

PHOTOPROCESS EFFECTS IN THE EARLY UNIVERSE

by

SHINYA MIYAKE

(Under the direction of Phillip C. Stancil)

ABSTRACT

In this dissertation, we show the importance of considering the interaction between photons and atomic and molecular species in the early Universe as well as in current day photodissociation regions (PDRs). First we calculated spectroscopic properties of the  $\text{HeH}^+$  molecular ion.  $\text{HeH}^+$  is believed to be formed first in the early Universe. Due to its permanent dipole moment, a high efficiency of radiative cooling is expected. We used the time-independent radial nuclear Schrödinger equation and obtained 162 rovibrational levels for the  $\text{X } ^1\Sigma^+$  electronic ground state. This is 4 levels more than the result previously calculated. Transition probabilities between all rovibrational levels were also computed and used to predict the emission spectra of  $\text{HeH}^+$  in local thermodynamic equilibrium (LTE). Then we calculated the radiative cooling coefficients for the LTE case. We found that the value of the radiative cooling coefficients of  $\text{HeH}^+$  is about ten orders of magnitude larger than those of  $\text{H}_2$ . However, the abundance of  $\text{HeH}^+$  is low compared to that of  $\text{H}_2$  in the early Universe. Therefore, the absolute cooling efficiency of  $\text{HeH}^+$  is a minor effect overall and depends highly on the primordial cloud circumstances.

Secondly, we have calculated photodissociation cross sections for  $\text{HeH}^+$ . Compared to its formation process, the cross sections for the destruction process are not always treated precisely which is important, especially for UV irradiated environments. Photodissociation cross sections for the  $\text{A } ^1\Sigma^+ \leftarrow \text{X } ^1\Sigma^+$  and  $\text{X } ^1\Sigma^+ \leftarrow \text{X } ^1\Sigma^+$  transitions were obtained using

a quantum method. We have calculated the respective cross sections as well as the case for LTE. Those data will be included in future releases of the plasma code Cloudy.

Thirdly, photodissociation cross sections of C<sub>2</sub> have been calculated from its ground electronic state X  $^1\Sigma^+$  to the electronic excited states A  $^1\Pi_u$ , 2  $^1\Pi_u$ , and 3  $^1\Pi_u$ . C<sub>2</sub> is important as a temperature diagnostic in diffuse interstellar clouds and PDRs. More accurate values have been obtained from the current calculation and important resonance features have also been found.

Next, we have considered the photodetachment cross section of H<sup>-</sup> involving a strong resonance around 11 eV. As for the radiation field, we have considered the case for a black-body, quasar, and the average intergalactic radiation field in the early Universe. We conclude that the photodetachment rate is enhanced by > 30 % if the resonance is included. A reduction of H<sup>-</sup> results in the loss of H<sub>2</sub>. Therefore the reduction of the H<sub>2</sub> abundance affects significantly the formation of Population III (Pop III) stars and may influence the era of the reionization of the Universe. We believe that this result may have a significant impact on large scale cosmological simulations because they adopt the H<sup>-</sup> cross section without the resonance contribution.

Lastly, we have considered the spectra of primordial objects at high redshift. We have used the publicly-available plasma code Cloudy in order to simulate the first generation star, Pop III star. We considered the case for the single Pop III star as well as for the case of a large star cluster in a dwarf galaxy. Strong features due to H I lines, He II lines as well as few H<sub>2</sub> lines are predicted. The simulated primordial emission features, may be observable with future far infrared or submillimeter detectors.

INDEX WORDS: The early Universe, Atomic and molecular processes,  
Radiative cooling processes, Population III star, Primordial gas

PHOTOPROCESS EFFECTS IN THE EARLY UNIVERSE

by

SHINYA MIYAKE

B.A., Saga University, Japan, 1999

M.S., Ibaraki University, Japan, 2002

A Dissertation Submitted to the Graduate Faculty

of The University of Georgia in Partial Fulfillment

of the

Requirements for the Degree

DOCTOR OF PHILOSOPHY

ATHENS, GEORGIA

2010

© 2010

Shinya Miyake

All Rights Reserved

PHOTOPROCESS EFFECTS IN THE EARLY UNIVERSE

by

SHINYA MIYAKE

Approved:

Major Professor: Phillip C. Stancil

Committee: Loris Magnani  
Craig Wiegert

Electronic Version Approved:

Maureen Grasso  
Dean of the Graduate School  
The University of Georgia  
May 2010

## DEDICATION

I dedicate this Ph.D. thesis to my family and relatives in Japan as well as to all of my friends who have supported me while I was studying at the University of Georgia. I especially would like to express my thankfulness to my research adviser, Dr. Phillip C. Stancil, who has supported and guided me during this academic life. Without all of their support, I wouldn't have come to this point. I really thank you.

## ACKNOWLEDGMENTS

This work was partially supported by NSF grant AST-0607733 from the Astronomy and Astrophysics Research Program and by Program HST-AR-11776.01-A which was provided by NASA through a grant from the Space Telescope Science Institute, which is operated by the Association of Universities for Research in Astronomy, Incorporated, under NASA contract NAS5-26555. I thank Chris Gay who is also in our research group as a graduate student. He worked hard for the modification of the photodissociation code which is used to generate the results in this dissertation. I also thank Dr. Gary Ferland who is the project leader of the plasma code Cloudy. He had made Cloudy code publicly available so that I could use it to generate the results in this dissertation. He generously gave me a lot of useful information while I visited the University of Kentucky. I would really appreciate everything.

## TABLE OF CONTENTS

	Page
ACKNOWLEDGMENTS . . . . .	v
LIST OF FIGURES . . . . .	vii
LIST OF TABLES . . . . .	viii
CHAPTER	
1 INTRODUCTION . . . . .	1
2 THE ROVIBRATIONAL SPECTRA AND RADIATIVE COOLING OF $\text{HeH}^+$ . . . . .	5
2.1 INTRODUCTION . . . . .	5
2.2 LINE LIST . . . . .	7
2.3 LTE SPECTRA OF BOUND-BOUND TRANSITIONS . . . . .	9
2.4 COOLING FUNCTION . . . . .	9
2.5 RESULTS AND DISCUSSION . . . . .	10
2.6 SUMMARY . . . . .	11
3 THE THEORY OF PHOTODISSOCIATION . . . . .	19
4 PHOTODISSOCIATION OF $\text{HeH}^+$ . . . . .	21
4.1 INTRODUCTION . . . . .	21
4.2 THEORY AND CALCULATION . . . . .	22
4.3 RESULTS AND DISCUSSION . . . . .	23
4.4 CONCLUSION . . . . .	26
5 PHOTODISSOCIATION OF $\text{C}_2$ . . . . .	42
5.1 INTRODUCTION . . . . .	42

5.2	THEORY AND CALCULATION . . . . .	43
5.3	RESULTS AND DISCUSSION . . . . .	43
5.4	SUMMARY . . . . .	44
6	RESONANT H <sup>-</sup> PHOTODETACHMENT: ENHANCED PHOTODESTRUCTION AND CONSEQUENCES FOR RADIATIVE FEEDBACK . . . . .	52
6.1	INTRODUCTION . . . . .	52
6.2	RESONANT PHOTODESTRUCTION . . . . .	54
6.3	CONCLUSIONS . . . . .	58
7	SIMULATED SPECTRA OF PRIMORDIAL OBJECTS AT HIGH REDSHIFT . . . . .	64
7.1	INTRODUCTION . . . . .	64
7.2	SIMULATIONAL MODEL . . . . .	65
7.3	RESULTS AND DISCUSSION . . . . .	67
7.4	CONCLUSION . . . . .	68
8	SUMMARY AND FUTURE RESEARCH . . . . .	78
	BIBLIOGRAPHY . . . . .	81
	APPENDIX	
A	HEH <sup>+</sup> SPECTROSCOPIC DATA IN LAMDA FORMAT . . . . .	87
B	ALL <i>v</i> AND <i>J</i> ENERGY LEVELS OF THE GROUND X $^1\Sigma_g^+$ STATE OF C <sub>2</sub> . . .	103

## LIST OF FIGURES

2.1	LTE spectrum of $\text{HeH}^+$ at $T = 100$ K. Red line: P-branch, a unit decrease in the rotational quantum number $J$ . Blue line: R-branch, a unit increase in the rotational quantum number $J$ . . . . .	12
2.2	Same as Fig. 2.1 but for $T = 500$ K. . . . .	13
2.3	Same as Fig. 2.1 but for $T = 1000$ K. . . . .	14
2.4	Same as Fig. 2.1 but for $T = 3500$ K. . . . .	15
2.5	Radiative cooling coefficients of $\text{HeH}^+$ in LTE (solid line), $\text{HeH}^+$ in the low density limit due to electron collisions (dashed line), and $\text{H}_2$ in the LTE limit (dotted line). . . . .	16
4.1	The plot of $\text{A } ^1\Sigma^+$ and $\text{X } ^1\Sigma^+$ state potentials obtained from Bishop & Cheung [20] and Kraemer et al. [14]. . . . .	27
4.2	The electric dipole moment for the ground electronic state, $\text{X } ^1\Sigma^+$ , of $\text{HeH}^+$ . Obtained from Jurek et al. [21]. . . . .	28
4.3	$\text{A } ^1\Sigma^+ \leftarrow \text{X } ^1\Sigma^+$ transition dipole moment of $\text{HeH}^+$ obtained from Kraemer et al. [14]. For actual calculation, values for smaller internuclear distance are smoothly extrapolated towards the origin. . . . .	29
4.4	The partial photodissociation cross sections $\sigma_{v''J''}$ as a function of wavelength $\lambda$ for the $\text{A } ^1\Sigma^+ \leftarrow \text{X } ^1\Sigma^+$ of $\text{HeH}^+$ from the vibrational level $v'' = 8$ (with $J'' = 1$ ). Solid line: current calculation. Dotted line: Saha et al. [36]. . . . .	30
4.5	Same as Fig. 4.4, but for $v'' = 0$ , $J'' = 1$ . . . . .	31
4.6	The partial photodissociation cross sections $\sigma_{v''J''}$ for the $\text{A } ^1\Sigma^+ \leftarrow \text{X } ^1\Sigma^+$ electronic transition of $\text{HeH}^+$ for $v'' = 10$ and all $J''$ . . . . .	32
4.7	Same as Fig. 4.6, but for $v'' = 0 - 11$ , $J'' = 0$ . . . . .	33

4.8 Total HeH <sup>+</sup> LTE photodissociation cross section for temperatures from 500 to 12,000 K, along with the partial cross section of $v'' = 0, J'' = 0$ of the A $^1\Sigma^+ \leftarrow$ X $^1\Sigma^+$ transition. . . . .	34
4.9 The partial photodissociation cross section of $v'' = 8, J'' = 1$ for the X $^1\Sigma^+ \leftarrow$ X $^1\Sigma^+$ rovibrational transition. Solid line: current calculation. Dotted line: Saha et al. [36]. . . . .	35
4.10 Same as Fig. 4.9 but for $v'' = 0, J'' = 0$ . . . . .	36
4.11 Same as Fig. 4.10 but for $v'' = 0, J'' = 0 - 23$ . . . . .	37
4.12 Same as Fig. 4.10 but for $v'' = 0 - 11, J'' = 0$ . . . . .	38
4.13 Total HeH <sup>+</sup> LTE photodissociation cross section for temperatures from 500 to 12,000 K, along with the partial cross section of $v'' = 0, J'' = 0$ for the X $^1\Sigma^+ \leftarrow$ X $^1\Sigma^+$ transition. . . . .	39
4.14 Total HeH <sup>+</sup> LTE photodissociation cross section at 1,000 K for both the X $^1\Sigma^+ \leftarrow$ X $^1\Sigma^+$ and A $^1\Sigma^+ \leftarrow$ X $^1\Sigma^+$ transitions. . . . .	41
5.1 Ab initio potential energy curves from Langhoff et al. [42] for the A $^1\Pi_u$ and X $^1\Sigma_g^+$ states. . . . .	45
5.2 Ab initio potential energy curves from Pouilly et al. [40] for the F $^1\Pi_u$ , $3^1\Pi_u$ and $4^1\Pi_u$ states. . . . .	46
5.3 The dipole transition moments from Pouilly et al. [40] for the F $^1\Pi_u \leftarrow$ X $^1\Sigma_g^+$ transition. . . . .	47
5.4 The dipole transition moments from Pouilly et al. [40] for the $3^1\Pi_u \leftarrow$ X $^1\Sigma_g^+$ transition. . . . .	48
5.5 The cross section of $v'' = 0, J'' = 0$ for A $^1\Pi_u \leftarrow$ X $^1\Sigma_g^+$ transition of C <sub>2</sub> . . .	49
5.6 The photodissociation cross sections as a function of photon energy for the C <sub>2</sub> F $^1\Pi_u \leftarrow$ X $^1\Sigma_g^+$ and $3^1\Pi_u \leftarrow$ X $^1\Sigma_g^+$ transitions for $v'' = 0, J'' = 0$ . Solid line: current calculation. Dotted line Pouilly et al. [40]. . . . .	50

6.1 $\text{H}^-$ photodetachment cross sections. Background without resonances from Chuzhoy et al. [67] fit to Wishart [70] (dashed); with resonances from McLaughlin et al. [74] (solid). The shape resonance just above $\text{H}(n = 2)$ is prominent at about 11 eV. There is also a narrow Feshbach resonance evident below $\text{H}(n = 2)$ and other less-prominent Feshbach resonances below $\text{H}(n = 3)$ near 12.8 eV. Also shown are blackbody spectra for temperatures from 5000 to 100,000 K (dotted). . . . .	60
6.2 $\text{H}^-$ photodetachment rate ratio, $R$ , for a blackbody radiation field as a function of effective temperature $T_{\text{eff}}$ (solid). As discussed in the text $R \sim F_r$ , the enhancement factor due to the resonances. Also shown are the photodetachment rates: using the Wishart [70] cross section with a cut-off energy of 13.6 eV (dotted), using the cross section of McLaughlin et al. [74] with the cut-off (dashed), and using [74] without the cut-off, i.e. a full blackbody (dot-dash). . . . .	61
6.3 $\text{H}^-$ photodetachment rate ratio, $R$ , for a power-law radiation field as a function of the power-law index $\alpha$ . Power-law rates computed over the photon energy ranges: 0.75-1000 eV (solid), 10-13.6 eV (dashed), and 10-1000 eV (dotted). The photodetachment rate ratio is also show for the IGM spectrum of Fig. 6.4 for photon energies 10-13.6 eV (dot-dash). . . . .	62
6.4 IGM sawtooth spectrum at $z \sim 20$ (long dashed) compared to an $\alpha = 0.7$ power-law spectrum (dotted) and $\text{H}^-$ photodetachment cross sections (same as Fig. 6.1). See text for a description of the sawtooth spectrum. Note the $\text{H}^-$ resonance between the Ly $\alpha$ and Ly $\beta$ features of the IGM spectrum. . . . .	63
7.1 Emergent spectrum for case I, for a single Pop III star at $z = 20$ . . . . .	70
7.2 Same as Fig. 7.1 with magnified wavelength range from 0.3 to 10 $\mu\text{m}$ . . . . .	71
7.3 Fractional abundance, electron density, ( $\text{cm}^{-3}$ ) and temperature of the shell as a function of the depth from the inner radius. . . . .	72

7.4	Column density (divided by the statistical weight) for $\text{H}_2(v = 0, J)$ as a function of $J$ rotational quantum number. Solid line: non-LTE, dotted line : LTE	73
7.5	Generated composite spectrum using multiple blackbody spectrum, corresponding to Pop III effective temperatures. . . . .	74
7.6	Same as Fig. 7.1, for primordial dwarf galaxy at $z = 10$ . . . . .	75
7.7	Emergent spectrum of the case of a primordial dwarf galaxy with magnified wavelength range from 0.3 to 10 $\mu\text{m}$ at $z = 10$ . . . . .	76
7.8	Same as Fig. 7.3, for primordial dwarf galaxy $z = 10$ . . . . .	77

## LIST OF TABLES

2.1 HeH <sup>+</sup> transition energies. [1] Experimental values are from Coxon & Hajigeorgiou [22]. . . . .	17
2.2 Spontaneous transition probabilities ( $s^{-1}$ ) for $\text{HeH}^+(v', J') \rightarrow \text{HeH}^+(v'', J'') + h\nu$ . . . . .	18
4.1 The partition function $Q_{\text{HeH}^+}$ for temperatures from 500 to 12,000 K. . . . .	40
5.1 Asymptotic separated-atom and united-atom limits for C <sub>2</sub> . . . . .	51

## CHAPTER 1

### INTRODUCTION

The first generation stars, so-called Population III (Pop III) stars, are predicted to have formed in minihalos which consist of baryonic matter and dark matter with a virial temperature of  $T \leq 10^4$  K at redshift  $z \geq 15$  [1, 2, 3, 4, 5]. Numerical simulations, which have investigated the collapse and the fragmentation of metal-free gas, showed that Pop III stars were predominantly very massive. Most current available understanding of the first generation stars is reviewed in Bromm & Larson [6]. The first stars must have formed from only primordial elements (H, He, Li), and the interaction between photons and the atoms and molecules made from these primordial elements is quite important especially in the early Universe. The next generation space telescope, the James Webb Space Telescope may be capable of spectroscopically detecting these primordial atomic and molecular species in the early Universe. The temperature drops as the Universe expands so at a redshift of  $z \sim 10^3$ , radiative recombination of hydrogen becomes effective so that the electron fraction decreases dramatically. As a result, the Universe became neutral and transparent to photons left over from the Big Bang. This phenomenon is called decoupling. At the recombination era ( $z \sim 10^3$ ), the gas density of the Universe was approximately  $10^{10}$  times larger ( $\sim 10^3 \text{ cm}^{-3}$ ) than today. Once atomic hydrogen formed, molecules could be created. It is believed that  $\text{HeH}^+$  was the first molecule to form followed by  $\text{He}_2^+$  (Lepp et al. [7]). At a slightly later time, the first neutral molecule  $\text{H}_2$  was formed from interaction between  $\text{H}_2^+$  and  $\text{H}^-$ . Cooling processes are likely to be important in the collapse of the first objects, with such cooling provided by molecules. It is still an active area of research to study how the first objects formed, how galaxies and clusters emerged, etc. In order to study these questions, we must start from

the initial fluctuations of the density of the matter in the early Universe and investigate the collapse of the primordial gas. A review of atomic and molecular process in the early Universe can be found in Lepp et al. [7]. In order to collapse further, cooling is needed. Saslaw & Zipoy [8] were the first to recognize the importance of H<sub>2</sub> cooling on the evolution of gas in the early Universe. The radiative cooling of molecular hydrogen can decrease the gas temperature to  $T \sim 500$  K.

In order to allow a primordial cloud to collapse and make a star, some energy has to be taken away from the cloud, otherwise the primordial cloud falls into virial equilibrium and would not collapse further. The dominant cooling mechanism available in the early Universe is through the radiation of photons. Due to its property that HeH<sup>+</sup> has a dipole moment, unlike H<sub>2</sub> (which has a only quadrupole moment), the HeH<sup>+</sup> may be a more efficient coolant. We study this property of HeH<sup>+</sup> and calculate the rovibrational spectra and radiative cooling coefficients.

Molecules may be destroyed once they are irradiated by a strong radiation field, like the UV radiation around a star. The transition region from atomic to molecular gas is called a photodissociation region (PDR). In order to determine the properties of PDRs, one has to obtain cross sections of photodissociation accurately. We study the photodissociation cross section of HeH<sup>+</sup>. Using the photodissociation cross sections mentioned above, we can calculate the total cross section for the case of local thermodynamic equilibrium (LTE) and for various temperatures.

We also study the photodissociation cross section of C<sub>2</sub>, an important temperature diagnostic in diffuse interstellar clouds and PDRs. Also in the early Universe, transition from Pop III stars to Pop II stars, which has more metals compare to the first generation stars, is dictated by the "critical metallicity". It is still an active field of research to determine when exactly that transition occurred and what value the critical metallicity should be. The abundance of C<sub>2</sub> highly depends on the circumstance of the clouds, especially once Pop III stars appeared and radiation turned on, because C<sub>2</sub> photodissociates when it is irradiated by

the UV photons. Therefore calculation of C<sub>2</sub> photodissociation cross sections can contribute to research deciding when exactly the transition from Pop III to Pop II occurred.

H<sup>-</sup> is one of the primordial atoms formed in the early Universe. It is closely connected to the formation reaction of H<sub>2</sub>, which is the most abundant molecule in the Universe and the important coolant in order for the cloud to collapse. There has still been an active debate whether “positive feedback” or “negative feedback” is dominant in the early Universe, once the Pop III stars emerged. The positive feedback process suggests that increase in the production of the FUV photons drives the increase in the number of free electrons, which ends up creating more H<sub>2</sub>. Therefore the increase in the number of H<sub>2</sub> molecules drives further creation of Pop III through enhanced H<sub>2</sub> radiative decay. Because Pop III stars are believed to be very massive,  $\sim 100 M_{\odot}$ , the negative feedback process suggests that once the Pop III star formed, its strong UV radiation destroys the ambient medium, especially H<sub>2</sub> and halts further collapse of the primordial clouds. In this dissertation, using the newly acquired H<sup>-</sup> cross section which has strong resonance peak around 11 eV and various radiation fields, we study the impact of the cross section resonance and important aspects about the argument of the feedback processes.

In order to investigate the history of Pop III stars and their effects on the ambient medium, one has to solve hydrodynamics, radiative transfer, and microphysics self-consistently. It is still beyond our current computer resource capability to follow from the collapse of the primordial cloud and emergence of the Pop III star, and to investigate the effect on the ambient medium produced by the star’s radiation and simulate the resulting emission spectra. Here we use the current version of publicly available plasma code, Cloudy, to simulate emission spectra in the early Universe assuming a single Pop III star and a cluster of Pop III stars are already formed. It is only a matter of time before we start to observe the spectra from these systems which includes Pop III stars and its ambient medium. Once we start to reach the capability of observing these systems, our simulated spectra in

this thesis might be useful to compare to the actual observed spectra and thus to improve our knowledge about the early Universe.

## CHAPTER 2

### THE ROVIBRATIONAL SPECTRA AND RADIATIVE COOLING OF $\text{HeH}^+$

#### 2.1 INTRODUCTION

A theoretical rotational and vibrational line list for the  $\text{HeH}^+$  molecular ion in the ground electronic state is computed and presented. The list includes transition energies and oscillator strengths for all possible allowed transitions and is used to compute the cooling function of  $\text{HeH}^+$  for a thermal population of rovibrational levels. The  $\text{HeH}^+$  cooling function per unit volume is found to be  $\sim 10^9$  times larger than that for  $\text{H}_2$  which suggests that it might play a role in the thermal balance of primordial gas with a significant ionization fraction.

Primordial atoms and molecules play important roles in the early Universe. We know that the first objects must have collapsed before a redshift of  $z \sim 9$ , as quasars are observed back to this redshift. We also know that the Universe had reionized by this time due to the observed absorption spectra of quasars. It is also believed that atomic and molecular processes controlled the evolution of the Universe after the recombination era. The scale of any object formed in the Universe is controlled by predominantly molecular cooling, and therefore radiative cooling processes have received considerable interest.

The possibility that  $\text{HeH}^+$  may exist in astrophysical environments was introduced by Dabrowski et al. [9].  $\text{HeH}^+$  is believed to be the first molecular ion formed in the early Universe. As it is composed of the two most abundant primordial elements,  $\text{HeH}^+$  is of fundamental astrophysical importance, particularly for the chemistry of the early Universe before the first generation of massive star formation, when the Universe was free of heavy elements [10, 11, 7].  $\text{HeH}^+$  is presumed to exist in diffuse ionizing environments and in these circumstances it is expected that, because of its large dipole moment,  $\text{HeH}^+$  will be

radiatively cooled and be present predominantly in its low-lying rotational and vibrational ground levels. Roberge & Dalgarno [13] discussed the possibility of detecting the  $J = 1 \rightarrow 0$  emission line of rotational transition at 149  $\mu\text{m}$  in planetary nebulae and dense molecular clouds. NGC 7027 had been a candidate for the detection of  $\text{HeH}^+$ , but without success [15].  $\text{HeH}^+$  may have been detected in the ejecta of SN 1987A [16].

$\text{HeH}^+$  is formed by the radiative association processes [13, 14]



and [17]



Additional  $\text{HeH}^+$  could be made by stimulated radiative association with Cosmic Microwave Background (CBR) photons [17]. With increasing density, the vibrational distribution of  $\text{H}_2^+$  [18] is a more efficient source of  $\text{HeH}^+$ . Therefore  $\text{H}_2^+$  ions and  $\text{H}_2$  produce  $\text{HeH}^+$  by the fast reaction



However, the  $\text{H}_2^+$  ions react preferentially with neutral atomic hydrogen to form molecular hydrogen [8, 19].

In this dissertation, we apply quantum-mechanical techniques to compute line lists for the bound-bound transitions of  $\text{HeH}^+$ . We also obtain local thermodynamic equilibrium (LTE) spectra and radiative cooling functions. In Section 2.2, an overview of the theory of molecular rovibrational lines is presented, while various LTE spectra are given in Section 2.3. In Section 2.4, the cooling function of the LTE case is presented. Finally, results are discussed in Section 2.5. Atomic units are used throughout this dissertation unless otherwise noted.

## 2.2 LINE LIST

### 2.2.1 ADOPTED POTENTIAL AND DIPOLE MOMENT FUNCTIONS

Accurate *ab initio* calculations of the ground electronic X  ${}^1\Sigma^+$  potential energy curve including adiabatic corrections have been made by Bishop & Cheung [20]. We performed a smooth fit to this *ab initio* potential. For the long-range interaction defined as an internuclear distances  $R \geq 10.0 a_0$ , we used

$$V_L = -\frac{\alpha}{2R^4}, \quad (2.4)$$

where  $\alpha$  is the static dipole polarizability of the helium atom. We adopt the value  $\alpha = 1.38309 a_0^3$ . For  $R \leq 0.9a_0$ , we fit the potential to the form  $A \exp(-BR)$  where  $A$  and  $B$  are the fitting parameters. For the dipole moment,  $D(R)$ , of the X  ${}^1\Sigma^+$  ground electronic state, we employed the calculations of Jurek & Kraemer [21]. The reduced mass of the molecular ion is taken to have the value  $\mu = 1467.4243$  a.u.

### 2.2.2 ENERGY LEVELS

We obtained eigenenergies and eigenfunctions for each rotation-vibration level for the HeH $^+$  X  ${}^1\Sigma^+$  electronic state. The time-independent radial nuclear Schrödinger equation

$$-\frac{\hbar^2}{2\mu} \frac{d^2\psi_{v,J}}{dR^2} + V_J(R)\psi_{v,J}(R) = E_{v,J}\psi_{v,J}(R) \quad (2.5)$$

is numerically solved with the Numerov method where  $\hbar$  is Plank's constant divided by  $2\pi$ ,  $J$  is the rotational quantum number,  $v$  is the vibrational quantum number, and  $V_J(R)$  is the effective potential of the molecule, defined by

$$V_J(R) = V_{BO}(R) + \frac{J(J+1)}{2\mu R^2} + \frac{V_{ad}}{\mu}, \quad (2.6)$$

where  $V_{BO}$  is the Born-Oppenheimer potential,  $V_{ad}$  is the adiabatic correction and  $R$  is the inter-nuclear distance. A total of 162 bound states were found, four more than obtained by Zygelman et al. [17] who also used the potential curve of Bishop & Cheung [20].

### 2.2.3 TRANSITION ENERGIES

Transition energies were obtained for all allowed transitions between bound rovibrational levels. Some examples are given in Table 2.1 and compared with the experimental data of Coxon & Hajigeorgiou [22]. Differences are typically less than  $1 \text{ cm}^{-1}$ , except for transitions between large  $v$ .

### 2.2.4 TRANSITION PROBABILITIES

We have calculated the radiative transition probabilities for all allowed electric dipole transitions between all bound rovibrational levels. The Einstein A coefficient is related to the transition dipole moment by

$$|\langle \psi_{v',J'} | D(R) | \psi_{v'',J''} \rangle|^2 = \frac{2J' + 1}{(2J'' + 1)\nu^3} A_{(v' J'; v'' J'')}, \quad (2.7)$$

Some examples are given in Table 2.2. The transition dipole moment is the electric dipole moment associated with the transition between the two states, an initial state  $\langle \psi_{v',J'} |$  and a final state  $| \psi_{v'',J''} \rangle$ . Our results are in good agreement with the transition probabilities of Engel et al. [23], but there is some discrepancy with those obtained by Roberge & Dalgarno [13].

### 2.2.5 OSCILLATOR STRENGTHS

The oscillator strength of a dipole transition,  $f$ , is

$$f = \frac{4\pi m_e \nu^2}{3\hbar e^2 \omega''} |\langle \psi_{v',J'} | D(R) | \psi_{v'',J''} \rangle|^2 \quad (2.8)$$

where  $\omega'' (=1)$  is the degeneracy of the lower  $X \ ^1\Sigma^+$  electronic state,  $m_e$  is the mass of the electron,  $e$  is electron charge, and  $\nu$  is the resonance frequency of the transition. The oscillator strength is also related to the Einstein A coefficient by

$$A = \frac{8\pi^2 e^2}{m_e c^3} \nu^2 \frac{g_1}{g_2} f \quad (2.9)$$

where  $c$  is the speed of light and  $g_1$  and  $g_2$  are the degeneracy factors of the two levels, given by  $(2J' + 1)$ ,  $(2J'' + 1)$ , respectively.

The line strength is defined by the double summation over Zeeman states:

$$\langle S_{v' J'} \rangle = \sum_{M'} \sum_{M''} |\langle \psi_{v', J'} | D(R) | \psi_{v'', J''} \rangle|^2 S_{J'}(J'') \quad (2.10)$$

The Hönl-London factors,  $S_{J'}(J'')$ , can be expressed for a  $\Sigma \leftarrow \Sigma$  electronic transition as

$$S_{J'}(J'') = \begin{cases} J'' & \text{for } J' = J'' - 1 \text{ (P-branch)} \\ J'' + 1 & \text{for } J' = J'' + 1 \text{ (R-branch).} \end{cases} \quad (2.11)$$

The Hönl-London factors indicate how the total intensity of a transition is distributed among the branches.

### 2.3 LTE SPECTRA OF BOUND-BOUND TRANSITIONS

We have plotted the radiative spectra for a local thermodynamic equilibrium (LTE) population distribution for temperatures between 100 K and 3500 K, shown as in Figs. 2.1–2.4. The relative spectrum intensity for a given transition  $i \rightarrow j$  is given by

$$I_{ij} = \frac{f_{ij}(2J_i + 1) \exp [(E_i - E_0)/k_b T]}{\sum_j (2J_j + 1) \exp [(E_j - E_0)/k_b T]} \quad (2.12)$$

### 2.4 COOLING FUNCTION

Cooling is important in the early Universe in that it controls the collapse of the first objects [25, 26]. In order to dissipate energy during the gravitational collapse of a gas cloud, the thermal energy must be transferred into radiation which escapes the cloud. This process is due to collisional excitation of atoms and/or molecules followed by the emission of a photon. To get significant cooling below 8000 K one must form molecules. As a cloud collapses, the efficiency of molecule formation increases. The most abundant molecule, and most important for the cooling, is H<sub>2</sub>. Since H<sub>2</sub> lacks a dipole moment, its emission is by quadrupole radiation. As a consequence, radiative cooling by HeH<sup>+</sup> may be important as it has a dipole moment;

therefore, we computed its cooling function over the range  $1 \leq T \leq 10^5$  K. The cooling function is given by for any substances

$$\frac{\Lambda}{n} = \sum_{v', J', v'', J''} A(v' J'; v'' J'') h\nu \exp \left[ \frac{E(v', J') - E(v'', J'')}{k_b T} \right] \quad (2.13)$$

and is expressed in  $\text{erg s}^{-1}\text{cm}^{-3}$  where  $A(v' J'; v'' J'')$  is the Einstein  $A$  coefficient for spontaneous emission,  $k_b$  is Boltzmann's constant, and  $T$  is the absolute temperature. This relation is valid in the high-density limit and assumes the levels are populated in LTE.

In the low-density limit, we assumed collisional de-excitation with electrons,

$$\Lambda \rightarrow n_1 n_0 q_{10} h\nu_{10} \quad (2.14)$$

where  $n_1, n_0$  are the number densities in units of  $\text{cm}^{-3}$ ,  $q_{01}$  is the collisional rate coefficient for excitation, and  $h\nu_{10}$  represents the energy of the emitted photon for  $J' = 1 \rightarrow J'' = 0$ .

In Figure 2.5 we have plot the  $\text{HeH}^+$  cooling coefficients as a function of the temperature. The  $\text{H}_2$  cooling coefficients for the LTE case is also included. We have adopted rate coefficients for electron– $\text{HeH}^+$  collisions for the  $J = 0 \rightarrow 1$  transition from Rabadan et al. [27]. The cooling function for an arbitrary density resides in between the LTE and low density limit curves.

## 2.5 RESULTS AND DISCUSSION

In gaseous nebulae, collisions with electrons, protons, or hydrogen atoms can excite  $\text{HeH}^+$  ions. The strongest emissions are from the  $(0, 1) - (0, 0)$  pure rotational line at  $149.13\ \mu\text{m}$  and the vibration rotation transition arising from the  $(1, 1)$  level [13].

In Figure 2.5, we have plotted the radiative cooling coefficients of  $\text{HeH}^+$  for LTE case, the low density limit case due to electron collisions as well as  $\text{H}_2$  in the LTE limit case. The efficiency of  $\text{HeH}^+$  is  $\sim 10$  times larger than  $\text{H}_2$ . True cooling function of  $\text{HeH}^+$  in the interstellar circumstances falls somewhere in between LTE and low density limit lines. In order to investigate which molecule can be efficient as a coolant, one has to know the

abundance of  $\text{HeH}^+$  and  $\text{H}_2$  in the gas cloud exactly. However, the abundance of  $\text{HeH}^+$  in the interstellar medium, especially in the early Universe is fairly low compared to the abundance of  $\text{H}_2$  [7]. Therefore we conclude that the role of cooling due to  $\text{HeH}^+$  is highly depends on the clouds circumstances.

In table 2.1, we list up the  $\text{HeH}^+$  transition energies and compared with the experimental data of Coxon & Hajigeorgiou [22]. Our data matched within  $< 1 \text{ cm}^{-1}$  for the low rovibrational transitions and agreed with the experimental data quite well. However as we go high rovibrational transitions, there is some deviations.

## 2.6 SUMMARY

We have calculated the rovibrational spectra and radiative cooling function of  $\text{HeH}^+$  for LTE and the low density limit. We point out that  $\text{HeH}^+$  could also be an important coolant comparable to the molecular hydrogen . However it is highly dependent on the clouds circumstances.

All data including binding energies, transition energies, and transition probabilities can be found on the UGA Molecular Opacity Project website (<http://www.physast.uga.edu/ugamop/>). The data is also available in a format following the Leiden Atomic and Molecular Database (LAMDA, Schöier et al. [28]).

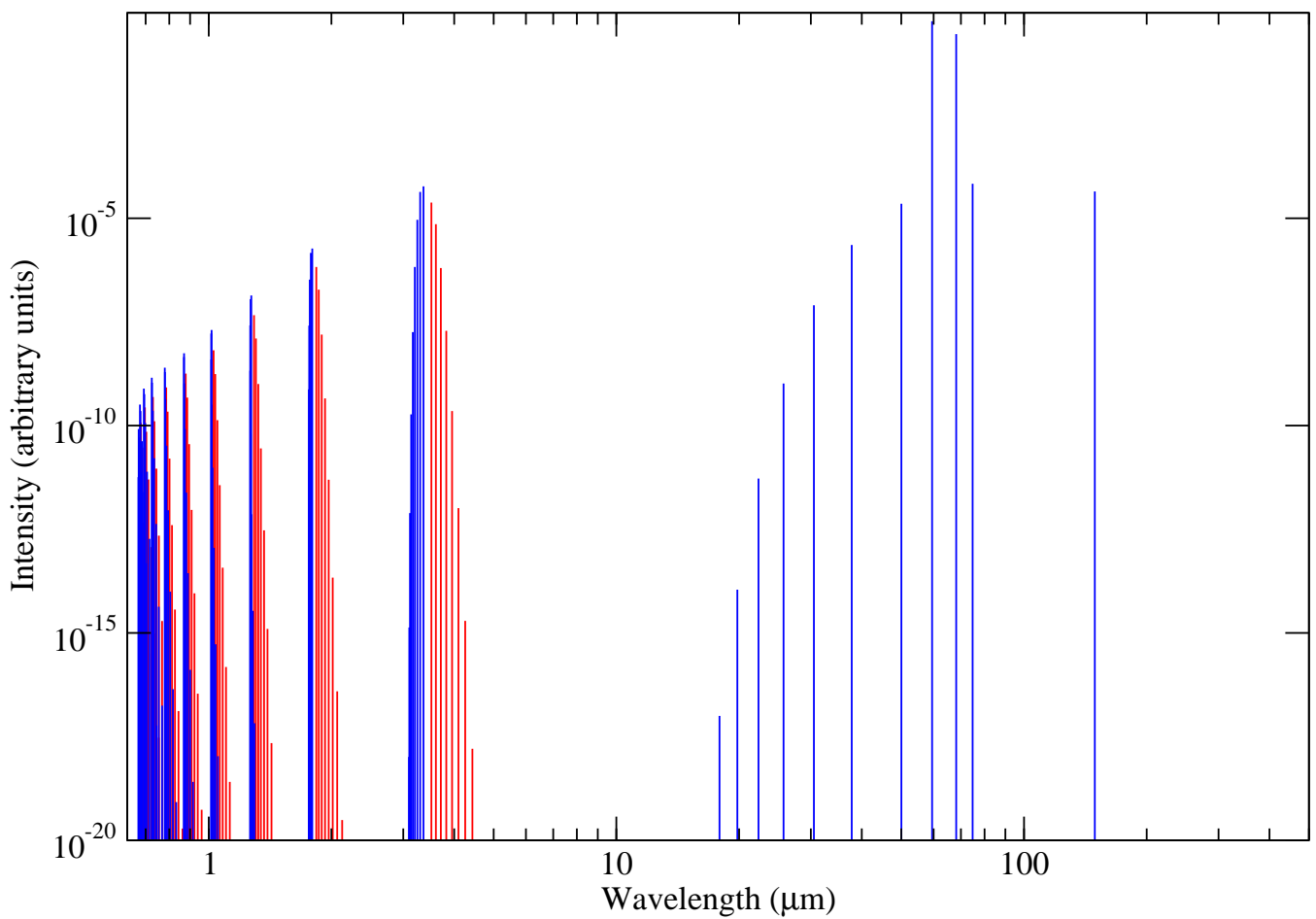


Figure 2.1: LTE spectrum of  $\text{HeH}^+$  at  $T = 100 \text{ K}$ . Red line: P-branch, a unit decrease in the rotational quantum number  $J$ . Blue line: R-branch, a unit increase in the rotational quantum number  $J$ .

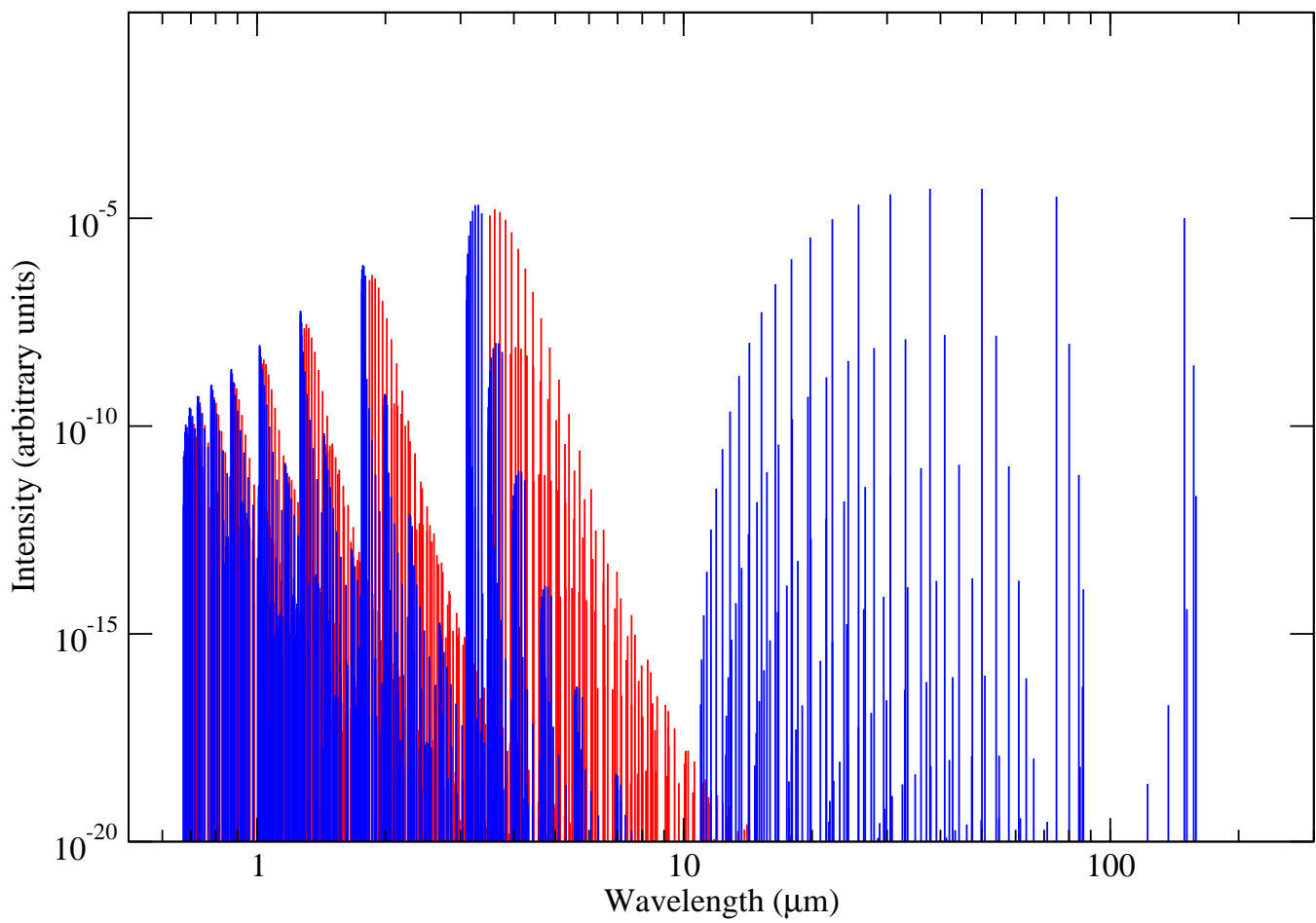


Figure 2.2: Same as Fig. 2.1 but for  $T = 500 \text{ K}$ .

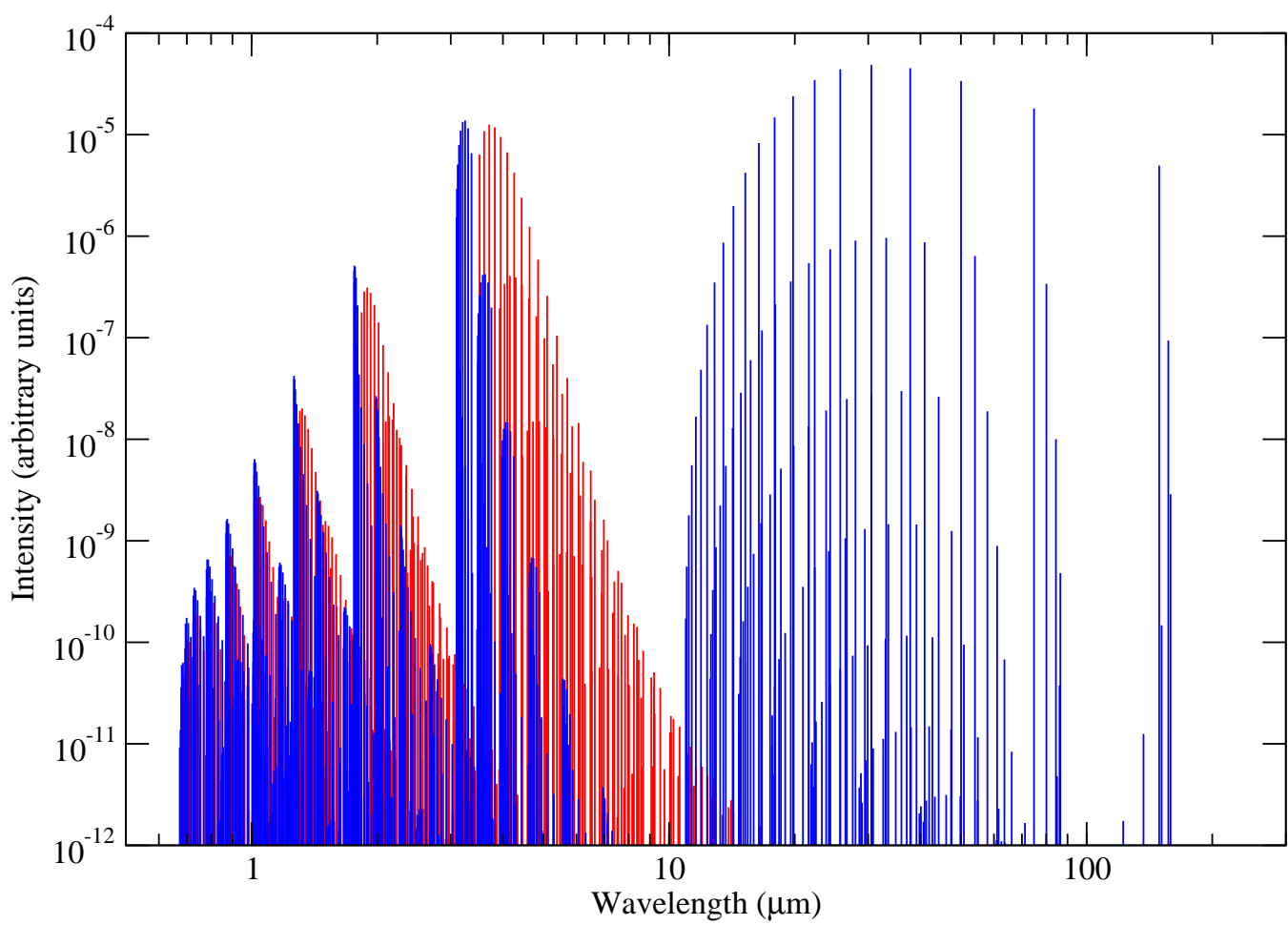


Figure 2.3: Same as Fig. 2.1 but for  $T = 1000 \text{ K}$ .

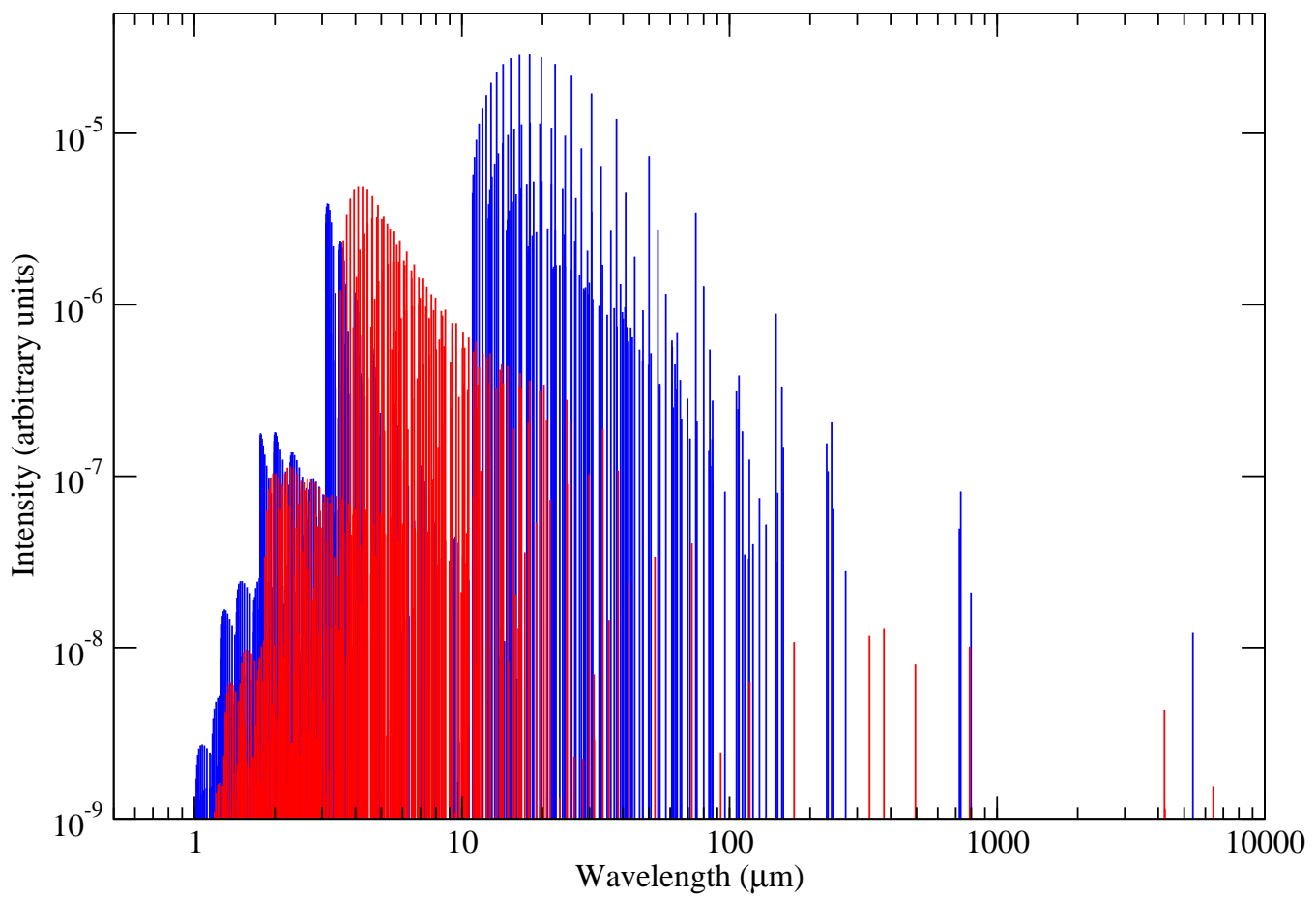


Figure 2.4: Same as Fig. 2.1 but for  $T = 3500 \text{ K}$ .

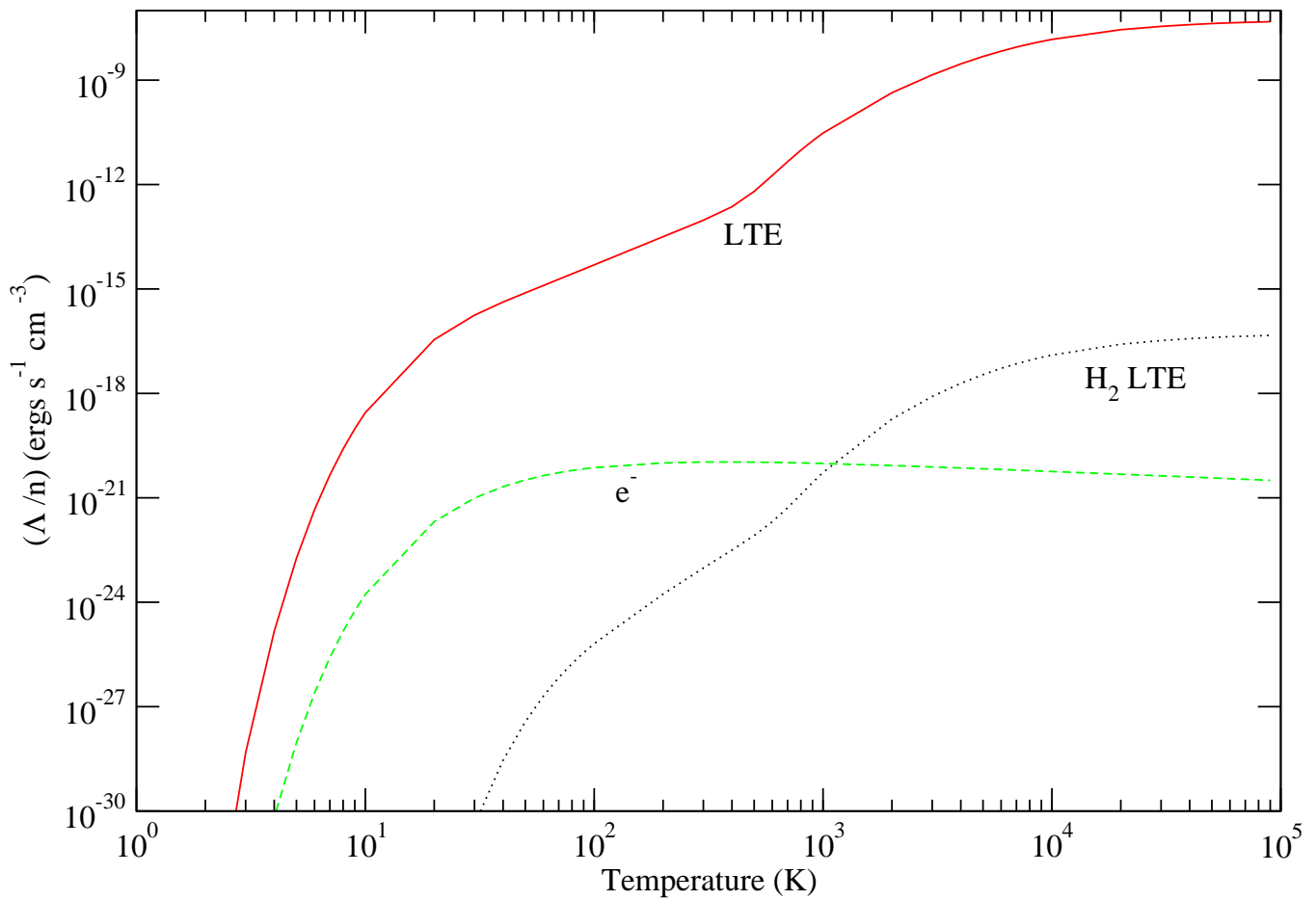


Figure 2.5: Radiative cooling coefficients of  $\text{HeH}^+$  in LTE (solid line),  $\text{HeH}^+$  in the low density limit due to electron collisions (dashed line), and  $\text{H}_2$  in the LTE limit (dotted line).

Table 2.1:  $\text{HeH}^+$  transition energies. [1]Experimental values are from Coxon & Hajigeorgiou [22].

$v'$	$v''$	$J$	$P(J)$ Transition		
			Experiment <sup>1</sup> (cm <sup>-1</sup> )	Calculated (cm <sup>-1</sup> )	obs-calc (cm <sup>-1</sup> )
1	0	1	2843.9035	2843.7873	0.1162
		2	2771.8095	2771.7048	0.1047
		3	2695.0500	2694.9639	0.0861
		4	2614.0295	2613.9571	0.0724
		5	2529.134	2529.0727	0.0613
		6	2440.742	2440.6897	0.0523
		9	2158.140	2158.1106	0.0294
		10	2059.210	2059.1187	0.0913
		11	1958.388	1958.4010	-0.013
		12	1855.905	1855.9232	-0.0182
		13	1751.971	1751.9919	-0.0209
		2	2542.531	2544.5116	-1.9806
			2475.814	2477.6580	-1.844
			2248.854	2250.0033	-1.1493
			2165.485	2166.3913	-0.9063
			2248.854	2250.0033	-1.1493
			2078.841	2079.5307	-0.696
			1989.251	1989.7540	-0.503
			1896.992	1897.3628	-0.3708
			1802.349	1802.623	-0.274
			1705.543	1705.761	-0.218
			862.529	863.05441	-0.52541
			745.624	746.18133	-0.55733
3	2	5	1966.356	1970.4648	-4.1088
		17	833.640	834.05857	-0.41857
		18	719.769	720.24819	-0.47919
5	4	11	901.963	904.034	-2.071
		12	807.806	809.21635	-1.41035
6	5	8	863.378	871.75314	-8.37514
		9	782.925	788.65176	-5.72676
7	6	4	817.337	848.80041	-31.46341
		5	760.367	784.65909	-24.29209

Table 2.2: Spontaneous transition probabilities ( $\text{s}^{-1}$ ) for  $\text{HeH}^+(v', J') \rightarrow \text{HeH}^+(v'', J'') + h\nu$ .

$v'$	$J'$	$v''$	$J''$	$\lambda$ (nm)	Roberge et al. $A$ ( $\text{s}^{-1}$ )	Engel et al. $A$ ( $\text{s}^{-1}$ )	this work $A$ ( $\text{s}^{-1}$ )
1	0	0	1	3516.0271	1098	830.802	826.076
1	1	0	0	3363.8480	293	283.663	282.019
1	1	0	2	3607.4759	811	542.764	539.711
1	2	0	1	3301.8692	311	341.654	339.661
2	0	0	1	1861.9524	224	82.4290	84.7687
2	1	0	0	1794.8580	72	30.5583	31.3875
2	1	0	2	1861.9524	150	51.7642	53.3310

## CHAPTER 3

### THE THEORY OF PHOTODISSOCIATION

The expression for the photodissociation cross section is given by Kirby & van Dishoeck [29]

$$\sigma_{v''J''} = \frac{2\pi e^2}{3mc} g \Delta E_{k',v''} |D_{k',v''}^{fi}(R)|^2, \quad (3.1)$$

where  $\Delta E_{k',v''}$  is the energy of the absorbed photon,  $D_{k',v''}^{fi}(R)$  is the matrix element of the electric dipole transition moment for absorption from the rovibrational level  $v'', J''$  in state  $i$  to continuum  $k'$  in state  $f$ , and  $g$  is the degeneracy factor given by

$$g = \frac{2 - \delta_{0,\Lambda' + \Lambda''}}{2 - \delta_{0,\Lambda''}}, \quad (3.2)$$

where  $\Lambda'$  and  $\Lambda''$  are the angular momenta projected along the nuclear axis for the final and initial electronic states, respectively. If both the matrix element and the transition energy are given in atomic units, the factor  $2\pi e^2/3mc$  has the numeric value  $2.69 \times 10^{-18}$  for the cross section in  $\text{cm}^2$ .

The rotational photodissociation cross section can be rewritten as

$$\sigma_{v''J''} = 2.69 \times 10^{-18} \Delta E_{k'J',v''J''} \frac{1}{2J'' + 1} S_{J'} |D_{k'J',v''J''}^{fi}|^2 \text{ cm}^2 \quad (3.3)$$

where the Hönl-London factors,  $S_{J'}(J'')$  for a  $\Sigma \leftarrow \Sigma$  electronic transition are the same as those given in eq. (2.11). For a  $\Pi \leftarrow \Sigma$  electronic transition, it is defined according to Whiting & Nicholls [24] as

$$S_{J'}(J'') = \begin{cases} (J'' - 1)/2 & \text{for } J' = J'' - 1 \text{ (P-branch)} \\ (2J'' + 1)/2 & \text{for } J' = J'' \text{ (Q-branch)} \\ (J'' + 2)/2 & \text{for } J' = J'' + 1 \text{ (R-branch)}. \end{cases} \quad (3.4)$$

The factor  $D_{k'J',v''J''}^{fi} = \langle \chi_{k'J'} | D^{fi}(R) | \chi_{v''J''} \rangle$  is the integral of the dipole moment function between rovibrational wave functions of electronic state  $i$  and  $f$ .  $J$  is the angular momentum of nuclear motion, and spin-splitting of doublet electronic states is neglected. The continuum wave functions  $\chi_{k'J'}$  are normalized such that they behave asymptotically as

$$\chi_{k'J'} \sim \sin\left(k'R - \frac{\pi}{2}J' + \eta_{J'}\right) \quad (3.5)$$

where  $\eta_{J'}$  is the phase shift. This wavefunction  $\chi_{k'J'}$  is necessary because it describes the unbound upper states. And since it is unbound, the wavefunction has to be in the form of the plane wave which is sinusoidal. The bound and continuum rotational-vibrational wave functions,  $\chi_{v''J''}$  and  $\chi_{k'J'}$ , respectively, are solutions of the radial Schrödinger equation for nuclear motion eq. (2.5) on the  $i$  and  $f$  state potential curves, respectively. The wave functions were obtained numerically using the standard Numerov method [30, 31, 32] with a step size of  $0.01a_0$  over internuclear distances  $0.1a_0 < R < 200a_0$ .

## CHAPTER 4

### PHOTODISSOCIATION OF $\text{HeH}^+$

#### 4.1 INTRODUCTION

Accurate photodissociation cross sections have been obtained for the  $A\ ^1\Sigma^+ \leftarrow X\ ^1\Sigma^+$  electronic transition of  $\text{HeH}^+$  using *ab initio* potential energies and dipole transition moments. The partial cross sections have been evaluated for all rotational transitions from vibrational levels  $v'' = 0 - 11$  and over the entire accessible wavelength range  $\lambda\lambda 100 - 1,200\ \text{\AA}$ . Assuming a Boltzmann distribution of the rovibrational levels of  $X\ ^1\Sigma^+$ , photodissociation cross sections are presented for temperatures between 500 and 12,000 K. A similar set of calculations were also performed for the pure rovibrational photodissociation from the  $X\ ^1\Sigma^+$  electronic ground state, but covering photon wavelengths into the far infrared. The resulting cross sections are applicable to the destruction of  $\text{HeH}^+$  in the early Universe and in UV-irradiated molecular clouds regions.

Photodissociation is an important mechanism for the destruction of interstellar molecules in diffuse and translucent clouds, in photodissociation regions, in circumstellar disks, in protoplanetary disks, and in many other environments with an intense radiation field.  $\text{HeH}^+$  is believed to be one of the first molecules formed in the early Universe [7]. Its abundance is kept low due to photodissociation by the cosmic background (CBR) radiation field. Schleicher et al. [33], however, have suggested that  $\text{HeH}^+$  can efficiently scatter CBR photons and may generate fluctuations in the cosmic background radiation. Within our galaxy, Roberge & Dalgarno [13] discussed the possibility of observing  $\text{HeH}^+$  in gaseous nebulae. However, to date this molecule has not been detected. Searches for  $\text{HeH}^+$  in the planetary nebulae NGC 7072 have placed upper limits on vibrational [34] and rotational [15, 35] line strengths.

Intensive UV radiation from the central white dwarf may result in efficient photodissociation, providing insight into the low abundance of this molecular ion.

We have performed extensive calculations of photodissociation cross sections for  $\text{HeH}^+$  using the most accurate available molecular data. Calculations were performed for the full range of 162 rovibrational levels ( $v'', J''$ ) in the ground electronic state. Atomic units are used throughout unless stated otherwise. In this work, we apply quantum-mechanical techniques to compute the photodissociation cross section. We also obtained LTE cross sections for  $\text{HeH}^+$ . In chapter 3, an overview of the theory of molecular photodissociation was presented. Results of the partial cross section as well as the LTE photodissociation cross section of  $\text{HeH}^+$  are discussed in section 4.4.

## 4.2 THEORY AND CALCULATION

### 4.2.1 POTENTIAL CURVES AND THE DIPOLE TRANSITION MOMENTS

Accurate *ab initio* calculations of the ground electronic  $X\ ^1\Sigma^+$  potential energy including adiabatic corrections have been made by Bishop & Cheung [20] and are adopted here. For internuclear distances  $R > 10 a_0$ , a smooth fit to the ab initio potentials have been performed using the average long-range interaction potential

$$V_L = -\frac{\alpha}{2R^4} \quad (4.1)$$

where  $\alpha$  is the static dipole polarizability of the neutral hydrogen or helium atom. We adopt the values  $\alpha_{\text{H}} = 4.5$  and  $\alpha_{\text{He}} = 1.38309$ . For  $R < 0.9 a_0$ , the potentials have been fit to the short-range interaction potential form  $A \exp(-BR) + C$ . Ab initio calculations of the excited electronic  $A\ ^1\Sigma^+$  state are obtained from Kraemer et al. [14] and smoothly fit in the same way described above. A plot of both  $A\ ^1\Sigma^+$  and  $X\ ^1\Sigma^+$  state potentials are given in Figure 4.1. The electric dipole moment for the ground electronic state,  $X\ ^1\Sigma^+$  are obtained from Jurek et al. [21] over the range of  $0.9 a_0 < R < 30.0 a_0$ . In Figure 4.2, the electric dipole moment for the ground state of  $\text{HeH}^+$  is shown. Values of the  $A\ ^1\Sigma^+ \leftarrow X\ ^1\Sigma^+$  transition dipole moment

function was obtained from Kraemer et al. [14] over the range of  $1.0a_0 < R < 30.0a_0$  and displayed in Figure 4.3.

### 4.3 RESULTS AND DISCUSSION

#### 4.3.1 PARTIAL CROSS SECTIONS FOR ELECTRONIC PHOTODISSOCIATION

In order to see the general trend to the contribution to the total cross sections, we plot partial cross sections here. A sampling of the partial cross sections  $\sigma_{v''J''}$  for the  $A\ ^1\Sigma^+ \leftarrow X\ ^1\Sigma^+$  transition are presented in Figures 4.4–4.7. Those partial cross sections are calculated from a single rovibrational state to the upper unbound states. Figure 4.4 shows the partial cross section  $\sigma_{v''J''}$  as a function of wavelength  $\lambda$  for photodissociation of  $\text{HeH}^+$  from the vibrational level  $v'' = 0, J'' = 1$ . Comparison is made with the earlier calculation performed by Saha et al. [36]. The overall trend is similar, but there is the shift in the peak.

Figure 4.4 shows our results for the partial cross section  $\sigma_{v''J''}$  from the vibrational level  $v'' = 8, J'' = 1$  in order to make comparison with the earlier calculations of Figure 4 in Saha et al. [36]. Given the ionization potentials of H and He and the binding energy of the  $v'' = 8, J'' = 1$  level, the photodissociation threshold is 1123 Å, which is consistent with the current results as seen by the sharp cutoff in the figure at that wavelength. Additional cross sections are presented in Figure 4.6 for  $v'' = 10$  and all bound  $J''$  and in Figure 4.7 for  $v'' = 0 - 11$ , for  $J'' = 0$ .

#### 4.3.2 LTE CROSS SECTIONS FOR ELECTRONIC PHOTODISSOCIATION

The total quantum-mechanical cross section for photodissociation as a function of both temperature and wavelength in LTE is given by Argyros [37]

$$\sigma(\lambda, T) = \frac{\sum_{v''} \sum_{J''} g_{iv''J''} \exp[-(E_g - E_{v''J''})/k_b T] \sigma_{v''J''}(\lambda)}{Q_{\text{HeH}^+}(T)} \quad (4.2)$$

where  $\sigma_{v''J''}$  is the partial cross section from the  $(v'', J'')$  level,  $g = 2J'' + 1$  is the total vibrational-rotational statistical weight,  $E_g$  is the binding energy of the lowest rovibrational

level,  $k_b$  is the Boltzmann constant and  $Q_{\text{HeH}^+}(T)$  is the partition function given by

$$Q_{\text{HeH}^+}(T) = \sum_{v''} \sum_{J''} g_{iv''J''} \exp [-(E_g - E_{v''J''})/k_b T], \quad (4.3)$$

Figure 4.8 displays LTE cross sections for the  $\text{A } ^1\Sigma^+ \leftarrow \text{X } ^1\Sigma^+$  photodissociation transition as a function of the wavelength. A Boltzmann population distribution of the rovibrational levels of the ground electronic state of  $\text{X } ^1\Sigma^+$  has been used for the temperatures between 500 and 12,000 K as given in equation (4.2). The threshold wavelength at 1129 Å corresponds to the asymptotic energy gap between the  $\text{A } ^1\Sigma^+$  and  $\text{X } ^1\Sigma^+$  electronic states. The partition function  $Q_{\text{HeH}^+}$  is tabulated in Table 4.1.

#### 4.3.3 THE PARTIAL CROSS SECTIONS FOR ROVIBRATIONAL PHOTODISSOCIATION

For irradiated environments with photon wavelength much greater than the Lyman limit, photodissociation via pure rovibrational transitions may dominate although the cross sections are typically small. For example, in Figure 4.9, the partial cross section for rovibrational photodissociation in the  $\text{X } ^1\Sigma^+$  electronic state is presented. Comparison is made with the earlier work of Saha et al. [36]. There is a significant shift in the threshold wavelength with the current results consistent with the  $v'' = 8, J'' = 1$  binding energy calculation of Zygelman et al. [17]. Additional examples of rovibrational photodissociation for the  $\text{X } ^1\Sigma^+ \leftarrow \text{X } ^1\Sigma^+$  transition are given in Figures 4.10–4.12. Figure 4.10 displays photodissociation from the ground rovibrational level ( $v'' = 0, J'' = 0$ ) which has a threshold of 6732 Å and a peak cross section magnitude that is  $10^7$  times smaller than for the  $\text{A } ^1\Sigma^+ \leftarrow \text{X } ^1\Sigma^+$  electronic transition. Figure 4.11 displays cross sections from  $v'' = 0$  and a selection of  $J''$ . Orbiting resonances due to quasi-bound levels are evident for  $J \geq 5$ , near thresholds. Figure 4.12 displays similar results, but for  $J'' = 0$  and a selection of  $v''$ .

#### 4.3.4 LTE CROSS SECTIONS FOR VIBRATIONAL PHOTODISSOCIATION

A Boltzmann population distribution of the rovibrational levels of the ground electronic state of  $\text{X } ^1\Sigma^+$  has been used for the temperatures between 500 and 12,000 K. For gas tem-

peratures less than  $\sim 1000$  K, the LTE cross section peaks at a wavelength corresponding to the  $v'' = 0, J'' = 0$  threshold. Photons in this wavelength range are primarily responsible for photodestruction of  $\text{HeH}^+$ . For higher temperature gas, the population in highly excited  $v'', J''$  levels contribute substantially to the cross section increasing its value at large wavelength. Figure 4.13 shows LTE cross sections for the  $\text{X}^1\Sigma^+ \leftarrow \text{X}^1\Sigma^+$  photodissociation of  $\text{HeH}^+$  as a function of the wavelength.

#### 4.3.5 ASTROPHYSICAL APPLICATIONS

Roberge & Dalgarno [13] discussed the mechanisms for the formation and destruction of  $\text{HeH}^+$  in astrophysical plasmas. They computed the photodissociation cross section for the  $\text{A}^1\Sigma^+ \leftarrow \text{X}^1\Sigma^+$  transition, but only for  $v'' = 0, J'' = 0$ . Their cross section is similar to the current results shown in Figure 4.7. As shown in Figure 4.8, since the minimum wavelength for the average interstellar radiation field is at the Lyman limit (911 Å), photodissociation of  $\text{HeH}^+$  through the  $\text{A}^1\Sigma^+ \leftarrow \text{X}^1\Sigma^+$  transition will only be efficient for gas with  $T \geq 2000$  K. However, in other environments, such as the inner regions of circumstellar shells, protoplanetary disks, or PDRs near massive Population III stars, significant photon flux in the far UV with  $\lambda < 911$  Å may result in efficient  $\text{HeH}^+$  photodestruction. Representative photodestruction rates can be found in Roberge & Dalgarno [13] for blackbody temperatures between 20,000 – 500,000 K.

In the early Universe, radiation from the cosmic microwave background can efficiently destroy  $\text{HeH}^+$  through the  $\text{X}^1\Sigma^+ \leftarrow \text{X}^1\Sigma^+$  transition until a redshift of  $z \sim 300$  [38, 33]. Early Universe chemical models typically obtain the destruction rate via detailed balance from the radiative association rate coefficients. The current results shown in Figure 4.12 could be used to improve such calculations by directly computing the photodissociation rate due to the cosmic background radiation field.

Once a population III star is formed, the  $\text{HeH}^+$  present in its primordial halo which consist of baryonic matter and dark matter will be photodissociated by both the Far UV

stellar radiation through the  $A\ ^1\Sigma^+ \leftarrow X\ ^1\Sigma^+$  transition and the high redshift CBR radiation through the  $X\ ^1\Sigma^+ \leftarrow X\ ^1\Sigma^+$  transition. Figure 4.13 compares the LTE photodissociation cross section for a gas temperature of 1,000 K.

#### 4.4 CONCLUSION

Using *ab initio* potentials and dipole moment functions, accurate cross section calculations have been performed for the photodissociation of  $\text{HeH}^+$  through the  $A\ ^1\Sigma^+ \leftarrow X\ ^1\Sigma^+$  as well as  $X\ ^1\Sigma^+ \leftarrow X\ ^1\Sigma^+$  transitions. The partial cross sections have been evaluated for all the rotational transitions from the vibrational levels  $v'' = 0 - 11$  of the  $X\ ^1\Sigma^+$  electronic state. LTE cross sections are also calculated for temperatures between 500 and 12,000 K. The resulting cross sections are applicable to the destruction of  $\text{HeH}^+$  in the early Universe and UV irradiated molecular regions. All photodissociation cross section data can be obtained from the UGA Molecular Opacity Project website (<http://www.physast.uga.edu/ugamop/>).

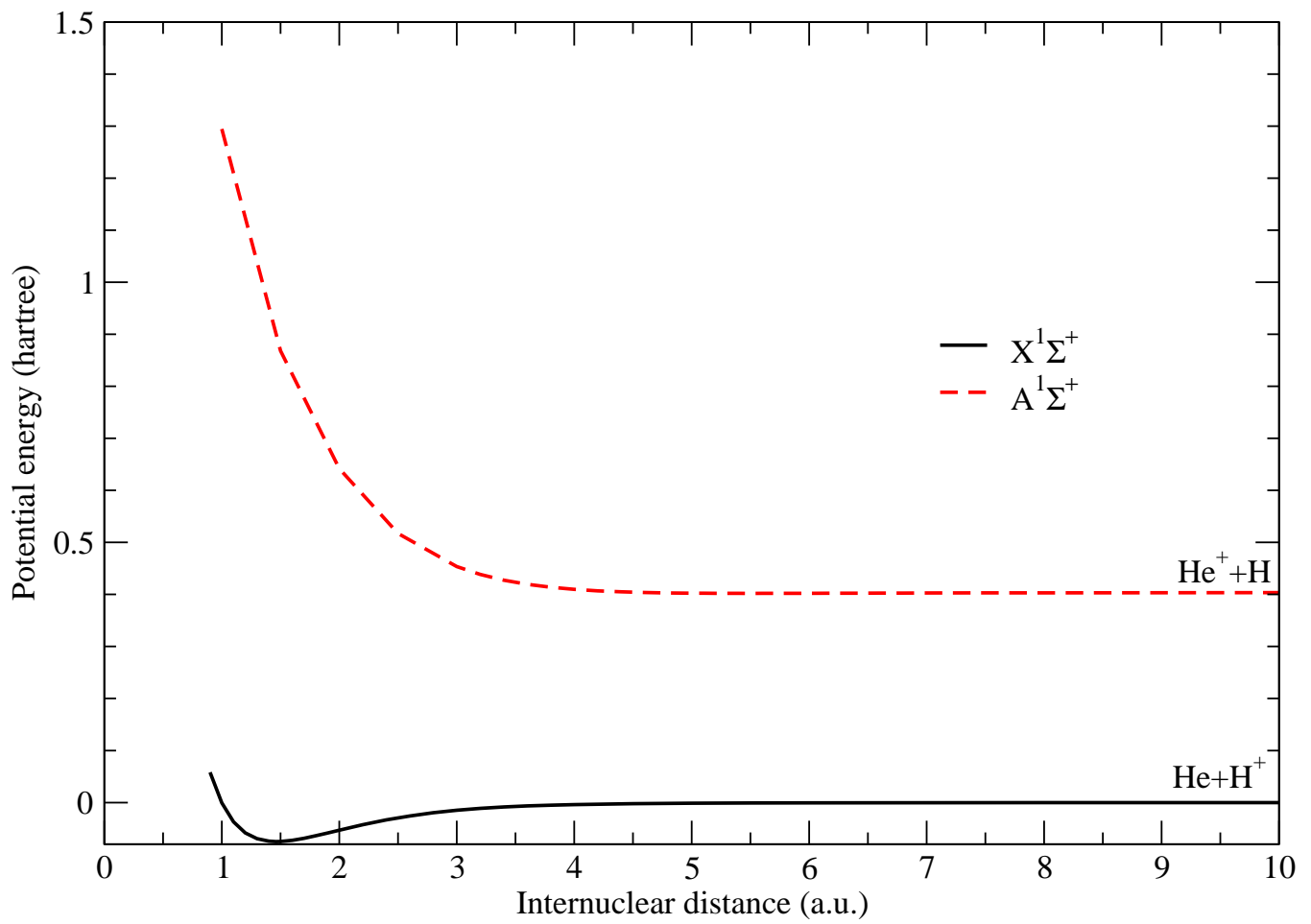


Figure 4.1: The plot of  $A^1\Sigma^+$  and  $X^1\Sigma^+$  state potentials obtained from Bishop & Cheung [20] and Kraemer et al. [14].

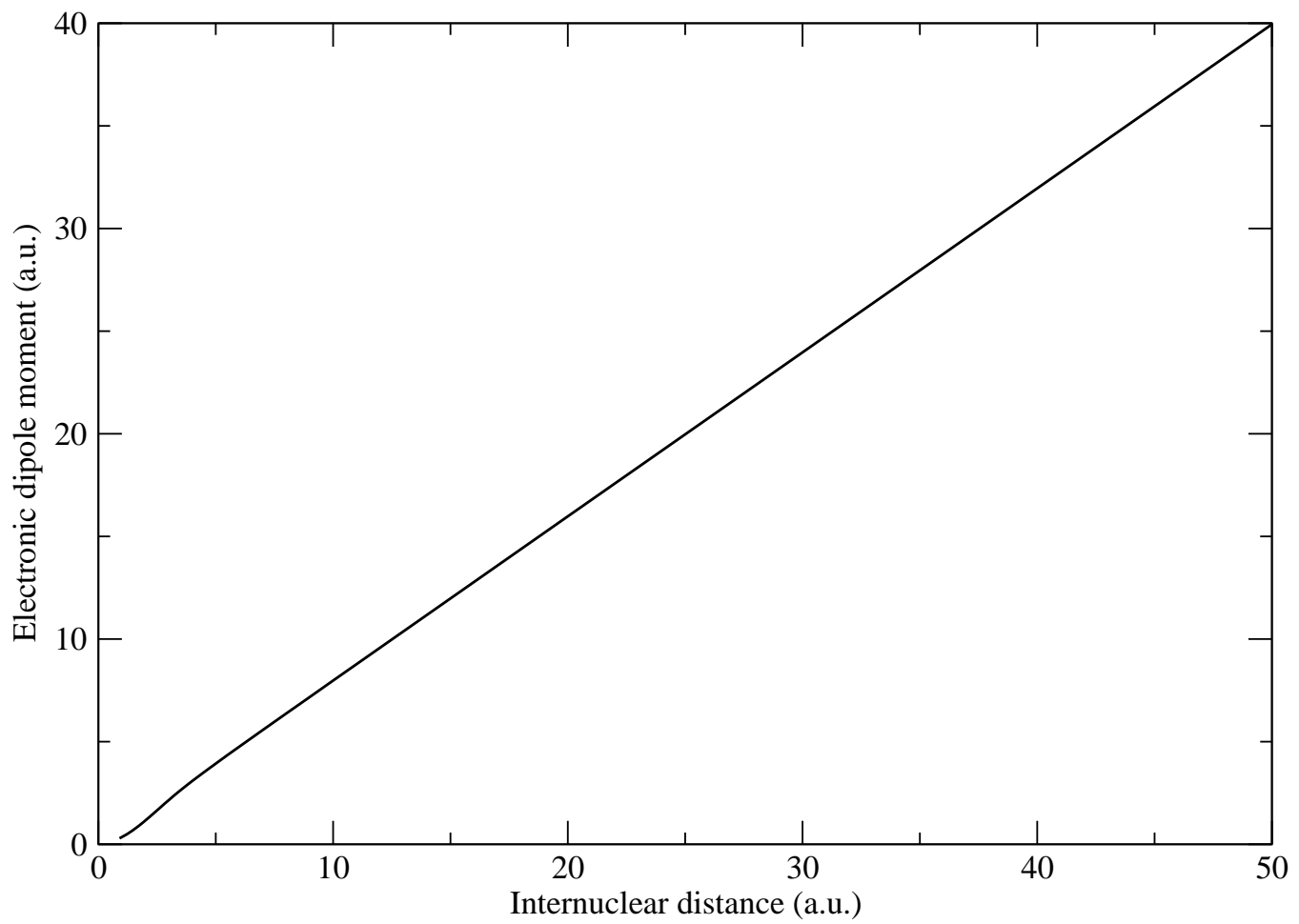


Figure 4.2: The electric dipole moment for the ground electronic state,  $X\ ^1\Sigma^+$ , of  $\text{HeH}^+$ . Obtained from Jurek et al. [21].

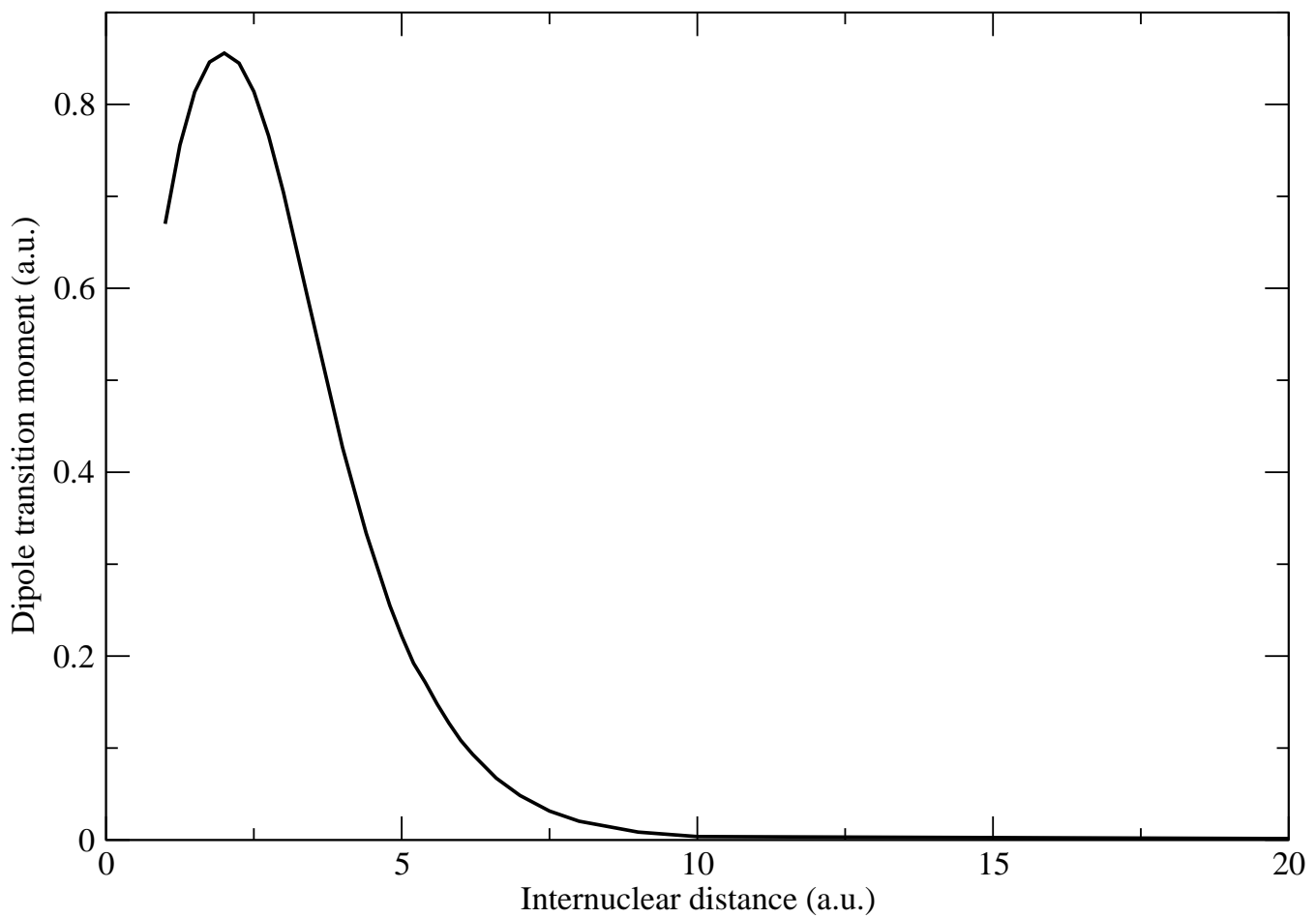


Figure 4.3: A  ${}^1\Sigma^+ \leftarrow X {}^1\Sigma^+$  transition dipole moment of  $\text{HeH}^+$  obtained from Kraemer et al. [14]. For actual calculation, values for smaller internuclear distance are smoothly extrapolated towards the origin.

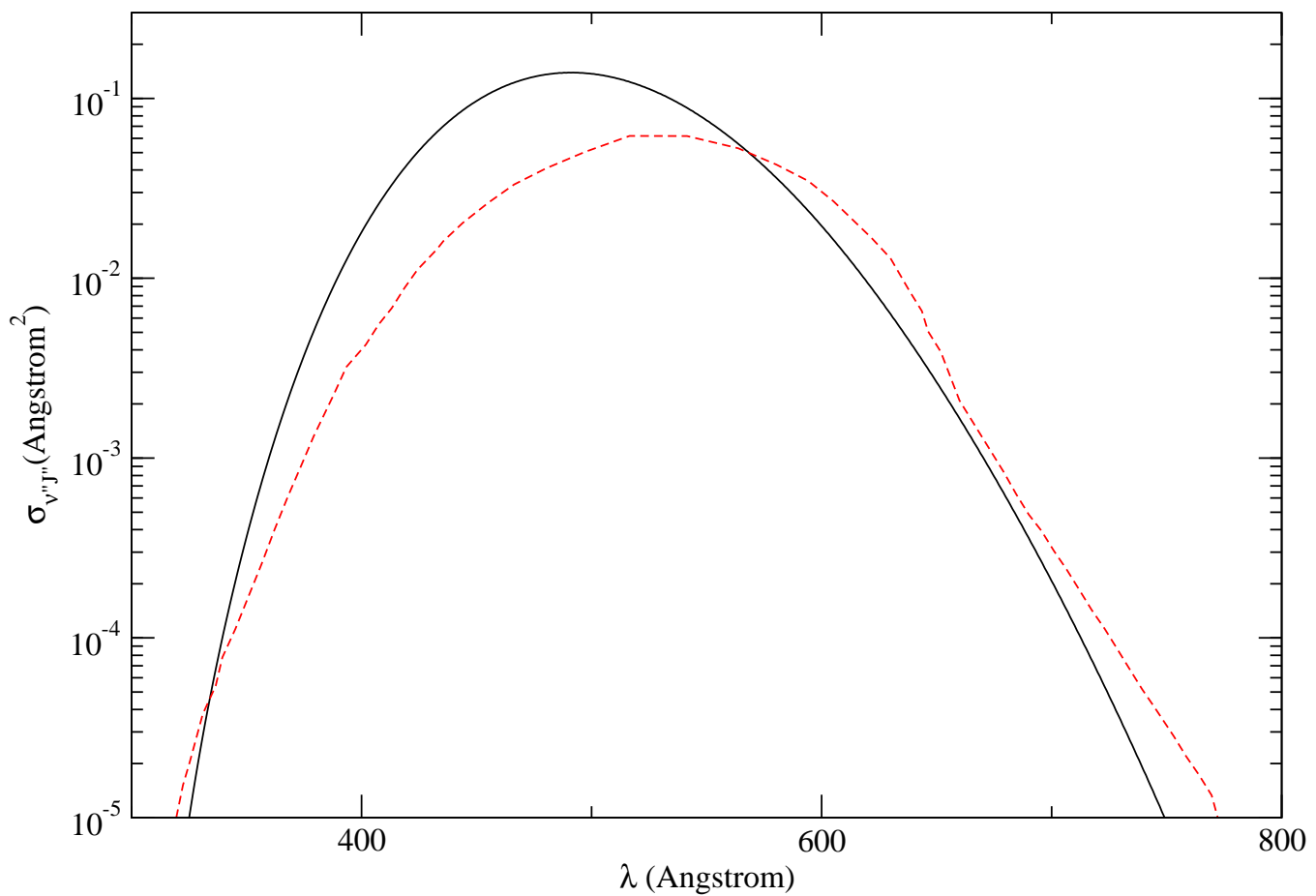


Figure 4.4: The partial photodissociation cross sections  $\sigma_{v''J''}$  as a function of wavelength  $\lambda$  for the  $\text{A } ^1\Sigma^+ \leftarrow \text{X } ^1\Sigma^+$  of  $\text{HeH}^+$  from the vibrational level  $v'' = 8$  (with  $J'' = 1$ ). Solid line: current calculation. Dotted line: Saha et al. [36].

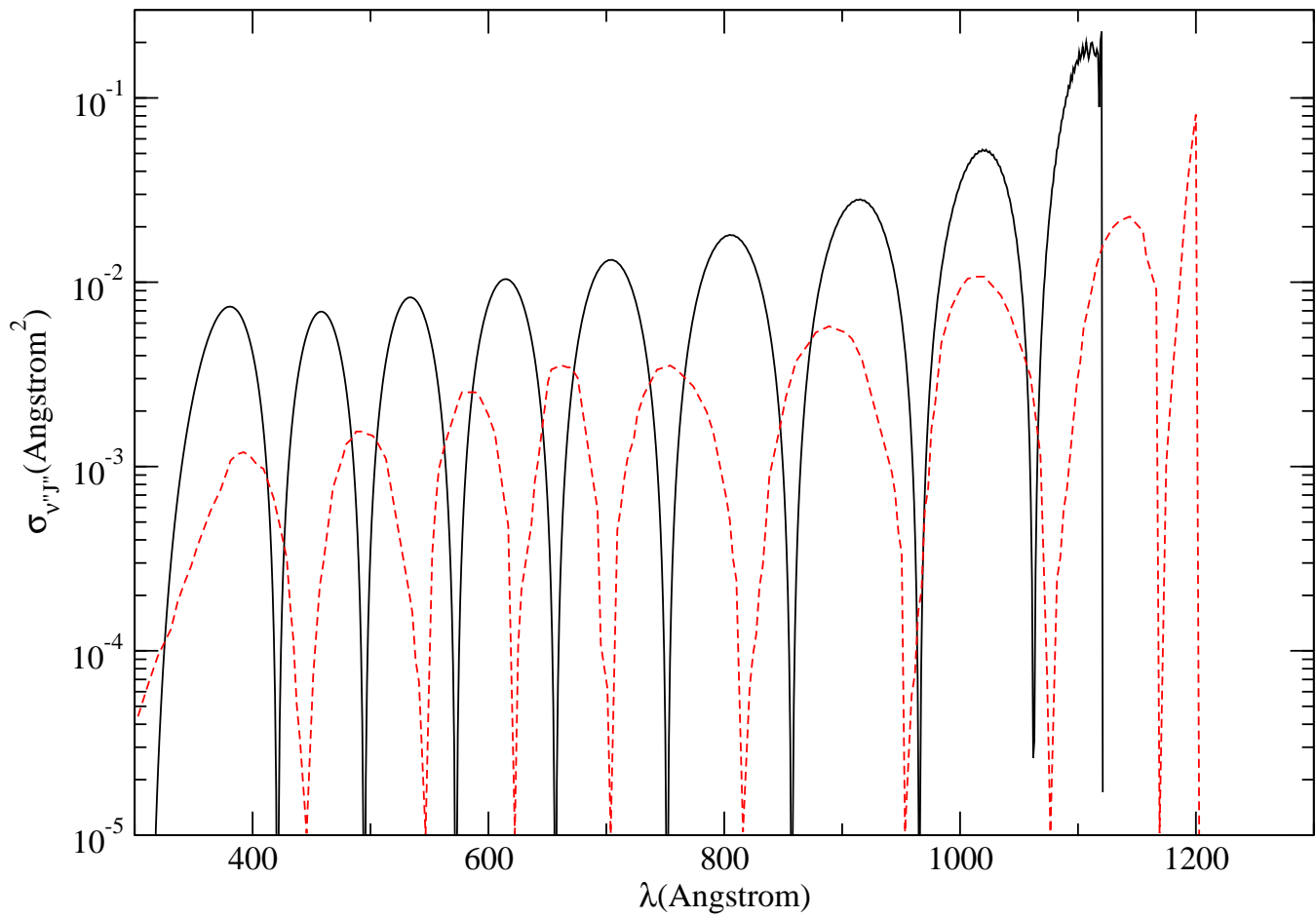


Figure 4.5: Same as Fig. 4.4, but for  $v'' = 0, J'' = 1$ .

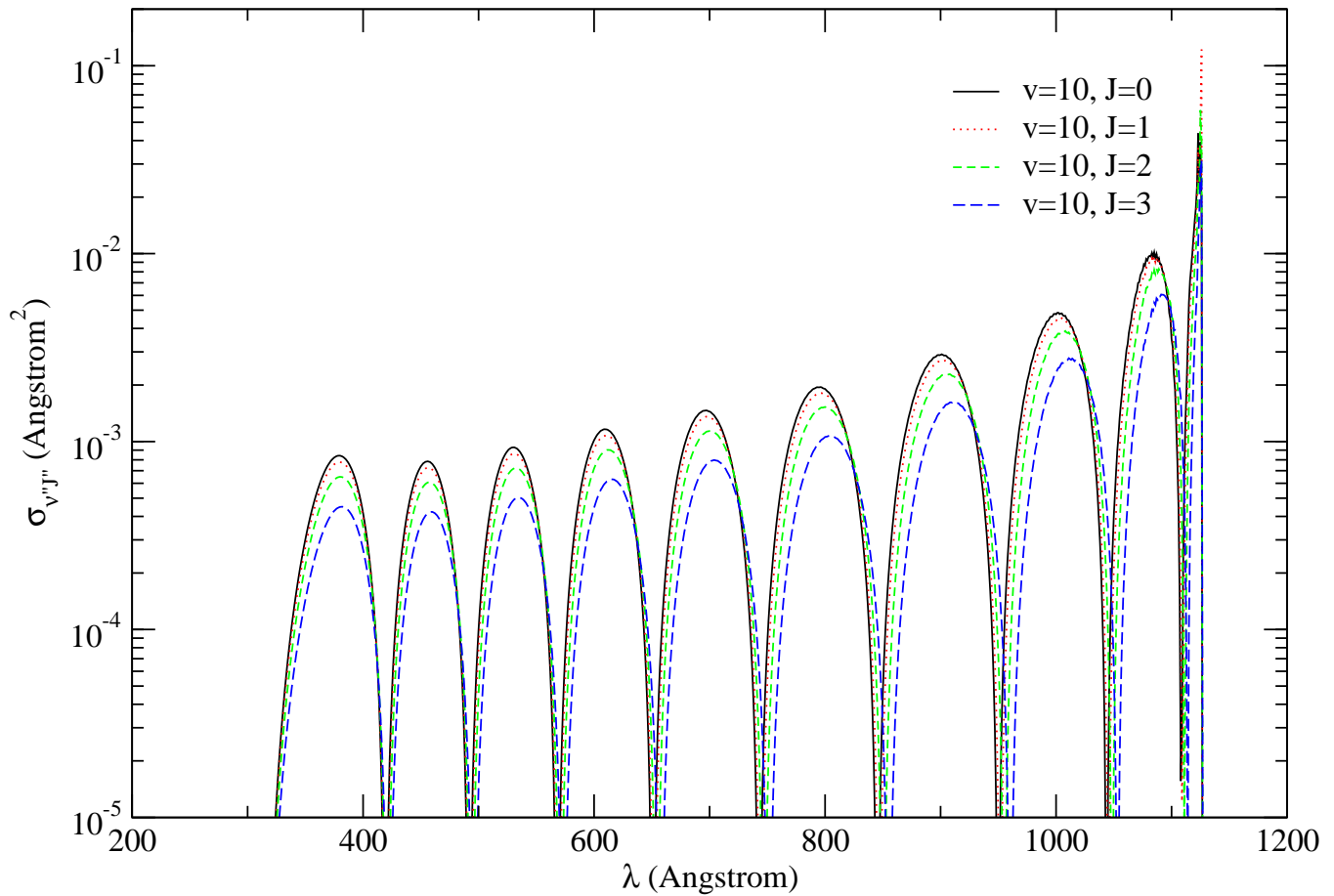


Figure 4.6: The partial photodissociation cross sections  $\sigma_{v''J''}$  for the  $A\ ^1\Sigma^+ \leftarrow X\ ^1\Sigma^+$  electronic transition of  $\text{HeH}^+$  for  $v'' = 10$  and all  $J''$ .

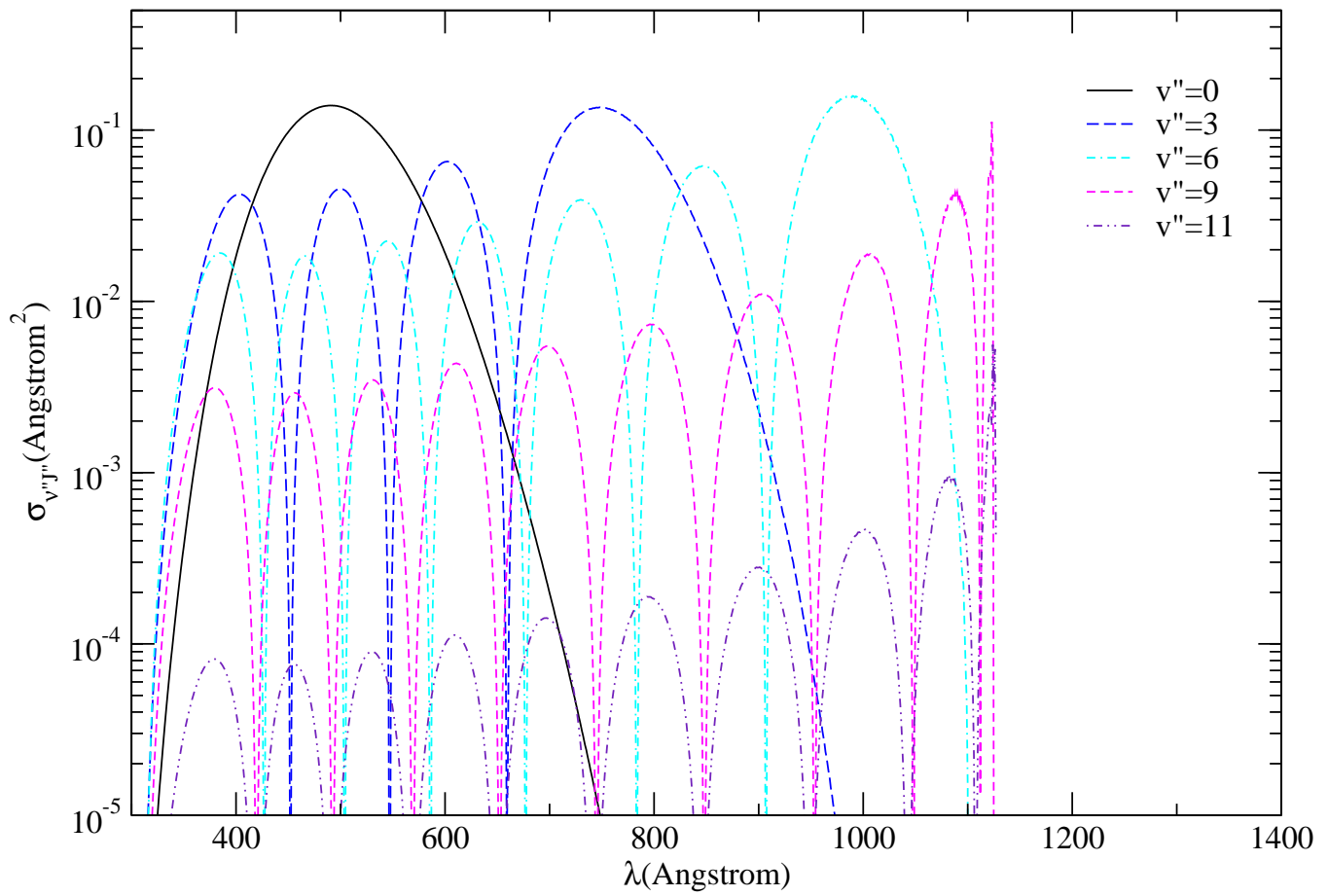


Figure 4.7: Same as Fig. 4.6, but for  $v'' = 0 - 11$ ,  $J'' = 0$ .

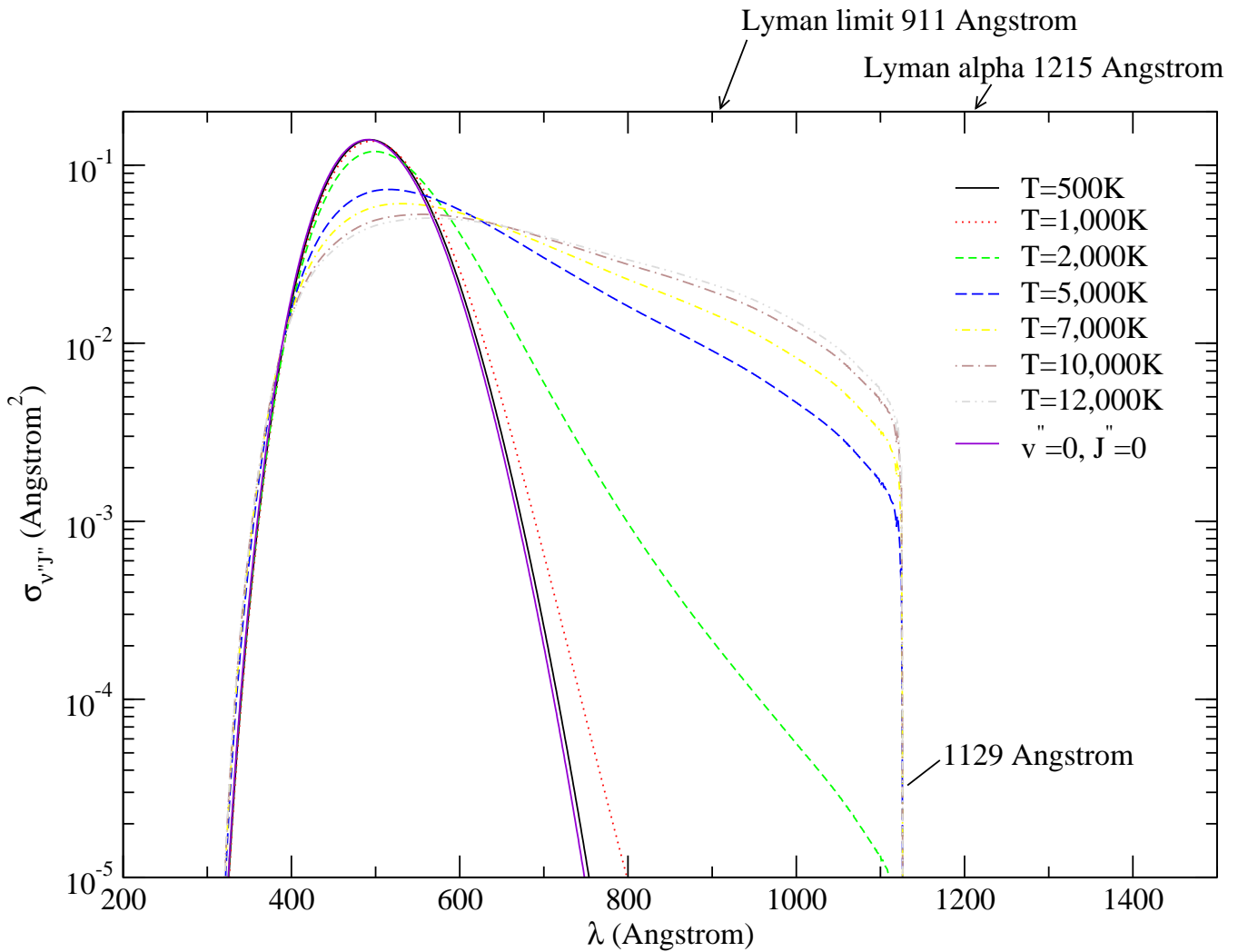


Figure 4.8: Total HeH<sup>+</sup> LTE photodissociation cross section for temperatures from 500 to 12,000 K, along with the partial cross section of  $v'' = 0, J'' = 0$  of the A  ${}^1\Sigma^+ \leftarrow$  X  ${}^1\Sigma^+$  transition.

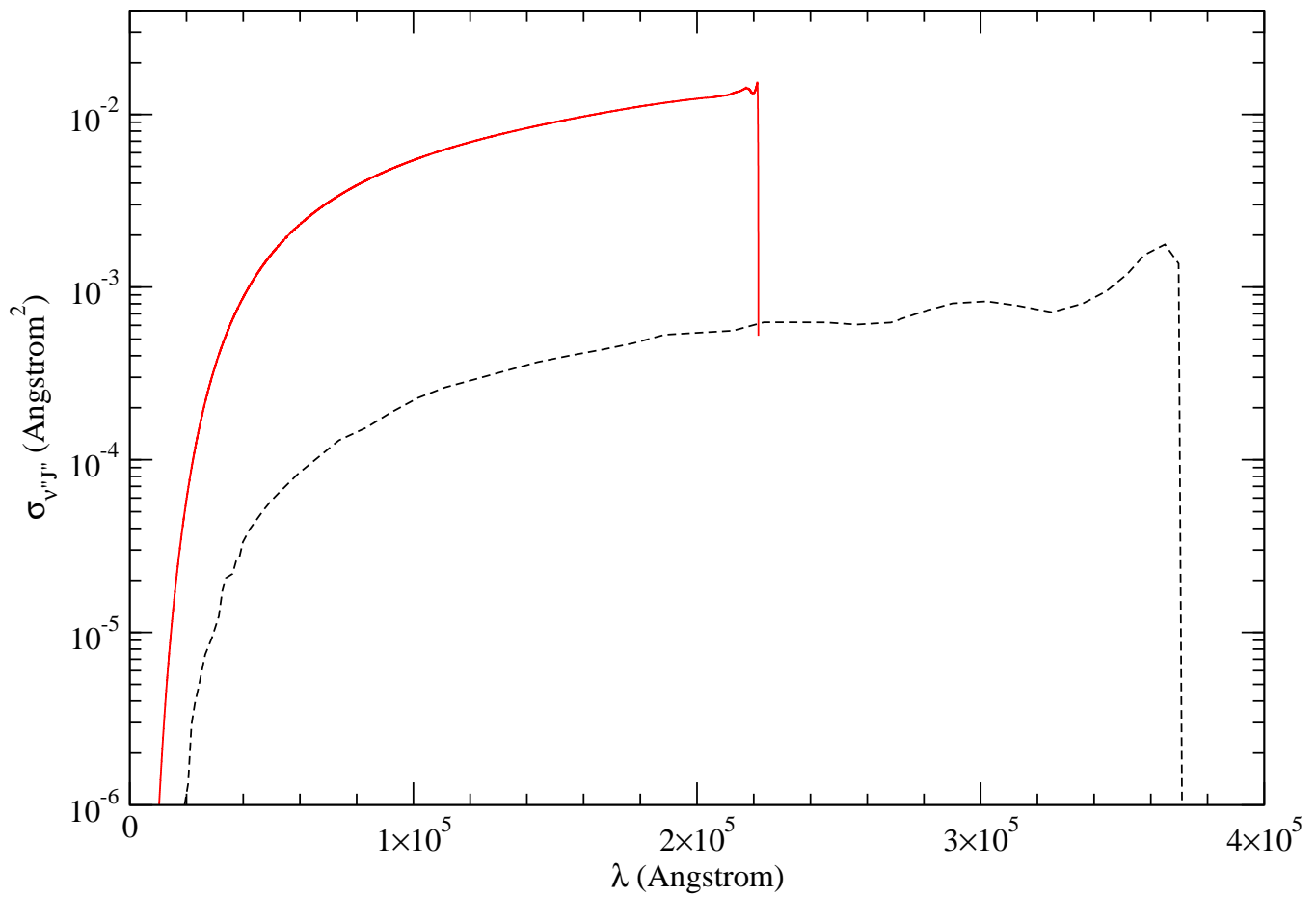


Figure 4.9: The partial photodissociation cross section of  $v'' = 8, J'' = 1$  for the  $X\ ^1\Sigma^+ \leftarrow X\ ^1\Sigma^+$  rovibrational transition. Solid line: current calculation. Dotted line: Saha et al. [36].

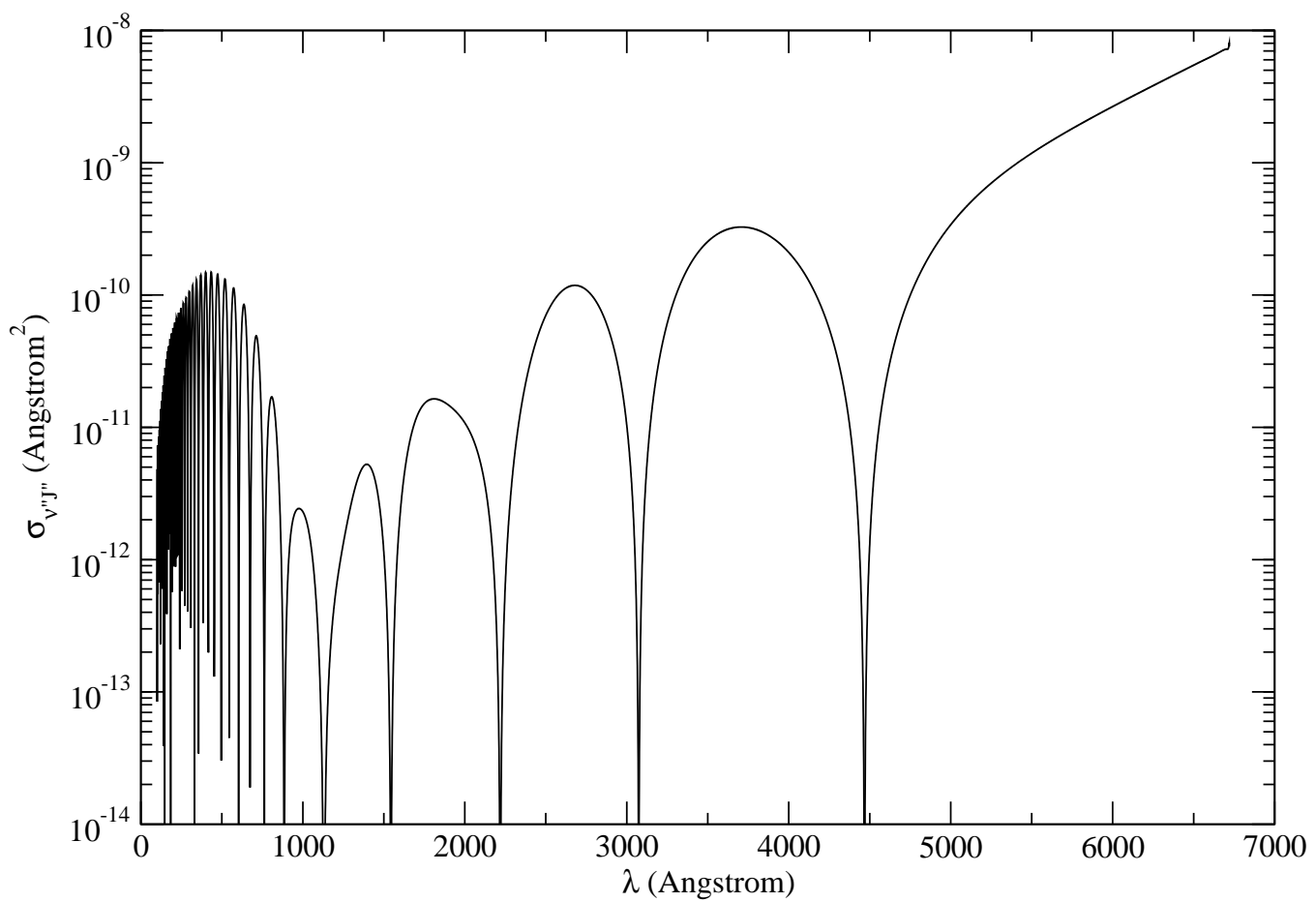


Figure 4.10: Same as Fig. 4.9 but for  $v'' = 0, J'' = 0$ .

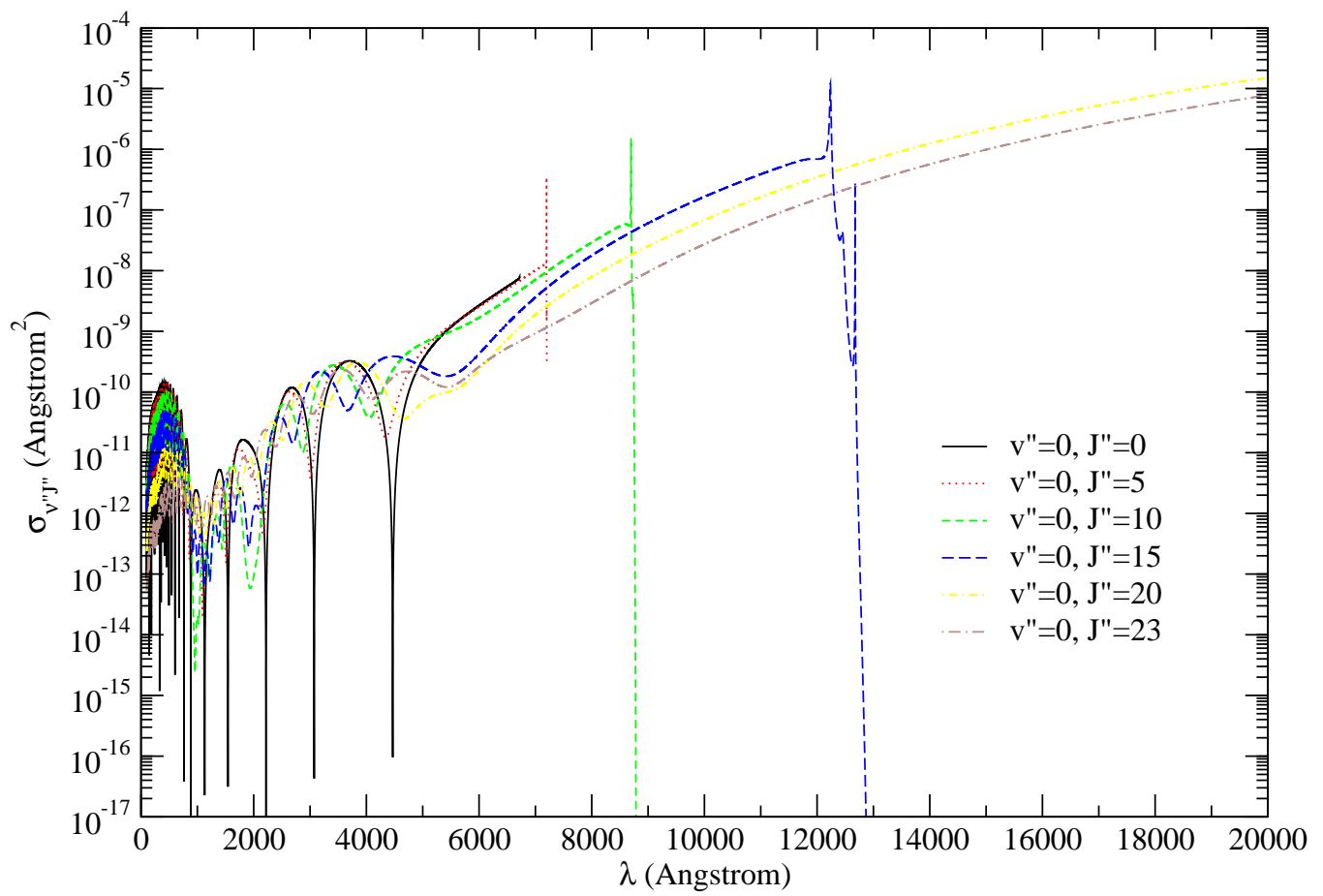


Figure 4.11: Same as Fig. 4.10 but for  $v'' = 0, J'' = 0 - 23$ .

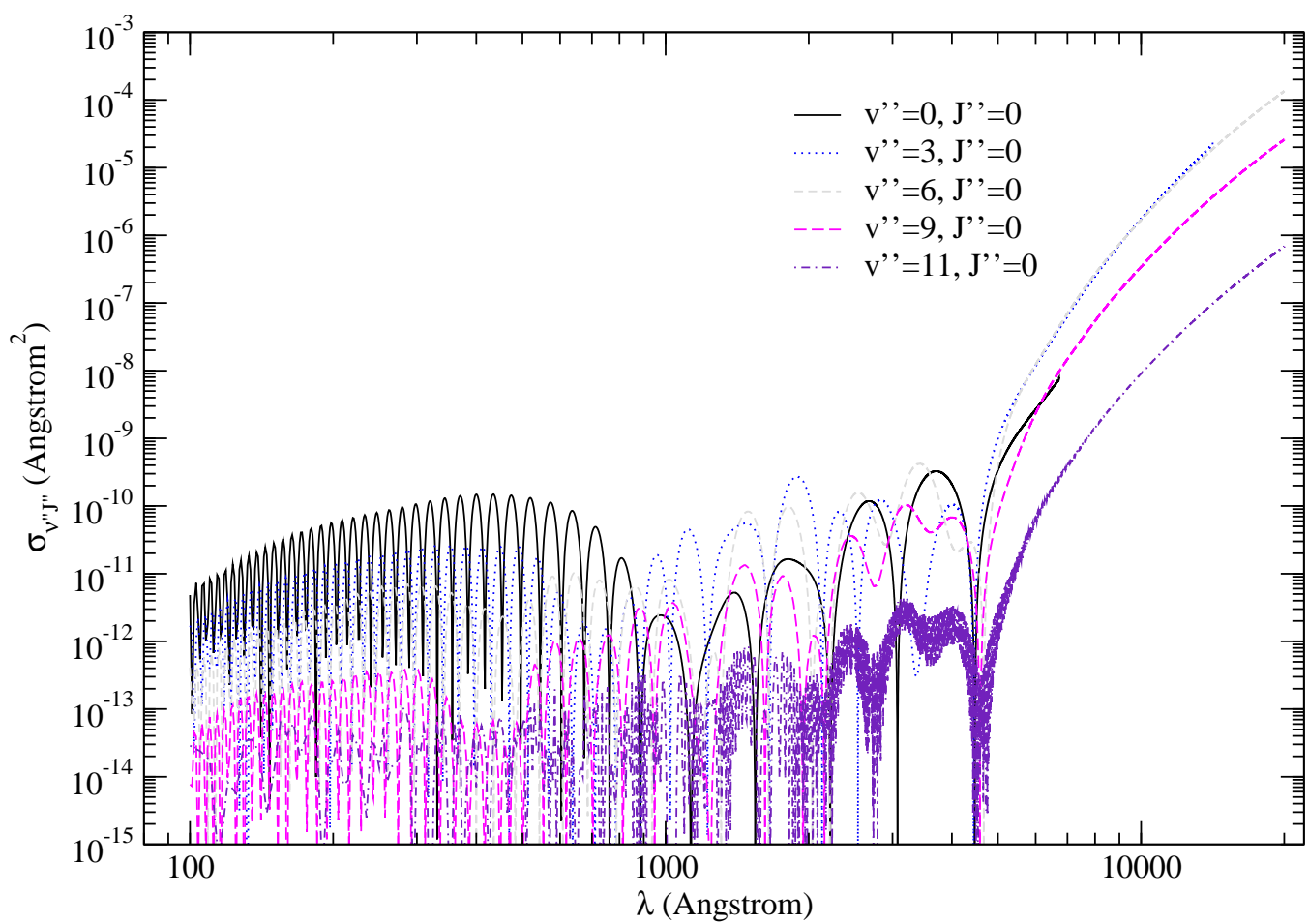


Figure 4.12: Same as Fig. 4.10 but for  $v'' = 0 - 11, J'' = 0$ .

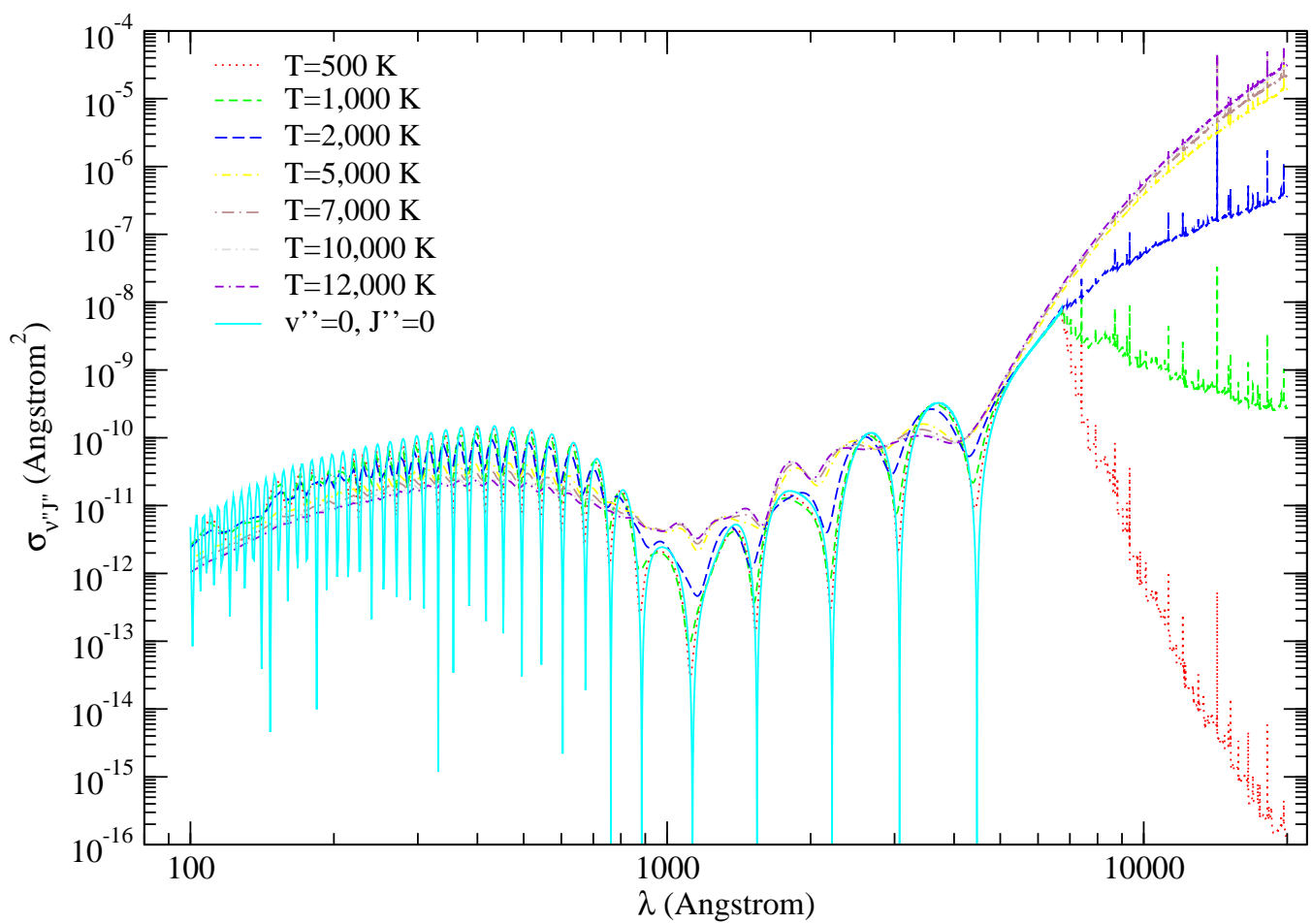


Figure 4.13: Total HeH<sup>+</sup> LTE photodissociation cross section for temperatures from 500 to 12,000 K, along with the partial cross section of  $v'' = 0, J'' = 0$  for the  $X \ ^1\Sigma^+ \leftarrow X \ ^1\Sigma^+$  transition.

Table 4.1: The partition function  $Q_{\text{HeH}^+}$  for temperatures from 500 to 12,000 K.

Temperature (K)	Partition function Q
500	10.63
1,000	21.47
2,000	49.65
5,000	233.69
7,000	393.31
10,000	654.08
12,000	812.84

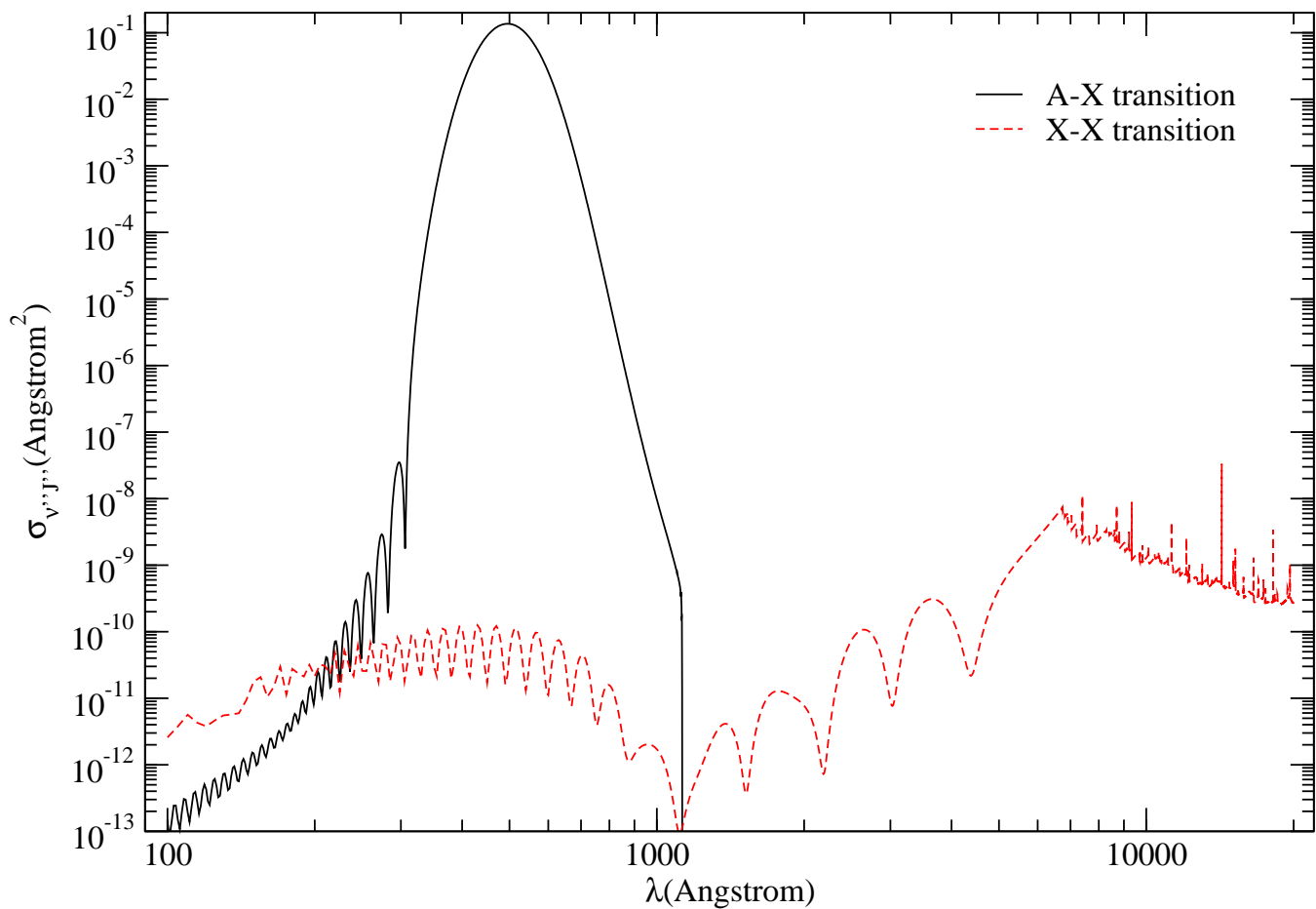


Figure 4.14: Total HeH<sup>+</sup> LTE photodissociation cross section at 1,000 K for both the X  $^1\Sigma^+$   $\leftarrow$  X  $^1\Sigma^+$  and A  $^1\Sigma^+$   $\leftarrow$  X  $^1\Sigma^+$  transitions.

## CHAPTER 5

### PHOTODISSOCIATION OF C<sub>2</sub>

#### 5.1 INTRODUCTION

Accurate photodissociation cross sections have been obtained for transitions from the ground X  $^1\Sigma_g^+$  of C<sub>2</sub> to the electronic excited states A  $^1\Pi_u$ , F  $^1\Pi_u$ , and 3  $^1\Pi_u$ .

Molecular clouds can be divided into three categories, diffuse cloud, translucent cloud and dark cloud depending on their opacity to ultraviolet radiation. Molecules are primarily destroyed in diffuse and translucent regions via photodissociation due to absorption of incident UV and optical radiation from luminous sources. The interstellar C<sub>2</sub> molecule has been detected at optical wavelengths in many locations [39] and other references cited therein. C<sub>2</sub> has also been detected in the visible spectrum of comets [43, 44, 45, 46] and in stellar atmospheres [47] including the Sun [48, 49, 50]. The earlier study of van Dishoeck & Black [51] found that the observed abundance of C<sub>2</sub> could not be reproduced by their models without significantly adjusting the photodissociation rates. Further, they performed a parameter study of photorates in translucent clouds by adopting various interstellar dust grain models and found that the photodissociation rates for C<sub>2</sub> varied by as much as 2 orders of magnitude. Therefore it is important to calculate accurate photodissociation cross sections for the C<sub>2</sub> molecule.

Martin [52] reviewed the spectroscopic and kinetic properties of C<sub>2</sub> for a large range of electronic states. The ground electronic state of C<sub>2</sub> is the X  $^1\Sigma_g^+$ , and the Phillips band (A  $^1\Pi_u \leftarrow$  X  $^1\Sigma_g^+$ ), which is a dipole allowed transition, had been observed in the laboratory by Ballik & Ramsay [53].

Experimental measurements of F  $^1\Pi_u$  have been made by Herzberg & Malmberg [54]. The transition  $C_2(F\ ^1\Pi_u \leftarrow X\ ^1\Sigma_g^+)$  is observed by vacuum UV absorption in the experimental system.

## 5.2 THEORY AND CALCULATION

### 5.2.1 POTENTIAL CURVES AND THE DIPOLE TRANSITION MOMENTS

*Ab initio* potential energy curves and dipole transition moments are adopted from Langhoff et al. [42] for the A  $^1\Pi_u$  and X  $^1\Sigma_g^+$  states and from Pouilly et al. [40] for the F  $^1\Pi_u$  and  $^3\Pi_u$  states and are shown in Figure 5.1–5.4. Those values were used to calculate the partial cross sections for  $C_2$  presented in this work. They reported potential energies for internuclear distance  $R = 1.8a_0$  to  $R = 7.0a_0$  for X  $^1\Sigma_g^+$  state,  $R = 1.8a_0$  to  $R = 5.0a_0$  for A  $^1\Sigma_g^+$  state,  $R = 1.8a_0$  to  $R = 5.0a_0$  for F  $^1\Pi_u$  state and  $R = 1.8a_0$  to  $R = 5.0a_0$  for  $^3\Pi_u$  state. For  $R > 7.0a_0$  for X  $^1\Sigma_g^+$  state,  $R > 5.0a_0$  for A  $^1\Sigma_g^+$  state,  $R > 5.0a_0$  for F  $^1\Pi_u$  state and  $R > 5.0a_0$  for  $^3\Pi_u$  state, the potential curves were extended using the long-range interaction potential

$$V(R) = -\frac{C_5}{R^5} - \frac{C_6}{R^6} \quad (5.1)$$

The values of the coefficients  $C_5$ , and  $C_6$  used are shown in Table 5.1. For  $R < 1.8a_0$ , the potential curves have been fit to the short-range interaction potential form  $A \exp(-BR) + C$ .

Similarly, the dipole transition moments were fit in the long-range and the short-range with an exponential function. The united-atom and the separated-atom limits were determined according to Wigner-Witmer rules [41] and are listed in Table 5.1.

## 5.3 RESULTS AND DISCUSSION

### 5.3.1 PARTIAL CROSS SECTIONS

The partial cross sections  $\sigma_{v''J''}$  for the A  $^1\Pi_u \leftarrow X\ ^1\Sigma_g^+$  transition are presented in Fig. 5.5. The cross section for this transition had not been computed previously. The results are small

because most of the oscillator strength for the transition resides in bound-bound transition. The partial cross sections  $\sigma_{v''J''}$  for  $F\ ^1\Pi_u \leftarrow X\ ^1\Sigma_g^+$  and  $3\ ^1\Pi_u \leftarrow X\ ^1\Sigma_g^+$  transition are presented in Fig. 5.6. The comparison is made with Pouilly et al. [40]. The feature around 10.5 eV corresponds to the  $F\ ^1\Pi_u \leftarrow X\ ^1\Sigma_g^+$  transition, while the feature around 12.5 eV corresponds to the  $3\ ^1\Pi_u \leftarrow X\ ^1\Sigma_g^+$  transition. We have reproduced the features obtained by Pouilly et al. [40]. We also have obtained some new resonance features and we believe that it is due to minor dips in the potentials.

#### 5.4 SUMMARY

The photodissociation cross sections of  $C_2$  has been calculated from its ground electronic state  $X\ ^1\Sigma^+$  to the electronic excited states  $A\ ^1\Pi_u$ ,  $F\ ^1\Pi_u$ , and  $3\ ^1\Pi_u$ . We have revisited the calculation of the photodissociation cross section of  $C_2$  molecule. More accurate values has been obtained from the current available calculation [40] and important resonance features has been obtained.

For the  $F\ ^1\Pi_u \leftarrow X\ ^1\Sigma_g^+$  and  $3\ ^1\Pi_u \leftarrow X\ ^1\Sigma_g^+$  transitions, we have successfully reproduced the features found by Pouilly et al. [40] and new resonance features has been newly obtained.

The contribution of the cross section of the  $A\ ^1\Pi_u \leftarrow X\ ^1\Sigma_g^+$  transition is minor in the interstellar medium since the magnitude of its cross section is many orders of magnitude smaller than those of the  $F\ ^1\Pi_u \leftarrow X\ ^1\Sigma_g^+$  and  $3\ ^1\Pi_u \leftarrow X\ ^1\Sigma_g^+$  transition. Therefore, we believe that it is probably not an important destruction channel.

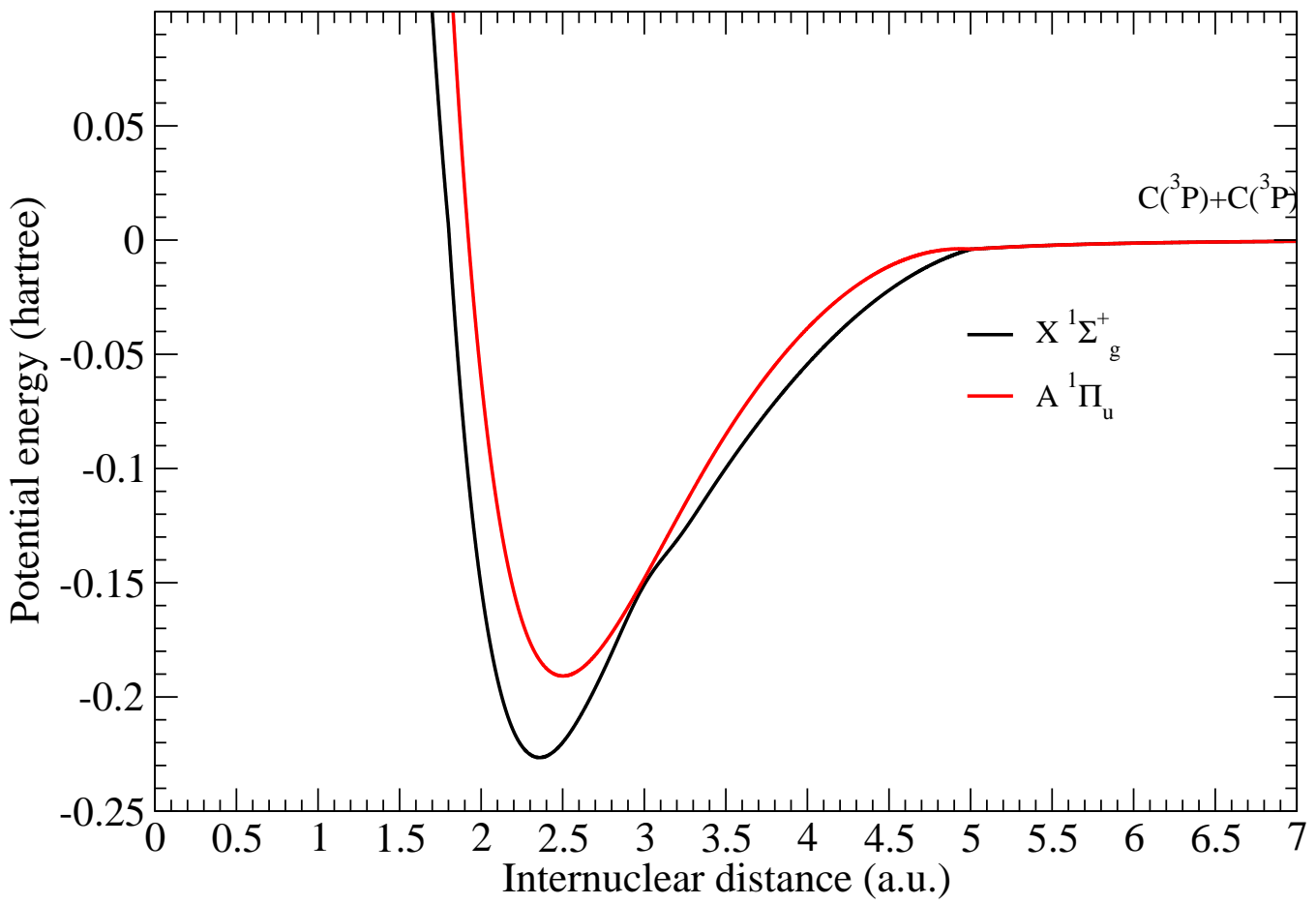


Figure 5.1: Ab initio potential energy curves from Langhoff et al. [42] for the  $A\ ^1\Pi_u$  and  $X\ ^1\Sigma_g^+$  states.

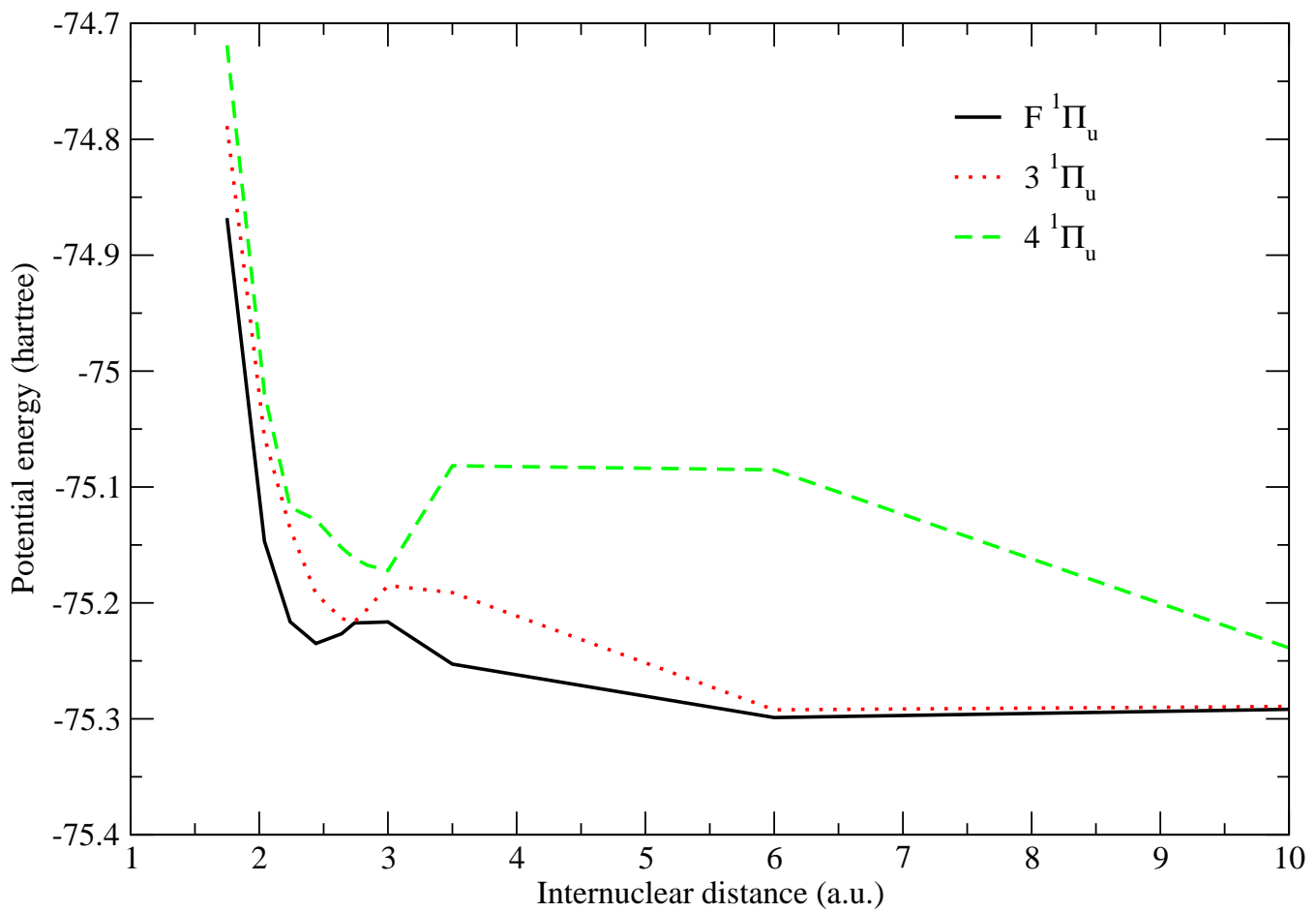


Figure 5.2: Ab initio potential energy curves from Pouilly et al. [40] for the  $F\ ^1\Pi_u$ ,  $3\ ^1\Pi_u$  and  $4\ ^1\Pi_u$  states.

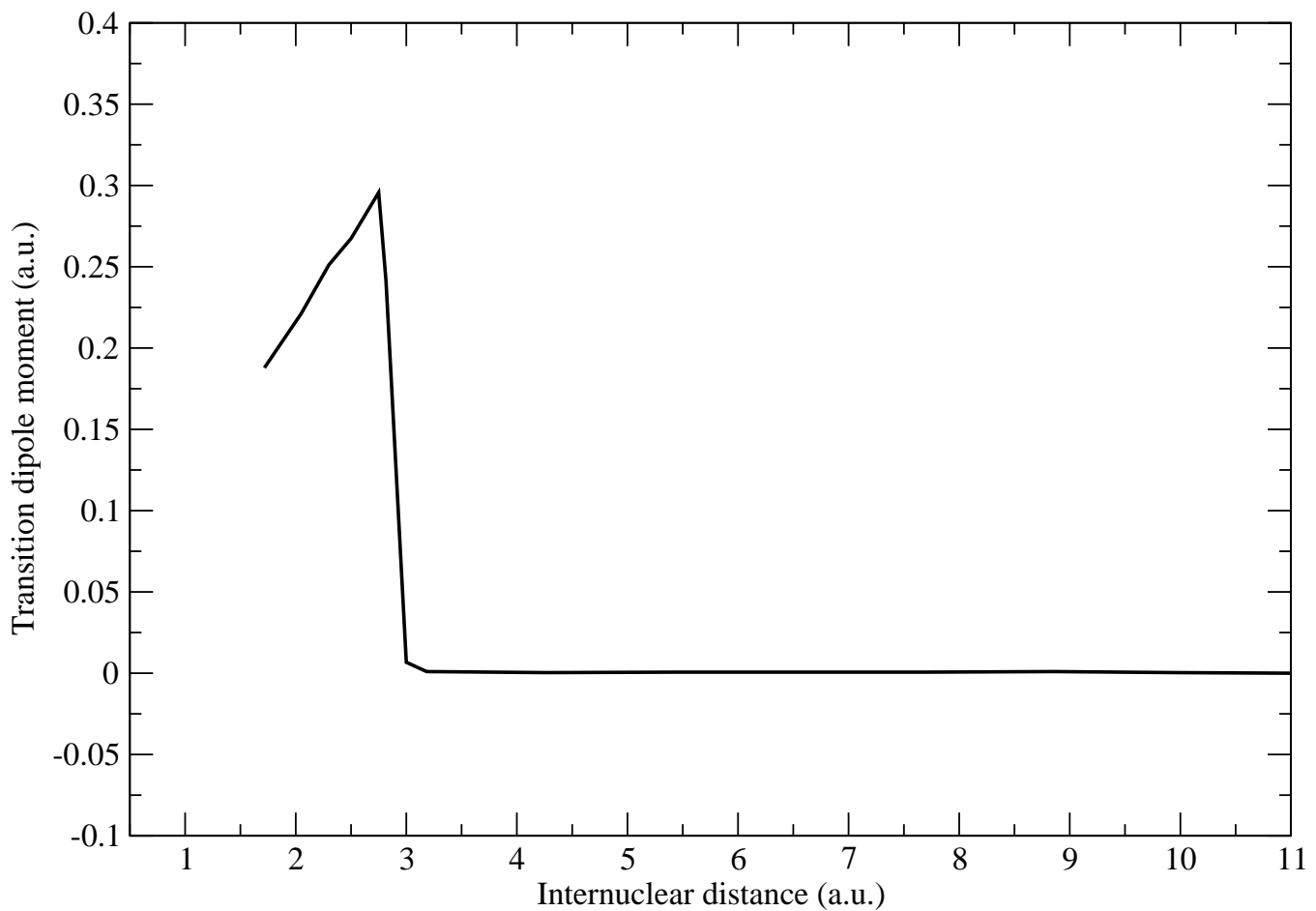


Figure 5.3: The dipole transition moments from Pouilly et al. [40] for the  $\text{F } ^1\Pi_u \leftarrow \text{X } ^1\Sigma_g^+$  transition.

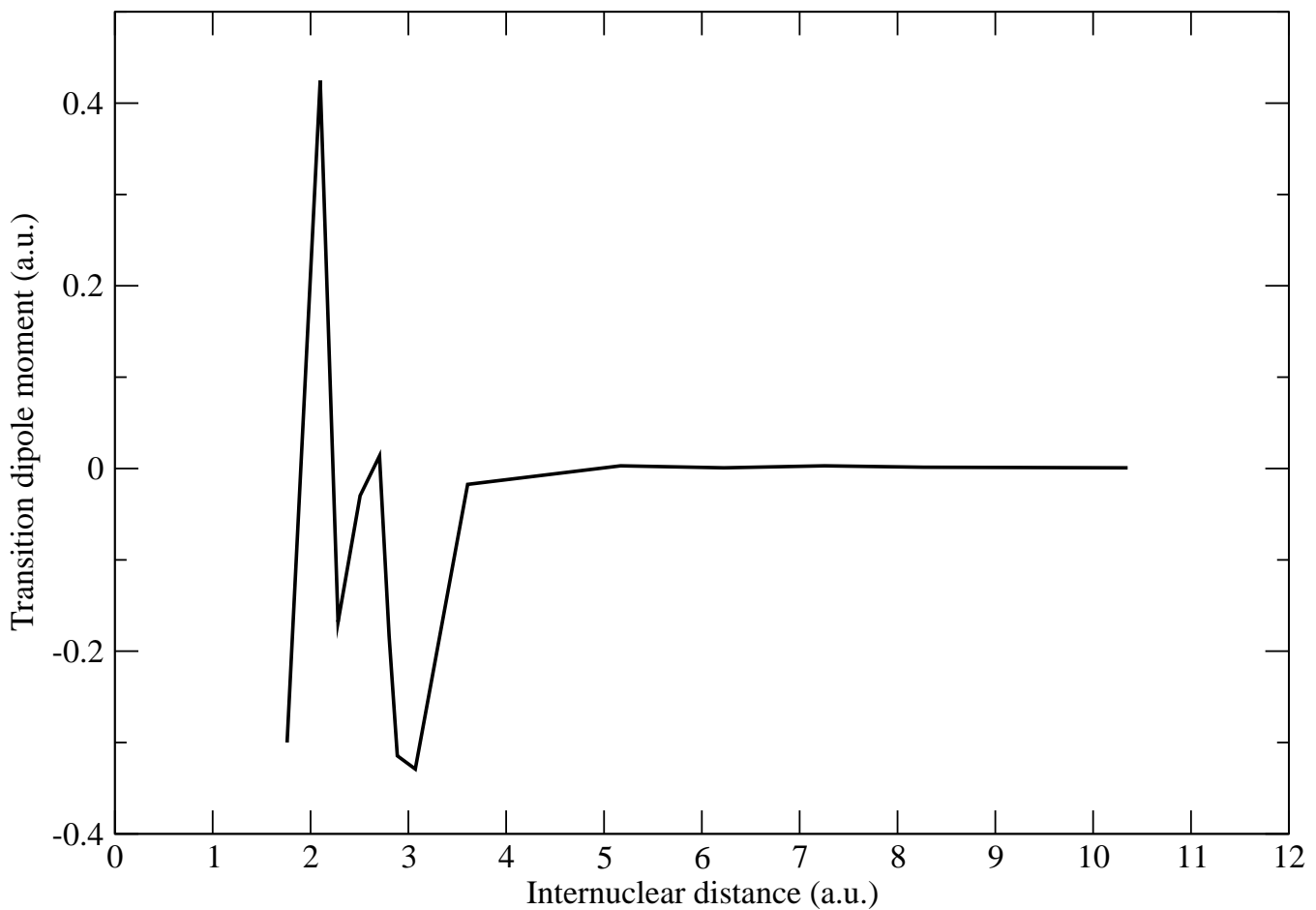


Figure 5.4: The dipole transition moments from Pouilly et al. [40] for the  $3\ ^1\Pi_u \leftarrow X\ ^1\Sigma_g^+$  transition.

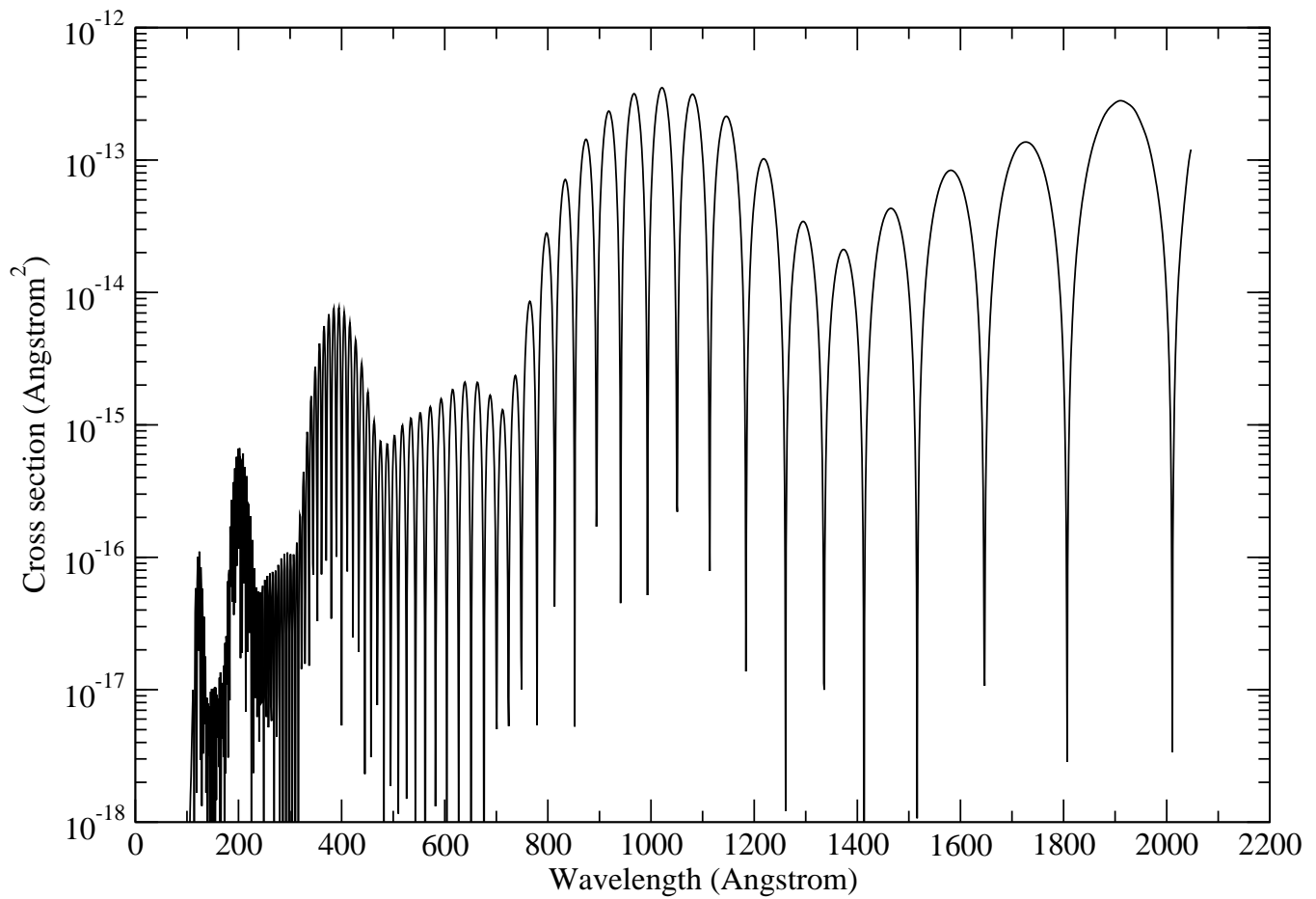


Figure 5.5: The cross section of  $v'' = 0, J'' = 0$  for  $A\ 1\Pi_u \leftarrow X\ 1\Sigma_g^+$  transition of  $C_2$ .

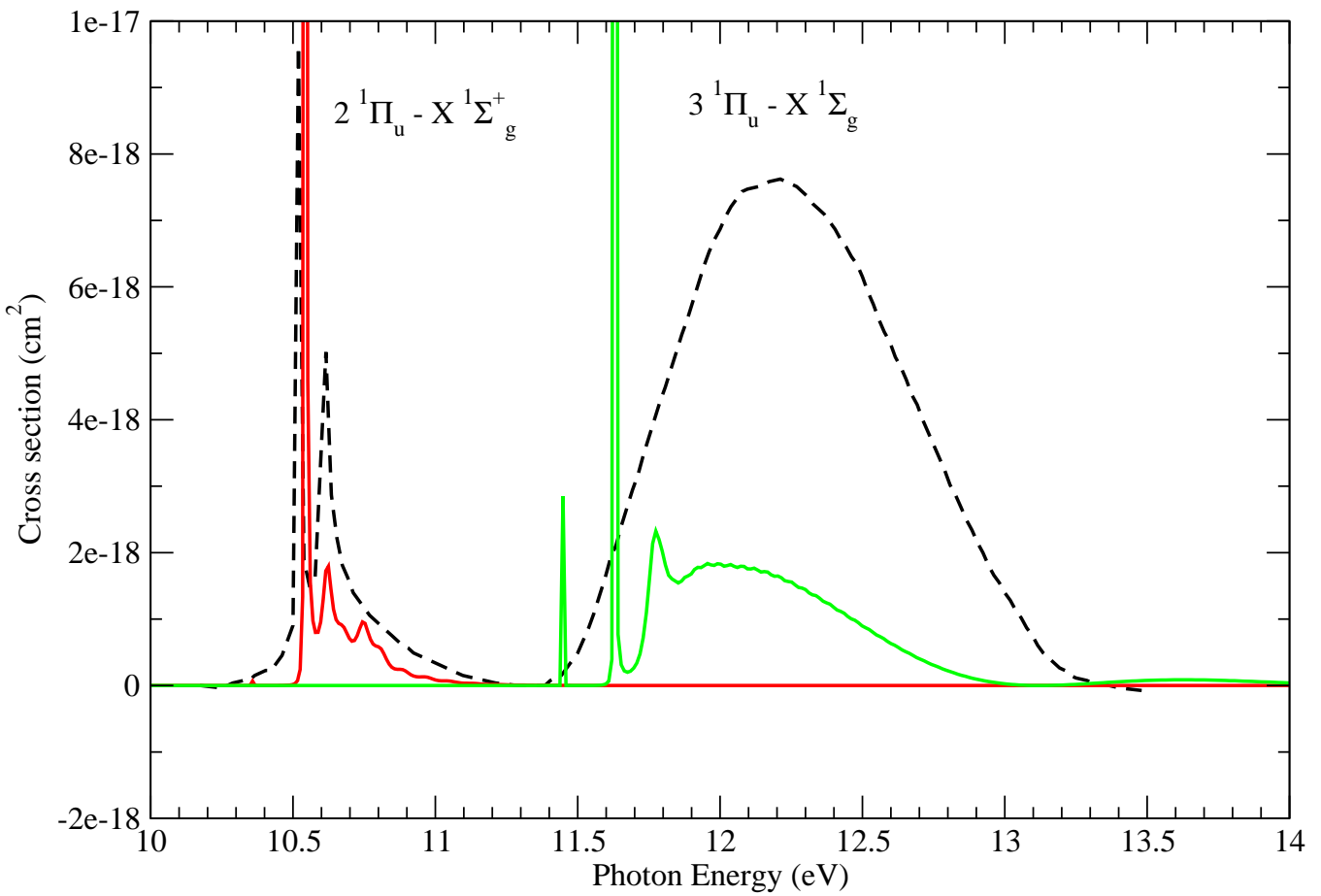


Figure 5.6: The photodissociation cross sections as a function of photon energy for the  $\text{C}_2\ \text{F}\ 1\Pi_u \leftarrow \text{X}\ 1\Sigma_g^+$  and  $3\ 1\Pi_u \leftarrow \text{X}\ 1\Sigma_g^+$  transitions for  $v'' = 0$ ,  $J'' = 0$ . Solid line: current calculation. Dotted line Pouilly et al. [40].

Table 5.1: Asymptotic separated-atom and united-atom limits for  $C_2$ 

Molecular state	Atomic states	Separated-atom			United-atom	
		Theory	Expt.	$C_5$ (a.u.) <sup>1</sup>	$C_6$ (a.u.)	Mg
$X^1\Sigma_g^+$	$C(^3P)+C(^3P)$	0.00	0.00	0.0	62.98 <sup>2</sup>	$3s^2\ ^1S$
$B'\ ^1\Sigma_g^+$	$C(^3P)+C(^3P)$			-20		$3s4s\ ^1S$
$A^1\Pi_u$	$C(^3P)+C(^3P)$			0.0	61.54 <sup>2</sup>	$3p3s\ ^1P^0$
$C^1\Pi_g$	$C(^3P)+C(^3P)$			14		$3s3d\ ^1D$
$1^1\Delta_g$	$C(^3P)+C(^3P)$			-3		$3s3d\ ^1D$
$1^1\Sigma_u^-$	$C(^3P)+C(^3P)$			0.0		
$3^1\Sigma_g^+$	$C(^1D)+C(^1D)$			7		$3s3d\ ^1D$
$F^1\Pi_u$	$C(^1D)+C(^1D)$	3.08	2.53	14	61.54 <sup>1</sup>	$3p4p\ ^1P^0$
$4^1\Sigma_g^+$	$C(^1D)+C(^1D)$			-23		$3s5s\ ^1S$
$5^1\Sigma_g^+$	$C(^1D)+C(^1D)$			-50		$3s4d\ ^1D$
$3^1\Pi_u$	$C(^1D)+C(^1D)$	3.08	2.53	-18	61.54 <sup>1</sup>	$3s4d\ ^1D$
$2^1\Delta_g$	$C(^1D)+C(^1D)$			28		$3s4d\ ^1D$

<sup>1</sup>Estimate<sup>2</sup>Le Bourlot & Roueff [55]

## CHAPTER 6

### RESONANT H<sup>-</sup> PHOTODETACHMENT: ENHANCED PHOTODESTRUCTION AND CONSEQUENCES FOR RADIATIVE FEEDBACK

#### 6.1 INTRODUCTION

The hydrogen negative ion plays a crucial role in the formation of hydrogen molecules in the early Universe. Cooling through excitation of H<sub>2</sub> drives the formation of the first cosmological objects. The H<sub>2</sub> molecules are produced primarily by a reaction sequence initiated by H<sup>-</sup>. We explore the influence of enhanced photodestruction rates that arise due to absorption by resonance states of H<sup>-</sup> lying near 11 eV. We examine the feedback effects that occur in radiation fields characteristic of Population III stars, blackbody sources, power-law spectra, and the hydrogen Lyman modulated sawtooth spectra of the high-redshift intergalactic medium. This chapter is based on Miyake et al. [56].

After the formation of the first luminous sources, an ultraviolet (UV) background radiation field was built up as the energetic photons traveled through the surrounding primordial gas. The photons ionized the neutral primordial hydrogen and helium atoms formed by recombination and the Universe entered the reionization era [57, 58]. These photons were produced by the first stars (Pop III stars), primordial galaxies, and early miniquasars that formed from halos of gas collapsing under the action of gravitational forces between baryons and dark matter. The gravitational energy resulting from the adiabatic collapse was dissipated by radiative cooling processes. The primary cooling agent for temperatures below 8000 K was molecular hydrogen [59, 60]. H<sub>2</sub>, therefore, played a critical role in the evolution of primordial halos and the subsequent formation of the first generation of luminous sources.

The UV photons from these sources ionized the intergalactic medium (IGM) and modified the chemistry that created and destroyed the hydrogen molecules. Feedback mechanisms, enhancing and suppressing the efficiency of subsequent star formation, may have occurred [61, 62, 63, 64, 5].

Molecular hydrogen was formed in the early Universe by the  $\text{H}^-$  reaction sequence



in which electrons behaved as catalysts. The process of associative detachment (Eq. 6.2) was introduced by Dalgarno [65], and McDowell [66] pointed to it as a source of  $\text{H}_2$  in the interstellar medium. The electrons produced by photoionization increase the production of  $\text{H}_2$  and constitute a positive feedback. A negative feedback arises from the photodissociation of  $\text{H}_2$  by UV radiation between the Lyman limit (13.6 eV) and the threshold for absorption in the Lyman and Werner systems of  $\text{H}_2$  (11.18 eV), followed by spontaneous radiative decay into the vibrational continuum. The negative feedback may therefore be amplified by the photodetachment of  $\text{H}^-$  [67, 68],



Chuzhoy et al. [67] estimated the magnitude of a radiative feedback effect due to the photodetachment of  $\text{H}^-$  by introducing a suppression factor

$$F_b = 1 + \frac{\beta_{6.3}}{k_{6.2} n_{\text{H}}}, \quad (6.4)$$

where  $\beta_{6.3}$  is the  $\text{H}^-$  photodetachment rate for a given radiation field,  $k_{6.2}$  is the rate coefficient for associative detachment (reaction 6.2), and  $n_{\text{H}}$  the number density of atomic hydrogen. This expression, however, ignores the effect of the removal of  $\text{H}^-$  by mutual neutralization [69]



The abundance of  $\text{H}^-$  is thereby reduced by  $F_b$ , hence suppressing the production of  $\text{H}_2$ .

In their analysis, Chuzhoy et al. [67] employed the commonly adopted  $\text{H}^-$  photodetachment cross section, from a fit to the results of Wishart [70], which includes only non-resonant contributions as shown in Fig. 6.1.  $\text{H}^-$  has two discrete levels: the ground state is  ${}^1S_e$ , while the other bound level has  ${}^3P_e$  symmetry whose decay to the ground state is spin-forbidden [71]. As such  $\text{H}^-$  has no discrete spectrum, but in the continuum region,  $\text{H}^-$  has a strong series of broad and narrow auto-detaching resonances, for photon energies greater than  $\sim 11$  eV [72, 73].

We have revisited the photodetachment of  $\text{H}^-$  and used accurate cross sections based on a hybrid approach of R-matrix calculations, incorporation of high-resolution cross section measurements, and previous theoretical results [74]. We then constructed a photodetachment cross section, displayed in Fig. 6.1, which is obtained after a number of oscillator strength sum rules are self-consistently satisfied [74]. The new cross section is in good agreement with the results of the eigenchannel R-matrix study of the auto-detaching resonances by [75], and use of the latter would not change the conclusions presented below.

Here, we point out that the  $\text{H}^-$  auto-detaching resonances provide an additional contribution to the radiative feedback considered by Chuzhoy et al. [67], which should be included in models of high redshift halo evolution. In the next section, we estimate the resonant contribution in three high redshift scenarios that are relevant to the reionization epoch following the formation of the first stars.

## 6.2 RESONANT PHOTODESTRUCTION

To estimate the effect of the auto-detaching resonant contribution to radiative feedback, we partition photodetachment into the continuum background (b) and resonant (r) contributions. If the rate due to the background is  $\beta_{6.3}^b$  and that due to the full cross section is  $\beta_{6.3}^{r+b}$ , their ratio  $R$  gives the enhancement factor due to the resonances only

$$R = \frac{\beta_{6.3}^{r+b}}{\beta_{6.3}^b}. \quad (6.6)$$

Similarly, a ratio of H<sub>2</sub> suppression factors can be written

$$F_r = \frac{F_{r+b}}{F_b} = \frac{1 + \frac{\beta_{6.3}^{r+b}}{n_H k_{6.2}}}{1 + \frac{\beta_{6.3}^b}{n_H k_{6.2}}}, \quad (6.7)$$

where  $F_r$  is the resonant contribution to H<sub>2</sub> suppression. Here we have followed the approach of Chuzhoy et al. [67] and neglected the mutual neutralization process (6.5). For any meaningful suppression of the rate of formation of H<sub>2</sub>, we would expect the ratio  $\beta_{6.3}/n_H k_{6.2} >> 1$ , so that,

$$F_r \approx \frac{\beta_{6.3}^{r+b}}{\beta_{6.3}^b} = R. \quad (6.8)$$

This is the case if fiducial values of the ionization fraction ( $x$ ) and the fraction of escaping ionizing photons ( $f_{\text{esc}}$ ) are adopted as in Eq. (10) of Chuzhoy et al. [67]. Therefore, the total H<sub>2</sub> suppression factor is given by  $F = F_b \times F_r$ , within the approximations discussed above.

### 6.2.1 POP III RADIATION AND RECOMBINATION

Radiation from Pop III stars will photoionize the primordial gas in halos in which the stars are formed, and in the gas beyond. The resulting protons recombine producing a spectrum whose photons have energies less than 10.25 eV (case B recombination for H), but greater than 0.755 eV. The negative feedback proposed by Chuzhoy et al. [67] is the photodetachment of H<sup>-</sup> by the recombination photons, yielding a suppression factor of  $F_b \sim 800$  (for  $x = 0.1$ ,  $f_{\text{esc}} = 0.1$ ). The Pop III stars also produce a blackbody continuum with a significant flux of photons less than the Lyman limit (13.6 eV). Depending on the mass of the Pop III star, inclusion of the blackbody spectrum as a source of H<sup>-</sup> photodetachment could increase the suppression by factors of 1.1 to  $\sim 10$  (see their Fig. 2), increasing as the stellar effective temperature  $T_{\text{eff}}$  decreases. The suppression factor arising from the blackbody continuum is enhanced compared to that due to the recombination photons because as  $T_{\text{eff}}$  is decreased, fewer photons contribute to H photoionization, but the Planck spectrum overlap with the H<sup>-</sup> photodetachment cross section peak, near 1.5 eV, is enhanced as illustrated in Fig. 6.1.

The enhancement factor  $R$  for resonant photodetachment is shown in Fig. 6.2 as a function of the Pop III stellar effective temperature where only photon energies less than the Lyman limit are included. The resonant contribution is seen to increase the H<sub>2</sub> suppression factor  $F_r$  for  $T_{\text{eff}} > 1000$  K reaching asymptotically  $R \sim F_r \sim 1.2$  as  $T_{\text{eff}}$  exceeds 100,000 K<sup>1</sup>. The behavior of  $R$  can be understood by comparing the blackbody spectrum to the photodetachment cross sections as shown in Fig. 6.1. As  $T_{\text{eff}}$  increases, a larger fraction of photons reside in the region of the resonances compared to the photodetachment cross section peak near 1.5 eV. For example, the blackbody radiation field enhances the suppression factor to  $F_b \sim 1600$  at 40,000 K [67] with the resonant contribution increasing this by another 20%.

Fig. 6.2 displays the H<sup>-</sup> photodetachment rates corresponding to the cross section of McLaughlin et al. [74], which includes the resonant enhancement, with and without the Lyman limit cut-off. Comparison is made to the rate computed with the Lyman limit cut-off using the fit to the non-resonant cross section of Wishart [70]. The difference in the rates are negligible for  $T_{\text{eff}} < 25,000$  K, but increase with increasing  $T_{\text{eff}}$ .

### 6.2.2 A SMOOTH POWER-LAW UV SPECTRUM

On cosmological scales, the accumulated UV spectrum due to a large number of sources, or to an early miniquasar, is typically represented by a simple power-law of the form

$$J(E_{\text{ph}}) = J_{21} \left( \frac{E_{\text{ph}}}{E_H} \right)^{-\alpha} \quad (6.9)$$

where  $J_{21}$  is the intensity in  $10^{-21}$  ergs cm<sup>-2</sup> Hz<sup>-1</sup> sr<sup>-1</sup>,  $E_{\text{ph}}$  the photon energy,  $E_H$  the ionization energy of H, and  $\alpha$  the power-law index. For  $\alpha = 1.7$ , typical of a miniquasar, Chuzhoy et al. [67] found that the H<sub>2</sub> suppression is enhanced by a factor of  $\sim 5$  over that due to recombination photons, assuming that the power-law field extends down to the H<sup>-</sup> photodetachment threshold of 0.755 eV.

---

<sup>1</sup>The shoulder between 5000 and 15,000 K is actually due to the 3% difference between the two cross sections at the peak near 1.5 eV. The fit given by Chuzhoy et al. [67] does not accurately reproduce the Wishart [70] cross section at these photon energies.

Enhancements to the photodetachment rate due to the auto-detaching resonances are shown in Fig. 6.3, where we have considered  $\alpha = 0.1$  to  $5$  and various photon energy windows. In addition to miniquasars with  $\alpha \sim 1.7$ , typical power-law indices for quasars, massive black holes, and the high redshift IGM are  $\sim 0.5\text{-}0.7$ ,  $\sim 1$ , and  $\sim 0.7\text{-}1$ , respectively. For the largest range in photon energies (0.75-1000 eV), the enhancement is seen to be small approaching only 4% for the flattest spectra. However, it might be unrealistic to assume that the radiation intensity extends down to the  $H^-$  threshold for very steep spectral indices or for sources that emit primarily in the UV. Some authors only considered photon energies greater than 13.6 eV for photoionization models due to quasar spectra [76, 77] or greater than the Lyman-Werner band threshold (11.18 eV) when modeling radiative feedback [63]. However, to include the  $H^-$  resonant and  $Ly\alpha$  energies, we computed photodestruction rates for  $E_{ph} > 10$  eV with and without the Lyman limit cut-off which resulted in significant resonant enhancement factors of  $R \sim 1.8$  and  $1.4\text{-}1.7$ , respectively. With a Lyman limit cut-off, the photodetachment rate integral is constrained to a narrow photon energy bin and is therefore relatively insensitive to the power-law index. Conversely, without a Lyman limit cut-off, the photodetachment rate integral can sample the higher-energy cross section away from the resonances which reduces the enhancement factor for smaller  $\alpha$ . However, as  $\alpha$  is increased  $R$  approaches the Lyman-limit value, as the steeper spectral profile favors photon energies near the resonances.

### 6.2.3 IGM BACKGROUND WITH H SAWTOOTH ABSORPTION MODULATION

While the use of power-law spectra is computationally convenient, a fraction of the UV photons will be removed from the IGM spectrum as radiation is transported through the partially neutral IGM. As in the interstellar medium of the Galaxy, photoionization of H will remove nearly all the photons with energies greater than the Lyman limit and red-shifted resonant Lyman lines will carve out flux from the IGM spectrum. We assume that all sources turn on simultaneously at some redshift  $z$ , the sources are distributed uniformly in space, and the emission spectrum is given by a power-law [62].

To construct a complete IGM spectrum to cover photon energies accessible for H<sup>-</sup> photodetachment, we combined the  $z \sim 20$  spectra presented in [5] from 11-13.6 eV and that given in Haiman et al. [62] from 6-11 eV with  $\alpha = 0.7$  power-law from 0.75-6 eV. For other power-laws, we appropriately scaled the full hybrid spectrum. The resulting  $\alpha = 0.7$  sawtooth spectrum is shown in Fig. 6.4, with  $\alpha = 0.7$  power-law spectrum shown for reference. The two H<sup>-</sup> photodetachment cross sections are also shown. Interestingly, the H<sup>-</sup> resonance lies in the window between the Ly $\alpha$  and Ly $\beta$  IGM spectral features. Because the power-law and IGM spectra are similar over most of the photon energy range, the resonant enhancement is expected to be comparable for the two cases. In fact,  $R$  for the IGM spectrum for 0.75-13.6 eV is nearly identical to the enhancement computed for the 0.75-1000 eV power-law spectrum shown in Fig. 6.3 giving only a modest 4% enhancement for the smallest power-law index. However, if we truncate the IGM photon energy range to 10-13.6 eV, the enhancement factor varies slowly between 1.3 and 1.4, somewhat less than the comparable smooth power-law cases, but still significant.

### 6.3 CONCLUSIONS

Cosmology is now a precision science and if the observations of the early Universe are to yield a comprehensive view of its evolution, an accurate detailed account of the atomic and molecular processes that occurred must be constructed. Following the formation of the first stars, Pop III stars, which are assumed to be massive, hot, and luminous, the subsequent role of their radiation on their host primordial halos and the surrounding IGM likely had a significant impact on subsequent primordial star formation. Whether this radiative feedback effect was positive or negative, i.e., enhancing or suppressing the efficiency of star formation, is not fully understood and therefore a topic of considerable current interest.

It has been suggested by Chuzhoy et al. [67] that H<sup>-</sup> photodetachment contributes a significant enhancement to a negative feedback effect. We point out here, that the H<sup>-</sup> auto-detaching resonances, which occur for photon energies near 11 eV, can provide an additional

negative feedback contribution. While the resonant contribution is not large for steep power-law spectra extending into the near infrared, it is significant for blackbody spectra with effective temperatures exceeding  $\sim 40,000$  K and for the UV background spectrum of the high redshift intergalactic medium. If the background radiation field, after the formation of the first luminous objects, was dominated by miniquasars, or similar sources, there may have been a significant negative radiative feedback effect on the creation of H<sub>2</sub>, its cooling efficiency, and on the ability of the residual primordial gas to coalesce into another generation of primordial stars<sup>2</sup>. Therefore H<sup>-</sup> photodetachment and its auto-detaching resonances should be accurately treated in radiation-hydrodynamics simulations of primordial halos, particularly in the early reionization epoch.

---

<sup>2</sup>Note that since the H<sup>-</sup> mechanism for forming H<sub>2</sub> is suppressed, other routes such as the charge exchange reaction  $H + H_2^+ \rightarrow H_2 + H^+$  would become important. However, the destruction of H<sub>2</sub><sup>+</sup> due to photodissociation via a far UV radiation field would also contribute to a negative feedback effect. We do not explore these effects here.

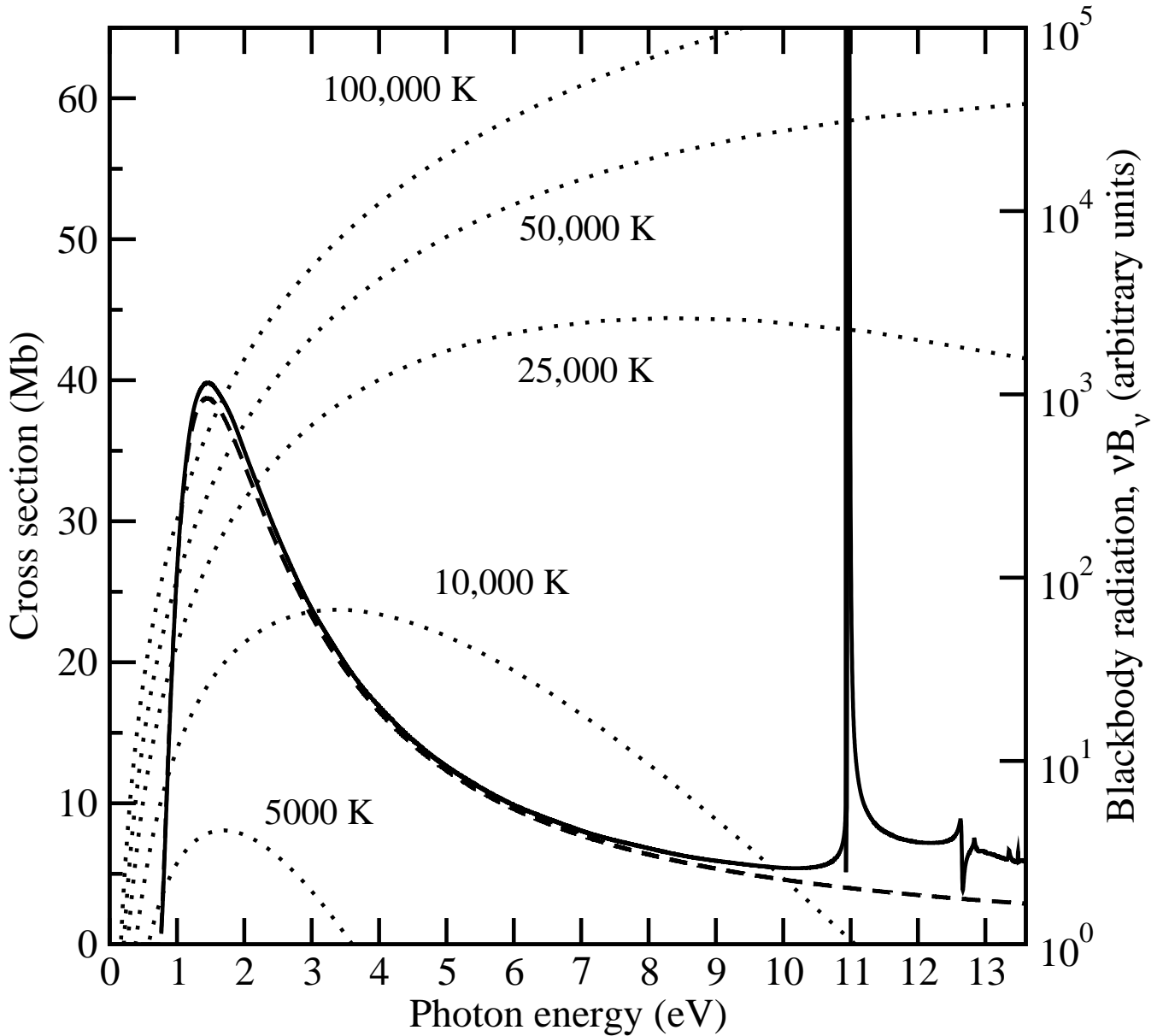


Figure 6.1: H<sup>-</sup> photodetachment cross sections. Background without resonances from Chuzhoy et al. [67] fit to Wishart [70] (dashed); with resonances from McLaughlin et al. [74] (solid). The shape resonance just above H( $n = 2$ ) is prominent at about 11 eV. There is also a narrow Feshbach resonance evident below H( $n = 2$ ) and other less-prominent Feshbach resonances below H( $n = 3$ ) near 12.8 eV. Also shown are blackbody spectra for temperatures from 5000 to 100,000 K (dotted).

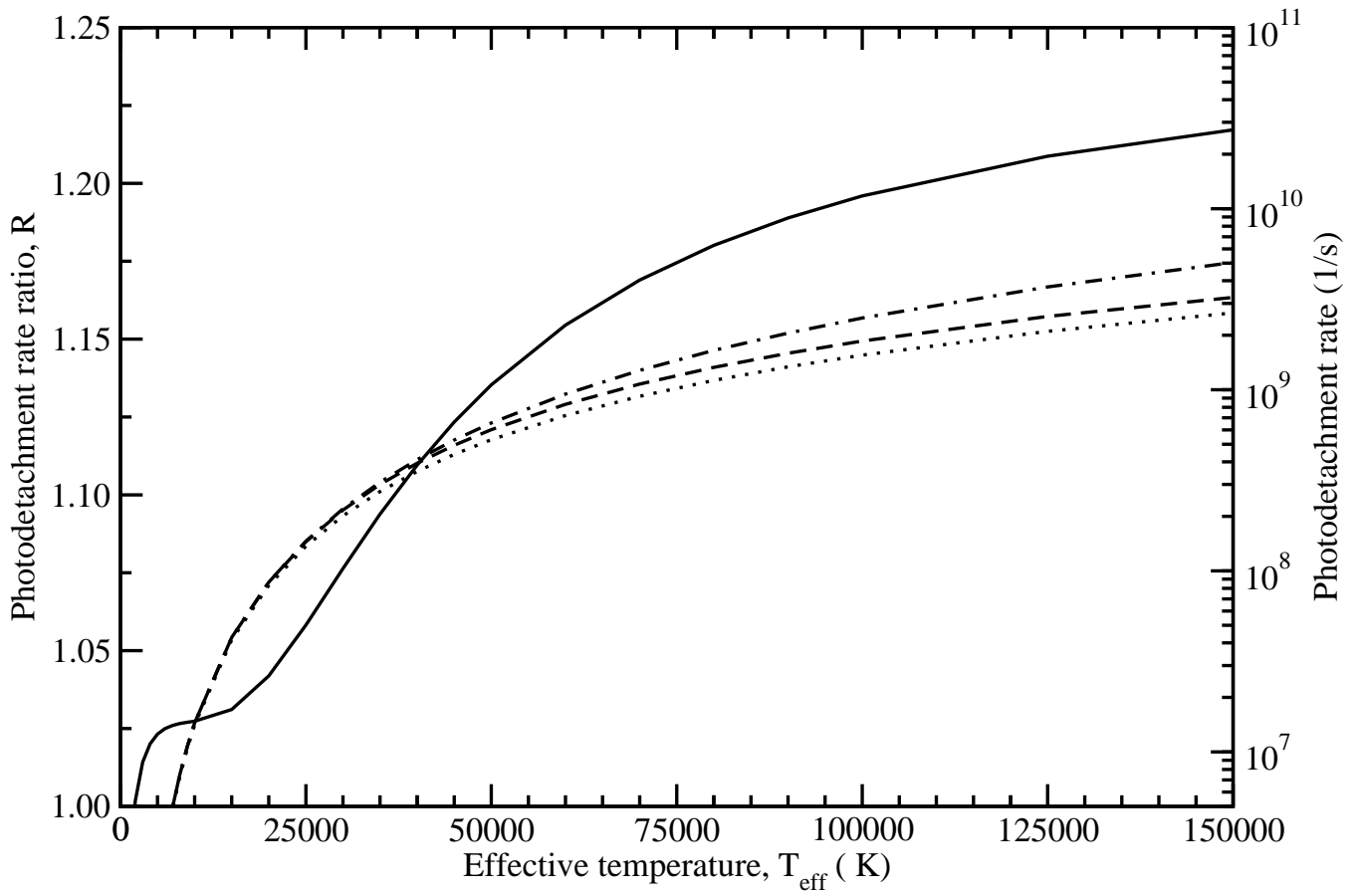


Figure 6.2:  $\text{H}^-$  photodetachment rate ratio,  $R$ , for a blackbody radiation field as a function of effective temperature  $T_{\text{eff}}$  (solid). As discussed in the text  $R \sim F_r$ , the enhancement factor due to the resonances. Also shown are the photodetachment rates: using the Wishart [70] cross section with a cut-off energy of 13.6 eV (dotted), using the cross section of McLaughlin et al. [74] with the cut-off (dashed), and using [74] without the cut-off, i.e. a full blackbody (dot-dash).

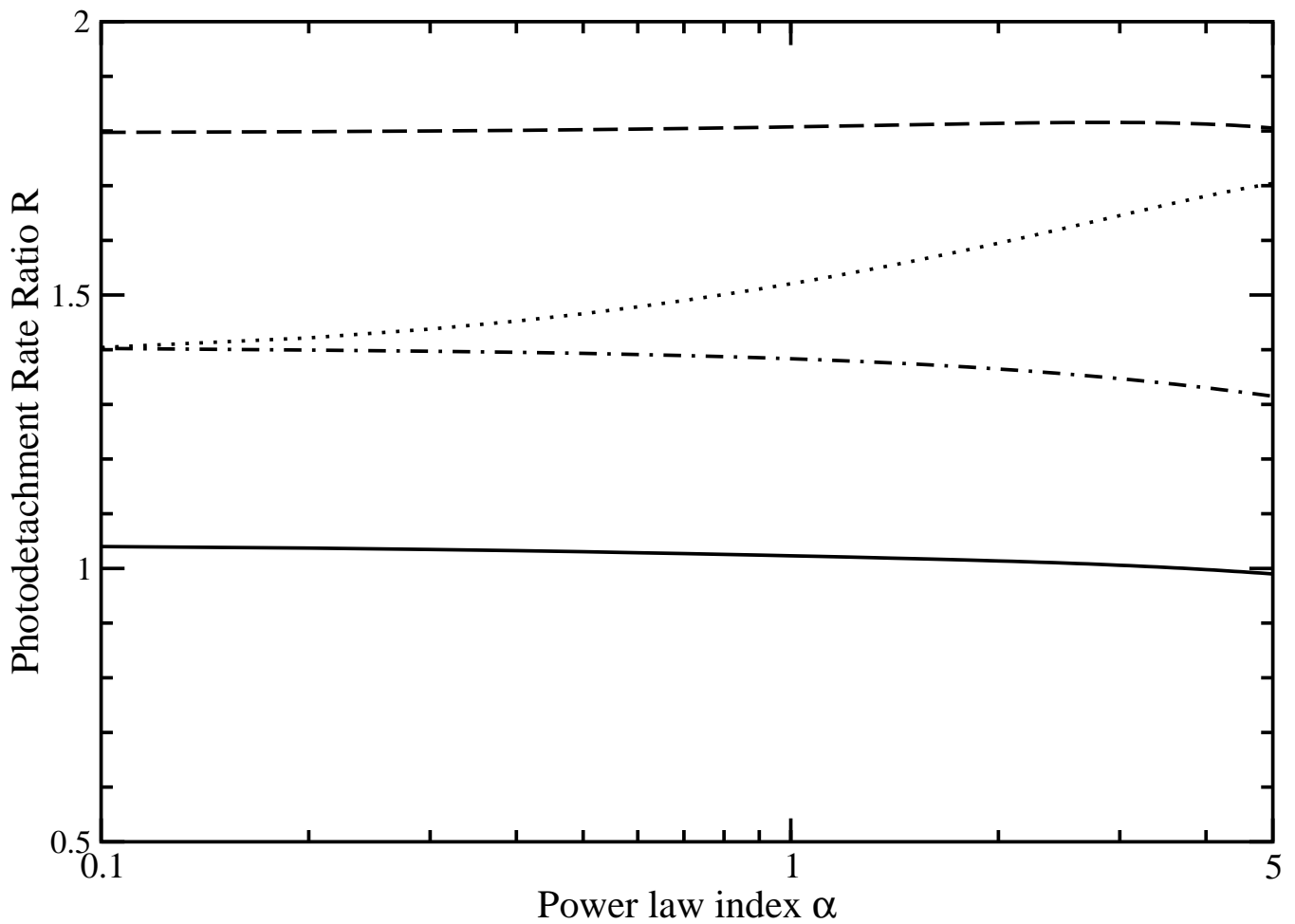


Figure 6.3:  $\text{H}^-$  photodetachment rate ratio,  $R$ , for a power-law radiation field as a function of the power-law index  $\alpha$ . Power-law rates computed over the photon energy ranges: 0.75-1000 eV (solid), 10-13.6 eV (dashed), and 10-1000 eV (dotted). The photodetachment rate ratio is also show for the IGM spectrum of Fig. 6.4 for photon energies 10-13.6 eV (dot-dash).

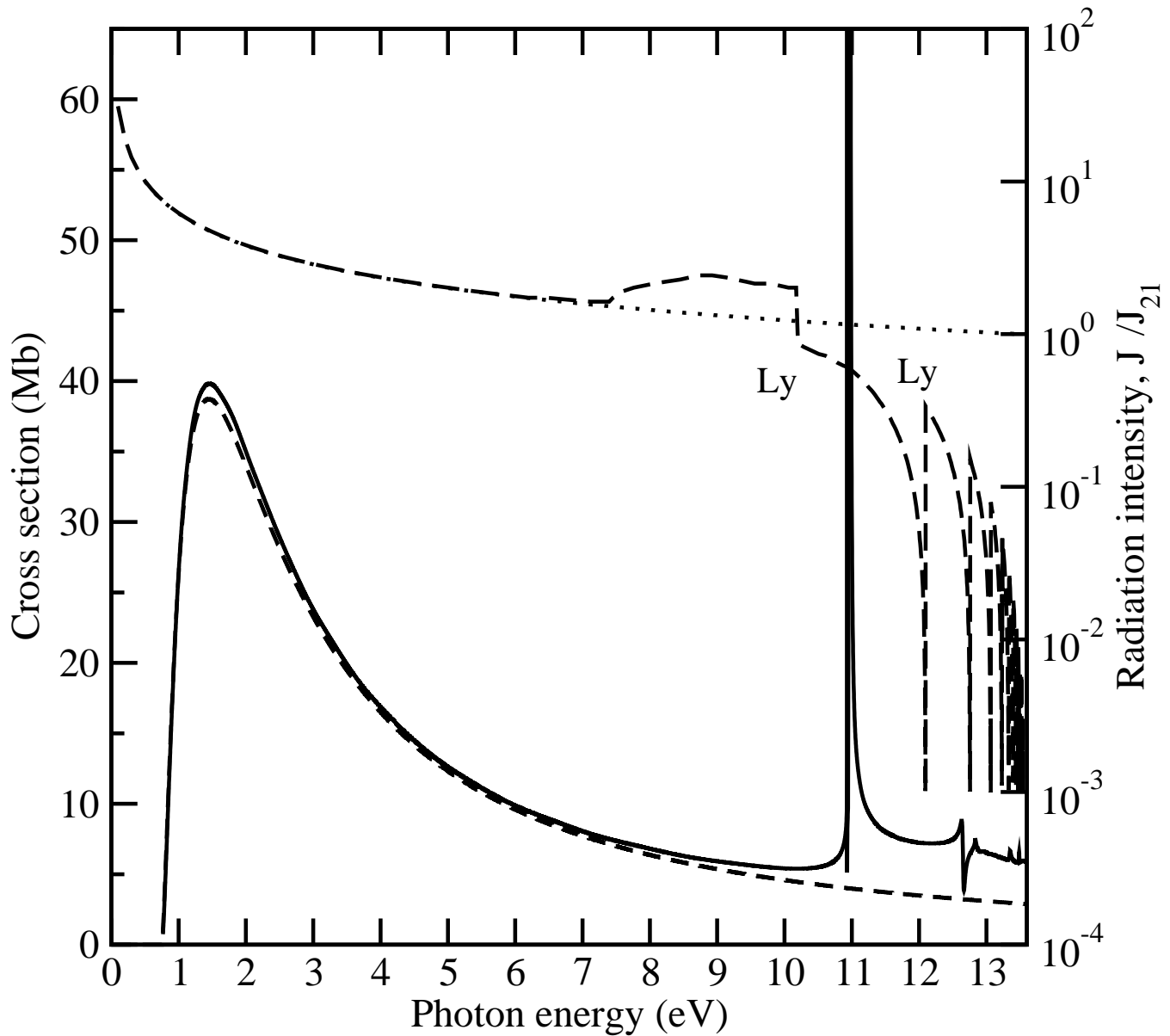


Figure 6.4: IGM sawtooth spectrum at  $z \sim 20$  (long dashed) compared to an  $\alpha = 0.7$  power-law spectrum (dotted) and  $H^-$  photodetachment cross sections (same as Fig. 6.1). See text for a description of the sawtooth spectrum. Note the  $H^-$  resonance between the Ly $\alpha$  and Ly $\beta$  features of the IGM spectrum.

## CHAPTER 7

### SIMULATED SPECTRA OF PRIMORDIAL OBJECTS AT HIGH REDSHIFT

#### 7.1 INTRODUCTION

We investigated the expected spectra from a primordial star and a dwarf galaxy in the early Universe. We used the plasma code Cloudy to simulate the physical, chemical, and thermal properties of those objects, as well as the radiative transfer. It is the public available code which calculates the microphysics self-consistently and simultaneously. In addition to H I, He I and He II lines, H<sub>2</sub> rotational lines may be observable with future infrared and submm telescopes.

The first generation stars, so-called Pop III stars, are predicted to have formed in mini-halos with virial temperature  $T \leq 10^4$  K at redshift  $z \geq 15$  [1, 2, 3, 4, 5]. The Pop III star itself is embedded inside its parent primordial halo. Therefore the emergent spectrum will be the reprocessed spectrum of the star through the primordial cloud. It is still computer resource demanding to fully resolve the cosmological hydrodynamic simulation as well as to follow the radiative transfer, chemical abundances, and level populations of the atoms and molecules simultaneously.

There have been several authors who considered H II regions in the early Universe [79, 80, 81, 82, 83]. They have shown that an ionization front (I-front) can be created by a Pop III star ( $M_* = 15 - 500 M_\odot$ ) at  $z \sim 20$ , within the density field of a cosmological simulation of primordial star formation, outward through the host minihalo and into the surrounding gas. Instead of doing a full treatment of hydrodynamics, one can adopt a steady-state shell approximation which can be applied in certain circumstances in the early Universe, as usually treated in current study of contemporary (i.e., Pop I) photodissociation regions (PDR).

Haehnelt [78], using an analytical model, suggested that Ly $\alpha$  photon radiation pressure can support a cloud from collapsing in the early Universe. Fully ionized, self-gravitating gaseous objects can be radiation-pressure-supported on a characteristic length scale  $R \sim 100$  pc – 3 kpc [78]. The impact of Ly $\alpha$  radiation pressure on the formation of current galaxies has been discussed extensively [84, 85, 86, 87, 88].

Dijkstra & Loeb [89] performed numerical models using a Monte Carlo Ly  $\alpha$  radiative transfer method [91]. They performed Monte Carlo simulations of the transfer of Ly $\alpha$  photons through spherically symmetric clouds of neutral collapsing gas. The characteristic length scale of their models was on the order of  $R \sim 10$  kpc. However, this radiation pressure due to the radiation coming out from Pop III stars are calculated to be an order of  $\sim$ Myr (Schaerer [93]) and may not hold long compared to the Hubble time.

## 7.2 SIMULATIONAL MODEL

### 7.2.1 PLASMA CODE CLOUDY

Calculations were performed with version 07.02 of the spectral/plasma simulation code Cloudy, last described by Ferland et al. [92]. It solves radiative transfer, chemical abundances, thermal balances, and level population self-consistently for a 1D spherical, static/steady flow geometry (1D plane parallel slabs can also be treated). Hydrodynamics, e.g. a radiative shock, are currently beyond the capability of the public version of Cloudy. An advective treatment is expected to be added in future releases. In each of our models, the chemical abundances, level populations, and temperature of the cloud are calculated self-consistently.

### 7.2.2 CASE I: A SINGLE MASSIVE STAR IN A MINIHALO AT $z=20$

We considered two cases for which a steady-state shell approximation is expected to be valid. A minihalo with halo mass,  $M_{\text{halo}}$  set to  $M_{\text{halo}} = 2 \times 10^6 M_{\odot}$ . 1D spherical geometry was adopted. We consider the case of a Pop III star inside a spherical shell. For the Pop III star, we adopted a mass  $M_*$ , luminosity  $L$ , and effective temperature  $T_{\text{eff}}$  of  $120 M_{\odot}$ ,

$\log L/L_{\odot} = 6.243$ , and  $\log T_{\text{eff}} = 4.981$ , respectively. The shell inner radius from the star was taken as  $R_{\text{in}} = 10$  kpc. The radius of the shell,  $R_{\text{shell}}$  was set as  $R_{\text{shell}} = 100$  pc. The density of the shell,  $n_{\text{shell}}$  was set as  $n_{\text{shell}} = 10^4$  cm $^{-3}$ . The simulation was performed for conditions consistent with  $z = 20$  with a cosmic microwave background (CMB). The cosmic ray ionization rate was also included, but set to the low value of  $10^{-19}$  s $^{-1}$ . This value was taken from Stacy & Bromm [94].

### 7.2.3 CASE II: DWARF GALAXY WITH IMF OF POP III STARS AT z=10

The initial mass function (IMF) for population I stars is observed to take the approximate Salpeter form [98, 99]

$$\frac{dN}{d\log M} \propto M^{-\alpha} \quad (7.1)$$

where

$$\alpha \simeq \begin{cases} 2.35 & \text{for } M \leq 0.5 M_{\odot} \\ 1.0 & \text{for } M \geq 0.5 M_{\odot}. \end{cases} \quad (7.2)$$

$M$  is the stellar mass and  $N$  is the stellar number density. Constraining the IMF of primordial stars is the key to understand chemical enrichment of the intergalactic medium (IGM), as well as primitive galaxy assembly, and the reionization of the early Universe. A top heavy Salpeter IMF is needed in order to reproduce the reionization of the universe. However the initial mass function in the early Universe is not known. Therefore we adopt a normal Salpeter IMF value  $\alpha = 2.35$  in our models.

For a preliminary study, we consider a star cluster of blackbody radiators. The composite spectrum was generated using the table of Pop III properties from Schaerer [93]. We have accumulated each of the blackbody spectra corresponding to effective temperatures of Pop III stars and a Salpeter IMF with a mass range  $5 \leq M \leq 100 M_{\odot}$ . We considered a halo mass of  $M_{\text{halo}} = 1.5 \times 10^7 M_{\odot}$ . The shell inner radius,  $R_{\text{in}}$ , was set as  $R_{\text{in}} = 20$  kpc for the case of a primordial dwarf galaxy.

#### 7.2.4 SHELL PROPERTY

The existence of a thin, neutral atomic hydrogen shell around H II regions is reported by HI observation in the Milky Way [95] and other nearby galaxies [96]. The largest of these shells, so-called 'supershells' have radii of  $r_{\max} \sim 1$  kpc [96, 97]. However in the early Universe, we suspect that circumstances of the primordial supershells are quite different to the currently observed supershells and not much has been done with this area of the research. Therefore as our model clouds, we take the spatial width of the supershell to be 10 percent of its radius as adopted by Dijkstra & Loeb [89]. In Bromm et al. [90], they performed the cosmological simulation in the early Universe and found that before the primordial clouds collapses, the gas settles into a quasi-hydrostatic state at the temperature,  $T \sim 200$  K and the density,  $n \sim 10^4 \text{ cm}^{-3}$ . Using this information, we solve for the temperature self-consistently using Cloudy and keep the fixed value of the density,  $n = 10^4 \text{ cm}^{-3}$  throughout the shell structure.

### 7.3 RESULTS AND DISCUSSION

Using the conditions described in section 7.2, we performed simulations with Cloudy for case I and II. We plot the emergent spectrum in Figures 7.1 and 7.2 for case I. The fractional abundances (density ratio relative to the total hydrogen) are plotted in Figure 7.3 for the hydrogen species as well as the electron number density. The temperature drops dramatically to  $\sim 30$  K within 1 pc as we move towards outside of the cloud shell. H I and H<sub>2</sub> are fairly abundant,  $\sim 10^0 - 10^{-1}$  respect to the total hydrogen density, with throughout the shell. The abundance of H<sup>+</sup> drops in a depth around  $10^{15} - 10^{16}$  cm along with the decline of free electron density and temperature. The abundance of H<sub>2</sub><sup>+</sup> and H<sub>3</sub><sup>+</sup> are low,  $\sim 10^{-8} - 10^{-10}$  respect to the total hydrogen density, and drops further with depth around  $10^{15} - 10^{16}$  cm.

Column densities (divided by the statistical weight) of the rotational levels of H<sub>2</sub> in the vibrational ground state as a function of  $J$  quantum number are plotted in Figure 7.4. Comparison with made to an LTE population for which a departure from LTE is seen for  $J > 2$ .

Figure 7.5 shows the generated composite spectrum using multiple blackbody spectrum, which corresponds to Pop III effective temperature. In order to generate this figure, we took the value of total mass,  $M_{total} = 1.0 \times 10^6 M_\odot$ , the slope of IMF,  $\alpha = 2.35$  with mass range  $5 - 100 M_\odot$ . We generated blackbody spectrum which corresponds with each effective temperature using table in Schaerer [93] and accumulate each spectrum in order to generate composite spectrum. This figure is comparable to Figure 4 in Tumlinson and Shull (2000). Their spectrum follows the features of He II, He I and H I because they adopted expected Pop III spectra. Since it is only accumulation of the blackbody radiation, we could not reproduce spectral features. However in this research, general trend of luminosity in corresponding wavelength range is generally reproduced.

Figure 7.6 and 7.7 show the emergent spectra for case II. As for case I, a large number of H I, He I, He II, and H<sub>2</sub> lines are evident from the UV to IR.

The fractional abundances for case II are plotted in Figure 7.8. The temperature never drops below  $\sim 100$  K throughout the shell. We believe it is because of the strong radiation from a cluster of Pop III stars. The electron density is an order of magnitude higher compared to case I. H I is fairly abundant,  $\sim 1$ , throughout the cloud shell. The abundance of H<sup>+</sup> relatively higher compared to case I and drops in a depth around  $10^{15} - 10^{16}$  cm<sup>-3</sup> along with the decline of the electron density. Basic behavior of H<sup>+</sup> is same for case I. H<sub>2</sub> abundance is compared to the primordial case,  $\sim 10^{-6}$ , and smaller than the case I. The abundance of H<sub>2</sub><sup>+</sup> and H<sub>3</sub><sup>+</sup> are also low as for case II,  $\sim 10^{-8} - 10^{-10}$ , and drops further with depth around  $10^{15} - 10^{16}$  cm. The features at a depth around  $10^{15} - 10^{16}$  cm are connected to the abundance of H<sub>2</sub> and the decline of H<sup>+</sup> and electron density abundances.

#### 7.4 CONCLUSION

We report the expected spectra from a Pop III star and a primordial dwarf galaxy in the early universe. We used the plasma code Cloudy to simulate the primordial dwarf galaxy. H<sub>2</sub> lines could be observable in the early Universe. Such lines could possibly be visible in

their rest-frame visible continua with the James Webb Space telescope (JWST) or planned ground-based infrared detectors.

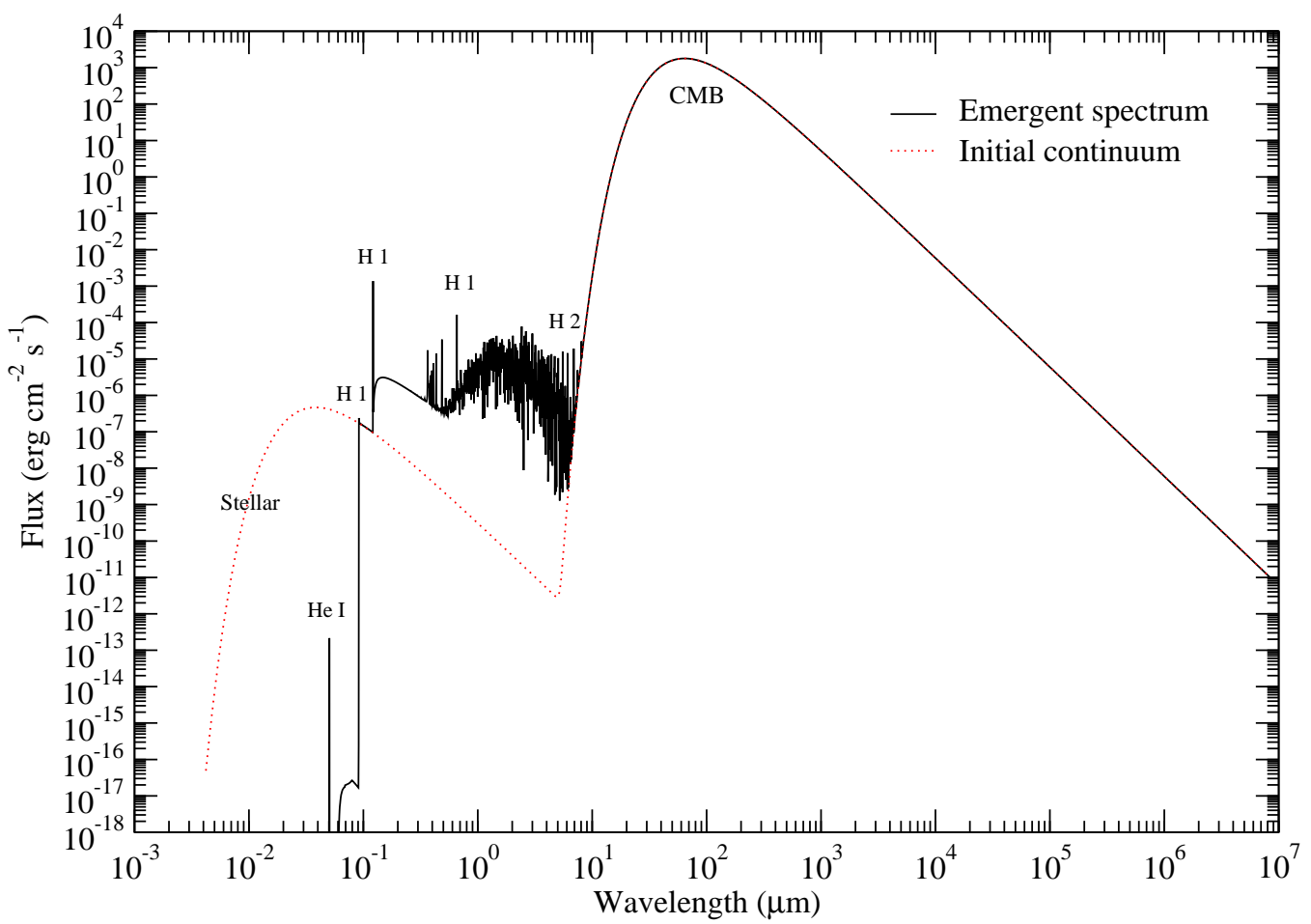


Figure 7.1: Emergent spectrum for case I, for a single Pop III star at  $z = 20$ .

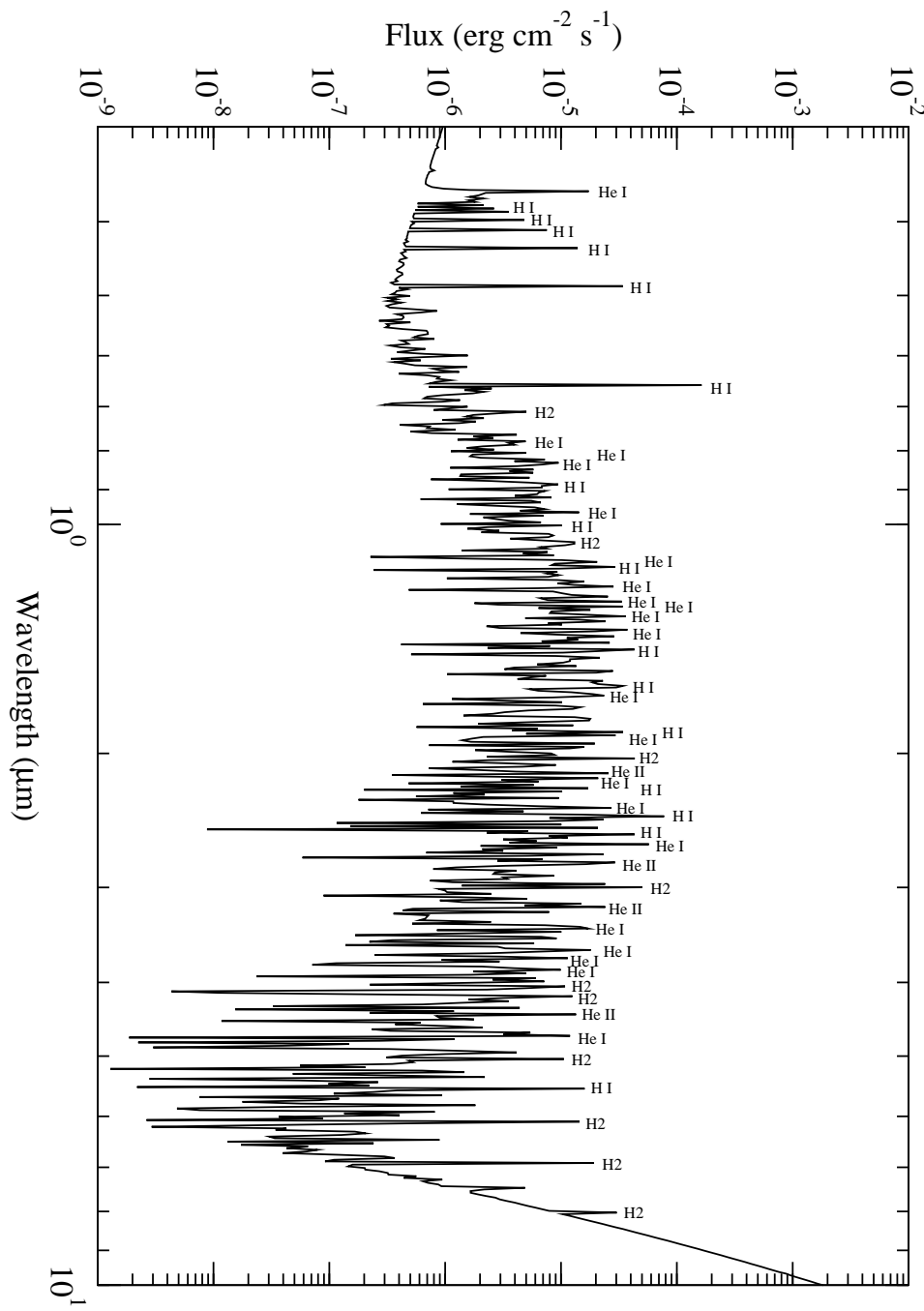


Figure 7.2: Same as Fig. 7.1 with magnified wavelength range from 0.3 to 10  $\mu\text{m}$ .

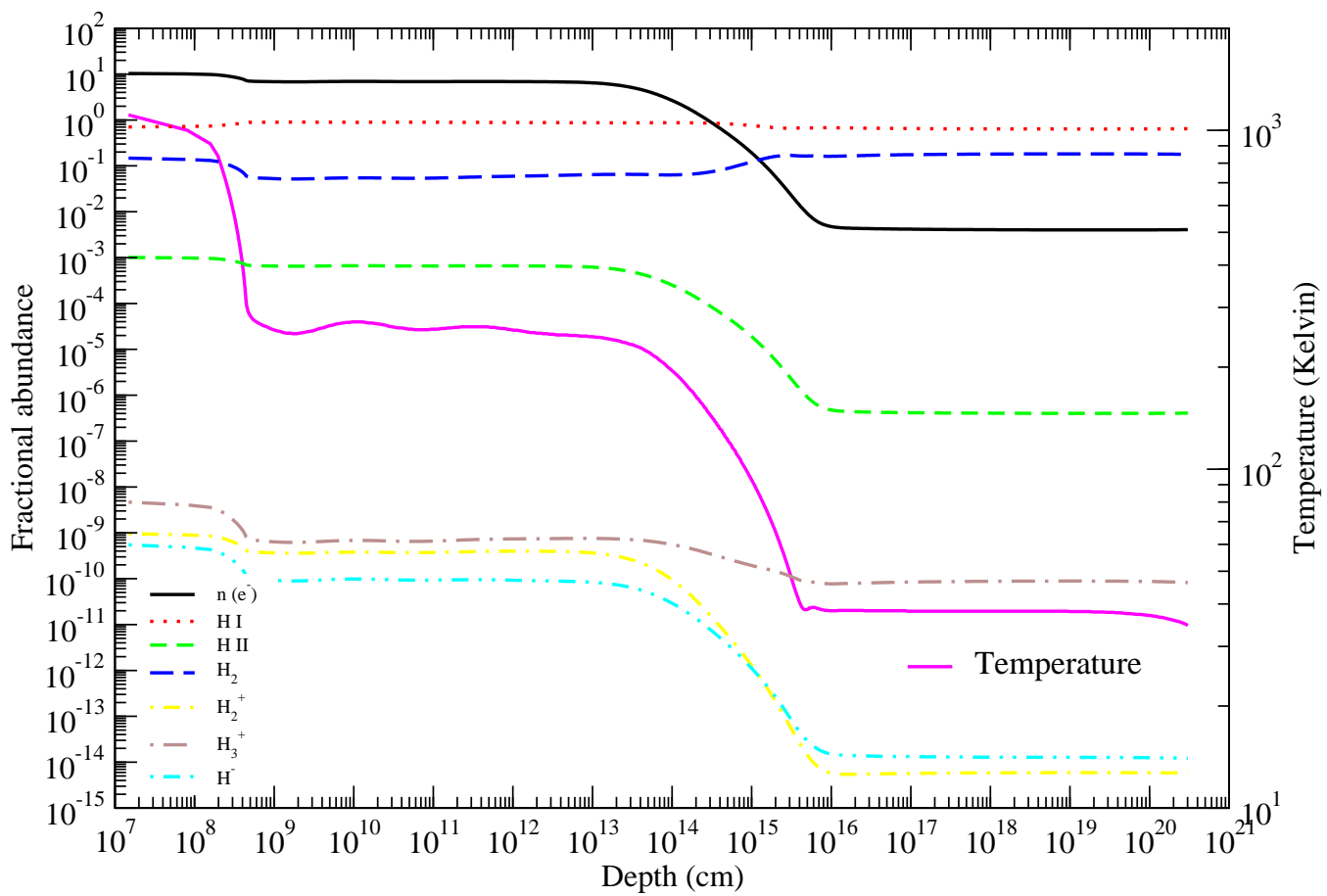


Figure 7.3: Fractional abundance, electron density, ( $\text{cm}^{-3}$ ) and temperature of the shell as a function of the depth from the inner radius.

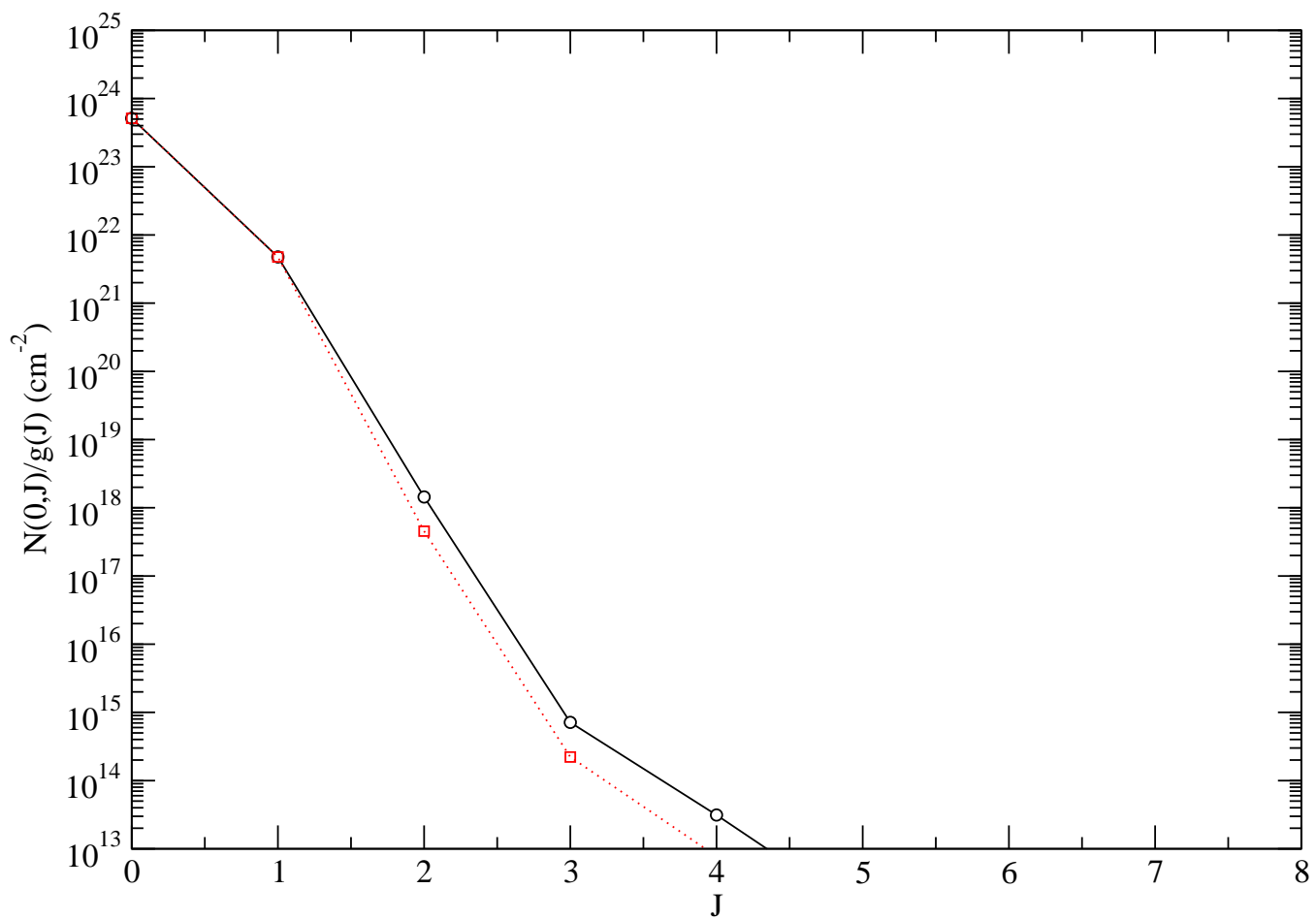


Figure 7.4: Column density (divided by the statistical weight) for  $\text{H}_2(v = 0, J)$  as a function of  $J$  rotational quantum number. Solid line: non-LTE, dotted line : LTE

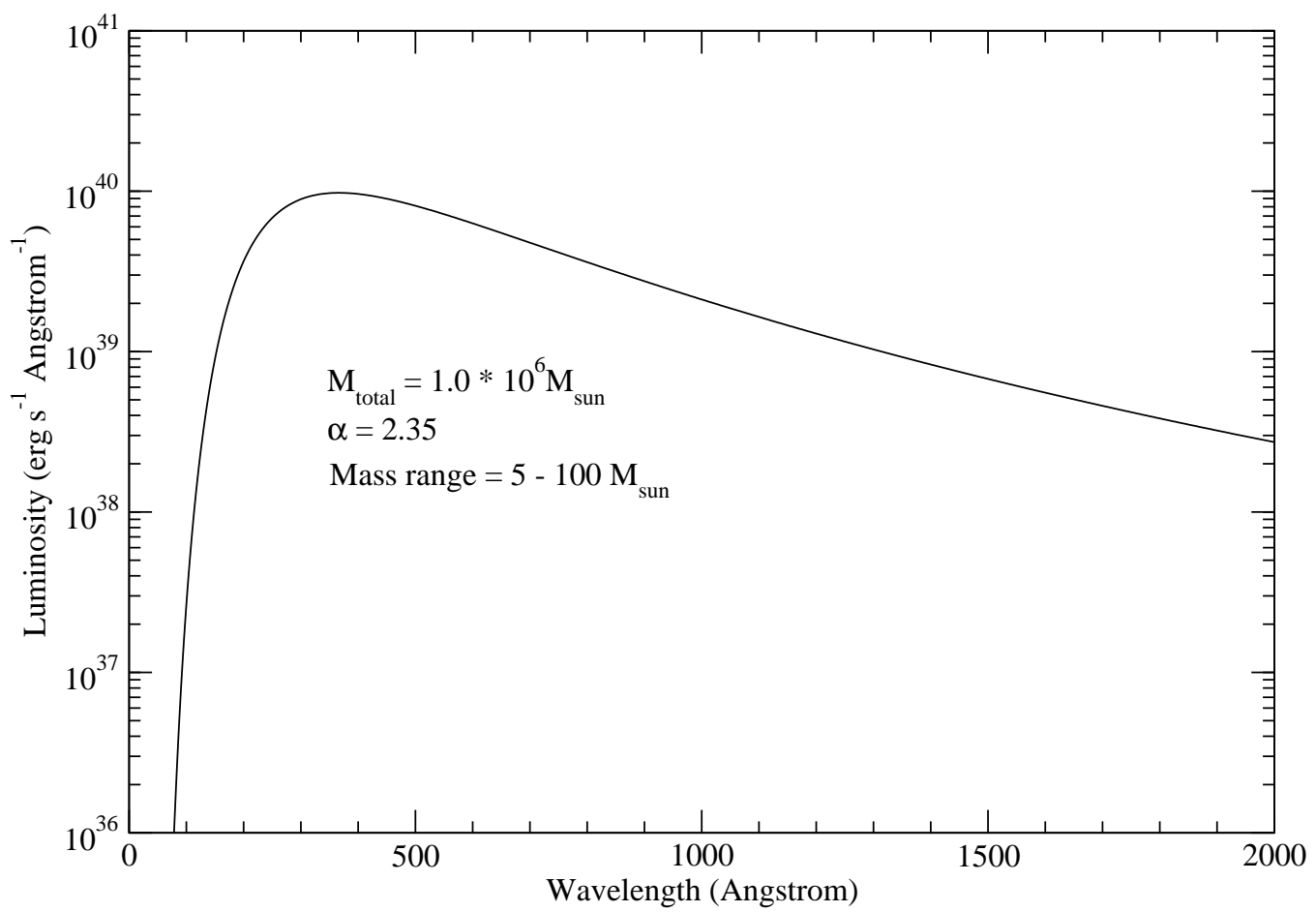


Figure 7.5: Generated composite spectrum using multiple blackbody spectrum, corresponding to Pop III effective temperatures.

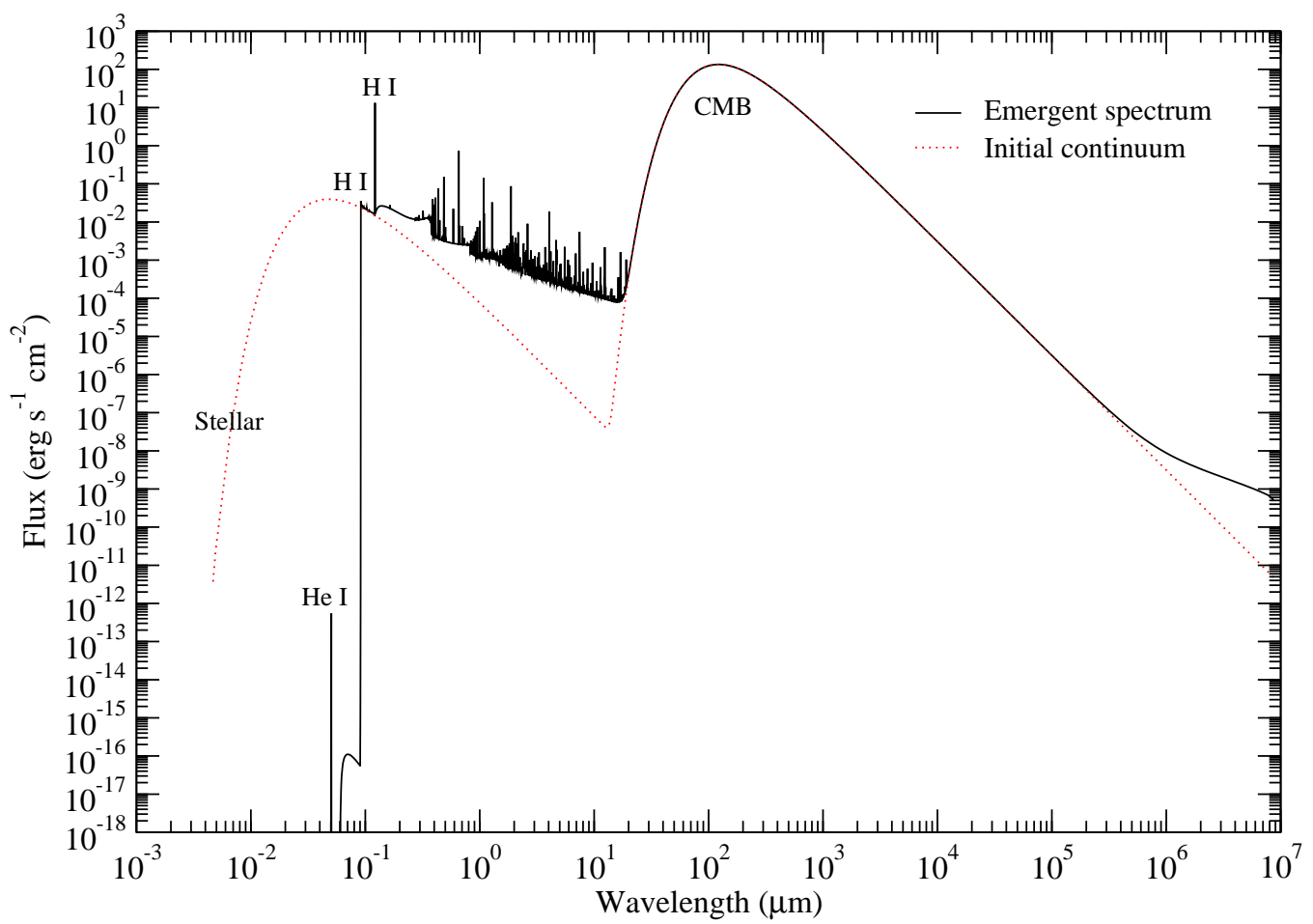


Figure 7.6: Same as Fig. 7.1, for primordial dwarf galaxy at  $z = 10$ .

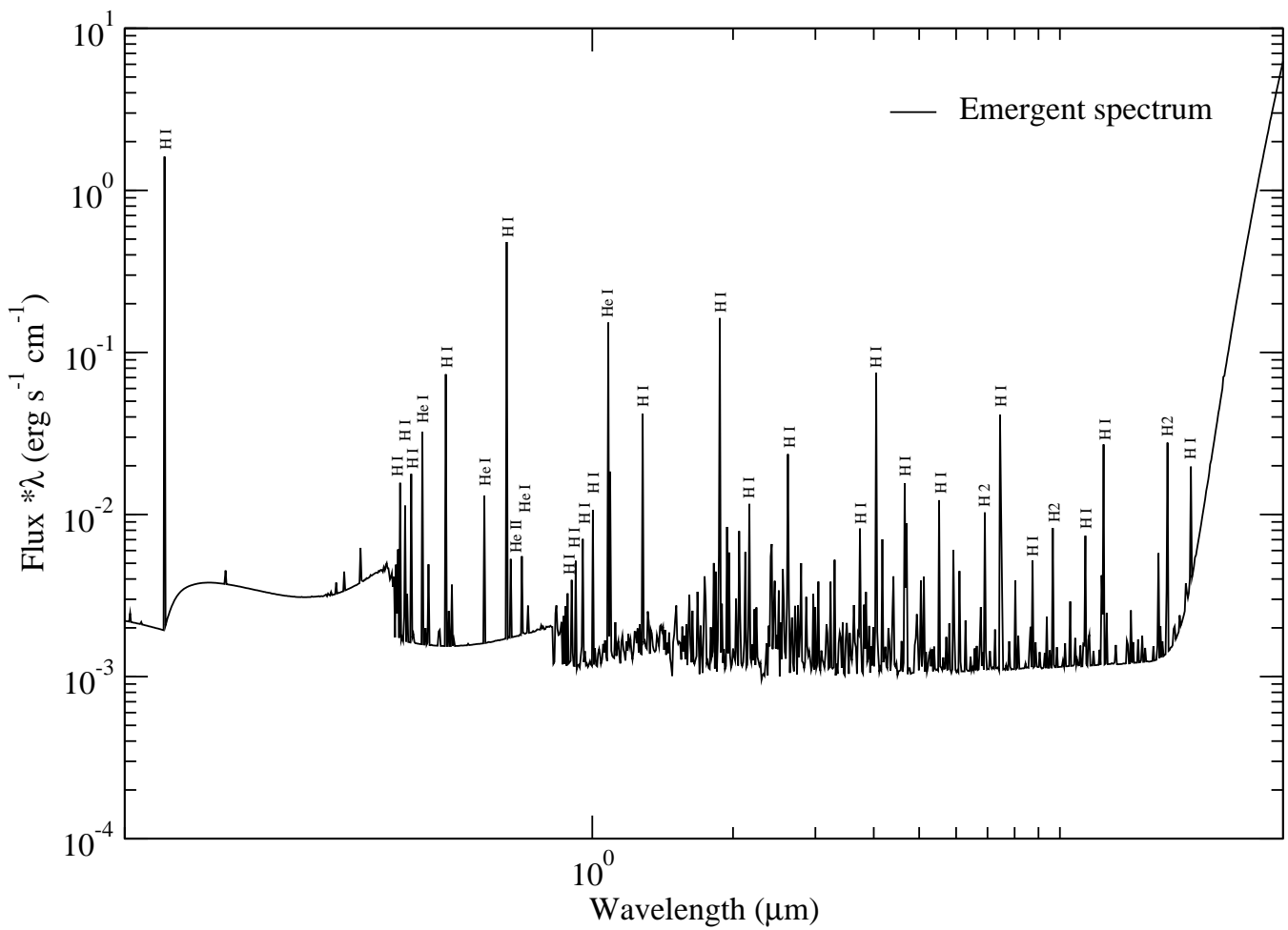


Figure 7.7: Emergent spectrum of the case of a primordial dwarf galaxy with magnified wavelength range from  $0.3$  to  $10\ \mu\text{m}$  at  $z = 10$ .

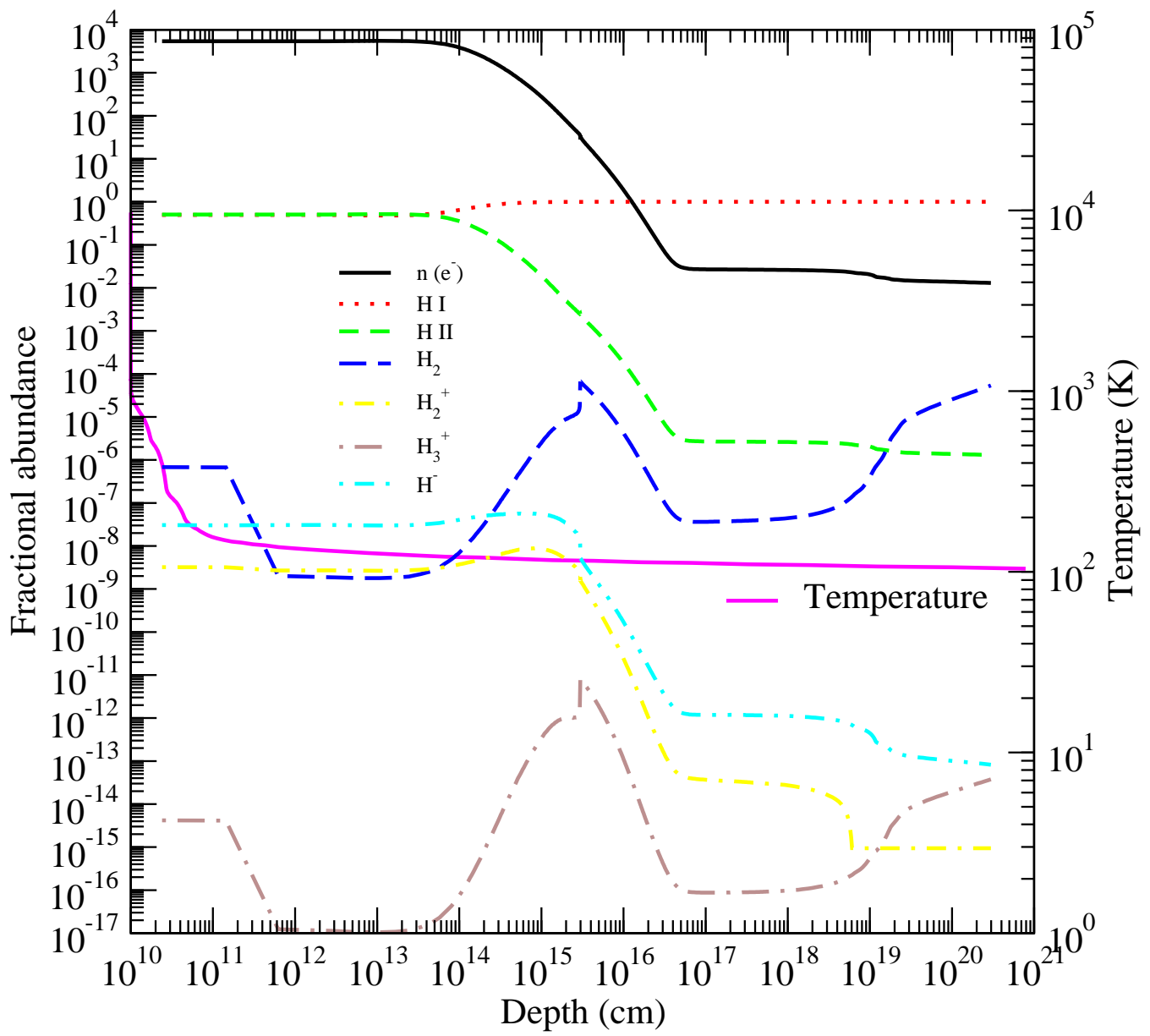


Figure 7.8: Same as Fig. 7.3, for primordial dwarf galaxy  $z = 10$ .

## CHAPTER 8

### SUMMARY AND FUTURE RESEARCH

We have shown in this dissertation that the photoprocesses of atoms and molecules may give quite significant effects in the early Universe. In chapter 2, we considered the rovibrational spectra and radiative cooling of  $\text{HeH}^+$ . We used the time-independent radial nuclear Schrödinger equation for the  $\text{X } ^1\Sigma^+$  electronic ground state and obtained 162 rovibrational states. Transition probabilities between all rovibrational states were also calculated and we obtained spectra for the local thermodynamic equilibrium (LTE) case. Then we calculated the radiative cooling coefficients for LTE. We found that the value of the radiative cooling coefficients of  $\text{HeH}^+$  is about ten orders of magnitude larger than those of  $\text{H}_2$ . However, abundance of  $\text{HeH}^+$  is low in the early Universe so that overall cooling efficiency highly depends on local primordial circumstances. Calculation of non-LTE cooling, which can be used to improve the current results, require information of rotational collisional excitation of  $\text{HeH}^+$  due to the dominant species atomic hydrogen. However, collisional data for the  $\text{HeH}^+ \text{-H}$  system is currently not available.

In chapter 4, we studied photodissociation cross section of  $\text{HeH}^+$ . Photodissociation cross sections for the  $\text{A } ^1\Sigma^+ \leftarrow \text{X } ^1\Sigma^+$  and  $\text{X } ^1\Sigma^+ \leftarrow \text{X } ^1\Sigma^+$  transitions were obtained. A total of 324 radiative transition have been obtained from this calculation. We also calculated total cross section for LTE case with both transitions. These data will be included in the future release of the plasma code Cloudy.

In chapter 5, we studied photodissociation of  $\text{C}_2$ . Photodissociation cross sections of  $\text{C}_2$  have been calculated from its ground electronic state  $\text{X } ^1\Sigma^+$  to the electronic excited

states A  $^1\Pi_u$ , 2  $^1\Pi_u$ , and 3  $^1\Pi_u$ . More accurate values have been obtained from the current calculation and important resonance features have also been obtained.

In chapter 6, we studied an enhanced photodestruction effect due to the resonant H $^-$  photodetachment. We have considered the radiation field with the photodetachment cross section of H $^-$  involving strong resonance around 11 eV. As for the radiation field, we have considered the case for a blackbody, quasar, and the average intergalactic radiation field in the early Universe. We conclude that the photodetachment rate is enhanced by > 30 % if the resonance is included. So far among large scale cosmological simulations, they adopt H $^-$  cross section without the resonance. A reduction of H $^-$  results in the loss of H<sub>2</sub>. Therefore the reduction of the H<sub>2</sub> abundance affects significantly the formation of Population III stars and may influence the era of the reionization of the Universe. Therefore, this result might give significant impact to the large scale cosmological simulations.

In chapter 7, we conclude that features of H I lines, He I, He II lines as well as few H<sub>2</sub> lines might be detected. Future research at high redshifts with the James Webb Space Telescope or large-aperture ground-based infrared telescopes will be capable of detecting atomic and molecular lines in the early Universe. As for this dissertation, we considered the possibility of a quasi-state gas evolution in which resides the Pop III star and the primordial gas. This is mainly due to the limitation of the current version of Cloudy. Due to the high mass property of Pop III stars, a radiative shock might be produced within the range of  $\sim 100$  pc. If a radiative shock is generated, the contribution from advection modifies the emission spectra and quasi-static assumption is no longer valid. In order to deal with the radiative shock and advection, one has to solve hydrodynamics, radiative transfer as well as microphysics consistently and simultaneously. The upcoming version of Cloudy will be able to incorporate all of these effects. Therefore it is quite interesting to see the effect of the advection term. We believe that the model coupled with hydrodynamics, radiative transfer and microphysics which deal with atomic and molecular processes self-consistently would give us a more precise picture. For the case of a large star cluster in a dwarf galaxy,

we have used multiple blackbody spectra with corresponding to effective temperatures in order to generate composite spectrum of a cluster of Pop III stars as input for our Cloudy simulation. Of course, the true spectra from Pop III stars is more than just a blackbody. Therefore, as a next step, one can improve this work by using true spectra of Pop III stars and produce composite spectrum. Another improvement might be changing the slope of initial mass function (IMF) of Pop III stars. So far we have assumed usual Salpeter IMF,  $\alpha = 2.35$ . It might be interesting to see how the result changes in terms of the slope of the IMF. Further improvement is to the shell structure of the primordial model clouds. As for this dissertation, we only assumed constant density for whole shell structure, but we can improve its structure by taking a  $r^{-2}$  density dependence. A clumping factor, which describe local clumpiness compared to the spatial average density, is also expected and was used in the calculation of Dijkstra & Loeb [89]. However, the clumping factor was not included in this simulation due to the structure of the Cloudy code. If we include the clumping factor, radiation could more easily escape. It might be interesting to see those effects as well.

As the future research personally, I would like to finalize constructing a Monte Carlo radiative transfer code. It is the continuation of my research while I was a Master's student. It deals with the radiative transfer using Monte Carlo method and will treat line/continuum, emission/absorption as well as level populations self-consistently. Its structure and logic are quite similar to Cloudy which I dealt with in this dissertation. Once it is complete, it will give us a seamless module to connect between current existing hydrodynamic code and radiative transfer calculations. I would like to make it available to the public and let everyone freely use it.

## BIBLIOGRAPHY

- [1] Couchman, H. M. P., & Rees, M. J. 1986, MNRAS, 221, 53
- [2] Haiman, Z., Thoul, A. A., & Loeb, A. 1996, ApJ, 464, 523
- [3] Gnedin, N. Y., & Ostriker, J. P. 1997, ApJ, 486, 581
- [4] Tegmark, M., Silk, J., Rees, M. J., Blanchard, A., Abel, T., & Palla, F. 1997, ApJ, 474, 1
- [5] Yoshida, N., Abel, T., Hernquist, L., & Sugiyama, N. 2003, ApJ, 592, 645
- [6] Bromm, V., & Larson, R. B. 2004, Annu. Rev. Astron. Astrophys., 42, 79
- [7] Lepp, S., Stancil, P. C., & Dalgarno, A. 2002, J. Phys. B Atomi., Molec., Phys., 35, 57
- [8] Saslaw, W. C., & Zipoy, D. 1967, Nature, 216, 976
- [9] Dabrowski, J., Piechocki, W., Rozynek, J., & Haensel, P. 1978, Phys. Rev. C, 17, 1516
- [10] Hirasawa, T. 1969, Progress of Theoretical Physics, 42, 523
- [11] Dalgarno, A., & Lepp, S. 1987, Astrochemistry, 120, 109
- [13] Roberge, W., & Dalgarno, A. 1982, ApJ, 255, 489
- [14] Kraemer, W. P., Spirko, V., & Jurek, M. 1995, Chemi. Phys. Lett., 236, 177
- [15] Liu, X.-W., et al. 1997, MNRAS, 290, L71
- [16] Miller, S., Tennyson, J., Lepp, S., & Dalgarno, A. 1992, Nature, 355, 420
- [17] Zygelman, B., Stancil, P. C., & Dalgarno, A. 1998, ApJ, 508, 151

- [18] Black, J. H. 1978, *ApJ*, 222, 125
- [19] Shchekinov, Y. A., & Entel, M. B. 1983, *Soviet Astronomy*, 27, 622
- [20] Bishop, D. M., & Cheung, L. M. 1979, *J. Molec. Spectrosc.*, 75, 462
- [21] Jurek, M., Spirko, V., & Kraemer, W. P. 1995, *Chem. Phys.*, 193, 287
- [22] Coxon, J. A., & Hajigeorgiou, P. G. 1999, *Journal of Molecular Spectroscopy*, 193, 306
- [23] Engel, E. A., Doss, N., Harris, G. J., & Tennyson, J. 2005, *MNRAS*, 357, 471
- [24] Whiting, E. E., & Nicholls, R. W. 1974, *ApJ*, 27, 1
- [25] Rees, M. J., & Ostriker, J. P. 1977, *MNRAS*, 179, 541
- [26] Silk, J. 1977, *ApJ*, 211, 638
- [27] Rabadan, I., Sarpal, B. K., & Tennyson, J. 1998, *MNRAS*, 299, 171
- [28] Schöier, F. L., van der Tak, F. F. S., van Dishoeck, E. F., & Black, J. H. 2005, *A&A*, 432, 369
- [29] Kirby, K. P. & van Dishoeck, E. F. 1988, *Adv. At. Mol. Phys.*, 25, 437
- [30] Cooley, J. W. 1961, *Math. Comput.*, 15, 363
- [31] Blatt, J. M. 1967, *J. Computat. Phys.*, 1, 382
- [32] Johnson, B. R. 1977, *J. Chem. Phys.*, 67, 4086
- [33] Schleicher, D. R. G., Galli, D., Palla, F., Camenzind, M., Klessen, R. S., Bartelmann, M., & Glover, S. C. O. 2008, *A&A*, 490, 521
- [34] Moorhead, J. M., Lowe, R. P., Wehlau, W. H., Maillard, J.-P., & Bernath, P. F. 1988, *ApJ*, 326, 899
- [35] Dinerstein, H. L., & Geballe, T. R. 2001, *ApJ*, 562, 515

- [36] Saha, S., Datta, K. K., & Barua, A. K. 1978, J. Phys. B Atomi., Molec., Phys., 11, 3349
- [37] Argyros, J. D., 1974, J. Phys. B, 7, 2025
- [38] Stancil, P. C., Lepp, S., & Dalgarno, A. 1998, ApJ, 509, 1
- [39] Gredel, R., van Dishoeck, E. F., & Black, J. H. 1989, ApJ, 338, 1047
- [40] Pouilly, B., Robbe, J. M., Schamps, J., & Roueff, E. 1983, Journal of Physics B Atomic Molecular Physics, 16, 437
- [41] Herzberg, G., 1950, Molecular spectra and molecular structure, Van Nostrand Reinhold company, Chapter VI, p. 315
- [42] Langhoff, S. R., Bauschlicher, C. W., Jr., Rendell, A. P., & Komornicki, A. 1990, J. Chem. Phys., 92, 3000
- [43] Mayer, P., & O'dell, C. R. 1968, ApJ, 153, 951
- [44] Johnson, J. R., Fink, U., & Larson, H. P. 1983, ApJ, 270, 769
- [45] Lambert, D. L., & Danks, A. C. 1983, ApJ, 268, 428
- [46] de Freitas Pacheco, J. A., Singh, P. D., & Landaberry, S. J. C. 1988, MNRAS, 235, 457
- [47] Goebel, J. H., Bregman, J. D., Cooper, D. M., Goorvitch, D., Langhoff, S. R., & Witteborn, F. C. 1983, ApJ, 270, 190
- [48] Grevesse, N., & Sauval, A. J. 1973, A&A, 27, 29
- [49] Lambert, D. L. 1978, MNRAS, 182, 249
- [50] Brault, J. W., Testerman, L., Grevesse, N., Sauval, A. J., Delbouille, L., & Roland, G. 1982, A&A, 108, 201
- [51] van Dishoeck, E. F., & Black, J. H. 1989, ApJ, 340, 273

- [52] Martin, M. 1992, Journal of Photochemistry and Photobiology A: Chemistry, 66, 263
- [53] Ballik, E. A., & Ramsay, D. A. 1963, ApJ, 137, 84
- [54] Herzberg, G, Lagerqvist, A & Malmberg, C, 1969, Can. J. Phys., 47, 2735
- [55] Le Bourlot, J. & Roueff, E., 1986, J. Mol. spectros., 120, 157
- [56] Miyake, S., Stancil, P. C., Sadeghpour, H. R., Dalgarno, A., McLaughlin, B. M., & Forrey, R. C. 2010, ApJ, 709, L168
- [57] Barkana, R., & Loeb, A. 1999, ApJ, 523, 54
- [58] Bromm, V. & Larson, R. B. 2004, Annu. Rev. Astron. Astrophys., 42, 1
- [59] Saslaw, W. C. & Zipoy, D. 1967, Nature, 216, 976
- [60] Peebles, P. J. E. & Dicke, R. H. 1968, ApJ, 154, 891
- [61] Haiman, Z., Rees, M. J., & Loeb, A. 1996, ApJ, 467, 522
- [62] Haiman, Z., Rees, M. J., & Loeb, A. 1997, ApJ, 476, 458
- [63] Haiman, Z., Abel, T., & Rees, M. J. 2000, ApJ, 534, 11
- [64] Kitayama, T., Susa, H., Umemura, M., & Ikeuchi, S. 2001, MNRAS, 326, 1353
- [65] Pagel, B. E. J. 1959, MNRAS, 119, 609
- [66] McDowell, M. R. C. 1962, The Observatory, 81, 240
- [67] Chuzhoy, L., Kuhlen, M., & Shapiro, P. R. 2007, ApJ, 665, L85
- [68] Glover, S. C. O. 2007, MNRAS, 379, 1352
- [69] Dalgarno, A. & McCray, R. 1973, ApJ, 180, 95
- [70] Wishart, A. W. 1979, MNRAS, 187, 59

- [71] Bylicki, M. & Bednarz, E. 2000, Phys. Rev. A, 67, 022503
- [72] Rau, A. R. P. 2002, *Astronomy-inspired Atomic and Molecular Physics*, Astrophys. Space Sci. Lib., Vol. 271, (Kluwer Acad. Publ., Dordrecht)
- [73] Stancil, P. C., Miyake, S., Sadeghpour, H. R., McLaughlin, B. M., & Forrey, R. C. 2010, Proc. Dalgarno Celebratory Symp. (Imperial College Press), p. 102
- [74] McLaughlin, B. M., Sadeghpour, H. R., Stancil, P. C., Dalgarno, A., & Forrey, R. C. 2010, in preparation
- [75] Sadeghpour, H. R., Greene, C. H., & Cavagnero, M. 1992, Phys. Rev. A, 45, 1587
- [76] Donahue, M. & Shull, J. M. 1991, ApJ, 383, 511
- [77] Thoul, A. A. & Weinberg, D. H. 1996, ApJ, 465, 608
- [78] Haehnelt, M. G. 1995, MNRAS, 273, 249
- [79] Ricotti, M., Gnedin, N. Y., & Shull, J. M. 2001, ApJ, 560, 580
- [80] Kitayama, T., Yoshida, N., Susa, H., & Umemura, M. 2004, ApJ, 613, 631
- [81] Alvarez, M. A., Bromm, V., & Shapiro, P. R. 2006, ApJ, 639, 621
- [82] Johnson, J. L., Greif, T. H., & Bromm, V. 2007, ApJ, 665, 85
- [83] Greif, T. H., Johnson, J. L., Klessen, R. S., & Bromm, V. 2009, MNRAS, 399, 639
- [84] Cox, D. P. 1985, ApJ, 288, 465
- [85] Elitzur, M., & Ferland, G. J. 1986, ApJ, 305, 35
- [86] Bithell, M. 1990, MNRAS, 244, 738
- [87] Oh, S. P., & Haiman, Z. 2002, ApJ, 569, 558
- [88] McKee, C. F., & Tan, J. C. 2008, ApJ, 681, 771

- [89] Dijkstra, M., & Loeb, A. 2008, MNRAS, 391, 457
- [90] Bromm, V., Coppi, P. S., & Larson, R. B. 2002, ApJ, 564, 23
- [91] Dijkstra, M., Haiman, Z., & Spaans, M. 2006, ApJ, 649, 14
- [92] Ferland, G. J., Korista, K. T., Verner, D. A., Ferguson, J. W., Kingdon, J. B., & Verner, E. M. 1998, The Astronomical Society of the Pacific, 110, 761
- [93] Schaerer, D. 2002, A&A, 382, 28
- [94] Stacy, A., & Bromm, V. 2007, MNRAS, 382, 229
- [95] Heiles, C. 1984, ApJ, 55, 585
- [96] Ryder, S. D., Staveley-Smith, L., Malin, D., & Walsh, W. 1995, Astronomical Journal, 109, 1592
- [97] McClure-Griffiths, N. M., Dickey, J. M., Gaensler, B. M., & Green, A. J. 2002, ApJ, 578, 176
- [98] Salpeter, E. E. 1955, ApJ, 121, 161
- [99] Kroupa, P. 2002, Science, 295, 82
- [100] Johnson, J. L., Greif, T. H., & Bromm, V. 2008, MNRAS, 388, 26

## APPENDIX A

### HEH<sup>+</sup> SPECTROSCOPIC DATA IN LAMDA FORMAT

```

!MOLECULE
HeH+
!MOLECULAR WEIGHT
5
!NUMBER OF ENERGY LEVELS
162
!LEVEL + ENERGIES(cm^-1) + WEIGHT + J, + v
    1    0.00    1    0    0
    2    67.03    3    1    0
    3   200.71    5    2    0
    4   400.26    7    3    0
    5   664.53    9    4    0
    6   992.03   11    5    0
    7  1380.88   13    6    0
    8  1828.91   15    7    0
    9  2333.62   17    8    0
   10  2892.23   19    9    0
   11  2910.81    1    0    1
   12  2972.41    3    1    1
   13  3095.22    5    2    1
   14  3278.49    7    3    1
   15  3501.71   21   10    0
   16  3521.09    9    4    1
   17  3821.57   11    5    1
   18  4158.76   23   11    0
   19  4178.08   13    6    1
   20  4588.49   15    7    1
   21  4859.89   25   12    0
   22  5050.34   17    8    1
   23  5514.85    1    0    2
   24  5560.90   19    9    1
   25  5570.96    3    1    2
   26  5601.42   27   13    0
   27  5682.81    5    2    2
   28  5849.65    7    3    2
   29  6070.37    9    4    2
   30  6117.14   21   10    1
   31  6343.53   11    5    2
   32  6379.45   29   14    0
   33  6667.31   13    6    2
   34  6715.80   23   11    1
   35  7039.58   15    7    2
   36  7189.98   31   15    0
   37  7353.40   25   12    1
   38  7457.90   17    8    2
   39  7810.64    1    0    3
   40  7861.16    3    1    3
   41  7919.52   19    9    2
   42  7961.81    5    2    3
   43  8026.21   27   13    1
   44  8028.81   33   16    0
   45  8111.87    7    3    3
   46  8310.21    9    4    3
   47  8421.41   21   10    2
   48  8555.38   11    5    3
   49  8730.32   29   14    1
   50  8845.55   13    6    3
   51  8891.61   35   17    0
   52  8960.27   23   11    2
   53  9178.58   15    7    3
   54  9461.58   31   15    1
   55  9532.52   25   12    2
   56  9551.96   17    8    3
   57  9773.92   37   18    0
   58  9793.00    1    0    4
   59  9837.71    3    1    4
   60  9926.75    5    2    4
   61  9962.90   19    9    3
   62 10059.36    7    3    4
   63 10134.31   27   13    2
   64 10215.67   33   16    1

```

65	10234.41	9	4	4
66	10408.25	21	10	3
67	10450.39	11	5	4
68	10671.07	39	19	0
69	10705.44	13	6	4
70	10761.54	29	14	2
71	10884.55	23	11	3
72	10987.99	35	17	1
73	10997.31	15	7	4
74	11323.40	17	8	4
75	11388.03	25	12	3
76	11409.78	31	15	2
77	11453.70	1	0	5
78	11492.29	3	1	5
79	11569.08	5	2	5
80	11578.24	41	20	0
81	11680.73	19	9	4
82	11683.27	7	3	5
83	11773.71	37	18	1
84	11833.66	9	4	5
85	11914.53	27	13	3
86	12018.66	11	5	5
87	12065.94	21	10	4
88	12074.27	33	16	2
89	12236.27	13	6	5
90	12459.48	29	14	3
91	12475.24	23	11	4
92	12484.07	15	7	5
93	12490.32	43	21	0
94	12567.62	39	19	1
95	12749.82	35	17	2
96	12759.20	17	8	5
97	12781.76	1	0	6
98	12813.78	3	1	6
99	12877.39	5	2	6
100	12904.36	25	12	4
101	12971.72	7	3	6
102	13017.83	31	15	3
103	13058.36	19	9	5
104	13095.46	9	4	6
105	13246.84	11	5	6
106	13348.46	27	13	4
107	13364.06	41	20	1
108	13377.67	21	10	5
109	13401.89	45	22	0
110	13423.63	13	6	6
111	13430.67	37	18	2
112	13583.87	33	16	3
113	13623.06	15	7	6
114	13712.64	23	11	5
115	13766.43	1	0	7
116	13791.30	3	1	7
117	13801.97	29	14	4
118	13840.53	5	2	7
119	13841.79	17	8	6
120	13913.15	7	3	7
121	14007.63	9	4	7
122	14057.97	25	12	5
123	14075.78	19	9	6
124	14110.24	39	19	2
125	14121.93	11	5	7
126	14150.91	35	17	3
127	14156.66	43	21	1
128	14253.34	13	6	7
129	14258.22	31	15	4
130	14306.98	47	23	0
131	14320.11	21	10	6
132	14398.44	15	7	7
133	14406.03	1	0	8
134	14407.14	27	13	5
135	14423.17	3	1	8
136	14456.87	5	2	8
137	14505.95	7	3	8
138	14552.89	17	8	7
139	14568.57	23	11	6
140	14568.61	9	4	8
141	14642.29	11	5	8
142	14708.86	33	16	4
143	14710.74	37	18	3
144	14710.94	19	9	7
145	14723.55	13	6	8
146	14733.02	1	0	9
147	14742.63	3	1	9
148	14751.74	29	14	5
149	14761.22	5	2	9
150	14780.59	41	20	2
151	14787.48	7	3	9
152	14807.62	15	7	8
153	14812.75	25	12	6
154	14819.35	9	4	9
155	14848.50	1	0	10
156	14852.53	3	1	10

157 14853.68 11 5 9  
 158 14859.97 5 2 10  
 159 14864.42 21 10 7  
 160 14869.46 7 3 10  
 161 14873.06 1 0 11  
 162 14873.90 3 1 11  
 !NUMBER OF RADIATIVE TRANSITIONS  
 1279  
 !TRANS + UP + LOW + EINSTEINA(s^-1) + FREQ(GHz) + E\_u(K)  
 1 2 1 0.10853484E+00 2009.56880 96.443072  
 2 3 2 0.10379910E+01 4007.50566 288.772098  
 3 4 3 0.37471929E+01 5982.32852 575.877224  
 4 5 4 0.91159184E+01 7922.76518 956.108181  
 5 6 5 0.17985857E+02 9818.02312 1427.296741  
 6 7 6 0.31102178E+02 11657.54965 1986.768233  
 7 8 7 0.49103352E+02 13431.60150 2631.380381  
 8 9 8 0.72505594E+02 15130.85513 3357.543454  
 9 10 9 0.10168996E+03 16746.79643 4161.259111  
 10 15 10 0.13689217E+03 18271.57085 5038.152052  
 11 18 15 0.17819514E+03 19697.92341 5983.498795  
 12 21 18 0.22552392E+03 21019.46852 6992.269399  
 13 26 21 0.27864282E+03 22230.25232 8059.148155  
 14 32 26 0.33715379E+03 23325.02842 9178.567689  
 15 36 32 0.40049545E+03 24298.94619 10344.727651  
 16 44 36 0.46794150E+03 25147.47576 11551.610418  
 17 51 44 0.53859708E+03 25866.24017 12792.988272  
 18 57 51 0.61139076E+03 26450.73354 14062.417250  
 19 68 57 0.68505917E+03 26896.00928 15353.215993  
 20 80 68 0.75811862E+03 27196.18547 16658.420852  
 21 93 80 0.82881388E+03 27343.69835 17970.705179  
 22 12 1 0.28201900E+03 89110.55005 4276.611062  
 23 12 11 0.12218413E+00 1846.54167 4276.611062  
 24 13 2 0.33966121E+03 90782.67246 4453.303535  
 25 13 12 0.11083740E+01 3681.69122 4453.303535  
 26 14 3 0.36320511E+03 92269.46318 4716.986923  
 27 14 13 0.39058675E+01 5494.29638 4716.986923  
 28 16 4 0.37376148E+03 93560.36950 5066.045488  
 29 16 14 0.94120556E+01 7273.23484 5066.045488  
 30 17 5 0.37708540E+03 94645.52826 5498.355604  
 31 17 16 0.18446378E+02 9007.92394 5498.355604  
 32 19 6 0.37540872E+03 95515.55596 6011.298710  
 33 19 17 0.31730005E+02 10688.05082 6011.298710  
 34 20 7 0.36980686E+03 96161.78858 6601.784329  
 35 20 19 0.49867397E+02 12303.78227 6601.784329  
 36 22 8 0.36089473E+03 96576.17071 7266.283588  
 37 22 20 0.73329252E+02 13845.98362 7266.283588  
 38 24 9 0.34908235E+03 96751.27948 8000.850518  
 39 24 22 0.10243704E+03 15305.96390 8000.850518  
 40 30 10 0.33468331E+03 96680.13274 8801.151686  
 41 30 24 0.13734956E+03 16675.64969 8801.151686  
 42 34 15 0.31796548E+03 96356.10805 9662.493968  
 43 34 30 0.17805188E+03 17947.54617 9662.493968  
 44 37 18 0.29917614E+03 95772.84684 10579.848720  
 45 37 34 0.22434674E+03 19114.66219 10579.848720  
 46 43 21 0.27855517E+03 94923.80162 11547.871774  
 47 43 37 0.27584776E+03 20170.42331 11547.871774  
 48 49 26 0.25634221E+03 93802.09816 12560.917539  
 49 49 43 0.33197325E+03 21108.54886 12560.917539  
 50 54 32 0.23278120E+03 92399.90887 13613.042890  
 51 54 49 0.39193850E+03 21922.83913 13613.042890  
 52 64 36 0.20812406E+03 90707.86225 14697.997807  
 53 64 54 0.45474338E+03 22606.89957 14697.997807  
 54 72 44 0.18263505E+03 88714.12849 15809.196898  
 55 72 64 0.51915058E+03 23153.74200 15809.196898  
 56 83 51 0.15659722E+03 86403.05541 16939.661263  
 57 83 72 0.58364686E+03 23555.16710 16939.661263  
 58 94 57 0.13032326E+03 83753.14191 18081.915054  
 59 94 83 0.64637347E+03 23800.82004 18081.915054  
 60 107 68 0.10417443E+03 80733.71621 19227.804905  
 61 107 94 0.70499792E+03 23876.58359 19227.804905  
 62 25 1 0.31387503E+02 167013.18218 8015.330012  
 63 25 11 0.45005401E+03 79749.17380 8015.330012  
 64 25 23 0.15457403E+00 1682.13548 8015.330012  
 65 27 2 0.39474452E+02 168356.69608 8176.251838  
 66 27 12 0.53955192E+03 81255.71484 8176.251838  
 67 27 25 0.12415412E+01 3353.08271 8176.251838  
 68 28 3 0.44154547E+02 169350.93978 8416.296810  
 69 28 13 0.57379728E+03 82575.77298 8416.296810  
 70 28 27 0.41782094E+01 5001.74936 8416.296810  
 71 29 4 0.47615561E+02 169985.85824 8733.873071  
 72 29 14 0.58667938E+03 83698.72358 8733.873071  
 73 29 28 0.98114343E+01 6617.24698 8733.873071  
 74 31 5 0.50435494E+02 170252.05595 9126.879443  
 75 31 16 0.58745078E+03 84614.45163 9126.879443  
 76 31 29 0.18899090E+02 8188.96290 9126.879443  
 77 33 6 0.52820753E+02 170140.66807 9592.722253  
 78 33 17 0.57971568E+03 85313.16293 9592.722253  
 79 33 31 0.32095904E+02 9706.63524 9592.722253  
 80 35 7 0.54853759E+02 169643.52823 10128.334908  
 81 35 19 0.56523230E+03 85785.52192 10128.334908  
 82 35 33 0.49937735E+02 11160.40981 10128.334908  
 83 38 8 0.56565704E+02 168752.80287 10730.199184

84	38	20	0.54503391E+03	86022.61578	10730.199184
85	38	35	0.72822917E+02	12540.87613	10730.199184
86	41	9	0.57963267E+02	167460.98817	11394.365224
87	41	22	0.51984200E+03	86015.67259	11394.365224
88	41	38	0.10099129E+03	13839.04043	11394.365224
89	47	10	0.59039936E+02	165760.53237	12116.472261
90	47	24	0.49024170E+03	85756.04932	12116.472261
91	47	41	0.13450256E+03	15046.34064	12116.472261
92	52	15	0.59781227E+02	163643.49097	12891.763721
93	52	30	0.45676309E+03	85234.92909	12891.763721
94	52	47	0.17321581E+03	16154.52945	12891.763721
95	55	18	0.60167087E+02	161101.13700	13715.097296
96	55	34	0.41992120E+03	84442.95236	13715.097296
97	55	52	0.21677088E+03	17155.56945	13715.097296
98	63	21	0.60172707E+02	158123.11564	14580.946094
99	63	37	0.38023750E+03	83369.73733	14580.946094
100	63	55	0.26457102E+03	18041.44717	14580.946094
101	70	26	0.59768161E+02	154696.71569	15483.384397
102	70	43	0.33825425E+03	82003.16639	15483.384397
103	70	63	0.31576391E+03	18803.85236	15483.384397
104	76	32	0.58916782E+02	150805.48753	16416.055288
105	76	49	0.29454830E+03	80328.41779	16416.055288
106	76	70	0.36921569E+03	19433.80026	16416.055288
107	88	36	0.57571853E+02	146427.45938	17372.104034
108	88	54	0.24974918E+03	78326.49669	17372.104034
109	88	76	0.42346871E+03	19920.91804	17372.104034
110	95	44	0.55670625E+02	141532.42114	18344.063131
111	95	64	0.20456629E+03	75972.03465	18344.063131
112	95	88	0.47666690E+03	20252.43753	18344.063131
113	111	51	0.53123722E+02	136077.50850	19323.647709
114	111	72	0.15983230E+03	73229.62019	19323.647709
115	111	95	0.52641607E+03	20411.32753	19323.647709
116	124	57	0.49795730E+02	129999.58756	20301.383870
117	124	83	0.11657637E+03	70047.26569	20301.383870
118	124	111	0.56950448E+03	20372.81260	20301.383870
119	40	1	0.46218947E+01	235671.54299	11310.396014
120	40	11	0.82225139E+02	148407.53460	11310.396014
121	40	23	0.51232962E+03	70340.49629	11310.396014
122	40	39	0.23670935E+00	1514.38361	11310.396014
123	42	2	0.59694973E+01	236679.55915	11455.216565
124	42	12	0.10276001E+03	149578.57791	11455.216565
125	42	25	0.61051746E+03	71675.94578	11455.216565
126	42	40	0.15271124E+01	3017.58497	11455.216565
127	45	3	0.68576409E+01	237170.56224	11671.109911
128	45	13	0.11417456E+03	150395.39543	11671.109911
129	45	27	0.64465252E+03	72821.37181	11671.109911
130	45	42	0.46987691E+01	4498.50875	11671.109911
131	46	4	0.75983904E+01	237134.43425	11956.481175
132	46	14	0.12224483E+03	150847.29959	11956.481175
133	46	28	0.65361078E+03	73765.82298	11956.481175
134	46	45	0.10479059E+02	5946.20053	11956.481175
135	48	5	0.82768753E+01	236561.59681	12309.220401
136	48	16	0.12849049E+03	150923.99249	12309.220401
137	48	29	0.64800518E+03	74498.50376	12309.220401
138	48	46	0.19498181E+02	7349.92775	12309.220401
139	50	6	0.89259891E+01	235442.77436	12726.714207
140	50	17	0.13344705E+03	150615.26922	12726.714207
141	50	31	0.63197397E+03	75008.74153	12726.714207
142	50	48	0.32289215E+02	8699.20067	12726.714207
143	53	7	0.95609295E+01	233769.04506	13205.859741
144	53	19	0.13732042E+03	149911.03875	13205.859741
145	53	33	0.60755957E+03	75285.92664	13205.859741
146	53	50	0.49277446E+02	9983.82034	13205.859741
147	56	8	0.10189004E+02	231531.27723	13743.076481
148	56	20	0.14017936E+03	148801.09015	13743.076481
149	56	35	0.57601074E+03	75319.35050	13743.076481
150	56	53	0.70757436E+02	11193.83367	13743.076481
151	61	9	0.10812978E+02	228719.93448	14334.317023
152	61	22	0.14202576E+03	147274.61890	14334.317023
153	61	38	0.53826855E+03	75097.98675	14334.317023
154	61	56	0.96860023E+02	12319.51238	14334.317023
155	66	10	0.11432345E+02	225324.38318	14975.072691
156	66	24	0.14282356E+03	145319.90013	14975.072691
157	66	41	0.49517453E+03	74610.19144	14975.072691
158	66	61	0.12751459E+03	13351.24513	14975.072691
159	71	15	0.12043822E+02	221332.16693	15660.370379
160	71	30	0.14251061E+03	142923.60505	15660.370379
161	71	47	0.44756686E+03	73843.20541	15660.370379
162	71	66	0.16240989E+03	14279.35461	15660.370379
163	75	18	0.12641503E+02	216728.08327	16384.757003
164	75	34	0.14100169E+03	140069.89663	16384.757003
165	75	52	0.39632769E+03	72782.51571	16384.757003
166	75	71	0.20095568E+03	15093.83975	16384.757003
167	85	21	0.13216676E+02	211492.52877	17142.261812
168	85	37	0.13818604E+03	136739.15046	17142.261812
169	85	55	0.34241051E+03	71410.86029	17142.261812
170	85	75	0.24224262E+03	15783.91402	17142.261812
171	90	26	0.13757098E+02	205599.58637	17926.325309
172	90	43	0.13391995E+03	132906.03707	17926.325309
173	90	63	0.28686650E+03	69706.72304	17926.325309
174	90	85	0.28499232E+03	16337.30992	17926.325309
175	102	32	0.14245090E+02	199013.59875	18729.668757

176	102	49	0.12801388E+03	128536.52901	18729.668757
177	102	70	0.23087252E+03	67641.91148	18729.668757
178	102	90	0.32747988E+03	16739.04080	18729.668757
179	112	36	0.14653088E+02	191683.98194	19544.064260
180	112	54	0.12021122E+03	123583.01926	19544.064260
181	112	76	0.17580543E+03	65177.44060	19544.064260
182	112	102	0.36739420E+03	16969.32938	19544.064260
183	126	44	0.14933301E+02	183536.04174	20359.909425
184	126	64	0.11015115E+03	117975.65525	20359.909425
185	126	88	0.12333148E+03	62256.05813	20359.909425
186	126	112	0.40155780E+03	16999.53557	20359.909425
187	143	51	0.14991896E+02	174453.08694	21165.376267
188	143	72	0.97292258E+02	111605.19863	21165.376267
189	143	95	0.75597547E+02	58786.90597	21165.376267
190	143	126	0.42529042E+03	16783.28537	21165.376267
191	59	1	0.10643275E+01	294927.18016	14154.204593
192	59	11	0.17009283E+02	207663.17178	14154.204593
193	59	23	0.13833460E+03	129596.13346	14154.204593
194	59	39	0.48000803E+03	60770.02079	14154.204593
195	59	58	0.42679627E+00	1340.36009	14154.204593
196	60	2	0.13844875E+01	295586.94242	14282.311672
197	60	12	0.21769949E+02	208455.96117	14282.311672
198	60	25	0.17159011E+03	130583.32904	14282.311672
199	60	40	0.56713216E+03	61924.96824	14282.311672
200	60	59	0.20680768E+01	2669.33106	14282.311672
201	62	3	0.15978390E+01	295555.00853	14473.108120
202	62	13	0.24825069E+02	208779.84172	14473.108120
203	62	27	0.18912865E+03	131205.81810	14473.108120
204	62	42	0.59290361E+03	62882.95504	14473.108120
205	62	60	0.55720679E+01	3975.57177	14473.108120
206	65	4	0.17769097E+01	294820.52300	14724.963667
207	65	14	0.27273780E+02	208533.38834	14724.963667
208	65	28	0.20074936E+03	131451.91174	14724.963667
209	65	45	0.59413814E+03	63632.28928	14724.963667
210	65	62	0.11461296E+02	5247.84299	14724.963667
211	67	5	0.19438289E+01	293372.77126	15035.713828
212	67	16	0.29448516E+02	207735.16694	15035.713828
213	67	29	0.20900189E+03	131309.67820	15035.713828
214	67	46	0.58085375E+03	64161.10219	15035.713828
215	67	65	0.20170571E+02	6475.01344	15035.713828
216	69	6	0.21095262E+01	291200.80788	15402.665081
217	69	17	0.31465717E+02	206373.30274	15402.665081
218	69	31	0.21475031E+03	130766.77505	15402.665081
219	69	48	0.55694724E+03	64457.23419	15402.665081
220	69	67	0.32064399E+02	7646.05974	15402.665081
221	73	7	0.22811785E+01	288293.28571	15822.598177
222	73	19	0.33374481E+02	204435.27940	15822.598177
223	73	33	0.21828799E+03	129810.16729	15822.598177
224	73	50	0.52438564E+03	64508.06100	15822.598177
225	73	69	0.47425299E+02	8750.02748	15822.598177
226	74	8	0.24640595E+01	284637.61648	16291.766705
227	74	20	0.35192973E+02	201907.42940	16291.766705
228	74	35	0.21966680E+03	128425.68975	16291.766705
229	74	53	0.48447392E+03	64300.17292	16291.766705
230	74	73	0.66416140E+02	9775.93226	16291.766705
231	81	9	0.26619555E+01	280219.34119	16805.887013
232	81	22	0.36920385E+02	198774.02561	16805.887013
233	81	38	0.21881826E+03	126597.39345	16805.887013
234	81	56	0.43833699E+03	63818.91908	16805.887013
235	81	74	0.89024409E+02	10712.57984	16805.887013
236	87	10	0.28771421E+01	275020.82604	17360.114475
237	87	24	0.38540354E+02	195016.34300	17360.114475
238	87	41	0.21560329E+03	124306.63431	17360.114475
239	87	61	0.38712835E+03	63047.68799	17360.114475
240	87	81	0.11499646E+03	11548.28129	17360.114475
241	91	15	0.31101919E+01	269019.67356	17948.998887
242	91	30	0.40020121E+02	190611.11167	17948.998887
243	91	47	0.20983178E+03	121530.71204	17948.998887
244	91	66	0.33212715E+03	61966.86123	17948.998887
245	91	87	0.14376702E+03	12270.41837	17948.998887
246	100	18	0.33596370E+01	262186.44110	18566.403749
247	100	34	0.41305969E+02	185528.25646	18566.403749
248	100	52	0.20126559E+03	118240.87355	18566.403749
249	100	71	0.27478982E+03	60552.19759	18566.403749
250	100	91	0.17438339E+03	12864.69096	18566.403749
251	106	21	0.36213208E+01	254480.86956	19205.366998
252	106	37	0.42313437E+02	179727.49125	19205.366998
253	106	55	0.18960961E+03	114399.20108	19205.366998
254	106	75	0.21679109E+03	58772.25481	19205.366998
255	106	100	0.20541425E+03	13313.89698	19205.366998
256	117	26	0.38869080E+01	245846.33412	19857.855405
257	117	43	0.42908004E+02	173152.78482	19857.855405
258	117	63	0.17449050E+03	109953.47080	19857.855405
259	117	85	0.16007936E+03	56584.05767	19857.855405
260	117	106	0.23481378E+03	13595.71688	19857.855405
261	129	32	0.41399942E+01	236199.56744	20514.305322
262	129	49	0.42865141E+02	165722.49770	20514.305322
263	129	70	0.15541696E+03	104827.88017	20514.305322
264	129	90	0.10697091E+03	53925.00949	20514.305322
265	129	117	0.28966806E+03	13678.26174	20514.305322
266	142	36	0.43446701E+01	225410.40532	21162.669624
267	142	54	0.41775290E+02	157309.44264	21162.669624

268	142	76	0.13169386E+03	98903.86398	21162.669624
269	142	102	0.60317105E+02	50695.75276	21162.669624
270	142	129	0.27560808E+03	13509.78407	21162.669624
271	78	1	0.39851518E+00	344530.30064	16534.767630
272	78	11	0.49491067E+01	257266.29225	16534.767630
273	78	23	0.37412247E+02	179199.25394	16534.767630
274	78	39	0.18164964E+03	110373.14126	16534.767630
275	78	58	0.37439483E+03	50943.48056	16534.767630
276	78	77	0.81149461E+00	1156.99203	16534.767630
277	79	2	0.50919482E+00	344822.78116	16645.248048
278	79	12	0.63905142E+01	257721.79991	16645.248048
279	79	25	0.47523957E+02	179819.16778	16645.248048
280	79	40	0.22307429E+03	111160.80697	16645.248048
281	79	59	0.43662709E+03	51905.16980	16645.248048
282	79	78	0.29298217E+01	2302.04932	16645.248048
283	82	3	0.57334453E+00	344238.51563	16809.536885
284	82	13	0.73257272E+01	257463.34983	16809.536885
285	82	27	0.53692182E+02	179889.32521	16809.536885
286	82	42	0.24318353E+03	111566.46215	16809.536885
287	82	60	0.44969175E+03	52659.07888	16809.536885
288	82	79	0.67286715E+01	3423.24014	16809.536885
289	84	4	0.61967065E+00	342764.79287	17025.914808
290	84	14	0.80932008E+01	256477.65821	17025.914808
291	84	28	0.58486620E+02	179396.18161	17025.914808
292	84	45	0.25496529E+03	111576.55916	17025.914808
293	84	62	0.44272868E+03	53192.11287	17025.914808
294	84	82	0.12459162E+02	4508.60576	17025.914808
295	86	5	0.65839124E+00	340388.18516	17292.087125
296	86	16	0.87919007E+01	254750.58084	17292.087125
297	86	29	0.62580862E+02	178325.09211	17292.087125
298	86	46	0.26172678E+03	111176.51610	17292.087125
299	86	65	0.42358134E+03	53490.42735	17292.087125
300	86	84	0.20334565E+02	5546.15748	17292.087125
301	89	6	0.69573789E+00	337093.88276	17605.174855
302	89	17	0.94661180E+01	252266.37762	17605.174855
303	89	31	0.66201305E+02	176659.84993	17605.174855
304	89	48	0.26450907E+03	110350.30907	17605.174855
305	89	67	0.39530238E+03	53539.13463	17605.174855
306	89	86	0.30544904E+02	6523.72072	17605.174855
307	92	7	0.73649672E+00	332865.16924	17961.701068
308	92	19	0.10140752E+02	249007.16293	17961.701068
309	92	33	0.69412244E+02	174382.05082	17961.701068
310	92	50	0.26358169E+03	109079.94453	17961.701068
311	92	69	0.35955957E+03	53321.91101	17961.701068
312	92	89	0.43220742E+02	7428.83612	17961.701068
313	96	8	0.78450151E+00	327681.98548	18357.560808
314	96	20	0.10830107E+02	244951.79840	18357.560808
315	96	35	0.72194309E+02	171470.05875	18357.560808
316	96	53	0.25889039E+03	107344.54192	18357.560808
317	96	73	0.31769067E+03	52820.30127	18357.560808
318	96	92	0.58363884E+02	8248.41774	18357.560808
319	103	9	0.84262926E+00	321519.47570	18787.971460
320	103	22	0.11539541E+02	240074.16012	18787.971460
321	103	38	0.74466596E+02	167897.52796	18787.971460
322	103	56	0.25022618E+03	105119.05359	18787.971460
323	103	74	0.27110936E+03	52012.71435	18787.971460
324	103	96	0.75757741E+02	8968.34534	18787.971460
325	108	10	0.91258967E+00	314345.34625	19247.384839
326	108	24	0.12264089E+02	234340.86320	19247.384839
327	108	41	0.76086478E+02	163631.15451	19247.384839
328	108	61	0.23729839E+03	102372.20819	19247.384839
329	108	81	0.22147770E+03	50872.80149	19247.384839
330	108	103	0.94864088E+02	9572.66698	19247.384839
331	114	15	0.99447604E+00	306116.07625	19729.336982
332	114	30	0.12984092E+02	227707.51437	19729.336982
333	114	47	0.76833437E+02	158627.11473	19729.336982
334	114	66	0.21976857E+03	99063.26393	19729.336982
335	114	87	0.17078356E+03	49366.82106	19729.336982
336	114	108	0.11470487E+03	10042.30086	19729.336982
337	122	18	0.10858244E+01	296770.71791	20226.179388
338	122	34	0.13655196E+02	220112.53326	20226.179388
339	122	52	0.76370649E+02	152825.15035	20226.179388
340	122	71	0.19726654E+03	95136.47439	20226.179388
341	122	91	0.12138482E+03	47448.96776	20226.179388
342	122	114	0.13371208E+03	10352.56507	20226.179388
343	134	21	0.11794444E+01	286219.37335	20728.567721
344	134	37	0.14184938E+02	211465.99504	20728.567721
345	134	55	0.74160710E+02	146137.70487	20728.567721
346	134	75	0.16939543E+03	90510.75861	20728.567721
347	134	100	0.76055960E+02	45052.40077	20728.567721
348	134	122	0.14948862E+03	10468.12397	20728.567721
349	148	26	0.12574158E+01	274319.87950	21224.363580
350	148	43	0.14370424E+02	201626.33020	21224.363580
351	148	63	0.69255936E+02	138427.01617	21224.363580
352	148	85	0.13569956E+03	85057.60305	21224.363580
353	148	106	0.38057790E+02	42069.26226	21224.363580
354	148	134	0.15828327E+03	10330.75846	21224.363580
355	98	1	0.22273207E+00	384147.37331	18436.078231
356	98	11	0.20088195E+01	296883.36492	18436.078231
357	98	23	0.12666905E+02	218816.32661	18436.078231
358	98	39	0.61938887E+02	149990.21394	18436.078231
359	98	58	0.19095653E+03	90560.55323	18436.078231

360	98	77	0.23075477E+03	40774.06470	18436.078231
361	98	97	0.14027405E+01	959.96543	18436.078231
362	99	2	0.27496396E+00	384044.77234	18527.597819
363	99	12	0.25707237E+01	296943.79109	18527.597819
364	99	25	0.16252006E+02	219041.15896	18527.597819
365	99	40	0.77767324E+02	150382.79816	18527.597819
366	99	59	0.23110400E+03	91127.16098	18527.597819
367	99	78	0.26338499E+03	41524.04050	18527.597819
368	99	98	0.39075176E+01	1906.96783	18527.597819
369	101	3	0.29593287E+00	382865.22092	18663.317573
370	101	13	0.29080367E+01	296090.05412	18663.317573
371	101	27	0.18528995E+02	218516.03050	18663.317573
372	101	42	0.86779850E+02	150193.16743	18663.317573
373	101	60	0.24776414E+03	91285.78417	18663.317573
374	101	79	0.26472247E+03	42049.94543	18663.317573
375	101	99	0.76016679E+01	2827.95425	18663.317573
376	104	4	0.30326045E+00	380592.55726	18841.352563
377	104	14	0.31626789E+01	294305.42260	18841.352563
378	104	28	0.20363817E+02	217223.94599	18841.352563
379	104	45	0.93249295E+02	149404.32354	18841.352563
380	104	62	0.25472439E+03	91019.87725	18841.352563
381	104	82	0.25305111E+03	42336.37014	18841.352563
382	104	101	0.12503163E+02	3709.66485	18841.352563
383	105	5	0.30411593E+00	377208.23917	19059.162638
384	105	16	0.33806785E+01	291570.63485	19059.162638
385	105	29	0.21993658E+02	215145.14611	19059.162638
386	105	46	0.98228660E+02	147996.57011	19059.162638
387	105	65	0.25535119E+03	90310.48135	19059.162638
388	105	84	0.23318478E+03	42366.21148	19059.162638
389	105	104	0.18672211E+02	4538.44710	19059.162638
390	110	6	0.30321476E+00	372690.18695	19313.519919
391	110	17	0.35860065E+01	287862.68181	19313.519919
392	110	31	0.23504233E+02	212256.15412	19313.519919
393	110	48	0.10198820E+03	145946.61326	19313.519919
394	110	67	0.25057363E+03	89135.43882	19313.519919
395	110	86	0.20711101E+03	42120.02491	19313.519919
396	110	105	0.26169640E+02	5299.97091	19313.519919
397	113	7	0.30405163E+00	367011.37431	19600.452680
398	113	19	0.37934563E+01	283153.36800	19600.452680
399	113	33	0.24918136E+02	208528.25589	19600.452680
400	113	50	0.10449049E+03	143226.14960	19600.452680
401	113	69	0.24052422E+03	87468.11608	19600.452680
402	113	89	0.17623825E+03	41575.04120	19600.452680
403	113	110	0.34972116E+02	5978.73701	19600.452680
404	119	8	0.30907950E+00	360137.08229	19915.152408
405	119	20	0.40105554E+01	277406.89520	19915.152408
406	119	35	0.26211677E+02	203925.15555	19915.152408
407	119	53	0.10551199E+03	139799.63872	19915.152408
408	119	73	0.22505620E+03	85275.39807	19915.152408
409	119	92	0.14209240E+03	40703.51454	19915.152408
410	119	113	0.44866794E+02	6557.30947	19915.152408
411	123	9	0.31962611E+00	352021.14373	20251.813710
412	123	22	0.42358766E+01	270575.82815	20251.813710
413	123	38	0.27307793E+02	198399.19599	20251.813710
414	123	56	0.10465978E+03	135620.72163	20251.813710
415	123	74	0.20396527E+03	82514.38238	20251.813710
416	123	96	0.10656415E+03	39470.01338	20251.813710
417	123	119	0.55327338E+02	7014.91657	20251.813710
418	131	10	0.33552277E+00	342599.16114	20603.347664
419	131	24	0.44539429E+01	262594.67809	20603.347664
420	131	41	0.28049554E+02	191884.96940	20603.347664
421	131	61	0.10133127E+03	130626.02309	20603.347664
422	131	81	0.17711922E+03	79126.61638	20603.347664
423	131	103	0.71980383E+02	37826.48187	20603.347664
424	131	123	0.65361504E+02	7324.81384	20603.347664
425	139	15	0.35397661E+00	331776.12397	20960.819206
426	139	30	0.46223607E+01	253367.56209	20960.819206
427	139	47	0.28135819E+02	184287.16245	20960.819206
428	139	66	0.94597387E+02	124723.31165	20960.819206
429	139	87	0.14456126E+03	75026.86878	20960.819206
430	139	108	0.41085197E+02	35702.34858	20960.819206
431	139	131	0.73291338E+02	7448.53369	20960.819206
432	153	18	0.36607841E+00	319398.69444	21312.145836
433	153	34	0.46334589E+01	242740.50980	21312.145836
434	153	52	0.26937564E+02	175453.12689	21312.145836
435	153	71	0.82862092E+02	117764.45093	21312.145836
436	153	91	0.10656708E+03	70076.94430	21312.145836
437	153	114	0.16945098E+02	32980.54161	21312.145836
438	153	139	0.76293750E+02	7320.49389	21312.145836
439	116	1	0.14711979E+00	413452.63769	19842.502434
440	116	11	0.10069723E+01	326188.62931	19842.502434
441	116	23	0.52267333E+01	248121.59100	19842.502434
442	116	39	0.23570751E+02	179295.47832	19842.502434
443	116	58	0.79016264E+02	119865.81762	19842.502434
444	116	77	0.14993461E+03	70079.32909	19842.502434
445	116	97	0.98302474E+02	30265.22982	19842.502434
446	116	115	0.18537458E+01	745.36499	19842.502434
447	118	2	0.17535936E+00	412919.08806	19913.339846
448	118	12	0.12623796E+01	325818.10682	19913.339846
449	118	25	0.66849522E+01	247915.47469	19913.339846
450	118	40	0.29876119E+02	179257.11388	19913.339846
451	118	59	0.97387207E+02	120001.47671	19913.339846

452	118	78	0.17712044E+03	70398.35623	19913.339846
453	118	98	0.10786110E+03	30781.28356	19913.339846
454	118	116	0.41697308E+01	1476.01917	19913.339846
455	120	3	0.17984498E+00	411088.56551	20017.818061
456	120	13	0.13888490E+01	324313.39871	20017.818061
457	120	27	0.75711284E+01	246739.37509	20017.818061
458	120	42	0.33615392E+02	178416.51202	20017.818061
459	120	60	0.10634646E+03	119509.12875	20017.818061
460	120	79	0.18444264E+03	70273.29001	20017.818061
461	120	99	0.10365598E+03	31051.29883	20017.818061
462	120	118	0.69263006E+01	2176.98311	20017.818061
463	121	4	0.17356715E+00	407938.91656	20153.764595
464	121	14	0.14611236E+01	321651.78190	20153.764595
465	121	28	0.82440265E+01	244570.30530	20153.764595
466	121	45	0.36372488E+02	176750.68285	20153.764595
467	121	62	0.11132150E+03	118366.23656	20153.764595
468	121	82	0.18284509E+03	69682.72945	20153.764595
469	121	101	0.93580161E+02	31056.02416	20153.764595
470	121	120	0.10105893E+02	2832.67958	20153.764595
471	125	5	0.16227737E+00	403442.56812	20318.205884
472	125	16	0.15053499E+01	317804.96380	20318.205884
473	125	29	0.88025002E+01	241379.47507	20318.205884
474	125	46	0.38508716E+02	174230.89906	20318.205884
475	125	65	0.11347175E+03	116544.81031	20318.205884
476	125	84	0.17484986E+03	68600.54043	20318.205884
477	125	104	0.79731750E+02	30772.77605	20318.205884
478	125	121	0.13727732E+02	3426.41674	20318.205884
479	128	6	0.14970592E+00	397564.12998	20507.275246
480	128	17	0.15351339E+01	312736.62484	20507.275246
481	128	31	0.92760104E+01	237130.09715	20507.275246
482	128	48	0.40057601E+02	170820.55629	20507.275246
483	128	67	0.11287548E+03	114009.38185	20507.275246
484	128	86	0.16113083E+03	66993.96794	20507.275246
485	128	105	0.63327962E+02	30173.91393	20507.275246
486	128	125	0.17745336E+02	3939.58498	20507.275246
487	132	7	0.13820303E+00	390256.78025	20716.050925
488	132	19	0.15563258E+01	306398.77394	20716.050925
489	132	33	0.96515834E+01	231773.66183	20716.050925
490	132	50	0.40872810E+02	166471.55554	20716.050925
491	132	69	0.10914844E+03	110713.52202	20716.050925
492	132	89	0.14194005E+03	64820.44714	20716.050925
493	132	110	0.45708565E+02	29224.14295	20716.050925
494	132	128	0.21944167E+02	4350.19992	20716.050925
495	138	8	0.12871022E+00	381455.24303	20938.257910
496	138	20	0.15652286E+01	298725.05595	20938.257910
497	138	35	0.98634091E+01	225243.31630	20938.257910
498	138	53	0.40617854E+02	161117.79947	20938.257910
499	138	73	0.10158664E+03	106593.55881	20938.257910
500	138	92	0.11762711E+03	62021.67529	20938.257910
501	138	113	0.28571117E+02	27875.47021	20938.257910
502	138	132	0.25824735E+02	4630.06427	20938.257910
503	144	9	0.12036000E+00	371062.64697	21165.657402
504	144	22	0.15414548E+01	289617.33139	21165.657402
505	144	38	0.97506619E+01	217440.69924	21165.657402
506	144	56	0.38648832E+02	154662.22487	21165.657402
507	144	74	0.89123139E+02	101555.88562	21165.657402
508	144	96	0.88930859E+02	58511.51662	21165.657402
509	144	119	0.13933188E+02	26056.41982	21165.657402
510	144	138	0.28439925E+02	4738.25907	21165.657402
511	159	10	0.10868053E+00	358917.04061	21386.478651
512	159	24	0.14238045E+01	278912.55756	21386.478651
513	159	41	0.89183183E+01	208202.84888	21386.478651
514	159	61	0.33600052E+02	146943.90256	21386.478651
515	159	81	0.69898581E+02	95444.49586	21386.478651
516	159	103	0.57108538E+02	54144.36135	21386.478651
517	159	123	0.38924536E+01	23642.69331	21386.478651
518	159	144	0.28042581E+02	4601.19007	21386.478651
519	135	1	0.88376911E-01	432395.78802	20751.625953
520	135	11	0.50685207E+00	345131.77964	20751.625953
521	135	23	0.22752783E+01	267064.74133	20751.625953
522	135	39	0.94304205E+01	198238.62865	20751.625953
523	135	58	0.31560792E+02	138808.96795	20751.625953
524	135	77	0.68693084E+02	89022.47942	20751.625953
525	135	97	0.71854606E+02	49208.38015	20751.625953
526	135	115	0.21338593E+02	19688.51532	20751.625953
527	135	133	0.14459396E+01	513.73545	20751.625953
528	136	2	0.10166888E+00	431396.42597	20800.108001
529	136	12	0.61752892E+00	344295.44472	20800.108001
530	136	25	0.28629629E+01	266392.81259	20800.108001
531	136	40	0.11889102E+02	197734.45179	20800.108001
532	136	59	0.38963953E+02	138478.81461	20800.108001
533	136	78	0.81733587E+02	88875.69414	20800.108001
534	136	98	0.80988220E+02	49258.62147	20800.108001
535	136	116	0.21490509E+02	19953.35708	20800.108001
536	136	135	0.27359179E+01	1010.20675	20800.108001
537	137	3	0.99103660E-01	428860.46058	20870.730461
538	137	13	0.65219920E+00	342085.29378	20870.730461
539	137	27	0.31613608E+01	264511.27016	20870.730461
540	137	42	0.13214358E+02	196188.40709	20870.730461
541	137	60	0.42377241E+02	137281.02382	20870.730461
542	137	79	0.85242109E+02	88045.18509	20870.730461
543	137	99	0.79410064E+02	48823.19391	20870.730461

544	137	118	0.18656730E+02	19948.87818	20870.730461
545	137	136	0.39585047E+01	1471.54027	20870.730461
546	140	4	0.89290559E-01	424756.59053	20960.881821
547	140	14	0.65026299E+00	338469.45587	20960.881821
548	140	28	0.33224929E+01	261387.97927	20960.881821
549	140	45	0.13997794E+02	193568.35682	20960.881821
550	140	62	0.43807496E+02	135183.91053	20960.881821
551	140	82	0.83897893E+02	86500.40342	20960.881821
552	140	101	0.72527198E+02	47873.69813	20960.881821
553	140	120	0.14557650E+02	19650.35354	20960.881821
554	140	137	0.51669225E+01	1878.45847	20960.881821
555	141	5	0.76289037E-01	419042.80440	21066.895593
556	141	16	0.62525368E+00	333405.20008	21066.895593
557	141	29	0.33779046E+01	256979.71135	21066.895593
558	141	46	0.14312755E+02	189831.13534	21066.895593
559	141	65	0.43493420E+02	132145.04659	21066.895593
560	141	84	0.78514403E+02	84200.77672	21066.895593
561	141	104	0.61741589E+02	46373.01233	21066.895593
562	141	121	0.98734721E+01	19026.65302	21066.895593
563	141	140	0.63258673E+01	2208.97906	21066.895593
564	145	6	0.62498793E-01	411660.67115	21183.799314
565	145	17	0.58153218E+00	326833.16601	21183.799314
566	145	31	0.33132991E+01	251226.63832	21183.799314
567	145	48	0.14041192E+02	184917.09746	21183.799314
568	145	67	0.41111484E+02	128105.92301	21183.799314
569	145	86	0.68909912E+02	81090.50911	21183.799314
570	145	105	0.47931615E+02	44270.45510	21183.799314
571	145	125	0.53484690E+01	18036.12615	21183.799314
572	145	141	0.72673610E+01	2435.88987	21183.799314
573	152	7	0.48764167E-01	402523.54136	21304.759816
574	152	19	0.51332673E+00	318665.53505	21304.759816
575	152	33	0.30596209E+01	244040.42294	21304.759816
576	152	50	0.12858347E+02	178738.31665	21304.759816
577	152	69	0.35883520E+02	122980.28313	21304.759816
578	152	89	0.54909612E+02	77087.20825	21304.759816
579	152	110	0.32247246E+02	41490.90405	21304.759816
580	152	128	0.18531750E+01	16616.96103	21304.759816
581	152	145	0.76237251E+01	2520.41986	21304.759816
582	147	1	0.37899455E-01	441972.85626	21211.250558
583	147	11	0.19984269E+00	354708.84787	21211.250558
584	147	23	0.83107751E+00	276641.80956	21211.250558
585	147	39	0.32722800E+01	207815.69689	21211.250558
586	147	58	0.10797456E+02	148386.03618	21211.250558
587	147	77	0.24517419E+02	98599.54765	21211.250558
588	147	97	0.29609715E+02	58785.44838	21211.250558
589	147	115	0.13746283E+02	29265.58356	21211.250558
590	147	133	0.11324156E+01	10090.80368	21211.250558
591	147	146	0.44095794E+00	288.09606	21211.250558
592	149	2	0.41513842E-01	440520.54018	21237.994344
593	149	12	0.23259764E+00	353419.55893	21237.994344
594	149	25	0.10062554E+01	275516.92680	21237.994344
595	149	40	0.39986551E+01	206858.56599	21237.994344
596	149	59	0.12980454E+02	147602.92882	21237.994344
597	149	78	0.28468099E+02	97999.80834	21237.994344
598	149	98	0.32649983E+02	58382.73567	21237.994344
599	149	116	0.13942876E+02	29077.47129	21237.994344
600	149	135	0.86765986E+00	10134.32096	21237.994344
601	149	147	0.75250513E+00	557.25272	21237.994344
602	151	3	0.37348242E-01	437300.42618	21275.783005
603	151	13	0.22802858E+00	350525.25938	21275.783005
604	151	27	0.10413441E+01	272951.23576	21275.783005
605	151	42	0.42020271E+01	204628.37270	21275.783005
606	151	60	0.13418523E+02	145720.98943	21275.783005
607	151	79	0.28269817E+02	96485.15069	21275.783005
608	151	99	0.30490960E+02	57263.15951	21275.783005
609	151	118	0.11814159E+02	28388.84378	21275.783005
610	151	136	0.51111104E+00	9911.50588	21275.783005
611	151	149	0.99230762E+00	787.39167	21275.783005
612	154	4	0.29617513E-01	432273.40378	21321.630250
613	154	14	0.20195085E+00	345986.26912	21321.630250
614	154	28	0.98347478E+00	268904.79252	21321.630250
615	154	45	0.40378393E+01	201085.17006	21321.630250
616	154	62	0.12649835E+02	142700.72377	21321.630250
617	154	82	0.25394326E+02	94017.21667	21321.630250
618	154	101	0.25356110E+02	55390.51138	21321.630250
619	154	120	0.86037216E+01	27167.16679	21321.630250
620	154	137	0.18413572E+00	9395.27172	21321.630250
621	154	151	0.11570452E+01	955.30612	21321.630250
622	157	5	0.20261934E-01	425379.91661	21371.027570
623	157	16	0.15755357E+00	339742.31229	21371.027570
624	157	29	0.82171796E+00	263316.82356	21371.027570
625	157	46	0.34240832E+01	196168.24755	21371.027570
626	157	65	0.10462508E+02	138482.15880	21371.027570
627	157	84	0.19778428E+02	90537.88892	21371.027570
628	157	104	0.17853399E+02	52710.12454	21371.027570
629	157	121	0.49745387E+01	25363.76523	21371.027570
630	157	140	0.97019760E-02	8546.09126	21371.027570
631	157	154	0.11662397E+01	1029.27802	21371.027570
632	156	1	0.98892630E-02	445267.67460	21369.376149
633	156	11	0.50716815E-01	358003.66622	21369.376149
634	156	23	0.20540478E+00	279936.62791	21369.376149
635	156	39	0.79360564E+00	211110.51523	21369.376149

636	156	58	0.26010346E+01	151680.85453	21369.376149
637	156	77	0.59725113E+01	101894.36600	21369.376149
638	156	97	0.75119585E+01	62080.26673	21369.376149
639	156	115	0.38870822E+01	32560.40190	21369.376149
640	156	133	0.50617059E+00	13385.62203	21369.376149
641	156	146	0.37113545E-04	3582.91440	21369.376149
642	156	155	0.40134963E-01	120.70906	21369.376149
643	158	2	0.96436065E-02	443481.16395	21380.081201
644	158	12	0.52673595E-01	356380.18270	21380.081201
645	158	25	0.22275039E+00	278477.55057	21380.081201
646	158	40	0.87168734E+00	209819.18977	21380.081201
647	158	59	0.28165299E+01	150563.55259	21380.081201
648	158	78	0.62484287E+01	100960.43212	21380.081201
649	158	98	0.74535147E+01	61343.35945	21380.081201
650	158	116	0.35469715E+01	32038.09506	21380.081201
651	158	135	0.37682707E+00	13094.94473	21380.081201
652	158	147	0.34141686E-02	3517.87649	21380.081201
653	158	156	0.69520374E-01	223.05815	21380.081201
654	160	3	0.66836745E-02	439758.27479	21393.740574
655	160	13	0.39937904E-01	352983.10798	21393.740574
656	160	27	0.17918491E+00	275409.08436	21393.740574
657	160	42	0.71510993E+00	207056.22130	21393.740574
658	160	60	0.22781232E+01	148178.83803	21393.740574
659	160	79	0.48532550E+01	98942.99929	21393.740574
660	160	99	0.54254400E+01	59721.00811	21393.740574
661	160	118	0.23284540E+01	30846.69238	21393.740574
662	160	136	0.18679700E+00	12369.35448	21393.740574
663	160	149	0.13161495E-01	3245.24027	21393.740574
664	160	158	0.80016491E-01	284.61650	21393.740574
665	162	1	0.68526242E-03	445908.31127	21400.121714
666	162	11	0.34956529E-02	358644.30288	21400.121714
667	162	23	0.14084746E-01	280577.26457	21400.121714
668	162	39	0.54214204E-01	211751.15190	21400.121714
669	162	58	0.17743421E+00	152321.49119	21400.121714
670	162	77	0.40823770E+00	102535.00266	21400.121714
671	162	97	0.51730562E+00	62720.90339	21400.121714
672	162	115	0.27289822E+00	33201.03857	21400.121714
673	162	133	0.38053055E-01	14026.25869	21400.121714
674	162	146	0.99570514E-04	4223.55106	21400.121714
675	162	155	0.47554089E-03	761.34573	21400.121714
676	162	161	0.51837642E-03	25.12845	21400.121714
677	11	2	0.82607650E+03	85254.43958	4187.991459
678	12	3	0.53971129E+03	83093.47558	4276.611062
679	13	4	0.47341886E+03	80792.83828	4453.303535
680	14	5	0.43700451E+03	78364.36948	4716.986923
681	16	6	0.40948172E+03	75819.58120	5066.045488
682	17	7	0.38525839E+03	73169.95549	5498.355604
683	19	8	0.36230188E+03	70426.40481	6011.298710
684	20	9	0.33976904E+03	67599.33196	6601.784329
685	22	10	0.31730668E+03	64698.51915	7266.283558
686	24	15	0.29479177E+03	61732.91219	8000.850518
687	30	18	0.27221867E+03	58710.63847	8801.151686
688	34	21	0.24964431E+03	55638.71612	9662.493968
689	37	26	0.22715921E+03	52523.12600	10579.848720
690	43	32	0.20487137E+03	49368.52088	11547.871774
691	49	36	0.18289700E+03	46178.12355	12560.917539
692	54	44	0.16135545E+03	42953.48692	13613.042890
693	64	51	0.14036672E+03	39694.14631	14697.997807
694	72	57	0.12005109E+03	36397.15477	15809.196898
695	83	68	0.10053056E+03	33056.31259	16939.661263
696	94	80	0.81932582E+02	29660.94715	18081.915054
697	107	93	0.64396872E+02	26193.83239	19227.804905
698	23	2	0.84768787E+02	163321.47789	7934.600624
699	23	12	0.13271786E+04	76220.49665	7934.600624
700	25	3	0.53331054E+02	160996.10771	8015.330012
701	25	13	0.86894887E+03	74220.94091	8015.330012
702	27	4	0.45141871E+02	158366.86190	8176.251838
703	27	14	0.76317560E+03	72079.72724	8176.251838
704	28	5	0.40303817E+02	155445.84608	8416.296810
705	28	16	0.70470856E+03	69808.24176	8416.296810
706	29	6	0.36623139E+02	152245.06993	8733.873071
707	29	17	0.65989024E+03	67417.56479	8733.873071
708	31	7	0.33513241E+02	148776.48318	9126.879443
709	31	19	0.61977931E+03	64918.47687	9126.879443
710	33	8	0.30756165E+02	145051.51692	9592.722253
711	33	20	0.58116163E+03	62321.32984	9592.722253
712	35	9	0.28254756E+02	141081.07161	10128.334908
713	35	22	0.54274511E+03	59635.75603	10128.334908
714	38	10	0.25959794E+02	136875.15130	10730.199184
715	38	24	0.50403338E+03	56870.66826	10730.199184
716	41	15	0.23843315E+02	132442.62088	11394.365224
717	41	30	0.46490518E+03	54034.05900	11394.365224
718	47	18	0.21887379E+02	127791.03811	12116.472261
719	47	34	0.42543018E+03	51132.85346	12116.472261
720	52	21	0.20078926E+02	122926.09903	12891.763721
721	52	37	0.38577881E+03	48172.72072	12891.763721
722	55	26	0.18407279E+02	117851.41616	13715.097296
723	55	43	0.34617501E+03	45157.86686	13715.097296
724	63	32	0.16862854E+02	112567.83491	14580.946094
725	63	49	0.30687058E+03	42090.76517	14580.946094
726	70	36	0.15436417E+02	107072.74108	15483.384397
727	70	54	0.26813201E+03	38971.77840	15483.384397

728	76	44	0.14118513E+02	101359.06558	16416.055288
729	76	64	0.23023499E+03	35798.67909	16416.055288
730	88	51	0.12898820E+02	95413.74344	17372.104034
731	88	72	0.19346486E+03	32565.85513	17372.104034
732	95	57	0.11765212E+02	89215.44743	18344.063131
733	95	83	0.15812236E+03	29263.12556	18344.063131
734	111	68	0.10702152E+02	82730.76568	19323.647709
735	111	94	0.12453593E+03	25873.63306	19323.647709
736	124	80	0.96876173E+01	75907.39281	20301.383870
737	124	107	0.93083548E+02	22369.86207	20301.383870
738	39	2	0.11822861E+02	232147.59057	11237.717408
739	39	12	0.22463482E+03	145046.60932	11237.717408
740	39	25	0.15245098E+04	67143.97719	11237.717408
741	40	3	0.72333585E+01	229654.46852	11310.396014
742	40	13	0.14205922E+03	142879.30172	11310.396014
743	40	27	0.10010720E+04	65305.27810	11310.396014
744	42	4	0.59516888E+01	226689.72497	11455.216565
745	42	14	0.12081996E+03	140402.59031	11455.216565
746	42	28	0.88074727E+03	63321.11371	11455.216565
747	45	5	0.51650554E+01	223265.46853	11671.109911
748	45	16	0.10833935E+03	137627.86421	11671.109911
749	45	29	0.81361510E+03	61202.37548	11671.109911
750	46	6	0.45638533E+01	219393.64594	11956.481175
751	46	17	0.99827875E+02	134566.14080	11956.481175
752	46	31	0.76107221E+03	58959.61311	11956.481175
753	48	7	0.40652488E+01	215086.02404	12309.220401
754	48	19	0.90744949E+02	131228.01773	12309.220401
755	48	33	0.71290015E+03	56602.90562	12309.220401
756	50	8	0.36378740E+01	210353.62322	12726.714207
757	50	20	0.83525038E+02	127623.43613	12726.714207
758	50	35	0.66549137E+03	54141.69648	12726.714207
759	53	9	0.32667516E+01	205206.58843	13205.859741
760	53	22	0.76921691E+02	123761.27285	13205.859741
761	53	38	0.61747838E+03	51584.64070	13205.859741
762	56	10	0.29430906E+01	199653.62567	13743.076481
763	56	24	0.70813973E+02	119649.14262	13743.076481
764	56	41	0.56843186E+03	48939.43393	13743.076481
765	61	15	0.26607006E+01	193701.56720	14334.317023
766	61	30	0.65135093E+02	115293.00531	14334.317023
767	61	47	0.51836843E+03	46212.60568	14334.317023
768	66	18	0.24146406E+01	187354.88891	14975.072691
769	66	34	0.59842023E+02	110696.70427	14975.072691
770	66	52	0.46753184E+03	43409.32135	14975.072691
771	71	21	0.22007313E+01	180614.77499	15660.370379
772	71	37	0.54901272E+02	105861.39668	15660.370379
773	71	55	0.41628536E+03	40533.10651	15660.370379
774	75	26	0.20154213E+01	173478.36243	16384.757003
775	75	43	0.50281625E+02	100784.81313	16384.757003
776	75	63	0.36505665E+03	37585.49910	16384.757003
777	85	32	0.18557843E+01	165937.24803	17142.261812
778	85	49	0.45949909E+02	95460.17829	17142.261812
779	85	70	0.31431077E+03	34565.56076	17142.261812
780	90	36	0.17195405E+01	157975.61176	17926.325309
781	90	54	0.41867749E+02	89874.64908	17926.325309
782	90	76	0.26454021E+03	31469.07042	17926.325309
783	102	44	0.16050268E+01	149567.17680	18729.668757
784	102	64	0.37987877E+02	84006.79031	18729.668757
785	102	88	0.21626693E+03	28287.19318	18729.668757
786	112	51	0.15110267E+01	140670.26600	19544.064260
787	112	72	0.34248285E+02	77822.37769	19544.064260
788	112	95	0.17005567E+03	25004.08503	19544.064260
789	126	57	0.14362511E+01	131219.06803	20359.909425
790	126	83	0.30561007E+02	71266.74616	20359.909425
791	126	111	0.12654194E+03	21592.29307	20359.909425
792	143	68	0.13777744E+01	121106.34412	21165.376267
793	143	94	0.26786466E+02	64249.21150	21165.376267
794	143	124	0.86485578E+02	18002.76584	21165.376267
795	58	2	0.26506771E+01	291577.25127	14089.877759
796	58	12	0.44216638E+02	204476.27002	14089.877759
797	58	25	0.38312256E+03	126573.63789	14089.877759
798	58	40	0.14473920E+04	57915.27709	14089.877759
799	59	3	0.15878163E+01	288910.10570	14154.204593
800	59	13	0.27268016E+02	202134.93889	14154.204593
801	59	27	0.24376991E+03	124560.91527	14154.204593
802	59	42	0.95471145E+03	56238.05221	14154.204593
803	60	4	0.12724007E+01	285597.10824	14282.311672
804	60	14	0.22612957E+02	199309.97358	14282.311672
805	60	28	0.20846856E+03	122228.49697	14282.311672
806	60	45	0.84226761E+03	54408.87452	14282.311672
807	62	5	0.10704009E+01	281649.91482	14473.108120
808	62	16	0.19775858E+02	196012.31050	14473.108120
809	62	29	0.18783474E+03	119586.82177	14473.108120
810	62	46	0.77861428E+03	52438.24576	14473.108120
811	65	6	0.91362686E+00	277079.73469	14724.963667
812	65	17	0.17606225E+02	192252.22955	14724.963667
813	65	31	0.17203168E+03	116645.70186	14724.963667
814	65	48	0.72713903E+03	50336.16100	14724.963667
815	67	7	0.78468618E+00	271897.19849	15035.713828
816	67	19	0.15799056E+02	188039.19218	15035.713828
817	67	33	0.15845179E+03	113414.08007	15035.713828
818	67	50	0.67820959E+03	48111.97377	15035.713828
819	69	8	0.67719810E+00	266111.65673	15402.665081

820	69	20	0.14241523E+02	183381.46965	15402.665081
821	69	35	0.14614835E+03	109899.73000	15402.665081
822	69	53	0.62854952E+03	45774.21317	15402.665081
823	73	9	0.58786396E+00	259730.82909	15822.598177
824	73	22	0.12882070E+02	178285.51351	15822.598177
825	73	38	0.13471713E+03	106108.88135	15822.598177
826	73	56	0.57707800E+03	43330.40698	15822.598177
827	74	10	0.51427059E+00	252759.96492	16291.766705
828	74	24	0.11692097E+02	172755.48187	16291.766705
829	74	41	0.12396425E+03	102045.77318	16291.766705
830	74	61	0.52365227E+03	40786.82687	16291.766705
831	81	15	0.45424428E+00	245200.97390	16805.887013
832	81	30	0.10652331E+02	166792.41202	16805.887013
833	81	47	0.11378229E+03	97712.01238	16805.887013
834	81	66	0.46858011E+03	38148.16158	16805.887013
835	87	18	0.40571350E+00	237051.33178	17360.114475
836	87	34	0.97474784E+01	160393.14713	17360.114475
837	87	52	0.10409666E+03	93105.76422	17360.114475
838	87	71	0.41239832E+03	35417.08826	17360.114475
839	91	21	0.36673995E+00	228302.28162	17948.998887
840	91	37	0.89640106E+01	153548.90331	17948.998887
841	91	55	0.94839371E+02	88220.61314	17948.998887
842	91	75	0.35576480E+03	32593.66687	17948.998887
843	100	26	0.33559239E+00	218936.72026	18566.403749
844	100	43	0.82890773E+01	146243.17096	18566.403749
845	100	63	0.85933932E+02	83043.85693	18566.403749
846	100	85	0.29940851E+03	29674.44381	18566.403749
847	106	32	0.31081653E+00	208925.58882	19205.366998
848	106	49	0.77095578E+01	138448.51908	19205.366998
849	106	70	0.77283307E+02	77553.90155	19205.366998
850	106	90	0.24411463E+03	26651.03088	19205.366998
851	117	36	0.29127344E+00	198222.35952	19857.855405
852	117	54	0.72104208E+01	130121.39683	19857.855405
853	117	76	0.68755182E+02	71715.81817	19857.855405
854	117	102	0.19073551E+03	23507.70695	19857.855405
855	129	44	0.27608276E+00	186753.14549	20514.305322
856	129	64	0.67707349E+01	121192.75900	20514.305322
857	129	88	0.60155891E+02	65473.16187	20514.305322
858	129	112	0.14022684E+03	20216.63931	20514.305322
859	142	51	0.26423429E+00	174396.68938	21162.669624
860	142	72	0.63519962E+01	111548.80107	21162.669624
861	142	95	0.51169595E+02	58730.50842	21162.669624
862	142	126	0.93715497E+02	16726.88782	21162.669624
863	77	2	0.99894937E+00	341363.73980	16479.241033
864	77	12	0.12550660E+02	254262.75856	16479.241033
865	77	25	0.98990917E+02	176360.12643	16479.241033
866	77	40	0.51191684E+03	107701.76562	16479.241033
867	77	59	0.11530294E+04	48446.12844	16479.241033
868	78	77	0.58751322E-04	1156.99203	16534.767630
869	78	3	0.58987014E+00	338513.22617	16534.767630
870	78	13	0.76021065E+01	251738.05937	16534.767630
871	78	27	0.61616694E+02	174164.03575	16534.767630
872	78	42	0.32807598E+03	105841.17268	16534.767630
873	78	60	0.76626512E+03	46933.78941	16534.767630
874	79	4	0.46016798E+00	334832.94697	16645.248048
875	79	14	0.61686084E+01	248545.81231	16645.248048
876	79	28	0.51586951E+02	171464.33571	16645.248048
877	79	45	0.28223876E+03	103644.71326	16645.248048
878	79	62	0.67916272E+03	45260.26697	16645.248048
879	82	5	0.37232087E+00	330333.42193	16809.536885
880	82	16	0.52610329E+01	244695.81761	16809.536885
881	82	29	0.45553374E+02	168270.32888	16809.536885
882	82	46	0.25543209E+03	101121.75287	16809.536885
883	82	65	0.62856414E+03	43435.66412	16809.536885
884	84	6	0.30237139E+00	325024.00456	17025.914808
885	84	17	0.45566921E+01	240196.49942	17025.914808
886	84	31	0.40952220E+02	164589.97173	17025.914808
887	84	48	0.23456666E+03	98280.43087	17025.914808
888	84	67	0.58530531E+03	41469.25643	17025.914808
889	86	7	0.24503812E+00	318912.61239	17292.087125
890	86	19	0.39731618E+01	235054.60608	17292.087125
891	86	33	0.37105909E+02	160429.49397	17292.087125
892	86	50	0.21619162E+03	95127.38768	17292.087125
893	86	69	0.54182790E+03	39369.35416	17292.087125
894	89	8	0.19857124E+00	312004.73162	17605.174855
895	89	20	0.34808815E+01	229274.54454	17605.174855
896	89	35	0.33766244E+02	155792.80489	17605.174855
897	89	53	0.19907585E+03	91667.28806	17605.174855
898	89	73	0.49579208E+03	37143.04740	17605.174855
899	92	9	0.16181242E+00	304302.71262	17961.701068
900	92	22	0.30656602E+01	222857.39703	17961.701068
901	92	38	0.30821322E+02	150680.76488	17961.701068
902	92	56	0.18270952E+03	87902.29051	17961.701068
903	92	74	0.44672778E+03	34795.95126	17961.701068
904	96	10	0.13352723E+00	295804.33392	18357.560808
905	96	24	0.27180997E+01	215799.85087	18357.560808
906	96	41	0.28208907E+02	145090.14218	18357.560808
907	96	61	0.16685284E+03	83831.19587	18357.560808
908	96	81	0.39498993E+03	32331.78917	18357.560808
909	103	15	0.11235256E+00	286501.10841	18787.971460
910	103	30	0.24302815E+01	208092.54653	18787.971460
911	103	47	0.25884770E+02	139012.14689	18787.971460

912	103	66	0.15136365E+03	79448.29609	18787.971460
913	103	87	0.34133745E+03	29751.85322	18787.971460
914	108	18	0.96900460E-01	276375.85198	19247.384839
915	108	34	0.21947993E+01	199717.66734	19247.384839
916	108	52	0.23809094E+02	132430.28442	19247.384839
917	108	71	0.13611918E+03	74741.60846	19247.384839
918	108	91	0.28674076E+03	27054.10184	19247.384839
919	114	21	0.85856675E-01	265398.68431	19729.336982
920	114	37	0.20044286E+01	190645.30600	19729.336982
921	114	55	0.21938342E+02	125317.01584	19729.336982
922	114	75	0.12097312E+03	69690.06957	19729.336982
923	114	100	0.23229701E+03	24231.71174	19729.336982
924	122	26	0.78022648E-01	253520.99707	20226.179388
925	122	43	0.18515956E+01	180827.44776	20226.179388
926	122	63	0.20215736E+02	117628.13374	20226.179388
927	122	85	0.10572130E+03	64258.72061	20226.179388
928	122	106	0.17920800E+03	21270.37982	20226.179388
929	134	32	0.72284620E-01	240664.09262	20728.567721
930	134	49	0.17267843E+01	170187.02288	20728.567721
931	134	70	0.18552058E+02	109292.40534	20728.567721
932	134	90	0.90053870E+02	58389.53467	20728.567721
933	134	117	0.12880363E+03	18142.78691	20728.567721
934	148	36	0.67437763E-01	226695.90489	21224.363580
935	148	54	0.16134200E+01	158594.94221	21224.363580
936	148	76	0.16774429E+02	100189.36355	21224.363580
937	148	102	0.73443570E+02	51981.25233	21224.363580
938	148	129	0.82606484E+02	14795.28364	21224.363580
939	97	2	0.57505583E+00	381177.83907	18390.007375
940	97	12	0.50880699E+01	294076.85783	18390.007375
941	97	25	0.32686141E+02	216174.22570	18390.007375
942	97	40	0.16756058E+03	147515.86489	18390.007375
943	97	59	0.55120458E+03	88260.22772	18390.007375
944	97	78	0.73739656E+03	38657.10724	18390.007375
945	98	97	0.51761925E-01	959.96543	18436.078231
946	98	3	0.33713397E+00	378130.29884	18436.078231
947	98	13	0.30448231E+01	291355.13204	18436.078231
948	98	27	0.20027469E+02	213781.10842	18436.078231
949	98	42	0.10539842E+03	145458.24535	18436.078231
950	98	60	0.35642497E+03	86550.86208	18436.078231
951	98	79	0.49676010E+03	37315.02335	18436.078231
952	99	4	0.25705676E+00	374054.93815	18527.597819
953	99	14	0.24214993E+01	287767.80350	18527.597819
954	99	28	0.16470987E+02	210686.32689	18527.597819
955	99	45	0.89117155E+02	142866.70444	18527.597819
956	99	62	0.30854290E+03	84482.25815	18527.597819
957	99	82	0.44394676E+03	35798.75104	18527.597819
958	101	5	0.20002321E+00	368960.12722	18663.317573
959	101	16	0.20090820E+01	283322.52290	18663.317573
960	101	29	0.14264150E+02	206897.03416	18663.317573
961	101	46	0.79402870E+02	139748.45816	18663.317573
962	101	65	0.28006257E+03	82062.36940	18663.317573
963	101	84	0.41151353E+03	34118.09953	18663.317573
964	104	6	0.15372016E+00	362851.76895	18841.352563
965	104	17	0.16821818E+01	278024.26381	18841.352563
966	104	31	0.12565410E+02	202417.73612	18841.352563
967	104	48	0.71938234E+02	136108.19526	18841.352563
968	104	67	0.25695177E+03	79297.02081	18841.352563
969	104	86	0.38080492E+03	32281.60691	18841.352563
970	105	7	0.11608798E+00	355732.66640	19059.162638
971	105	19	0.14114763E+01	271874.66009	19059.162638
972	105	33	0.11157673E+02	197249.54798	19059.162638
973	105	50	0.65584519E+02	131947.44169	19059.162638
974	105	69	0.23554717E+03	76189.40817	19059.162638
975	105	89	0.34722731E+03	30296.33328	19059.162638
976	110	8	0.86528845E-01	347601.03581	19313.519919
977	110	20	0.11870850E+01	264870.84873	19313.519919
978	110	35	0.99623054E+01	191389.10908	19313.519919
979	110	53	0.59924644E+02	127263.59225	19313.519919
980	110	73	0.21458562E+03	72739.35159	19313.519919
981	110	92	0.30977623E+03	28167.46807	19313.519919
982	113	9	0.64295178E-01	338448.91769	19600.452680
983	113	22	0.10034355E+01	257003.60211	19600.452680
984	113	38	0.89410015E+01	184826.96995	19600.452680
985	113	56	0.54763566E+02	122048.49558	19600.452680
986	113	74	0.19357503E+03	68942.15634	19600.452680
987	113	96	0.26882234E+03	25897.78733	19600.452680
988	119	10	0.48288199E-01	328259.43072	19915.152408
989	119	24	0.85541613E+00	248254.94768	19915.152408
990	119	41	0.80669273E+01	177545.23899	19915.152408
991	119	61	0.49974411E+02	116286.29267	19915.152408
992	119	81	0.17229105E+03	64786.88597	19915.152408
993	119	103	0.22537595E+03	23486.75146	19915.152408
994	123	15	0.37221235E-01	317002.77644	20251.813710
995	123	30	0.73754491E+00	238594.21456	20251.813710
996	123	47	0.73140554E+01	169513.81493	20251.813710
997	123	66	0.45433595E+02	109949.96412	20251.813710
998	123	87	0.15057627E+03	60253.52126	20251.813710
999	123	108	0.18077651E+03	20929.00105	20251.813710
1000	131	18	0.29815322E-01	304629.66687	20603.347664
1001	131	34	0.64383730E+00	227971.48223	20603.347664
1002	131	52	0.66508276E+01	160684.09931	20603.347664
1003	131	71	0.40977401E+02	102995.42335	20603.347664

1004	131	91	0.12823943E+03	55307.91673	20603.347664
1005	131	114	0.13655872E+03	18211.51403	20603.347664
1006	139	21	0.24891791E-01	291058.73203	20960.819206
1007	139	37	0.56722215E+00	216305.35372	20960.819206
1008	139	55	0.60298959E+01	150977.06355	20960.819206
1009	139	75	0.36342282E+02	95350.11729	20960.819206
1010	139	100	0.10497261E+03	49891.75945	20960.819206
1011	139	122	0.94417354E+02	15307.48265	20960.819206
1012	153	26	0.21279367E-01	276148.97360	21312.145836
1013	153	43	0.49673013E+00	203455.42430	21312.145836
1014	153	63	0.53563526E+01	140256.11028	21312.145836
1015	153	85	0.31010404E+02	86886.69715	21312.145836
1016	153	106	0.80169512E+02	43898.35636	21312.145836
1017	153	134	0.56233823E+02	12159.85257	21312.145836
1018	115	2	0.39239347E+00	410697.70390	19806.730725
1019	115	12	0.25856019E+01	323596.72265	19806.730725
1020	115	25	0.13385748E+02	245694.09052	19806.730725
1021	115	40	0.62327965E+02	177035.72971	19806.730725
1022	115	59	0.22031913E+03	117780.09254	19806.730725
1023	115	78	0.44923656E+03	68176.97206	19806.730725
1024	115	98	0.33810832E+03	28559.89939	19806.730725
1025	116	115	0.25018682E+00	745.36499	19842.502434
1026	116	3	0.22908097E+00	407435.56323	19842.502434
1027	116	13	0.15337454E+01	320660.39643	19842.502434
1028	116	27	0.81054617E+01	243066.37281	19842.502434
1029	116	42	0.38682312E+02	174763.50974	19842.502434
1030	116	60	0.14019993E+03	115856.12647	19842.502434
1031	116	79	0.29397994E+03	66620.28773	19842.502434
1032	116	99	0.23413838E+03	27398.29655	19842.502434
1033	118	4	0.17147762E+00	402929.25388	19913.339846
1034	118	14	0.11959963E+01	316642.11922	19913.339846
1035	118	28	0.65519907E+01	239560.64262	19913.339846
1036	118	45	0.32228872E+02	171741.02017	19913.339846
1037	118	62	0.11956198E+03	113356.57388	19913.339846
1038	118	82	0.25594812E+03	64673.06677	19913.339846
1039	118	101	0.21250074E+03	26046.36148	19913.339846
1040	120	5	0.12900770E+00	397183.47180	20017.818061
1041	120	16	0.96267086E+00	311545.86748	20017.818061
1042	120	29	0.55491092E+01	235120.37875	20017.818061
1043	120	46	0.28264720E+02	167971.80274	20017.818061
1044	120	65	0.10703625E+03	110285.71399	20017.818061
1045	120	84	0.23188579E+03	62341.44412	20017.818061
1046	120	104	0.19709277E+03	24513.67973	20017.818061
1047	121	6	0.94271255E-01	390198.12826	20153.764595
1048	121	17	0.77426862E+00	305370.62312	20153.764595
1049	121	31	0.47603415E+01	229764.09543	20153.764595
1050	121	48	0.25183272E+02	163454.55457	20153.764595
1051	121	67	0.96966240E+02	106643.38012	20153.764595
1052	121	86	0.21043428E+03	59627.96622	20153.764595
1053	121	105	0.17944467E+03	22807.91221	20153.764595
1054	125	7	0.66472156E-01	381966.99535	20318.205884
1055	125	19	0.61865039E+00	298108.98904	20318.205884
1056	125	33	0.41026548E+01	223483.87693	20318.205884
1057	125	50	0.22560966E+02	158181.77064	20318.205884
1058	125	69	0.87842893E+02	102423.73712	20318.205884
1059	125	89	0.18873133E+03	56530.66224	20318.205884
1060	125	110	0.15791083E+03	20934.35805	20318.205884
1061	128	8	0.45371420E-01	372474.97884	20507.275246
1062	128	20	0.49180259E+00	289744.79175	20507.275246
1063	128	35	0.35453399E+01	216263.05210	20507.275246
1064	128	53	0.20232546E+02	152137.53528	20507.275246
1065	128	73	0.79078334E+02	97613.29462	20507.275246
1066	128	92	0.16591830E+03	53041.41110	20507.275246
1067	128	113	0.13281861E+03	18895.20602	20507.275246
1068	132	9	0.30273842E-01	361694.32363	20716.050925
1069	132	22	0.39031249E+00	280249.00805	20716.050925
1070	132	38	0.30687854E+01	208072.37589	20716.050925
1071	132	56	0.18096978E+02	145293.90153	20716.050925
1072	132	74	0.70328621E+02	92187.56228	20716.050925
1073	132	96	0.14178158E+03	49143.19328	20716.050925
1074	132	119	0.10534757E+03	16688.09647	20716.050925
1075	138	10	0.20044265E-01	349577.59147	20938.257910
1076	138	24	0.30975222E+00	269573.10842	20938.257910
1077	138	41	0.26512313E+01	198863.39973	20938.257910
1078	138	61	0.16046401E+02	137604.45342	20938.257910
1079	138	81	0.61252302E+02	86105.04672	20938.257910
1080	138	103	0.11631656E+03	44804.91220	20938.257910
1081	138	123	0.77110456E+02	14303.24417	20938.257910
1082	144	15	0.13360429E-01	336044.27969	21165.657402
1083	144	30	0.24429139E+00	257635.71780	21165.657402
1084	144	47	0.22597243E+01	188555.31817	21165.657402
1085	144	66	0.13907385E+02	128991.46737	21165.657402
1086	144	87	0.51335444E+02	79295.02450	21165.657402
1087	144	108	0.89526287E+02	39970.50430	21165.657402
1088	144	131	0.49967536E+02	11716.68940	21165.657402
1089	159	18	0.88700415E-02	320947.54635	21386.478651
1090	159	34	0.18505872E+00	244289.36170	21386.478651
1091	159	52	0.18272243E+01	177001.97879	21386.478651
1092	159	71	0.11298070E+02	119313.30283	21386.478651
1093	159	91	0.39507100E+02	71625.79620	21386.478651
1094	159	114	0.61109313E+02	34529.39351	21386.478651
1095	159	139	0.25936562E+02	8869.34579	21386.478651

1096	133	2	0.24200207E+00	429872.48377	20726.970657
1097	133	12	0.13268683E+01	342771.50253	20726.970657
1098	133	25	0.58585918E+01	264868.87040	20726.970657
1099	133	40	0.24765466E+02	196210.50959	20726.970657
1100	133	59	0.86654861E+02	136954.87241	20726.970657
1101	133	78	0.20067980E+03	87351.75194	20726.970657
1102	133	98	0.23075618E+03	47734.67927	20726.970657
1103	133	116	0.87821456E+02	18429.41488	20726.970657
1104	135	133	0.27712322E+00	513.73545	20751.625953
1105	135	3	0.14022359E+00	426378.71356	20751.625953
1106	135	13	0.77919008E+00	339803.54676	20751.625953
1107	135	27	0.35064787E+01	262029.52314	20751.625953
1108	135	42	0.15185749E+02	193706.66007	20751.625953
1109	135	60	0.54436489E+02	134799.27680	20751.625953
1110	135	79	0.12913805E+03	85563.43806	20751.625953
1111	135	99	0.15383161E+03	46341.44688	20751.625953
1112	135	118	0.64822137E+02	17467.13116	20751.625953
1113	136	135	0.39245074E-04	1010.20675	20800.108001
1114	136	4	0.10263902E+00	421406.59179	20800.108001
1115	136	14	0.59317050E+00	335119.45713	20800.108001
1116	136	28	0.27734665E+01	258037.98052	20800.108001
1117	136	45	0.12424271E+02	190218.35807	20800.108001
1118	136	62	0.45657007E+02	131833.91178	20800.108001
1119	136	82	0.11024558E+03	83150.40467	20800.108001
1120	136	101	0.13427413E+03	44523.69938	20800.108001
1121	136	120	0.60558894E+02	16300.35480	20800.108001
1122	137	5	0.74247578E-01	414955.36688	20870.730461
1123	137	16	0.45922990E+00	329317.76256	20870.730461
1124	137	29	0.22741151E+01	252892.27382	20870.730461
1125	137	46	0.10626206E+02	185743.69781	20870.730461
1126	137	65	0.40009400E+02	128057.60906	20870.730461
1127	137	84	0.97564981E+02	80113.33919	20870.730461
1128	137	104	0.11959537E+03	42285.57481	20870.730461
1129	137	121	0.55647347E+02	14939.21550	20870.730461
1130	140	6	0.51121786E-01	407015.80222	20960.881821
1131	140	17	0.34948666E+00	322188.29708	20960.881821
1132	140	31	0.18666652E+01	246581.76939	20960.881821
1133	140	48	0.91543497E+01	180272.22853	20960.881821
1134	140	67	0.35237154E+02	123461.05409	20960.881821
1135	140	86	0.85956848E+02	76445.64018	20960.881821
1136	140	105	0.10416446E+03	39625.58618	20960.881821
1137	140	125	0.48127290E+02	13391.25723	20960.881821
1138	141	7	0.33091446E-01	397567.23163	21066.895593
1139	141	19	0.25913016E+00	313709.22532	21066.895593
1140	141	33	0.15169018E+01	239084.11321	21066.895593
1141	141	50	0.78321851E+01	173782.00692	21066.895593
1142	141	69	0.30687220E+02	118023.97340	21066.895593
1143	141	89	0.74026215E+02	72130.89852	21066.895593
1144	141	110	0.86899714E+02	36534.59433	21066.895593
1145	141	128	0.38220905E+02	11660.65130	21066.895593
1146	145	8	0.19993032E-01	386571.52001	21183.799314
1147	145	20	0.18607569E+00	303841.33292	21183.799314
1148	145	35	0.12084739E+01	230359.59327	21183.799314
1149	145	53	0.65663431E+01	166234.07644	21183.799314
1150	145	73	0.26005882E+02	111709.83579	21183.799314
1151	145	92	0.61164613E+02	67137.95226	21183.799314
1152	145	113	0.67910212E+02	32991.74719	21183.799314
1153	145	132	0.26976721E+02	9746.34125	21183.799314
1154	152	9	0.11121126E-01	373961.08474	21304.759816
1155	152	22	0.12704573E+00	292515.76916	21304.759816
1156	152	38	0.92147218E+00	220339.13700	21304.759816
1157	152	56	0.52468633E+01	157560.66263	21304.759816
1158	152	74	0.20793432E+02	104454.32339	21304.759816
1159	152	96	0.46836151E+02	61409.95438	21304.759816
1160	152	119	0.47728248E+02	28954.85758	21304.759816
1161	152	138	0.15838658E+02	7636.69683	21304.759816
1162	146	2	0.10672022E+00	439675.19140	21197.424193
1163	146	12	0.53643649E+00	352574.21015	21197.424193
1164	146	25	0.21784348E+01	274671.57802	21197.424193
1165	146	40	0.86831609E+01	206013.21722	21197.424193
1166	146	59	0.29802329E+02	146757.58004	21197.424193
1167	146	78	0.71707948E+02	97154.45957	21197.424193
1168	146	98	0.94223389E+02	57537.38690	21197.424193
1169	146	116	0.52004111E+02	28232.12251	21197.424193
1170	146	135	0.85925574E+01	9288.97218	21197.424193
1171	147	146	0.57092874E-01	288.09606	21211.250558
1172	147	3	0.60706797E-01	438955.78179	21211.250558
1173	147	13	0.30910840E+00	349180.61499	21211.250558
1174	147	27	0.12794087E+01	271606.59137	21211.250558
1175	147	42	0.52274689E+01	203283.72830	21211.250558
1176	147	60	0.18382649E+02	144376.34504	21211.250558
1177	147	79	0.45240786E+02	95140.50630	21211.250558
1178	147	99	0.61169585E+02	55918.51512	21211.250558
1179	147	118	0.36069660E+02	27044.19939	21211.250558
1180	147	136	0.749646818E+01	8566.86149	21211.250558
1181	149	4	0.42565876E-01	430530.70599	21237.994344
1182	149	14	0.22548404E+00	344243.57133	21237.994344
1183	149	28	0.97224845E+00	267162.09473	21237.994344
1184	149	45	0.41234394E+01	199342.47228	21237.994344
1185	149	62	0.14892753E+02	140958.02599	21237.994344
1186	149	82	0.37267514E+02	92274.51888	21237.994344
1187	149	101	0.51147953E+02	53647.81359	21237.994344

1188	149	120	0.31310196E+02	25424.46901	21237.994344
1189	149	137	0.73513125E+01	7652.57393	21237.994344
1190	151	5	0.28570358E-01	423395.33248	21275.783005
1191	151	16	0.16228375E+00	337757.72816	21275.783005
1192	151	29	0.74524938E+00	261332.23943	21275.783005
1193	151	46	0.33174264E+01	194183.66342	21275.783005
1194	151	65	0.12318128E+02	136497.57467	21275.783005
1195	151	84	0.31105835E+02	88553.30479	21275.783005
1196	151	104	0.42634801E+02	50725.54041	21275.783005
1197	151	121	0.26240381E+02	23379.18110	21275.783005
1198	151	140	0.63630265E+01	6561.50713	21275.783005
1199	154	6	0.17378593E-01	414532.61547	21321.630250
1200	154	17	0.10963656E+00	329705.11033	21321.630250
1201	154	31	0.54787826E+00	254098.58264	21321.630250
1202	154	48	0.26813303E+01	187789.04178	21321.630250
1203	154	67	0.98426421E+01	130977.86734	21321.630250
1204	154	86	0.24841631E+02	83962.45343	21321.630250
1205	154	105	0.33370117E+02	47142.39943	21321.630250
1206	154	125	0.19944610E+02	20908.07047	21321.630250
1207	154	141	0.45715266E+01	5307.83419	21321.630250
1208	157	7	0.90136502E-02	403904.34384	21371.027570
1209	157	19	0.65765111E-01	320046.33753	21371.027570
1210	157	33	0.36464938E+00	245421.22542	21371.027570
1211	157	50	0.18267574E+01	180119.11913	21371.027570
1212	157	69	0.71242903E+01	124361.08561	21371.027570
1213	157	89	0.17752150E+02	78468.01073	21371.027570
1214	157	110	0.22858364E+02	42871.70654	21371.027570
1215	157	128	0.12739741E+02	17997.76351	21371.027570
1216	157	145	0.24528051E+01	3901.22234	21371.027570
1217	155	2	0.29289558E-01	443137.39673	21363.583055
1218	155	12	0.14298786E+00	356036.41549	21363.583055
1219	155	25	0.56376136E+00	278133.78336	21363.583055
1220	155	40	0.21979104E+01	209475.42255	21363.583055
1221	155	59	0.74768710E+01	150219.78538	21363.583055
1222	155	78	0.18170431E+02	100616.66490	21363.583055
1223	155	98	0.24815425E+02	60999.59223	21363.583055
1224	155	116	0.15064318E+02	31694.32784	21363.583055
1225	155	135	0.32796322E+01	12751.17751	21363.583055
1226	155	147	0.27420253E+00	3174.10928	21363.583055
1227	156	155	0.89511886E-03	120.70906	21369.376149
1228	156	3	0.15890888E-01	439250.60014	21369.376149
1229	156	13	0.78626058E-01	352475.43334	21369.376149
1230	156	27	0.31619901E+00	274901.40971	21369.376149
1231	156	42	0.12646587E+01	206578.54665	21369.376149
1232	156	60	0.44093823E+01	147671.16338	21369.376149
1233	156	79	0.10953967E+02	98435.32464	21369.376149
1234	156	99	0.15352300E+02	59213.33346	21369.376149
1235	156	118	0.98580404E+01	30339.01774	21369.376149
1236	156	136	0.25481060E+01	11861.67983	21369.376149
1237	156	149	0.33358924E+00	2737.56562	21369.376149
1238	158	4	0.99369657E-02	433491.32977	21380.081201
1239	158	14	0.51229360E-01	347204.19511	21380.081201
1240	158	28	0.21513888E+00	270122.71850	21380.081201
1241	158	45	0.89535255E+00	202303.09605	21380.081201
1242	158	62	0.32103410E+01	143918.64976	21380.081201
1243	158	82	0.81045015E+01	95235.14265	21380.081201
1244	158	101	0.11488018E+02	56608.43736	21380.081201
1245	158	120	0.75751951E+01	28385.09278	21380.081201
1246	158	137	0.21278281E+01	10613.19771	21380.081201
1247	158	151	0.31524988E+00	2173.23210	21380.081201
1248	160	5	0.51436864E-02	425853.18108	21393.740574
1249	160	16	0.28521253E-01	340215.57676	21393.740574
1250	160	29	0.12810480E+00	263790.08803	21393.740574
1251	160	46	0.56175691E+00	196641.51202	21393.740574
1252	160	65	0.20748717E+01	138955.42327	21393.740574
1253	160	84	0.52817316E+01	91011.15339	21393.740574
1254	160	104	0.74414694E+01	53183.38901	21393.740574
1255	160	121	0.48742636E+01	25837.02970	21393.740574
1256	160	140	0.13747069E+01	9019.35573	21393.740574
1257	160	154	0.18316068E+00	1502.54249	21393.740574
1258	161	2	0.30317302E-02	443873.61401	21398.915745
1259	161	12	0.14710296E-01	356772.63277	21398.915745
1260	161	25	0.57635466E-01	278870.00064	21398.915745
1261	161	40	0.22362307E+00	210211.63983	21398.915745
1262	161	59	0.75917961E+00	150956.00265	21398.915745
1263	161	78	0.18484859E+01	101352.88218	21398.915745
1264	161	98	0.25440756E+01	61735.80951	21398.915745
1265	161	116	0.15733644E+01	32430.54512	21398.915745
1266	161	135	0.35933069E+00	13487.39479	21398.915745
1267	161	147	0.34624344E-01	3910.32656	21398.915745
1268	161	156	0.41392752E-02	615.50821	21398.915745
1269	162	3	0.11018109E-02	439891.23680	21400.121714
1270	162	13	0.54217549E-02	353116.07000	21400.121714
1271	162	27	0.21682235E-01	275542.04638	21400.121714
1272	162	42	0.86353578E-01	207219.18331	21400.121714
1273	162	60	0.30054776E+00	148311.80005	21400.121714
1274	162	79	0.74786188E+00	99075.96131	21400.121714
1275	162	99	0.10550856E+01	59853.97013	21400.121714
1276	162	118	0.68793660E+00	30979.65440	21400.121714
1277	162	136	0.18423244E+00	12502.31649	21400.121714
1278	162	149	0.26176748E-01	3378.20229	21400.121714
1279	162	158	0.36272902E-02	417.57851	21400.121714

## APPENDIX B

### ALL $v$ AND $J$ ENERGY LEVELS OF THE GROUND X $^1\Sigma_g^+$ STATE OF C<sub>2</sub>

```

# Rovibrational energy levels for C_2
# v J           -binding energy
#      a.u.          cm-1
0   0  0.22238213E+00  0.48807229E+05
0   1  0.22236577E+00  0.48803638E+05
0   2  0.22233304E+00  0.48796456E+05
0   3  0.22228396E+00  0.48785682E+05
0   4  0.22221851E+00  0.48771319E+05
0   5  0.22213671E+00  0.48753366E+05
0   6  0.22203856E+00  0.48731825E+05
0   7  0.22192407E+00  0.48706696E+05
0   8  0.22179323E+00  0.48677980E+05
0   9  0.22164605E+00  0.48645679E+05
0  10  0.22148255E+00  0.48609794E+05
0  11  0.22130273E+00  0.48570328E+05
0  12  0.22110659E+00  0.48527281E+05
0  13  0.22089415E+00  0.48480656E+05
0  14  0.22066542E+00  0.48430455E+05
0  15  0.22042041E+00  0.48376680E+05
0  16  0.22015912E+00  0.48319335E+05
0  17  0.21988157E+00  0.48258421E+05
0  18  0.21958778E+00  0.48193941E+05
0  19  0.21927776E+00  0.48125899E+05
0  20  0.21895152E+00  0.48054297E+05
0  21  0.21860908E+00  0.47979140E+05
0  22  0.21825045E+00  0.47900430E+05
0  23  0.21787565E+00  0.47818171E+05
0  24  0.21748470E+00  0.47732367E+05
0  25  0.21707776E+00  0.47643022E+05
0  26  0.21665441E+00  0.47550141E+05
0  27  0.21621512E+00  0.47453727E+05
0  28  0.21575975E+00  0.47353785E+05
0  29  0.21528833E+00  0.47250320E+05
0  30  0.21480087E+00  0.47143336E+05
0  31  0.21429741E+00  0.47032839E+05
0  32  0.21377797E+00  0.46918834E+05
0  33  0.21324256E+00  0.46801326E+05
0  34  0.21269122E+00  0.46680320E+05
0  35  0.21212397E+00  0.46555823E+05
0  36  0.21154083E+00  0.46427840E+05
0  37  0.21094185E+00  0.46296377E+05
0  38  0.21032703E+00  0.46161440E+05
0  39  0.20969641E+00  0.46023036E+05
0  40  0.20905003E+00  0.45881717E+05
0  41  0.20838790E+00  0.45735852E+05
0  42  0.20771007E+00  0.45587085E+05
0  43  0.20701656E+00  0.45434877E+05
0  44  0.20630741E+00  0.45279237E+05
0  45  0.20558265E+00  0.45120170E+05
1   0  0.21414178E+00  0.46998682E+05
1   1  0.21412558E+00  0.46995125E+05
1   2  0.21409317E+00  0.4698012E+05
1   3  0.21404455E+00  0.46977343E+05
1   4  0.21397974E+00  0.46963118E+05
1   5  0.21389873E+00  0.46945339E+05
1   6  0.21380153E+00  0.46924005E+05
1   7  0.21368814E+00  0.46899118E+05
1   8  0.21355586E+00  0.46870680E+05
1   9  0.21341281E+00  0.46838690E+05
1  10  0.21325088E+00  0.46803152E+05
1  11  0.21307280E+00  0.46764067E+05
1  12  0.21287855E+00  0.46721436E+05
1  13  0.21266817E+00  0.46675261E+05
1  14  0.21244165E+00  0.46625545E+05
1  15  0.21219900E+00  0.46572291E+05
1  16  0.21194024E+00  0.46515500E+05
1  17  0.21166538E+00  0.46455175E+05
1  18  0.21137443E+00  0.46391319E+05
1  19  0.21106741E+00  0.46323936E+05
1  20  0.21074433E+00  0.46253027E+05
1  21  0.21040520E+00  0.46178598E+05

```

1 22 0.21005005E+00 0.46100651E+05  
 1 23 0.20967889E+00 0.46019190E+05  
 1 24 0.202929173E+00 0.45934219E+05  
 1 25 0.20888860E+00 0.45845741E+05  
 1 26 0.20846951E+00 0.45753762E+05  
 1 27 0.20803448E+00 0.45658285E+05  
 1 28 0.20758354E+00 0.45559315E+05  
 1 29 0.20711671E+00 0.45456837E+05  
 1 30 0.20663400E+00 0.45350915E+05  
 1 31 0.20613545E+00 0.45241496E+05  
 1 32 0.20562107E+00 0.45128603E+05  
 1 33 0.20509089E+00 0.45012242E+05  
 1 34 0.20454494E+00 0.44892419E+05  
 1 35 0.20398324E+00 0.44769139E+05  
 1 36 0.20340581E+00 0.44642409E+05  
 1 37 0.20281269E+00 0.44512235E+05  
 1 38 0.20220391E+00 0.44378622E+05  
 1 39 0.20157949E+00 0.44241577E+05  
 1 40 0.20093946E+00 0.44101107E+05  
 1 41 0.20028338E+00 0.43957218E+05  
 1 42 0.19961270E+00 0.43809171E+05  
 1 43 0.19892604E+00 0.43659212E+05  
 1 44 0.19822389E+00 0.43505110E+05  
 1 45 0.19750630E+00 0.43347617E+05  
 2 0 0.20601908E+00 0.45215956E+05  
 2 1 0.20600305E+00 0.45212438E+05  
 2 2 0.20597099E+00 0.45209402E+05  
 2 3 0.20592291E+00 0.45194848E+05  
 2 4 0.20585880E+00 0.45180777E+05  
 2 5 0.20577866E+00 0.45163190E+05  
 2 6 0.20568251E+00 0.45142087E+05  
 2 7 0.20557034E+00 0.45117469E+05  
 2 8 0.20544217E+00 0.45089338E+05  
 2 9 0.20529799E+00 0.45057695E+05  
 2 10 0.20513782E+00 0.45022542E+05  
 2 11 0.20496166E+00 0.44983879E+05  
 2 12 0.20476953E+00 0.44941710E+05  
 2 13 0.20456142E+00 0.44896036E+05  
 2 14 0.20433735E+00 0.44846859E+05  
 2 15 0.20409734E+00 0.44794182E+05  
 2 16 0.20384139E+00 0.44738007E+05  
 2 17 0.20356951E+00 0.44678337E+05  
 2 18 0.20328172E+00 0.44615175E+05  
 2 19 0.20297804E+00 0.44548524E+05  
 2 20 0.20265847E+00 0.44478387E+05  
 2 21 0.20232303E+00 0.44404767E+05  
 2 22 0.20197175E+00 0.44327669E+05  
 2 23 0.20160463E+00 0.44247095E+05  
 2 24 0.20122169E+00 0.44163050E+05  
 2 25 0.20082295E+00 0.44075538E+05  
 2 26 0.20040844E+00 0.43984562E+05  
 2 27 0.19997817E+00 0.43890129E+05  
 2 28 0.19953216E+00 0.43792241E+05  
 2 29 0.19907043E+00 0.43690904E+05  
 2 30 0.19859302E+00 0.43586123E+05  
 2 31 0.19809993E+00 0.43477902E+05  
 2 32 0.19759119E+00 0.43366248E+05  
 2 33 0.19706684E+00 0.43251165E+05  
 2 34 0.19652688E+00 0.43132659E+05  
 2 35 0.19597136E+00 0.43010736E+05  
 2 36 0.19540029E+00 0.42885401E+05  
 2 37 0.19481371E+00 0.42756662E+05  
 2 38 0.19421165E+00 0.42624524E+05  
 2 39 0.19359412E+00 0.42488993E+05  
 2 40 0.19296117E+00 0.42350076E+05  
 2 41 0.19231282E+00 0.42207780E+05  
 2 42 0.19164911E+00 0.42062112E+05  
 2 43 0.19097007E+00 0.41913080E+05  
 2 44 0.19027573E+00 0.41760689E+05  
 2 45 0.18956612E+00 0.41604948E+05  
 3 0 0.19803168E+00 0.43462924E+05  
 3 1 0.19801583E+00 0.43459445E+05  
 3 2 0.19798413E+00 0.43452487E+05  
 3 3 0.19793658E+00 0.43442051E+05  
 3 4 0.19787318E+00 0.43428137E+05  
 3 5 0.19779394E+00 0.43410745E+05  
 3 6 0.19769886E+00 0.43389777E+05  
 3 7 0.19758794E+00 0.43365534E+05  
 3 8 0.19746119E+00 0.43337716E+05  
 3 9 0.19731862E+00 0.43306426E+05  
 3 10 0.19716024E+00 0.43271664E+05  
 3 11 0.19698604E+00 0.43233433E+05  
 3 12 0.19679605E+00 0.43191734E+05  
 3 13 0.19659026E+00 0.43146569E+05  
 3 14 0.19636870E+00 0.43097941E+05  
 3 15 0.19613136E+00 0.43045852E+05  
 3 16 0.19587827E+00 0.42990304E+05  
 3 17 0.19560943E+00 0.42931301E+05  
 3 18 0.19532486E+00 0.42868845E+05  
 3 19 0.19502457E+00 0.42802940E+05  
 3 20 0.19470858E+00 0.42733588E+05  
 3 21 0.19437690E+00 0.42660793E+05

3 22 0.19402955E+00 0.42584558E+05  
 3 23 0.19366655E+00 0.42504888E+05  
 3 24 0.19328791E+00 0.42421766E+05  
 3 25 0.19289365E+00 0.42335256E+05  
 3 26 0.19248379E+00 0.42245303E+05  
 3 27 0.19205836E+00 0.42151932E+05  
 3 28 0.19161737E+00 0.42055145E+05  
 3 29 0.19116084E+00 0.41954950E+05  
 3 30 0.19068880E+00 0.41851349E+05  
 3 31 0.19020128E+00 0.41744349E+05  
 3 32 0.18969828E+00 0.41633955E+05  
 3 33 0.18917985E+00 0.41520172E+05  
 3 34 0.18864600E+00 0.41403006E+05  
 3 35 0.18809677E+00 0.41282463E+05  
 3 36 0.18753217E+00 0.41158548E+05  
 3 37 0.18695224E+00 0.41031268E+05  
 3 38 0.18635700E+00 0.40900629E+05  
 3 39 0.18574649E+00 0.40766637E+05  
 3 40 0.18512073E+00 0.40629299E+05  
 3 41 0.18447976E+00 0.40488622E+05  
 3 42 0.18382361E+00 0.40344613E+05  
 3 43 0.18315230E+00 0.40197278E+05  
 3 44 0.18246588E+00 0.40046626E+05  
 3 45 0.18176437E+00 0.39892663E+05  
 4 0 0.19018093E+00 0.41739884E+05  
 4 1 0.19016525E+00 0.41736443E+05  
 4 2 0.19013390E+00 0.41729561E+05  
 4 3 0.19008686E+00 0.41719239E+05  
 4 4 0.19002416E+00 0.41705476E+05  
 4 5 0.18994578E+00 0.41688274E+05  
 4 6 0.18985174E+00 0.41667634E+05  
 4 7 0.18974203E+00 0.41643556E+05  
 4 8 0.18961667E+00 0.41616043E+05  
 4 9 0.18947566E+00 0.41585094E+05  
 4 10 0.18931900E+00 0.41550712E+05  
 4 11 0.18914671E+00 0.41512898E+05  
 4 12 0.18895879E+00 0.41471654E+05  
 4 13 0.18875525E+00 0.41426983E+05  
 4 14 0.18853611E+00 0.41378887E+05  
 4 15 0.18830137E+00 0.41327367E+05  
 4 16 0.18805104E+00 0.41272427E+05  
 4 17 0.18778514E+00 0.41214069E+05  
 4 18 0.18750369E+00 0.41152296E+05  
 4 19 0.18720668E+00 0.4087112E+05  
 4 20 0.18689415E+00 0.41018519E+05  
 4 21 0.18656610E+00 0.40946521E+05  
 4 22 0.18622256E+00 0.40871121E+05  
 4 23 0.18586355E+00 0.40792324E+05  
 4 24 0.18548904E+00 0.40710133E+05  
 4 25 0.18509910E+00 0.40624552E+05  
 4 26 0.18469374E+00 0.40535585E+05  
 4 27 0.18427298E+00 0.40443238E+05  
 4 28 0.18383683E+00 0.40347514E+05  
 4 29 0.18338532E+00 0.40248419E+05  
 4 30 0.18291846E+00 0.40145957E+05  
 4 31 0.18243630E+00 0.40040133E+05  
 4 32 0.18193884E+00 0.39930953E+05  
 4 33 0.18142611E+00 0.39818422E+05  
 4 34 0.18089814E+00 0.39702546E+05  
 4 35 0.18035495E+00 0.39583331E+05  
 4 36 0.17979658E+00 0.39460782E+05  
 4 37 0.17922304E+00 0.39334905E+05  
 4 38 0.17863437E+00 0.39205708E+05  
 4 39 0.17803060E+00 0.39073196E+05  
 4 40 0.17741176E+00 0.38937376E+05  
 4 41 0.17677789E+00 0.38798254E+05  
 4 42 0.17612898E+00 0.38655838E+05  
 4 43 0.17546511E+00 0.38510136E+05  
 4 44 0.17478630E+00 0.38361153E+05  
 4 45 0.17409257E+00 0.38208898E+05  
 5 0 0.18245508E+00 0.40044256E+05  
 5 1 0.18243957E+00 0.40040852E+05  
 5 2 0.18240855E+00 0.40034045E+05  
 5 3 0.18236203E+00 0.40023834E+05  
 5 4 0.18230001E+00 0.40010221E+05  
 5 5 0.18222248E+00 0.39993205E+05  
 5 6 0.18212945E+00 0.39972789E+05  
 5 7 0.18202094E+00 0.39948972E+05  
 5 8 0.18189693E+00 0.39921757E+05  
 5 9 0.18175745E+00 0.39891143E+05  
 5 10 0.18160249E+00 0.39857134E+05  
 5 11 0.18143207E+00 0.39819731E+05  
 5 12 0.18124619E+00 0.39778935E+05  
 5 13 0.18104486E+00 0.39734749E+05  
 5 14 0.18082810E+00 0.39687175E+05  
 5 15 0.18059591E+00 0.39636215E+05  
 5 16 0.18034830E+00 0.39581872E+05  
 5 17 0.18008530E+00 0.39524148E+05  
 5 18 0.17980690E+00 0.39463047E+05  
 5 19 0.17951313E+00 0.39398572E+05  
 5 20 0.17920400E+00 0.39330726E+05  
 5 21 0.17887953E+00 0.39259512E+05

5 22 0.17853972E+00 0.39184934E+05  
 5 23 0.17818461E+00 0.39106996E+05  
 5 24 0.17781421E+00 0.39025702E+05  
 5 25 0.17742853E+00 0.38941056E+05  
 5 26 0.17702760E+00 0.38853062E+05  
 5 27 0.17661144E+00 0.38761724E+05  
 5 28 0.17618006E+00 0.38667048E+05  
 5 29 0.17573349E+00 0.38569038E+05  
 5 30 0.17527176E+00 0.38467699E+05  
 5 31 0.174794488E+00 0.38363037E+05  
 5 32 0.17430288E+00 0.38255056E+05  
 5 33 0.17379579E+00 0.38143762E+05  
 5 34 0.17327363E+00 0.38029161E+05  
 5 35 0.17273643E+00 0.37911259E+05  
 5 36 0.17218421E+00 0.37790062E+05  
 5 37 0.17161701E+00 0.37665575E+05  
 5 38 0.17103485E+00 0.37537806E+05  
 5 39 0.17043777E+00 0.37406761E+05  
 5 40 0.16982578E+00 0.37272446E+05  
 5 41 0.16919894E+00 0.37134869E+05  
 5 42 0.16855726E+00 0.36994036E+05  
 5 43 0.16790078E+00 0.36849956E+05  
 5 44 0.16722953E+00 0.36702634E+05  
 5 45 0.16654355E+00 0.36552080E+05  
 6 0 0.17485360E+00 0.38375925E+05  
 6 1 0.17483827E+00 0.38372559E+05  
 6 2 0.17480760E+00 0.38365828E+05  
 6 3 0.17476160E+00 0.38355733E+05  
 6 4 0.17470028E+00 0.38342273E+05  
 6 5 0.17462362E+00 0.38325449E+05  
 6 6 0.17453165E+00 0.38305263E+05  
 6 7 0.17442435E+00 0.38281715E+05  
 6 8 0.17430175E+00 0.38254807E+05  
 6 9 0.17416384E+00 0.38224539E+05  
 6 10 0.17401063E+00 0.38190914E+05  
 6 11 0.17384214E+00 0.38153933E+05  
 6 12 0.17365836E+00 0.38113599E+05  
 6 13 0.17345931E+00 0.38069912E+05  
 6 14 0.17324500E+00 0.38022877E+05  
 6 15 0.17301544E+00 0.37972494E+05  
 6 16 0.17277064E+00 0.37918767E+05  
 6 17 0.17251062E+00 0.37861699E+05  
 6 18 0.17223539E+00 0.37801292E+05  
 6 19 0.17194496E+00 0.37737550E+05  
 6 20 0.17163934E+00 0.37670476E+05  
 6 21 0.17131857E+00 0.37600074E+05  
 6 22 0.17098264E+00 0.37526347E+05  
 6 23 0.17063159E+00 0.37449300E+05  
 6 24 0.17026542E+00 0.37368935E+05  
 6 25 0.16988416E+00 0.37285258E+05  
 6 26 0.16948783E+00 0.37198274E+05  
 6 27 0.16907645E+00 0.37107985E+05  
 6 28 0.16865003E+00 0.37014398E+05  
 6 29 0.16820861E+00 0.36917518E+05  
 6 30 0.16775221E+00 0.36817349E+05  
 6 31 0.16728085E+00 0.36713897E+05  
 6 32 0.16679455E+00 0.36607167E+05  
 6 33 0.16629335E+00 0.36497166E+05  
 6 34 0.16577726E+00 0.36383898E+05  
 6 35 0.16524632E+00 0.36267371E+05  
 6 36 0.16470056E+00 0.36147590E+05  
 6 37 0.16414000E+00 0.36024562E+05  
 6 38 0.16356463E+00 0.35898293E+05  
 6 39 0.16297462E+00 0.35768791E+05  
 6 40 0.16236987E+00 0.35636061E+05  
 6 41 0.16175044E+00 0.35500113E+05  
 6 42 0.16111638E+00 0.35360952E+05  
 6 43 0.16046771E+00 0.35218588E+05  
 6 44 0.15980449E+00 0.35073026E+05  
 6 45 0.15912673E+00 0.34924276E+05  
 7 0 0.16739216E+00 0.36738328E+05  
 7 1 0.16737702E+00 0.36735004E+05  
 7 2 0.16734673E+00 0.36728357E+05  
 7 3 0.16730131E+00 0.36718387E+05  
 7 4 0.16724074E+00 0.36705094E+05  
 7 5 0.16716504E+00 0.36688480E+05  
 7 6 0.16707421E+00 0.36668545E+05  
 7 7 0.16696825E+00 0.36645289E+05  
 7 8 0.16684717E+00 0.36618716E+05  
 7 9 0.16671098E+00 0.36588825E+05  
 7 10 0.16655963E+00 0.36555620E+05  
 7 11 0.16639329E+00 0.36519101E+05  
 7 12 0.16621181E+00 0.36479270E+05  
 7 13 0.16601525E+00 0.36436130E+05  
 7 14 0.16580362E+00 0.36389684E+05  
 7 15 0.16557694E+00 0.36339934E+05  
 7 16 0.16533522E+00 0.36286882E+05  
 7 17 0.16507847E+00 0.36230532E+05  
 7 18 0.16480671E+00 0.36170887E+05  
 7 19 0.16451995E+00 0.36107950E+05  
 7 20 0.16421821E+00 0.36041726E+05  
 7 21 0.16390150E+00 0.35972216E+05

7 22 0.16356985E+00 0.36899427E+05  
 7 23 0.16322327E+00 0.35823361E+05  
 7 24 0.16286178E+00 0.35744024E+05  
 7 25 0.16248540E+00 0.35661419E+05  
 7 26 0.16209416E+00 0.35575551E+05  
 7 27 0.16168808E+00 0.35486426E+05  
 7 28 0.16126717E+00 0.35394049E+05  
 7 29 0.16083148E+00 0.35298424E+05  
 7 30 0.16038101E+00 0.35199558E+05  
 7 31 0.15991580E+00 0.35097456E+05  
 7 32 0.15943588E+00 0.34992125E+05  
 7 33 0.15894126E+00 0.34883570E+05  
 7 34 0.15843199E+00 0.34771798E+05  
 7 35 0.15790809E+00 0.34656816E+05  
 7 36 0.15736960E+00 0.34538629E+05  
 7 37 0.15681654E+00 0.34417247E+05  
 7 38 0.15624895E+00 0.34292675E+05  
 7 39 0.15566686E+00 0.34164921E+05  
 7 40 0.15507031E+00 0.34033993E+05  
 7 41 0.15445933E+00 0.33899900E+05  
 7 42 0.15383397E+00 0.33762648E+05  
 7 43 0.15319425E+00 0.33622248E+05  
 7 44 0.15254023E+00 0.33478706E+05  
 7 45 0.15187194E+00 0.33332033E+05  
 8 0 0.16010914E+00 0.35139890E+05  
 8 1 0.16009422E+00 0.35136616E+05  
 8 2 0.16006439E+00 0.35130068E+05  
 8 3 0.16001964E+00 0.35120247E+05  
 8 4 0.15995999E+00 0.35107154E+05  
 8 5 0.15988542E+00 0.35090788E+05  
 8 6 0.15979595E+00 0.35071152E+05  
 8 7 0.15969158E+00 0.35048247E+05  
 8 8 0.15957233E+00 0.35022073E+05  
 8 9 0.15943819E+00 0.34992633E+05  
 8 10 0.15928917E+00 0.34959928E+05  
 8 11 0.15912530E+00 0.34923961E+05  
 8 12 0.15894656E+00 0.34884733E+05  
 8 13 0.15875298E+00 0.34842247E+05  
 8 14 0.15854457E+00 0.34796507E+05  
 8 15 0.15832135E+00 0.34747514E+05  
 8 16 0.15808332E+00 0.34695273E+05  
 8 17 0.15783050E+00 0.34639786E+05  
 8 18 0.15756291E+00 0.34581056E+05  
 8 19 0.15728056E+00 0.34519088E+05  
 8 20 0.15698349E+00 0.34453886E+05  
 8 21 0.15667168E+00 0.34385454E+05  
 8 22 0.15634518E+00 0.34313796E+05  
 8 23 0.15600401E+00 0.34238918E+05  
 8 24 0.15564818E+00 0.34160823E+05  
 8 25 0.15527773E+00 0.34079517E+05  
 8 26 0.15489266E+00 0.33995006E+05  
 8 27 0.15449302E+00 0.33907294E+05  
 8 28 0.15407883E+00 0.33816389E+05  
 8 29 0.15365010E+00 0.33722295E+05  
 8 30 0.15320688E+00 0.33625020E+05  
 8 31 0.15274920E+00 0.33524569E+05  
 8 32 0.15227708E+00 0.33420950E+05  
 8 33 0.15179055E+00 0.33314170E+05  
 8 34 0.15128965E+00 0.33204236E+05  
 8 35 0.15077442E+00 0.33091156E+05  
 8 36 0.15024489E+00 0.32974937E+05  
 8 37 0.14970109E+00 0.32855587E+05  
 8 38 0.14914307E+00 0.32733116E+05  
 8 39 0.14857087E+00 0.32607532E+05  
 8 40 0.14798452E+00 0.32478843E+05  
 8 41 0.14738407E+00 0.32347060E+05  
 8 42 0.14676956E+00 0.32212191E+05  
 8 43 0.14614104E+00 0.32074246E+05  
 8 44 0.14549855E+00 0.31933237E+05  
 8 45 0.14484215E+00 0.31789172E+05  
 9 0 0.15307227E+00 0.33595474E+05  
 9 1 0.15305763E+00 0.33592263E+05  
 9 2 0.15302837E+00 0.33585841E+05  
 9 3 0.15298448E+00 0.33576208E+05  
 9 4 0.15292596E+00 0.33563364E+05  
 9 5 0.15285282E+00 0.33547312E+05  
 9 6 0.15276507E+00 0.33528053E+05  
 9 7 0.15266271E+00 0.33505587E+05  
 9 8 0.15254574E+00 0.33479916E+05  
 9 9 0.15241418E+00 0.33451042E+05  
 9 10 0.15226804E+00 0.33418968E+05  
 9 11 0.15210733E+00 0.33383696E+05  
 9 12 0.15193206E+00 0.33345228E+05  
 9 13 0.15174224E+00 0.33303567E+05  
 9 14 0.15153789E+00 0.33258717E+05  
 9 15 0.15131902E+00 0.33210680E+05  
 9 16 0.15108565E+00 0.33159462E+05  
 9 17 0.15083779E+00 0.33105064E+05  
 9 18 0.15057548E+00 0.33047492E+05  
 9 19 0.15029871E+00 0.32986750E+05  
 9 20 0.15000753E+00 0.32922843E+05  
 9 21 0.14970195E+00 0.32855775E+05

9 22 0.14938199E+00 0.32785552E+05  
 9 23 0.14904768E+00 0.32712180E+05  
 9 24 0.14869904E+00 0.32635663E+05  
 9 25 0.14833611E+00 0.32556008E+05  
 9 26 0.14795891E+00 0.32473222E+05  
 9 27 0.14756747E+00 0.32387311E+05  
 9 28 0.14716182E+00 0.32298281E+05  
 9 29 0.14674200E+00 0.32206141E+05  
 9 30 0.14630803E+00 0.32110897E+05  
 9 31 0.14585996E+00 0.32012557E+05  
 9 32 0.14539783E+00 0.31911130E+05  
 9 33 0.14492166E+00 0.31806624E+05  
 9 34 0.14443151E+00 0.31699047E+05  
 9 35 0.14392740E+00 0.31588409E+05  
 9 36 0.14340939E+00 0.31474719E+05  
 9 37 0.14287752E+00 0.31357987E+05  
 9 38 0.14233184E+00 0.31238223E+05  
 9 39 0.14177238E+00 0.31115437E+05  
 9 40 0.14119921E+00 0.30989640E+05  
 9 41 0.14061237E+00 0.30860844E+05  
 9 42 0.14001192E+00 0.30729060E+05  
 9 43 0.13939791E+00 0.30594300E+05  
 9 44 0.13877039E+00 0.30456576E+05  
 9 45 0.13812943E+00 0.30315901E+05  
 10 0 0.14637141E+00 0.32124807E+05  
 10 1 0.14635714E+00 0.32121675E+05  
 10 2 0.14632860E+00 0.32115412E+05  
 10 3 0.14628580E+00 0.32106018E+05  
 10 4 0.14622874E+00 0.32093495E+05  
 10 5 0.14615742E+00 0.32077842E+05  
 10 6 0.14607186E+00 0.32059062E+05  
 10 7 0.14597205E+00 0.32037156E+05  
 10 8 0.14585800E+00 0.32012127E+05  
 10 9 0.14572974E+00 0.31983976E+05  
 10 10 0.14558726E+00 0.31952707E+05  
 10 11 0.14543059E+00 0.31918321E+05  
 10 12 0.14525973E+00 0.31880822E+05  
 10 13 0.14507471E+00 0.31840214E+05  
 10 14 0.14487553E+00 0.31796500E+05  
 10 15 0.14466222E+00 0.31749684E+05  
 10 16 0.14443480E+00 0.31699770E+05  
 10 17 0.14419329E+00 0.31646764E+05  
 10 18 0.14393770E+00 0.31590670E+05  
 10 19 0.14366807E+00 0.31531493E+05  
 10 20 0.14338442E+00 0.31469238E+05  
 10 21 0.14308677E+00 0.31403912E+05  
 10 22 0.14277516E+00 0.31335521E+05  
 10 23 0.14244961E+00 0.31264072E+05  
 10 24 0.14211016E+00 0.31189570E+05  
 10 25 0.14175683E+00 0.31112023E+05  
 10 26 0.14138966E+00 0.31031439E+05  
 10 27 0.14100869E+00 0.30947825E+05  
 10 28 0.14061395E+00 0.30861190E+05  
 10 29 0.14020548E+00 0.30771541E+05  
 10 30 0.13978332E+00 0.30678888E+05  
 10 31 0.13934751E+00 0.30583239E+05  
 10 32 0.13889810E+00 0.30484605E+05  
 10 33 0.13843513E+00 0.30382995E+05  
 10 34 0.13795865E+00 0.30278419E+05  
 10 35 0.13746870E+00 0.30170887E+05  
 10 36 0.13696533E+00 0.30060411E+05  
 10 37 0.13644860E+00 0.29947002E+05  
 10 38 0.13591856E+00 0.29830671E+05  
 10 39 0.13537526E+00 0.29711430E+05  
 10 40 0.13481875E+00 0.29589292E+05  
 10 41 0.13424911E+00 0.29464269E+05  
 10 42 0.13366637E+00 0.29336374E+05  
 10 43 0.13307062E+00 0.29205621E+05  
 10 44 0.13246190E+00 0.29072022E+05  
 10 45 0.13184028E+00 0.28935593E+05  
 11 0 0.14009540E+00 0.30747382E+05  
 11 1 0.14008156E+00 0.30744345E+05  
 11 2 0.14005388E+00 0.30738269E+05  
 11 3 0.14001236E+00 0.30729157E+05  
 11 4 0.13995701E+00 0.30717008E+05  
 11 5 0.13988783E+00 0.30701825E+05  
 11 6 0.13980483E+00 0.30683609E+05  
 11 7 0.13970801E+00 0.30662361E+05  
 11 8 0.13959740E+00 0.30638083E+05  
 11 9 0.13947299E+00 0.30610779E+05  
 11 10 0.13933480E+00 0.30580450E+05  
 11 11 0.13918285E+00 0.30547100E+05  
 11 12 0.13901715E+00 0.30510732E+05  
 11 13 0.13883771E+00 0.30471350E+05  
 11 14 0.13864455E+00 0.30428958E+05  
 11 15 0.13843770E+00 0.30383559E+05  
 11 16 0.13821717E+00 0.30335159E+05  
 11 17 0.13798299E+00 0.30283762E+05  
 11 18 0.13773518E+00 0.30229373E+05  
 11 19 0.13747376E+00 0.30171998E+05  
 11 20 0.13719876E+00 0.30111642E+05  
 11 21 0.13691020E+00 0.30048312E+05

11 22 0.13660812E+00 0.29982013E+05  
 11 23 0.13629255E+00 0.29912752E+05  
 11 24 0.13596351E+00 0.29840537E+05  
 11 25 0.13562104E+00 0.29765374E+05  
 11 26 0.13526517E+00 0.29687270E+05  
 11 27 0.13489594E+00 0.29606233E+05  
 11 28 0.13451339E+00 0.29522272E+05  
 11 29 0.13411754E+00 0.29435394E+05  
 11 30 0.13370844E+00 0.29348607E+05  
 11 31 0.13328614E+00 0.29252921E+05  
 11 32 0.13285066E+00 0.29157345E+05  
 11 33 0.13240205E+00 0.29058887E+05  
 11 34 0.13194036E+00 0.28957557E+05  
 11 35 0.13146562E+00 0.28853364E+05  
 11 36 0.13097788E+00 0.28746319E+05  
 11 37 0.13047720E+00 0.28636431E+05  
 11 38 0.12996360E+00 0.28523710E+05  
 11 39 0.12943715E+00 0.28408167E+05  
 11 40 0.12889789E+00 0.28289812E+05  
 11 41 0.12834586E+00 0.28168656E+05  
 11 42 0.12778111E+00 0.28044709E+05  
 11 43 0.12720371E+00 0.27917983E+05  
 11 44 0.12661368E+00 0.27788488E+05  
 11 45 0.12601109E+00 0.27656235E+05  
 12 0 0.13423255E+00 0.29460636E+05  
 12 1 0.13421909E+00 0.29457681E+05  
 12 2 0.13419216E+00 0.29451771E+05  
 12 3 0.13415177E+00 0.29442907E+05  
 12 4 0.13409793E+00 0.29431089E+05  
 12 5 0.13403063E+00 0.29416319E+05  
 12 6 0.13394989E+00 0.29398598E+05  
 12 7 0.13385570E+00 0.29377927E+05  
 12 8 0.13374809E+00 0.29354308E+05  
 12 9 0.13362705E+00 0.29327743E+05  
 12 10 0.13349260E+00 0.29298234E+05  
 12 11 0.13334474E+00 0.29265784E+05  
 12 12 0.13318350E+00 0.29230396E+05  
 12 13 0.13300889E+00 0.29192072E+05  
 12 14 0.13282091E+00 0.29150817E+05  
 12 15 0.13261959E+00 0.29106632E+05  
 12 16 0.13240494E+00 0.29059522E+05  
 12 17 0.13217699E+00 0.29009491E+05  
 12 18 0.13193574E+00 0.28956543E+05  
 12 19 0.13168122E+00 0.28900683E+05  
 12 20 0.13141345E+00 0.28841914E+05  
 12 21 0.13113245E+00 0.28780242E+05  
 12 22 0.13083824E+00 0.28715671E+05  
 12 23 0.13053085E+00 0.28648207E+05  
 12 24 0.13021031E+00 0.28577855E+05  
 12 25 0.12987663E+00 0.28504621E+05  
 12 26 0.12952984E+00 0.28428510E+05  
 12 27 0.12916997E+00 0.28349529E+05  
 12 28 0.12879706E+00 0.28267682E+05  
 12 29 0.12841111E+00 0.28182978E+05  
 12 30 0.12801217E+00 0.28095421E+05  
 12 31 0.12760027E+00 0.28005019E+05  
 12 32 0.12717543E+00 0.27911778E+05  
 12 33 0.12673769E+00 0.27815704E+05  
 12 34 0.12628708E+00 0.27716806E+05  
 12 35 0.12582363E+00 0.27615090E+05  
 12 36 0.12534737E+00 0.27510564E+05  
 12 37 0.12485834E+00 0.27403233E+05  
 12 38 0.12435656E+00 0.27293107E+05  
 12 39 0.12384209E+00 0.27180193E+05  
 12 40 0.12331494E+00 0.27064497E+05  
 12 41 0.12277516E+00 0.26946029E+05  
 12 42 0.12222278E+00 0.26824795E+05  
 12 43 0.12165783E+00 0.26700805E+05  
 12 44 0.12108036E+00 0.26574065E+05  
 12 45 0.12049041E+00 0.26444583E+05  
 13 0 0.12861883E+00 0.28228565E+05  
 13 1 0.12860561E+00 0.28225664E+05  
 13 2 0.12857917E+00 0.28219862E+05  
 13 3 0.12853952E+00 0.28211160E+05  
 13 4 0.12848666E+00 0.28199559E+05  
 13 5 0.12842059E+00 0.28185058E+05  
 13 6 0.12834132E+00 0.28167659E+05  
 13 7 0.12824884E+00 0.28147363E+05  
 13 8 0.12814318E+00 0.28124172E+05  
 13 9 0.12802433E+00 0.28098088E+05  
 13 10 0.12789230E+00 0.28069111E+05  
 13 11 0.12774710E+00 0.28037244E+05  
 13 12 0.12758875E+00 0.28002489E+05  
 13 13 0.12741725E+00 0.27964849E+05  
 13 14 0.12723261E+00 0.27924326E+05  
 13 15 0.12703485E+00 0.27880923E+05  
 13 16 0.12682398E+00 0.27834642E+05  
 13 17 0.12660001E+00 0.27785487E+05  
 13 18 0.12636297E+00 0.27733462E+05  
 13 19 0.12611286E+00 0.27678569E+05  
 13 20 0.12584970E+00 0.27620812E+05  
 13 21 0.12557351E+00 0.27560195E+05

13 22 0.12528430E+00 0.27496722E+05  
 13 23 0.12498211E+00 0.27430398E+05  
 13 24 0.12466694E+00 0.27361226E+05  
 13 25 0.12433881E+00 0.27289211E+05  
 13 26 0.12399776E+00 0.27214358E+05  
 13 27 0.12364379E+00 0.27136672E+05  
 13 28 0.12327694E+00 0.27056157E+05  
 13 29 0.12289722E+00 0.26972818E+05  
 13 30 0.12250466E+00 0.26886662E+05  
 13 31 0.12209929E+00 0.26797693E+05  
 13 32 0.12168113E+00 0.26705918E+05  
 13 33 0.12125021E+00 0.26611341E+05  
 13 34 0.12080655E+00 0.26513969E+05  
 13 35 0.12035018E+00 0.26413808E+05  
 13 36 0.11988113E+00 0.26310864E+05  
 13 37 0.11939943E+00 0.26205143E+05  
 13 38 0.11890511E+00 0.26096652E+05  
 13 39 0.11839820E+00 0.25985398E+05  
 13 40 0.11787873E+00 0.25871387E+05  
 13 41 0.11734673E+00 0.25754627E+05  
 13 42 0.11680223E+00 0.25635123E+05  
 13 43 0.11624527E+00 0.25512884E+05  
 13 44 0.11567588E+00 0.25387917E+05  
 13 45 0.11509409E+00 0.25260230E+05  
 14 0 0.12311383E+00 0.27020359E+05  
 14 1 0.12310079E+00 0.27017496E+05  
 14 2 0.12307470E+00 0.27011770E+05  
 14 3 0.12303557E+00 0.27003183E+05  
 14 4 0.12298340E+00 0.26991733E+05  
 14 5 0.12291820E+00 0.26977422E+05  
 14 6 0.12283966E+00 0.26960252E+05  
 14 7 0.12274870E+00 0.26940222E+05  
 14 8 0.12264442E+00 0.26917334E+05  
 14 9 0.12252712E+00 0.26891590E+05  
 14 10 0.12239681E+00 0.26862991E+05  
 14 11 0.12225350E+00 0.26831539E+05  
 14 12 0.12209721E+00 0.26797236E+05  
 14 13 0.12192793E+00 0.26760083E+05  
 14 14 0.12174568E+00 0.26720084E+05  
 14 15 0.12155047E+00 0.26677241E+05  
 14 16 0.12134232E+00 0.26631556E+05  
 14 17 0.12112123E+00 0.26583033E+05  
 14 18 0.12088721E+00 0.26531673E+05  
 14 19 0.12064030E+00 0.26477481E+05  
 14 20 0.12038049E+00 0.26420459E+05  
 14 21 0.12010780E+00 0.26360612E+05  
 14 22 0.11982226E+00 0.26297943E+05  
 14 23 0.11952388E+00 0.26232455E+05  
 14 24 0.11921267E+00 0.26164153E+05  
 14 25 0.11888866E+00 0.26093040E+05  
 14 26 0.11855186E+00 0.26019122E+05  
 14 27 0.11820230E+00 0.25942403E+05  
 14 28 0.11784000E+00 0.25862887E+05  
 14 29 0.11746498E+00 0.25780580E+05  
 14 30 0.11707726E+00 0.25695486E+05  
 14 31 0.11667687E+00 0.25607610E+05  
 14 32 0.11626384E+00 0.25516959E+05  
 14 33 0.11583818E+00 0.25423537E+05  
 14 34 0.11539992E+00 0.25327351E+05  
 14 35 0.11494909E+00 0.25228406E+05  
 14 36 0.11448572E+00 0.25126708E+05  
 14 37 0.11400984E+00 0.25022264E+05  
 14 38 0.11352148E+00 0.24915081E+05  
 14 39 0.11302066E+00 0.24805164E+05  
 14 40 0.11250742E+00 0.24692522E+05  
 14 41 0.11198180E+00 0.24577160E+05  
 14 42 0.11144382E+00 0.24459087E+05  
 14 43 0.11089351E+00 0.24338309E+05  
 14 44 0.11033092E+00 0.24214835E+05  
 14 45 0.10975609E+00 0.24086737E+05  
 15 0 0.11766972E+00 0.25825514E+05  
 15 1 0.11765683E+00 0.25822685E+05  
 15 2 0.11763105E+00 0.25817028E+05  
 15 3 0.11759239E+00 0.25808543E+05  
 15 4 0.11754084E+00 0.25797230E+05  
 15 5 0.11747642E+00 0.25783090E+05  
 15 6 0.11739912E+00 0.25766124E+05  
 15 7 0.11730894E+00 0.25746334E+05  
 15 8 0.11720591E+00 0.25723719E+05  
 15 9 0.11709001E+00 0.25698283E+05  
 15 10 0.11696126E+00 0.25670026E+05  
 15 11 0.11681967E+00 0.25638950E+05  
 15 12 0.11666524E+00 0.25605058E+05  
 15 13 0.11649799E+00 0.25568351E+05  
 15 14 0.11631793E+00 0.25528831E+05  
 15 15 0.11612507E+00 0.25486502E+05  
 15 16 0.11591941E+00 0.25441366E+05  
 15 17 0.11570098E+00 0.25393426E+05  
 15 18 0.11546979E+00 0.25342685E+05  
 15 19 0.11522585E+00 0.25289146E+05  
 15 20 0.11496917E+00 0.25232813E+05  
 15 21 0.11469979E+00 0.25173690E+05

15	22	0.11441770E+00	0.25111780E+05
15	23	0.11412294E+00	0.25047087E+05
15	24	0.11381552E+00	0.24979616E+05
15	25	0.11349546E+00	0.24909371E+05
15	26	0.11316278E+00	0.24836356E+05
15	27	0.11281751E+00	0.24760577E+05
15	28	0.11245966E+00	0.24682039E+05
15	29	0.11208926E+00	0.24600746E+05
15	30	0.11170634E+00	0.24516705E+05
15	31	0.11131092E+00	0.24429920E+05
15	32	0.11090303E+00	0.24340398E+05
15	33	0.11048269E+00	0.24248145E+05
15	34	0.11004994E+00	0.24153166E+05
15	35	0.10960480E+00	0.24055469E+05
15	36	0.10914730E+00	0.23955060E+05
15	37	0.10867744E+00	0.23851946E+05
15	38	0.10819536E+00	0.23746133E+05
15	39	0.10770098E+00	0.23637630E+05
15	40	0.10719438E+00	0.23526444E+05
15	41	0.10667559E+00	0.23412581E+05
15	42	0.10614464E+00	0.23296051E+05
15	43	0.10560157E+00	0.23176862E+05
15	44	0.10504642E+00	0.23055021E+05
15	45	0.10447923E+00	0.22930536E+05
16	0	0.11229501E+00	0.24645903E+05
16	1	0.11228230E+00	0.24643112E+05
16	2	0.11225687E+00	0.24637531E+05
16	3	0.11221872E+00	0.24629160E+05
16	4	0.11216787E+00	0.24617999E+05
16	5	0.11210431E+00	0.24604049E+05
16	6	0.11202805E+00	0.24587312E+05
16	7	0.11193909E+00	0.24567788E+05
16	8	0.11183745E+00	0.24545479E+05
16	9	0.11172311E+00	0.24520386E+05
16	10	0.11159610E+00	0.24492510E+05
16	11	0.11145643E+00	0.24461855E+05
16	12	0.11130409E+00	0.24428421E+05
16	13	0.11113911E+00	0.24392212E+05
16	14	0.11096149E+00	0.24353229E+05
16	15	0.11077125E+00	0.24311476E+05
16	16	0.11056840E+00	0.24266954E+05
16	17	0.11035294E+00	0.24219668E+05
16	18	0.11012491E+00	0.24169621E+05
16	19	0.10988431E+00	0.24116815E+05
16	20	0.10963116E+00	0.24061254E+05
16	21	0.10936547E+00	0.24002943E+05
16	22	0.10908727E+00	0.23941885E+05
16	23	0.10879657E+00	0.23878085E+05
16	24	0.10849340E+00	0.23811546E+05
16	25	0.10817777E+00	0.23742274E+05
16	26	0.10784971E+00	0.23670272E+05
16	27	0.10750924E+00	0.23595547E+05
16	28	0.10715638E+00	0.23518103E+05
16	29	0.10679115E+00	0.23437946E+05
16	30	0.10641359E+00	0.23355080E+05
16	31	0.10602371E+00	0.23269512E+05
16	32	0.10562155E+00	0.23181248E+05
16	33	0.10520713E+00	0.23090293E+05
16	34	0.10478048E+00	0.22996654E+05
16	35	0.10434163E+00	0.22900337E+05
16	36	0.10389061E+00	0.22801350E+05
16	37	0.10342745E+00	0.22699698E+05
16	38	0.10295218E+00	0.22595388E+05
16	39	0.10246484E+00	0.22488429E+05
16	40	0.10196545E+00	0.22378827E+05
16	41	0.10145406E+00	0.22266590E+05
16	42	0.10093070E+00	0.22151726E+05
16	43	0.10039541E+00	0.22034242E+05
16	44	0.99848214E-01	0.21914147E+05
16	45	0.99289162E-01	0.21791449E+05
17	0	0.10701018E+00	0.23486018E+05
17	1	0.10699765E+00	0.23483266E+05
17	2	0.10697258E+00	0.23477764E+05
17	3	0.10693497E+00	0.23469510E+05
17	4	0.10688484E+00	0.23458507E+05
17	5	0.10682217E+00	0.23444754E+05
17	6	0.10674699E+00	0.23428252E+05
17	7	0.10665928E+00	0.23409003E+05
17	8	0.10655907E+00	0.23387008E+05
17	9	0.10644634E+00	0.23362269E+05
17	10	0.10632113E+00	0.23334787E+05
17	11	0.10618342E+00	0.23304563E+05
17	12	0.10603323E+00	0.23271601E+05
17	13	0.10587058E+00	0.23235903E+05
17	14	0.10569547E+00	0.23197470E+05
17	15	0.10550791E+00	0.23156307E+05
17	16	0.10530792E+00	0.23112414E+05
17	17	0.10509552E+00	0.23065797E+05
17	18	0.10487071E+00	0.23016457E+05
17	19	0.10463351E+00	0.22964398E+05
17	20	0.10438394E+00	0.22909624E+05
17	21	0.10412202E+00	0.22852139E+05

17 22 0.10384777E+00 0.22791947E+05  
 17 23 0.10356119E+00 0.22729052E+05  
 17 24 0.10326233E+00 0.22663458E+05  
 17 25 0.10295119E+00 0.22595170E+05  
 17 26 0.10262779E+00 0.22524193E+05  
 17 27 0.10229217E+00 0.22450533E+05  
 17 28 0.10194434E+00 0.22374193E+05  
 17 29 0.10158433E+00 0.22295180E+05  
 17 30 0.10121216E+00 0.22213499E+05  
 17 31 0.10082787E+00 0.22129156E+05  
 17 32 0.10043147E+00 0.22042157E+05  
 17 33 0.10002300E+00 0.21952509E+05  
 17 34 0.99602493E-01 0.21860217E+05  
 17 35 0.99169970E-01 0.21765289E+05  
 17 36 0.98725465E-01 0.21667732E+05  
 17 37 0.98269011E-01 0.21567552E+05  
 17 38 0.97800642E-01 0.21464757E+05  
 17 39 0.97320391E-01 0.21359354E+05  
 17 40 0.96828295E-01 0.21251351E+05  
 17 41 0.96324389E-01 0.21140757E+05  
 17 42 0.95808710E-01 0.21027578E+05  
 17 43 0.95281298E-01 0.20911825E+05  
 17 44 0.94742191E-01 0.20793504E+05  
 17 45 0.94191428E-01 0.20672626E+05  
 18 0 0.10181957E+00 0.22346809E+05  
 18 1 0.10180722E+00 0.22344098E+05  
 18 2 0.10178252E+00 0.22338677E+05  
 18 3 0.10174546E+00 0.22330545E+05  
 18 4 0.10169607E+00 0.22319704E+05  
 18 5 0.10163433E+00 0.22306154E+05  
 18 6 0.10156025E+00 0.22289896E+05  
 18 7 0.10147384E+00 0.22270931E+05  
 18 8 0.10137511E+00 0.22249261E+05  
 18 9 0.10126405E+00 0.22224887E+05  
 18 10 0.10114069E+00 0.22197812E+05  
 18 11 0.10100502E+00 0.22168036E+05  
 18 12 0.10085706E+00 0.22135563E+05  
 18 13 0.10069682E+00 0.22100394E+05  
 18 14 0.10052431E+00 0.22062533E+05  
 18 15 0.10033954E+00 0.22021981E+05  
 18 16 0.10014253E+00 0.21978742E+05  
 18 17 0.99933292E-01 0.21932819E+05  
 18 18 0.99711839E-01 0.21884216E+05  
 18 19 0.99478189E-01 0.21832936E+05  
 18 20 0.99232358E-01 0.21778982E+05  
 18 21 0.98974365E-01 0.21722359E+05  
 18 22 0.98704229E-01 0.21663071E+05  
 18 23 0.98421970E-01 0.21601122E+05  
 18 24 0.98127607E-01 0.21536517E+05  
 18 25 0.97821164E-01 0.21469261E+05  
 18 26 0.97502662E-01 0.21399358E+05  
 18 27 0.97172126E-01 0.21326813E+05  
 18 28 0.96829578E-01 0.21251633E+05  
 18 29 0.96475045E-01 0.21173822E+05  
 18 30 0.96108553E-01 0.21093386E+05  
 18 31 0.95730129E-01 0.21010332E+05  
 18 32 0.95339800E-01 0.20924664E+05  
 18 33 0.94937596E-01 0.20836391E+05  
 18 34 0.94523546E-01 0.20745517E+05  
 18 35 0.94097680E-01 0.20652051E+05  
 18 36 0.93660031E-01 0.20555998E+05  
 18 37 0.93210630E-01 0.20457366E+05  
 18 38 0.92749511E-01 0.20356162E+05  
 18 39 0.92276707E-01 0.20252393E+05  
 18 40 0.91792254E-01 0.20146068E+05  
 18 41 0.91296187E-01 0.20037194E+05  
 18 42 0.90788543E-01 0.19925779E+05  
 18 43 0.90269359E-01 0.19811832E+05  
 18 44 0.89738674E-01 0.19695360E+05  
 18 45 0.89196527E-01 0.19576372E+05  
 19 0 0.96733152E-01 0.21230470E+05  
 19 1 0.96720990E-01 0.21227801E+05  
 19 2 0.96696667E-01 0.21222462E+05  
 19 3 0.96660184E-01 0.21214455E+05  
 19 4 0.96611545E-01 0.21203780E+05  
 19 5 0.96550753E-01 0.21190438E+05  
 19 6 0.96477812E-01 0.21174429E+05  
 19 7 0.96392728E-01 0.21155755E+05  
 19 8 0.96295507E-01 0.21134418E+05  
 19 9 0.96186157E-01 0.21110418E+05  
 19 10 0.96064684E-01 0.21083758E+05  
 19 11 0.95931099E-01 0.21054440E+05  
 19 12 0.95785411E-01 0.21022465E+05  
 19 13 0.95627631E-01 0.20987836E+05  
 19 14 0.95457771E-01 0.20950556E+05  
 19 15 0.95275842E-01 0.20910627E+05  
 19 16 0.95081860E-01 0.20868053E+05  
 19 17 0.94875837E-01 0.20822836E+05  
 19 18 0.94657789E-01 0.20774980E+05  
 19 19 0.94427732E-01 0.20724489E+05  
 19 20 0.94185683E-01 0.20671365E+05  
 19 21 0.93931660E-01 0.20615614E+05

19	22	0.93665682E-01	0.20557238E+05
19	23	0.93387769E-01	0.20496243E+05
19	24	0.93097941E-01	0.20432633E+05
19	25	0.92796218E-01	0.20366413E+05
19	26	0.92482625E-01	0.20297587E+05
19	27	0.92157184E-01	0.20226161E+05
19	28	0.91819918E-01	0.20152140E+05
19	29	0.91470853E-01	0.20075529E+05
19	30	0.91110015E-01	0.19996334E+05
19	31	0.90737431E-01	0.19914561E+05
19	32	0.90353128E-01	0.19830217E+05
19	33	0.89957134E-01	0.19743306E+05
19	34	0.89549479E-01	0.19653836E+05
19	35	0.89130193E-01	0.19561813E+05
19	36	0.88699307E-01	0.19467245E+05
19	37	0.88256854E-01	0.19370138E+05
19	38	0.87802865E-01	0.19270499E+05
19	39	0.87337376E-01	0.19168336E+05
19	40	0.86860420E-01	0.19063656E+05
19	41	0.86372032E-01	0.18956467E+05
19	42	0.85872251E-01	0.18846778E+05
19	43	0.85361112E-01	0.18734596E+05
19	44	0.84838653E-01	0.18619929E+05
19	45	0.84304915E-01	0.18502787E+05
20	0	0.91750402E-01	0.20136883E+05
20	1	0.91738425E-01	0.20134254E+05
20	2	0.91714473E-01	0.20128997E+05
20	3	0.91678546E-01	0.20121112E+05
20	4	0.91630648E-01	0.20110600E+05
20	5	0.91570783E-01	0.20097461E+05
20	6	0.91498954E-01	0.20081696E+05
20	7	0.91415167E-01	0.20063307E+05
20	8	0.91319428E-01	0.20042295E+05
20	9	0.91211745E-01	0.20018661E+05
20	10	0.91092125E-01	0.19992408E+05
20	11	0.90960577E-01	0.19963536E+05
20	12	0.90817112E-01	0.19932049E+05
20	13	0.90661739E-01	0.19897949E+05
20	14	0.90494471E-01	0.19861238E+05
20	15	0.90315319E-01	0.19821919E+05
20	16	0.90124298E-01	0.19779994E+05
20	17	0.89921421E-01	0.19735468E+05
20	18	0.89706703E-01	0.19688343E+05
20	19	0.89480161E-01	0.19638623E+05
20	20	0.89241812E-01	0.19586311E+05
20	21	0.88991673E-01	0.19531412E+05
20	22	0.88729762E-01	0.19473929E+05
20	23	0.88456101E-01	0.19413867E+05
20	24	0.88170708E-01	0.19351231E+05
20	25	0.87873606E-01	0.19286025E+05
20	26	0.87564817E-01	0.19218253E+05
20	27	0.87244363E-01	0.19147922E+05
20	28	0.86912270E-01	0.19075036E+05
20	29	0.865685861E-01	0.18999600E+05
20	30	0.86213263E-01	0.18921621E+05
20	31	0.85846403E-01	0.18841105E+05
20	32	0.85468008E-01	0.18758057E+05
20	33	0.85078107E-01	0.18672484E+05
20	34	0.84676730E-01	0.18584391E+05
20	35	0.84263906E-01	0.18493787E+05
20	36	0.83839668E-01	0.18400678E+05
20	37	0.83404047E-01	0.18305070E+05
20	38	0.82957076E-01	0.18206971E+05
20	39	0.82498791E-01	0.18106389E+05
20	40	0.82029225E-01	0.18003331E+05
20	41	0.81548415E-01	0.17897806E+05
20	42	0.81056398E-01	0.17789821E+05
20	43	0.80553212E-01	0.17679384E+05
20	44	0.80038895E-01	0.17566504E+05
20	45	0.79513487E-01	0.17451191E+05
21	0	0.86868360E-01	0.19065399E+05
21	1	0.86856567E-01	0.19062810E+05
21	2	0.86832982E-01	0.19057634E+05
21	3	0.86797607E-01	0.19049870E+05
21	4	0.86750444E-01	0.19039519E+05
21	5	0.86691498E-01	0.19026582E+05
21	6	0.86620772E-01	0.19011059E+05
21	7	0.86538272E-01	0.18992953E+05
21	8	0.86444005E-01	0.18972263E+05
21	9	0.86337977E-01	0.18948993E+05
21	10	0.86220197E-01	0.18923143E+05
21	11	0.86090673E-01	0.18894716E+05
21	12	0.85949415E-01	0.18863714E+05
21	13	0.85796435E-01	0.18830138E+05
21	14	0.85631744E-01	0.18793993E+05
21	15	0.85455355E-01	0.18755280E+05
21	16	0.85267281E-01	0.18714002E+05
21	17	0.85067536E-01	0.18670163E+05
21	18	0.84856136E-01	0.18623766E+05
21	19	0.84633096E-01	0.18574815E+05
21	20	0.84398436E-01	0.18523313E+05
21	21	0.84152171E-01	0.18469264E+05

```

21 22 0.83894321E-01 0.18412673E+05
21 23 0.83624906E-01 0.18353543E+05
21 24 0.83343946E-01 0.18291879E+05
21 25 0.83051464E-01 0.18227687E+05
21 26 0.82747481E-01 0.18160970E+05
21 27 0.82432022E-01 0.18091735E+05
21 28 0.82105109E-01 0.18019986E+05
21 29 0.81766769E-01 0.17945729E+05
21 30 0.81417028E-01 0.17868970E+05
21 31 0.81055911E-01 0.17789714E+05
21 32 0.80683449E-01 0.17707968E+05
21 33 0.80299668E-01 0.17623737E+05
21 34 0.79904598E-01 0.17537030E+05
21 35 0.79498271E-01 0.17447851E+05
21 36 0.79080717E-01 0.17356209E+05
21 37 0.78651963E-01 0.17262109E+05
21 38 0.78212058E-01 0.17165560E+05
21 39 0.77761020E-01 0.17066569E+05
21 40 0.77298889E-01 0.16965143E+05
21 41 0.76825701E-01 0.16861290E+05
21 42 0.76341492E-01 0.16755018E+05
21 43 0.75846299E-01 0.16646336E+05
21 44 0.75340161E-01 0.16535252E+05
21 45 0.74823116E-01 0.16421774E+05
22 0 0.82088010E-01 0.18016233E+05
22 1 0.82076402E-01 0.18013685E+05
22 2 0.82053185E-01 0.18008590E+05
22 3 0.82018362E-01 0.18000947E+05
22 4 0.81971936E-01 0.17990758E+05
22 5 0.81913911E-01 0.17978023E+05
22 6 0.81844289E-01 0.17962743E+05
22 7 0.81763078E-01 0.17944919E+05
22 8 0.81670283E-01 0.17924553E+05
22 9 0.81565912E-01 0.17901646E+05
22 10 0.81449972E-01 0.17876200E+05
22 11 0.81322472E-01 0.17848217E+05
22 12 0.81183423E-01 0.17817699E+05
22 13 0.81032834E-01 0.17784649E+05
22 14 0.80870718E-01 0.17749069E+05
22 15 0.80697087E-01 0.17710961E+05
22 16 0.80511955E-01 0.17670329E+05
22 17 0.80315335E-01 0.17627176E+05
22 18 0.80107243E-01 0.17581505E+05
22 19 0.79886769E-01 0.17533320E+05
22 20 0.79656709E-01 0.17482624E+05
22 21 0.79414299E-01 0.17429422E+05
22 22 0.79160488E-01 0.17373717E+05
22 23 0.78895294E-01 0.17315513E+05
22 24 0.78618738E-01 0.17254816E+05
22 25 0.78330841E-01 0.17191630E+05
22 26 0.78031625E-01 0.17125960E+05
22 27 0.77721114E-01 0.17057810E+05
22 28 0.77399331E-01 0.16987187E+05
22 29 0.77066302E-01 0.16914096E+05
22 30 0.76722053E-01 0.16838542E+05
22 31 0.76366610E-01 0.16760531E+05
22 32 0.76000001E-01 0.16680070E+05
22 33 0.75622256E-01 0.16597164E+05
22 34 0.75233403E-01 0.16511821E+05
22 35 0.74833472E-01 0.16424046E+05
22 36 0.74422497E-01 0.16333848E+05
22 37 0.74000508E-01 0.16241232E+05
22 38 0.73567539E-01 0.16146206E+05
22 39 0.73123624E-01 0.16048778E+05
22 40 0.72668798E-01 0.15948955E+05
22 41 0.72203098E-01 0.15846746E+05
22 42 0.71726560E-01 0.15742158E+05
22 43 0.71239223E-01 0.15635200E+05
22 44 0.70741124E-01 0.15525880E+05
22 45 0.70232304E-01 0.15414207E+05
23 0 0.77407417E-01 0.16988962E+05
23 1 0.77395990E-01 0.16988454E+05
23 2 0.77373136E-01 0.16981438E+05
23 3 0.77338859E-01 0.16973915E+05
23 4 0.77293160E-01 0.16963885E+05
23 5 0.77236042E-01 0.16951349E+05
23 6 0.77167511E-01 0.16936309E+05
23 7 0.770087572E-01 0.16918764E+05
23 8 0.76996231E-01 0.16898717E+05
23 9 0.76893495E-01 0.16876169E+05
23 10 0.76779373E-01 0.16851122E+05
23 11 0.76653873E-01 0.16823578E+05
23 12 0.76517006E-01 0.16793539E+05
23 13 0.76368781E-01 0.16761008E+05
23 14 0.76209211E-01 0.16725986E+05
23 15 0.76038309E-01 0.16688477E+05
23 16 0.75856087E-01 0.16648484E+05
23 17 0.75662561E-01 0.16606010E+05
23 18 0.75457745E-01 0.16561058E+05
23 19 0.75241656E-01 0.16513632E+05
23 20 0.75014311E-01 0.16463736E+05
23 21 0.74775728E-01 0.16411373E+05

```

```

23 22 0.74525925E-01 0.16356548E+05
23 23 0.74264922E-01 0.16299264E+05
23 24 0.73992741E-01 0.16239527E+05
23 25 0.73709402E-01 0.16177342E+05
23 26 0.73414928E-01 0.16112712E+05
23 27 0.73109343E-01 0.16045644E+05
23 28 0.72792670E-01 0.15976142E+05
23 29 0.72464935E-01 0.15904213E+05
23 30 0.72126164E-01 0.15829861E+05
23 31 0.71776382E-01 0.15753093E+05
23 32 0.71415620E-01 0.15673915E+05
23 33 0.71043904E-01 0.15592323E+05
23 34 0.70661264E-01 0.15508353E+05
23 35 0.70267732E-01 0.15421982E+05
23 36 0.69863337E-01 0.15333228E+05
23 37 0.69448113E-01 0.15242097E+05
23 38 0.69022092E-01 0.15148596E+05
23 39 0.68585308E-01 0.15052733E+05
23 40 0.68137796E-01 0.14954516E+05
23 41 0.67679592E-01 0.14853951E+05
23 42 0.67210733E-01 0.14751049E+05
23 43 0.66731255E-01 0.14645815E+05
23 44 0.66241198E-01 0.14538260E+05
23 45 0.65740600E-01 0.14428392E+05
24 0 0.72826281E-01 0.15983519E+05
24 1 0.72815035E-01 0.15981051E+05
24 2 0.72792544E-01 0.15976114E+05
24 3 0.72758809E-01 0.15968710E+05
24 4 0.72713833E-01 0.15958839E+05
24 5 0.72657621E-01 0.15946502E+05
24 6 0.72590175E-01 0.15931700E+05
24 7 0.72511502E-01 0.15914433E+05
24 8 0.72421609E-01 0.15894704E+05
24 9 0.72320501E-01 0.15872513E+05
24 10 0.72208188E-01 0.15847863E+05
24 11 0.72084678E-01 0.15820756E+05
24 12 0.71949981E-01 0.15791193E+05
24 13 0.71804107E-01 0.15759178E+05
24 14 0.71647069E-01 0.15724712E+05
24 15 0.71478880E-01 0.15687799E+05
24 16 0.71299551E-01 0.15648441E+05
24 17 0.71109099E-01 0.15606641E+05
24 18 0.70907538E-01 0.15562403E+05
24 19 0.70694884E-01 0.15515731E+05
24 20 0.70471154E-01 0.15466628E+05
24 21 0.70236367E-01 0.15415099E+05
24 22 0.69990541E-01 0.15361146E+05
24 23 0.69733696E-01 0.15304775E+05
24 24 0.69465853E-01 0.15245990E+05
24 25 0.69187033E-01 0.15184796E+05
24 26 0.68897259E-01 0.15121198E+05
24 27 0.68596554E-01 0.15055201E+05
24 28 0.68284943E-01 0.14986810E+05
24 29 0.67962450E-01 0.14916032E+05
24 30 0.67629103E-01 0.14842870E+05
24 31 0.67284927E-01 0.14767332E+05
24 32 0.66929952E-01 0.14689424E+05
24 33 0.66564205E-01 0.14609152E+05
24 34 0.66187711E-01 0.14526523E+05
24 35 0.65800519E-01 0.14441543E+05
24 36 0.65402642E-01 0.14354219E+05
24 37 0.64994119E-01 0.14264558E+05
24 38 0.64574983E-01 0.14172569E+05
24 39 0.64145268E-01 0.14078257E+05
24 40 0.63705011E-01 0.13981632E+05
24 41 0.63254246E-01 0.13882700E+05
24 42 0.62793011E-01 0.13781471E+05
24 43 0.62321344E-01 0.13677952E+05
24 44 0.61839283E-01 0.13572152E+05
24 45 0.61346869E-01 0.13464080E+05
25 0 0.68343350E-01 0.14999629E+05
25 1 0.68332284E-01 0.14997201E+05
25 2 0.68310154E-01 0.14992344E+05
25 3 0.68276961E-01 0.14985059E+05
25 4 0.68232708E-01 0.14975346E+05
25 5 0.68177398E-01 0.14963207E+05
25 6 0.68111037E-01 0.14948643E+05
25 7 0.68033628E-01 0.14931653E+05
25 8 0.67945180E-01 0.14912241E+05
25 9 0.67845698E-01 0.14890407E+05
25 10 0.67735192E-01 0.14866154E+05
25 11 0.67613669E-01 0.14839483E+05
25 12 0.67481140E-01 0.14810396E+05
25 13 0.67337617E-01 0.14778896E+05
25 14 0.67183109E-01 0.14744986E+05
25 15 0.67017631E-01 0.14708668E+05
25 16 0.66841196E-01 0.14669945E+05
25 17 0.66653817E-01 0.14628820E+05
25 18 0.66455511E-01 0.14585297E+05
25 19 0.66246294E-01 0.14539379E+05
25 20 0.66026182E-01 0.14491070E+05
25 21 0.65795194E-01 0.14440374E+05

```

25	22	0.65553348E-01	0.14387295E+05
25	23	0.65300665E-01	0.14331837E+05
25	24	0.65037165E-01	0.14274006E+05
25	25	0.64762869E-01	0.14213805E+05
25	26	0.64477801E-01	0.14151240E+05
25	27	0.64181983E-01	0.14086315E+05
25	28	0.63875439E-01	0.14019036E+05
25	29	0.63558196E-01	0.13949410E+05
25	30	0.63230278E-01	0.13877440E+05
25	31	0.62891713E-01	0.13803134E+05
25	32	0.62542529E-01	0.13726497E+05
25	33	0.62182755E-01	0.13647535E+05
25	34	0.61812419E-01	0.13566256E+05
25	35	0.61431554E-01	0.13482666E+05
25	36	0.61040189E-01	0.13396771E+05
25	37	0.60638359E-01	0.13308580E+05
25	38	0.60226095E-01	0.13218098E+05
25	39	0.59803433E-01	0.13125335E+05
25	40	0.59370408E-01	0.13030297E+05
25	41	0.58927056E-01	0.12932992E+05
25	42	0.58473413E-01	0.12833429E+05
25	43	0.58009519E-01	0.12731616E+05
25	44	0.57535413E-01	0.12627562E+05
25	45	0.57051133E-01	0.12521275E+05
26	0	0.63958435E-01	0.14037252E+05
26	1	0.63947548E-01	0.14034863E+05
26	2	0.63925776E-01	0.14030084E+05
26	3	0.63893120E-01	0.14022917E+05
26	4	0.63849584E-01	0.14013362E+05
26	5	0.63795170E-01	0.14001419E+05
26	6	0.63729883E-01	0.13987090E+05
26	7	0.63653728E-01	0.13970377E+05
26	8	0.63566713E-01	0.13951279E+05
26	9	0.63468843E-01	0.13929799E+05
26	10	0.63360128E-01	0.13905939E+05
26	11	0.63240576E-01	0.13879700E+05
26	12	0.63110198E-01	0.13851085E+05
26	13	0.62969004E-01	0.13820097E+05
26	14	0.62817005E-01	0.13786737E+05
26	15	0.62654216E-01	0.13751009E+05
26	16	0.62480648E-01	0.13712915E+05
26	17	0.62296318E-01	0.13672459E+05
26	18	0.62101240E-01	0.13629645E+05
26	19	0.61895430E-01	0.13584475E+05
26	20	0.61678906E-01	0.13536953E+05
26	21	0.61451686E-01	0.13487084E+05
26	22	0.61213789E-01	0.13434872E+05
26	23	0.60965235E-01	0.13380321E+05
26	24	0.60706045E-01	0.13323435E+05
26	25	0.60436241E-01	0.13264220E+05
26	26	0.60155845E-01	0.13202680E+05
26	27	0.59864882E-01	0.13138821E+05
26	28	0.59563375E-01	0.13072648E+05
26	29	0.59251351E-01	0.13004167E+05
26	30	0.58928836E-01	0.12933383E+05
26	31	0.58595856E-01	0.12860302E+05
26	32	0.58252441E-01	0.12784931E+05
26	33	0.57898619E-01	0.12707276E+05
26	34	0.57534420E-01	0.12627344E+05
26	35	0.57159876E-01	0.12545141E+05
26	36	0.56775018E-01	0.12460674E+05
26	37	0.56379879E-01	0.12373951E+05
26	38	0.55974493E-01	0.12284979E+05
26	39	0.55558893E-01	0.12193766E+05
26	40	0.55133117E-01	0.12100319E+05
26	41	0.54697199E-01	0.12004646E+05
26	42	0.54251178E-01	0.11906756E+05
26	43	0.53795090E-01	0.11806656E+05
26	44	0.53328977E-01	0.11704356E+05
26	45	0.52852876E-01	0.11599864E+05
27	0	0.59671058E-01	0.13096282E+05
27	1	0.59660352E-01	0.13093932E+05
27	2	0.59638940E-01	0.13089233E+05
27	3	0.59606824E-01	0.13082184E+05
27	4	0.59564008E-01	0.13072787E+05
27	5	0.59510494E-01	0.13061042E+05
27	6	0.59446287E-01	0.13046950E+05
27	7	0.59371392E-01	0.13030513E+05
27	8	0.59285817E-01	0.13011731E+05
27	9	0.59189568E-01	0.12990607E+05
27	10	0.59082654E-01	0.12967142E+05
27	11	0.58965083E-01	0.12941338E+05
27	12	0.58836866E-01	0.12913198E+05
27	13	0.58698013E-01	0.12882723E+05
27	14	0.58548536E-01	0.12849916E+05
27	15	0.58388448E-01	0.12814781E+05
27	16	0.58217763E-01	0.12777320E+05
27	17	0.58036495E-01	0.12737537E+05
27	18	0.57844660E-01	0.12695434E+05
27	19	0.57642273E-01	0.12651015E+05
27	20	0.57429353E-01	0.12604284E+05
27	21	0.57205917E-01	0.12555246E+05

27 22 0.56971985E-01 0.12503904E+05  
 27 23 0.56727576E-01 0.12450262E+05  
 27 24 0.56472712E-01 0.12394326E+05  
 27 25 0.56207413E-01 0.12336100E+05  
 27 26 0.55931704E-01 0.12275588E+05  
 27 27 0.55645607E-01 0.12212797E+05  
 27 28 0.55349148E-01 0.12147732E+05  
 27 29 0.55042351E-01 0.12080398E+05  
 27 30 0.54725243E-01 0.12010801E+05  
 27 31 0.54397852E-01 0.11938947E+05  
 27 32 0.54060205E-01 0.11864842E+05  
 27 33 0.53712333E-01 0.11788493E+05  
 27 34 0.53354265E-01 0.11709906E+05  
 27 35 0.52986032E-01 0.11629088E+05  
 27 36 0.52607667E-01 0.11546047E+05  
 27 37 0.52219203E-01 0.11460789E+05  
 27 38 0.51820673E-01 0.11373322E+05  
 27 39 0.51412113E-01 0.11283653E+05  
 27 40 0.50993559E-01 0.11191791E+05  
 27 41 0.50565047E-01 0.11097744E+05  
 27 42 0.50126616E-01 0.11001519E+05  
 27 43 0.49678304E-01 0.10903126E+05  
 27 44 0.49220152E-01 0.10802573E+05  
 27 45 0.48752200E-01 0.10699870E+05  
 28 0 0.55481074E-01 0.12176686E+05  
 28 1 0.55470546E-01 0.12174376E+05  
 28 2 0.55449493E-01 0.12169755E+05  
 28 3 0.55417915E-01 0.12162825E+05  
 28 4 0.55375815E-01 0.12153585E+05  
 28 5 0.55323198E-01 0.12142037E+05  
 28 6 0.55260067E-01 0.12128181E+05  
 28 7 0.55186428E-01 0.12112019E+05  
 28 8 0.55102288E-01 0.12093553E+05  
 28 9 0.55007653E-01 0.12072783E+05  
 28 10 0.54902533E-01 0.12049712E+05  
 28 11 0.54786936E-01 0.12024341E+05  
 28 12 0.54660873E-01 0.1196673E+05  
 28 13 0.54524354E-01 0.11966711E+05  
 28 14 0.54377392E-01 0.11934456E+05  
 28 15 0.54220000E-01 0.11899913E+05  
 28 16 0.54052190E-01 0.11863083E+05  
 28 17 0.53873978E-01 0.11823970E+05  
 28 18 0.53685380E-01 0.11782577E+05  
 28 19 0.53486413E-01 0.11738909E+05  
 28 20 0.53277093E-01 0.11692969E+05  
 28 21 0.53057439E-01 0.11644760E+05  
 28 22 0.52827470E-01 0.11594288E+05  
 28 23 0.52587208E-01 0.11541556E+05  
 28 24 0.52336672E-01 0.11486570E+05  
 28 25 0.52075885E-01 0.11429334E+05  
 28 26 0.51804870E-01 0.11369853E+05  
 28 27 0.51523652E-01 0.11308133E+05  
 28 28 0.51232254E-01 0.11244179E+05  
 28 29 0.50930703E-01 0.11177996E+05  
 28 30 0.50619026E-01 0.11109590E+05  
 28 31 0.50297250E-01 0.11038969E+05  
 28 32 0.49965403E-01 0.10966137E+05  
 28 33 0.49623516E-01 0.10891101E+05  
 28 34 0.49271618E-01 0.10813869E+05  
 28 35 0.48909741E-01 0.10734446E+05  
 28 36 0.48537917E-01 0.10652840E+05  
 28 37 0.48156180E-01 0.10569058E+05  
 28 38 0.47764563E-01 0.10483108E+05  
 28 39 0.47363102E-01 0.10394998E+05  
 28 40 0.46951832E-01 0.10304735E+05  
 28 41 0.46530791E-01 0.10212327E+05  
 28 42 0.46100016E-01 0.10117783E+05  
 28 43 0.45659547E-01 0.10021111E+05  
 28 44 0.45209422E-01 0.99223199E+04  
 28 45 0.44749684E-01 0.98214190E+04  
 29 0 0.51388962E-01 0.11278572E+05  
 29 1 0.51378615E-01 0.11276301E+05  
 29 2 0.51357922E-01 0.11271759E+05  
 29 3 0.51326885E-01 0.11264948E+05  
 29 4 0.51285507E-01 0.11255866E+05  
 29 5 0.51233791E-01 0.11244516E+05  
 29 6 0.51171742E-01 0.11230898E+05  
 29 7 0.51099366E-01 0.11215013E+05  
 29 8 0.51016669E-01 0.11196863E+05  
 29 9 0.50923658E-01 0.11176449E+05  
 29 10 0.50820341E-01 0.11153774E+05  
 29 11 0.50706729E-01 0.11128839E+05  
 29 12 0.50582831E-01 0.11101647E+05  
 29 13 0.50448658E-01 0.11072199E+05  
 29 14 0.50304223E-01 0.11040499E+05  
 29 15 0.50149538E-01 0.11006550E+05  
 29 16 0.49984617E-01 0.10970354E+05  
 29 17 0.49809474E-01 0.10931914E+05  
 29 18 0.49624127E-01 0.10891235E+05  
 29 19 0.49428591E-01 0.10848320E+05  
 29 20 0.49222884E-01 0.10803173E+05  
 29 21 0.49007024E-01 0.10755797E+05

29 22 0.48781032E-01 0.10706197E+05  
 29 23 0.48544927E-01 0.10654378E+05  
 29 24 0.48298731E-01 0.10600345E+05  
 29 25 0.48042466E-01 0.10544101E+05  
 29 26 0.47776155E-01 0.10485652E+05  
 29 27 0.47499823E-01 0.10425005E+05  
 29 28 0.47213494E-01 0.10362163E+05  
 29 29 0.46917196E-01 0.10297133E+05  
 29 30 0.46610954E-01 0.10229920E+05  
 29 31 0.46294797E-01 0.10160532E+05  
 29 32 0.45968754E-01 0.10088974E+05  
 29 33 0.45632855E-01 0.10015253E+05  
 29 34 0.45287130E-01 0.99393747E+04  
 29 35 0.44931612E-01 0.98613475E+04  
 29 36 0.44566333E-01 0.97811781E+04  
 29 37 0.44191327E-01 0.96988739E+04  
 29 38 0.43806629E-01 0.96144425E+04  
 29 39 0.43412275E-01 0.95278917E+04  
 29 40 0.43008301E-01 0.94392296E+04  
 29 41 0.42594745E-01 0.93484645E+04  
 29 42 0.42171645E-01 0.92556049E+04  
 29 43 0.41739041E-01 0.91606593E+04  
 29 44 0.41296974E-01 0.90636368E+04  
 29 45 0.40845484E-01 0.89645463E+04  
 30 0 0.47394768E-01 0.10401948E+05  
 30 1 0.47384602E-01 0.10399716E+05  
 30 2 0.47364271E-01 0.10395254E+05  
 30 3 0.47333777E-01 0.10388562E+05  
 30 4 0.47293123E-01 0.10379639E+05  
 30 5 0.47242312E-01 0.10368488E+05  
 30 6 0.47181350E-01 0.10355108E+05  
 30 7 0.47110241E-01 0.10339501E+05  
 30 8 0.47028993E-01 0.10321669E+05  
 30 9 0.46937613E-01 0.10301614E+05  
 30 10 0.46836109E-01 0.10279336E+05  
 30 11 0.46724490E-01 0.10254839E+05  
 30 12 0.46602768E-01 0.10228124E+05  
 30 13 0.46470953E-01 0.10199194E+05  
 30 14 0.46329057E-01 0.10168051E+05  
 30 15 0.46177094E-01 0.10134699E+05  
 30 16 0.46015078E-01 0.10099141E+05  
 30 17 0.45843023E-01 0.10061379E+05  
 30 18 0.45660946E-01 0.10021418E+05  
 30 19 0.45468863E-01 0.99792605E+04  
 30 20 0.45266792E-01 0.99349111E+04  
 30 21 0.45054753E-01 0.98883739E+04  
 30 22 0.44832764E-01 0.98396530E+04  
 30 23 0.44600847E-01 0.97887530E+04  
 30 24 0.44359022E-01 0.97356787E+04  
 30 25 0.44107314E-01 0.96804350E+04  
 30 26 0.43845743E-01 0.96230270E+04  
 30 27 0.43574337E-01 0.95634601E+04  
 30 28 0.43293119E-01 0.95017399E+04  
 30 29 0.43002116E-01 0.94378722E+04  
 30 30 0.42701355E-01 0.93718628E+04  
 30 31 0.42390865E-01 0.93037181E+04  
 30 32 0.42070674E-01 0.92334444E+04  
 30 33 0.41740813E-01 0.91610483E+04  
 30 34 0.41401313E-01 0.90865367E+04  
 30 35 0.41052206E-01 0.90099165E+04  
 30 36 0.40693525E-01 0.89311951E+04  
 30 37 0.40325304E-01 0.88503799E+04  
 30 38 0.39947577E-01 0.87674785E+04  
 30 39 0.39560382E-01 0.86824990E+04  
 30 40 0.39163754E-01 0.85954493E+04  
 30 41 0.38757733E-01 0.85063379E+04  
 30 42 0.38342356E-01 0.84151733E+04  
 30 43 0.37917665E-01 0.83219643E+04  
 30 44 0.37483699E-01 0.82267198E+04  
 30 45 0.37040501E-01 0.81294492E+04  
 31 0 0.43499221E-01 0.95469741E+04  
 31 1 0.43489237E-01 0.95447828E+04  
 31 2 0.43469269E-01 0.95404005E+04  
 31 3 0.43439321E-01 0.95338275E+04  
 31 4 0.43399394E-01 0.95250645E+04  
 31 5 0.43349492E-01 0.95141124E+04  
 31 6 0.43289620E-01 0.95009720E+04  
 31 7 0.43219784E-01 0.94856448E+04  
 31 8 0.43139990E-01 0.94681321E+04  
 31 9 0.43050247E-01 0.94484356E+04  
 31 10 0.42950561E-01 0.94265573E+04  
 31 11 0.42840944E-01 0.94024991E+04  
 31 12 0.42721405E-01 0.93762634E+04  
 31 13 0.42591956E-01 0.93478526E+04  
 31 14 0.42452610E-01 0.93172695E+04  
 31 15 0.42303378E-01 0.92845170E+04  
 31 16 0.42144276E-01 0.92495982E+04  
 31 17 0.41975319E-01 0.92125164E+04  
 31 18 0.41796523E-01 0.91732753E+04  
 31 19 0.41607906E-01 0.91318784E+04  
 31 20 0.41409484E-01 0.90883299E+04  
 31 21 0.41201277E-01 0.90426338E+04

31 22 0.40983306E-01 0.89947946E+04  
 31 23 0.40755590E-01 0.89448168E+04  
 31 24 0.40518152E-01 0.88927053E+04  
 31 25 0.40271016E-01 0.88384650E+04  
 31 26 0.40014203E-01 0.87821012E+04  
 31 27 0.39747740E-01 0.87236194E+04  
 31 28 0.39471652E-01 0.86630250E+04  
 31 29 0.39185966E-01 0.86003241E+04  
 31 30 0.38890709E-01 0.85355227E+04  
 31 31 0.38585910E-01 0.84686271E+04  
 31 32 0.38271598E-01 0.83996438E+04  
 31 33 0.37947805E-01 0.83285794E+04  
 31 34 0.37614562E-01 0.82554409E+04  
 31 35 0.37271901E-01 0.81802356E+04  
 31 36 0.36919856E-01 0.81029706E+04  
 31 37 0.36558461E-01 0.80236536E+04  
 31 38 0.36187752E-01 0.79422924E+04  
 31 39 0.35807766E-01 0.78588950E+04  
 31 40 0.35418539E-01 0.77734696E+04  
 31 41 0.35020111E-01 0.76860248E+04  
 31 42 0.34612520E-01 0.75965690E+04  
 31 43 0.34195808E-01 0.75051113E+04  
 31 44 0.33770016E-01 0.74116608E+04  
 31 45 0.33335187E-01 0.73162268E+04  
 32 0 0.39702667E-01 0.87137270E+04  
 32 1 0.39692866E-01 0.87115759E+04  
 32 2 0.39673265E-01 0.87072739E+04  
 32 3 0.39643865E-01 0.87008214E+04  
 32 4 0.39604670E-01 0.86922190E+04  
 32 5 0.39555683E-01 0.86814677E+04  
 32 6 0.39496909E-01 0.86685684E+04  
 32 7 0.39428355E-01 0.86535224E+04  
 32 8 0.39350026E-01 0.86363313E+04  
 32 9 0.39261931E-01 0.86169966E+04  
 32 10 0.39164078E-01 0.85955203E+04  
 32 11 0.39056476E-01 0.85719045E+04  
 32 12 0.38939137E-01 0.85461515E+04  
 32 13 0.38812071E-01 0.85182639E+04  
 32 14 0.38675292E-01 0.84882443E+04  
 32 15 0.38528813E-01 0.84560958E+04  
 32 16 0.38372648E-01 0.84218216E+04  
 32 17 0.38206813E-01 0.83854249E+04  
 32 18 0.38031323E-01 0.83469095E+04  
 32 19 0.37846197E-01 0.83062790E+04  
 32 20 0.37651453E-01 0.82635375E+04  
 32 21 0.37447109E-01 0.82186893E+04  
 32 22 0.37233187E-01 0.81717388E+04  
 32 23 0.37009707E-01 0.81226906E+04  
 32 24 0.36776692E-01 0.80715497E+04  
 32 25 0.36534164E-01 0.80183210E+04  
 32 26 0.36282148E-01 0.79630099E+04  
 32 27 0.36020669E-01 0.79056219E+04  
 32 28 0.35749753E-01 0.78461628E+04  
 32 29 0.35469428E-01 0.77846384E+04  
 32 30 0.35179720E-01 0.77210550E+04  
 32 31 0.34880660E-01 0.76554189E+04  
 32 32 0.34572277E-01 0.75877367E+04  
 32 33 0.34254603E-01 0.75180153E+04  
 32 34 0.33927669E-01 0.74462616E+04  
 32 35 0.33591509E-01 0.73724829E+04  
 32 36 0.33246156E-01 0.72966868E+04  
 32 37 0.32891646E-01 0.72188808E+04  
 32 38 0.32528015E-01 0.71390731E+04  
 32 39 0.32155300E-01 0.70572716E+04  
 32 40 0.31773539E-01 0.69734848E+04  
 32 41 0.31382772E-01 0.68877214E+04  
 32 42 0.30983039E-01 0.67999901E+04  
 32 43 0.30574381E-01 0.67103000E+04  
 32 44 0.30156840E-01 0.66186605E+04  
 32 45 0.29730461E-01 0.65250811E+04  
 33 0 0.36005831E-01 0.79023653E+04  
 33 1 0.35996214E-01 0.79002546E+04  
 33 2 0.35976981E-01 0.78960335E+04  
 33 3 0.35948135E-01 0.78897025E+04  
 33 4 0.35909677E-01 0.78812621E+04  
 33 5 0.35861613E-01 0.78707131E+04  
 33 6 0.35803946E-01 0.78580568E+04  
 33 7 0.35736684E-01 0.78432943E+04  
 33 8 0.35659831E-01 0.78264272E+04  
 33 9 0.35573398E-01 0.78074572E+04  
 33 10 0.35477391E-01 0.77863862E+04  
 33 11 0.35371821E-01 0.77632163E+04  
 33 12 0.35256700E-01 0.77379500E+04  
 33 13 0.35132037E-01 0.77105898E+04  
 33 14 0.34997847E-01 0.76811385E+04  
 33 15 0.34854143E-01 0.76495991E+04  
 33 16 0.34700940E-01 0.76159748E+04  
 33 17 0.34538252E-01 0.75802691E+04  
 33 18 0.34366098E-01 0.75424857E+04  
 33 19 0.34184495E-01 0.75026283E+04  
 33 20 0.33993461E-01 0.74607011E+04  
 33 21 0.33793015E-01 0.74167085E+04

33 22 0.335683179E-01 0.73706548E+04  
 33 23 0.33363975E-01 0.73225450E+04  
 33 24 0.33135424E-01 0.72723838E+04  
 33 25 0.32897550E-01 0.72201766E+04  
 33 26 0.32650378E-01 0.71659287E+04  
 33 27 0.32393934E-01 0.71096457E+04  
 33 28 0.32128244E-01 0.70513335E+04  
 33 29 0.31853336E-01 0.69909981E+04  
 33 30 0.31569238E-01 0.69286459E+04  
 33 31 0.31275980E-01 0.68642833E+04  
 33 32 0.30973593E-01 0.67979170E+04  
 33 33 0.30662109E-01 0.67295540E+04  
 33 34 0.30341559E-01 0.66592016E+04  
 33 35 0.30011979E-01 0.65868670E+04  
 33 36 0.29673402E-01 0.65125580E+04  
 33 37 0.29325864E-01 0.64362823E+04  
 33 38 0.28969403E-01 0.63580482E+04  
 33 39 0.28609405E-01 0.62778639E+04  
 33 40 0.28229863E-01 0.61957379E+04  
 33 41 0.27846863E-01 0.61116791E+04  
 33 42 0.27455097E-01 0.60256964E+04  
 33 43 0.27054608E-01 0.59377992E+04  
 33 44 0.26645439E-01 0.58479970E+04  
 33 45 0.26227634E-01 0.57562994E+04  
 34 0 0.32409716E-01 0.71131096E+04  
 34 1 0.32400286E-01 0.71110399E+04  
 34 2 0.32381427E-01 0.71069008E+04  
 34 3 0.32353141E-01 0.71006926E+04  
 34 4 0.32315430E-01 0.70924162E+04  
 34 5 0.32268300E-01 0.70820722E+04  
 34 6 0.32211754E-01 0.70696619E+04  
 34 7 0.32145799E-01 0.70551864E+04  
 34 8 0.32070442E-01 0.70386475E+04  
 34 9 0.31985691E-01 0.70200468E+04  
 34 10 0.31891555E-01 0.69993862E+04  
 34 11 0.31788043E-01 0.69766680E+04  
 34 12 0.31675167E-01 0.69518946E+04  
 34 13 0.31552939E-01 0.69250687E+04  
 34 14 0.31421371E-01 0.68961929E+04  
 34 15 0.31280479E-01 0.68652706E+04  
 34 16 0.31130276E-01 0.68323048E+04  
 34 17 0.30970777E-01 0.67972991E+04  
 34 18 0.30802003E-01 0.67602573E+04  
 34 19 0.30623969E-01 0.67211833E+04  
 34 20 0.30436694E-01 0.66800813E+04  
 34 21 0.30240199E-01 0.66369557E+04  
 34 22 0.30034505E-01 0.65918110E+04  
 34 23 0.29819633E-01 0.65446521E+04  
 34 24 0.29595608E-01 0.64954841E+04  
 34 25 0.29362451E-01 0.64443123E+04  
 34 26 0.29120190E-01 0.63911421E+04  
 34 27 0.28868850E-01 0.63359794E+04  
 34 28 0.28608458E-01 0.62788300E+04  
 34 29 0.28339043E-01 0.62197001E+04  
 34 30 0.28060633E-01 0.61585963E+04  
 34 31 0.27773260E-01 0.60955251E+04  
 34 32 0.27476953E-01 0.60304934E+04  
 34 33 0.27171747E-01 0.59635083E+04  
 34 34 0.26857674E-01 0.58945772E+04  
 34 35 0.26534768E-01 0.58237076E+04  
 34 36 0.26203066E-01 0.57509075E+04  
 34 37 0.25862605E-01 0.56761848E+04  
 34 38 0.25513421E-01 0.55995479E+04  
 34 39 0.25155555E-01 0.55210053E+04  
 34 40 0.24789045E-01 0.54406568E+04  
 34 41 0.24413935E-01 0.53582385E+04  
 34 42 0.24030264E-01 0.52740326E+04  
 34 43 0.23638078E-01 0.51879577E+04  
 34 44 0.23237421E-01 0.51000236E+04  
 34 45 0.22828338E-01 0.50102404E+04  
 35 0 0.28915663E-01 0.63462535E+04  
 35 1 0.28906422E-01 0.63442254E+04  
 35 2 0.28887941E-01 0.63401694E+04  
 35 3 0.28860223E-01 0.63340859E+04  
 35 4 0.28823270E-01 0.63259756E+04  
 35 5 0.28777086E-01 0.63158395E+04  
 35 6 0.28721677E-01 0.63036786E+04  
 35 7 0.28657049E-01 0.62894943E+04  
 35 8 0.28583208E-01 0.62732882E+04  
 35 9 0.28500164E-01 0.62550620E+04  
 35 10 0.28407924E-01 0.62348178E+04  
 35 11 0.28306500E-01 0.62125579E+04  
 35 12 0.28195903E-01 0.61882846E+04  
 35 13 0.28076145E-01 0.61620007E+04  
 35 14 0.27947239E-01 0.61337092E+04  
 35 15 0.27809200E-01 0.61034131E+04  
 35 16 0.27662043E-01 0.60711158E+04  
 35 17 0.27505784E-01 0.60368210E+04  
 35 18 0.27340442E-01 0.60005325E+04  
 35 19 0.27166033E-01 0.59622542E+04  
 35 20 0.26982578E-01 0.59219906E+04  
 35 21 0.26790098E-01 0.58797460E+04

35 22 0.26588614E-01 0.58355253E+04  
 35 23 0.26378148E-01 0.57893334E+04  
 35 24 0.26158724E-01 0.57411755E+04  
 35 25 0.25930367E-01 0.56910569E+04  
 35 26 0.25693103E-01 0.56389834E+04  
 35 27 0.25446958E-01 0.55849609E+04  
 35 28 0.25191960E-01 0.5528954E+04  
 35 29 0.24928139E-01 0.54710933E+04  
 35 30 0.24655824E-01 0.54112612E+04  
 35 31 0.24374146E-01 0.53495059E+04  
 35 32 0.24084037E-01 0.52858345E+04  
 35 33 0.23785232E-01 0.52202542E+04  
 35 34 0.23477763E-01 0.51527727E+04  
 35 35 0.23161667E-01 0.50833976E+04  
 35 36 0.22836980E-01 0.50121371E+04  
 35 37 0.22503741E-01 0.49389995E+04  
 35 38 0.22161987E-01 0.48639931E+04  
 35 39 0.218111759E-01 0.47871270E+04  
 35 40 0.21453098E-01 0.47084100E+04  
 35 41 0.21086046E-01 0.46278516E+04  
 35 42 0.20710649E-01 0.45454613E+04  
 35 43 0.20326949E-01 0.44612490E+04  
 35 44 0.19934994E-01 0.43752248E+04  
 35 45 0.19534830E-01 0.42873990E+04  
 36 0 0.25525518E-01 0.56022029E+04  
 36 1 0.25516470E-01 0.56002171E+04  
 36 2 0.25498375E-01 0.55962457E+04  
 36 3 0.25471235E-01 0.55902892E+04  
 36 4 0.25435054E-01 0.55823483E+04  
 36 5 0.25389835E-01 0.55724238E+04  
 36 6 0.25335584E-01 0.55608171E+04  
 36 7 0.25272306E-01 0.55466293E+04  
 36 8 0.25200011E-01 0.55307622E+04  
 36 9 0.25118705E-01 0.55129176E+04  
 36 10 0.25028339E-01 0.54930977E+04  
 36 11 0.24929101E-01 0.54713046E+04  
 36 12 0.24820826E-01 0.54475409E+04  
 36 13 0.24703585E-01 0.54218094E+04  
 36 14 0.24577392E-01 0.53941132E+04  
 36 15 0.24442261E-01 0.53644555E+04  
 36 16 0.24298209E-01 0.53328397E+04  
 36 17 0.24145252E-01 0.52992695E+04  
 36 18 0.23983408E-01 0.52637489E+04  
 36 19 0.23812697E-01 0.52262821E+04  
 36 20 0.23633139E-01 0.51868735E+04  
 36 21 0.23444753E-01 0.51455277E+04  
 36 22 0.23247563E-01 0.51022496E+04  
 36 23 0.23041593E-01 0.50570443E+04  
 36 24 0.22826866E-01 0.50099172E+04  
 36 25 0.22603408E-01 0.49608740E+04  
 36 26 0.22371246E-01 0.49099203E+04  
 36 27 0.22130408E-01 0.48570623E+04  
 36 28 0.21580921E-01 0.48023064E+04  
 36 29 0.21622817E-01 0.47456591E+04  
 36 30 0.21356126E-01 0.46871271E+04  
 36 31 0.21080880E-01 0.46267177E+04  
 36 32 0.20797112E-01 0.45644379E+04  
 36 33 0.20504858E-01 0.45002955E+04  
 36 34 0.20204152E-01 0.44342983E+04  
 36 35 0.19895032E-01 0.43664542E+04  
 36 36 0.19577535E-01 0.42967716E+04  
 36 37 0.19251700E-01 0.42252591E+04  
 36 38 0.18917567E-01 0.41519255E+04  
 36 39 0.185751179E-01 0.40767800E+04  
 36 40 0.18224577E-01 0.39998318E+04  
 36 41 0.17865807E-01 0.39210908E+04  
 36 42 0.17498912E-01 0.38405667E+04  
 36 43 0.17123940E-01 0.37582698E+04  
 36 44 0.16740938E-01 0.36742107E+04  
 36 45 0.16349956E-01 0.35884001E+04  
 37 0 0.222241599E-01 0.48814661E+04  
 37 1 0.22232749E-01 0.48795237E+04  
 37 2 0.22215049E-01 0.48756390E+04  
 37 3 0.22188502E-01 0.48698126E+04  
 37 4 0.22153111E-01 0.48620452E+04  
 37 5 0.22108881E-01 0.48523377E+04  
 37 6 0.22055816E-01 0.48406914E+04  
 37 7 0.21993924E-01 0.48271076E+04  
 37 8 0.21923211E-01 0.48115880E+04  
 37 9 0.21843688E-01 0.47941346E+04  
 37 10 0.21755363E-01 0.47747495E+04  
 37 11 0.21658247E-01 0.47534351E+04  
 37 12 0.21552353E-01 0.47301940E+04  
 37 13 0.21437693E-01 0.47050290E+04  
 37 14 0.21314281E-01 0.46779434E+04  
 37 15 0.21182134E-01 0.46489404E+04  
 37 16 0.21041267E-01 0.46180236E+04  
 37 17 0.20891698E-01 0.45851970E+04  
 37 18 0.20733444E-01 0.45504644E+04  
 37 19 0.20566527E-01 0.45138304E+04  
 37 20 0.20390967E-01 0.44752994E+04  
 37 21 0.20206786E-01 0.44348762E+04

37 22 0.20014006E-01 0.43925660E+04  
 37 23 0.19812652E-01 0.43483740E+04  
 37 24 0.19602750E-01 0.43023057E+04  
 37 25 0.19384325E-01 0.42543671E+04  
 37 26 0.19157406E-01 0.42045641E+04  
 37 27 0.18922021E-01 0.41529030E+04  
 37 28 0.18678200E-01 0.40939050E+04  
 37 29 0.18425974E-01 0.40440333E+04  
 37 30 0.18165376E-01 0.39868385E+04  
 37 31 0.17896438E-01 0.39278136E+04  
 37 32 0.17619196E-01 0.38669660E+04  
 37 33 0.17333686E-01 0.38043037E+04  
 37 34 0.17039944E-01 0.37398349E+04  
 37 35 0.16738009E-01 0.36735679E+04  
 37 36 0.16427922E-01 0.36055115E+04  
 37 37 0.16109721E-01 0.35356746E+04  
 37 38 0.15783451E-01 0.34640666E+04  
 37 39 0.15449154E-01 0.33906969E+04  
 37 40 0.15106875E-01 0.33155753E+04  
 37 41 0.14756660E-01 0.32387122E+04  
 37 42 0.14398558E-01 0.31601177E+04  
 37 43 0.14032616E-01 0.30798028E+04  
 37 44 0.13658886E-01 0.29977785E+04  
 37 45 0.13277419E-01 0.29140561E+04  
 38 0 0.19066897E-01 0.41846997E+04  
 38 1 0.19058250E-01 0.41828019E+04  
 38 2 0.19040958E-01 0.41790066E+04  
 38 3 0.19015022E-01 0.41733143E+04  
 38 4 0.18980445E-01 0.41657256E+04  
 38 5 0.18937233E-01 0.41562417E+04  
 38 6 0.18885391E-01 0.41448637E+04  
 38 7 0.18824927E-01 0.41315932E+04  
 38 8 0.18755846E-01 0.41164319E+04  
 38 9 0.18678160E-01 0.40993817E+04  
 38 10 0.18591878E-01 0.40804450E+04  
 38 11 0.18497012E-01 0.40596242E+04  
 38 12 0.18393573E-01 0.40369220E+04  
 38 13 0.18281576E-01 0.40123415E+04  
 38 14 0.18161035E-01 0.39858859E+04  
 38 15 0.18031967E-01 0.39575587E+04  
 38 16 0.17894388E-01 0.39273636E+04  
 38 17 0.17748316E-01 0.38953046E+04  
 38 18 0.17593772E-01 0.38613860E+04  
 38 19 0.17430775E-01 0.38256124E+04  
 38 20 0.17259347E-01 0.37879883E+04  
 38 21 0.17079512E-01 0.37485190E+04  
 38 22 0.16891293E-01 0.37072097E+04  
 38 23 0.16694715E-01 0.36640658E+04  
 38 24 0.16489805E-01 0.36190933E+04  
 38 25 0.16276590E-01 0.35722982E+04  
 38 26 0.16055101E-01 0.35236868E+04  
 38 27 0.15825365E-01 0.34732657E+04  
 38 28 0.15587415E-01 0.34210418E+04  
 38 29 0.15341284E-01 0.33670222E+04  
 38 30 0.15087005E-01 0.33112144E+04  
 38 31 0.14824613E-01 0.32536261E+04  
 38 32 0.14554145E-01 0.31942653E+04  
 38 33 0.14275639E-01 0.31331402E+04  
 38 34 0.13989133E-01 0.30702594E+04  
 38 35 0.13694668E-01 0.30056318E+04  
 38 36 0.13392286E-01 0.29392665E+04  
 38 37 0.13082029E-01 0.28711731E+04  
 38 38 0.12763943E-01 0.28013613E+04  
 38 39 0.12438074E-01 0.27298413E+04  
 38 40 0.12104469E-01 0.26566235E+04  
 38 41 0.11763177E-01 0.25817185E+04  
 38 42 0.11414249E-01 0.25051377E+04  
 38 43 0.11057737E-01 0.24268924E+04  
 38 44 0.10693695E-01 0.23469943E+04  
 38 45 0.10322178E-01 0.22654558E+04  
 39 0 0.16005391E-01 0.35127767E+04  
 39 1 0.15996955E-01 0.35109253E+04  
 39 2 0.15980085E-01 0.35072227E+04  
 39 3 0.15954783E-01 0.35016696E+04  
 39 4 0.15921052E-01 0.34942665E+04  
 39 5 0.15878898E-01 0.34850147E+04  
 39 6 0.15828326E-01 0.34739154E+04  
 39 7 0.15769343E-01 0.34609702E+04  
 39 8 0.15701958E-01 0.34461809E+04  
 39 9 0.15626180E-01 0.34295497E+04  
 39 10 0.15542021E-01 0.34110788E+04  
 39 11 0.15449491E-01 0.33907708E+04  
 39 12 0.15348604E-01 0.33686288E+04  
 39 13 0.15239375E-01 0.33446557E+04  
 39 14 0.15121819E-01 0.33188552E+04  
 39 15 0.14995953E-01 0.32912307E+04  
 39 16 0.14861794E-01 0.32617863E+04  
 39 17 0.14719362E-01 0.32305261E+04  
 39 18 0.14568678E-01 0.31974548E+04  
 39 19 0.14409763E-01 0.31625770E+04  
 39 20 0.14242640E-01 0.31258977E+04  
 39 21 0.14067333E-01 0.30874223E+04

39 22 0.13883867E-01 0.30471563E+04  
 39 23 0.13692270E-01 0.30051056E+04  
 39 24 0.13492569E-01 0.29612763E+04  
 39 25 0.13284794E-01 0.29156748E+04  
 39 26 0.13068974E-01 0.28683079E+04  
 39 27 0.12845143E-01 0.28191825E+04  
 39 28 0.12613332E-01 0.27683060E+04  
 39 29 0.12373577E-01 0.27156858E+04  
 39 30 0.12125913E-01 0.26613299E+04  
 39 31 0.11870378E-01 0.26052465E+04  
 39 32 0.11607010E-01 0.25474440E+04  
 39 33 0.11335850E-01 0.24879312E+04  
 39 34 0.11056939E-01 0.24267173E+04  
 39 35 0.10770321E-01 0.23638118E+04  
 39 36 0.10476039E-01 0.22992244E+04  
 39 37 0.10174140E-01 0.22329653E+04  
 39 38 0.98646716E-02 0.21650449E+04  
 39 39 0.95476838E-02 0.20954741E+04  
 39 40 0.92232272E-02 0.20242641E+04  
 39 41 0.88913549E-02 0.19514266E+04  
 39 42 0.85521215E-02 0.18769734E+04  
 39 43 0.82055835E-02 0.18009171E+04  
 39 44 0.78517992E-02 0.17232705E+04  
 39 45 0.74908291E-02 0.16440467E+04  
 40 0 0.13062272E-01 0.26668370E+04  
 40 1 0.13054058E-01 0.28650342E+04  
 40 2 0.13037632E-01 0.28614290E+04  
 40 3 0.13012995E-01 0.28560218E+04  
 40 4 0.12980152E-01 0.28488136E+04  
 40 5 0.12939107E-01 0.28398054E+04  
 40 6 0.12889868E-01 0.28289986E+04  
 40 7 0.12832441E-01 0.28163949E+04  
 40 8 0.12766836E-01 0.28019962E+04  
 40 9 0.12693062E-01 0.27858048E+04  
 40 10 0.12611132E-01 0.27678231E+04  
 40 11 0.12521057E-01 0.27480540E+04  
 40 12 0.12422852E-01 0.27265005E+04  
 40 13 0.12316532E-01 0.27031659E+04  
 40 14 0.12202113E-01 0.26780539E+04  
 40 15 0.12079614E-01 0.26511684E+04  
 40 16 0.11949053E-01 0.26225137E+04  
 40 17 0.11810452E-01 0.25920942E+04  
 40 18 0.11663831E-01 0.25599147E+04  
 40 19 0.11509214E-01 0.25259802E+04  
 40 20 0.11346626E-01 0.24902963E+04  
 40 21 0.11176092E-01 0.24528684E+04  
 40 22 0.10997640E-01 0.24137027E+04  
 40 23 0.10811298E-01 0.23728053E+04  
 40 24 0.10617096E-01 0.23301829E+04  
 40 25 0.10415066E-01 0.22858424E+04  
 40 26 0.10205240E-01 0.22397909E+04  
 40 27 0.99876521E-02 0.21920359E+04  
 40 28 0.97623390E-02 0.21425855E+04  
 40 29 0.95293376E-02 0.20914476E+04  
 40 30 0.92886866E-02 0.20386308E+04  
 40 31 0.90404263E-02 0.19841440E+04  
 40 32 0.87845987E-02 0.19279963E+04  
 40 33 0.85212473E-02 0.18701974E+04  
 40 34 0.82504173E-02 0.18107570E+04  
 40 35 0.79721556E-02 0.17496857E+04  
 40 36 0.76865108E-02 0.16869939E+04  
 40 37 0.73935333E-02 0.16226928E+04  
 40 38 0.70932756E-02 0.15567938E+04  
 40 39 0.67857918E-02 0.14893089E+04  
 40 40 0.64711381E-02 0.14202505E+04  
 40 41 0.61493730E-02 0.13496312E+04  
 40 42 0.58205567E-02 0.12774643E+04  
 40 43 0.54847520E-02 0.12037638E+04  
 40 44 0.51420240E-02 0.11285437E+04  
 40 45 0.47924401E-02 0.10518189E+04  
 41 0 0.10244475E-01 0.22484021E+04  
 41 1 0.10236497E-01 0.22466511E+04  
 41 2 0.10220543E-01 0.22431495E+04  
 41 3 0.10196615E-01 0.22378979E+04  
 41 4 0.10164717E-01 0.22308971E+04  
 41 5 0.10124854E-01 0.22221483E+04  
 41 6 0.10077034E-01 0.22116531E+04  
 41 7 0.10021265E-01 0.21994132E+04  
 41 8 0.99575566E-02 0.21854308E+04  
 41 9 0.98859190E-02 0.21697081E+04  
 41 10 0.98063649E-02 0.21522480E+04  
 41 11 0.97189079E-02 0.21330534E+04  
 41 12 0.96235633E-02 0.21121277E+04  
 41 13 0.95203474E-02 0.20894744E+04  
 41 14 0.94092782E-02 0.20650976E+04  
 41 15 0.92903750E-02 0.20390013E+04  
 41 16 0.91636586E-02 0.20111903E+04  
 41 17 0.90291512E-02 0.19816693E+04  
 41 18 0.88868764E-02 0.19504436E+04  
 41 19 0.87368593E-02 0.19175187E+04  
 41 20 0.85791267E-02 0.18829004E+04  
 41 21 0.84137066E-02 0.18465949E+04

41	22	0.82406287E-02	0.18086087E+04
41	23	0.80599242E-02	0.17689486E+04
41	24	0.78716259E-02	0.17276219E+04
41	25	0.76757682E-02	0.168464362E+04
41	26	0.74723872E-02	0.16399992E+04
41	27	0.72615205E-02	0.15937193E+04
41	28	0.70432075E-02	0.15458052E+04
41	29	0.68174894E-02	0.14962658E+04
41	30	0.65844092E-02	0.14451106E+04
41	31	0.63440115E-02	0.13923494E+04
41	32	0.60963430E-02	0.13379924E+04
41	33	0.58414523E-02	0.12820504E+04
41	34	0.55793900E-02	0.12245454E+04
41	35	0.53102087E-02	0.11654559E+04
41	36	0.50339632E-02	0.11048270E+04
41	37	0.47507104E-02	0.10426603E+04
41	38	0.44605096E-02	0.97896857E+03
41	39	0.41634227E-02	0.91376552E+03
41	40	0.38595137E-02	0.84706522E+03
41	41	0.35488496E-02	0.7788234E+03
41	42	0.32315000E-02	0.70923216E+03
41	43	0.29075374E-02	0.63813061E+03
41	44	0.25770376E-02	0.56559430E+03
41	45	0.22400796E-02	0.49164056E+03
42	0	0.75615827E-02	0.16595753E+04
42	1	0.75538611E-02	0.16578806E+04
42	2	0.75384193E-02	0.16544916E+04
42	3	0.75152605E-02	0.16494088E+04
42	4	0.74843890E-02	0.16426333E+04
42	5	0.74458108E-02	0.16341664E+04
42	6	0.73995536E-02	0.16240097E+04
42	7	0.73455662E-02	0.16121652E+04
42	8	0.72839193E-02	0.15986353E+04
42	9	0.72146049E-02	0.15834225E+04
42	10	0.71376366E-02	0.15665299E+04
42	11	0.70530294E-02	0.15479608E+04
42	12	0.69608002E-02	0.15277188E+04
42	13	0.68609672E-02	0.15058080E+04
42	14	0.67535502E-02	0.14822327E+04
42	15	0.66385706E-02	0.14569976E+04
42	16	0.65160515E-02	0.14301078E+04
42	17	0.63860177E-02	0.14015687E+04
42	18	0.62484953E-02	0.13713860E+04
42	19	0.61035126E-02	0.13395660E+04
42	20	0.59510992E-02	0.13061151E+04
42	21	0.57912866E-02	0.12710403E+04
42	22	0.56241081E-02	0.12343489E+04
42	23	0.54495987E-02	0.11960485E+04
42	24	0.52677955E-02	0.11561473E+04
42	25	0.50787373E-02	0.11146538E+04
42	26	0.48824649E-02	0.10715770E+04
42	27	0.46790211E-02	0.10269263E+04
42	28	0.44684508E-02	0.98071144E+03
42	29	0.42508010E-02	0.93294285E+03
42	30	0.40261211E-02	0.88363132E+03
42	31	0.37944626E-02	0.83278816E+03
42	32	0.35558794E-02	0.78042521E+03
42	33	0.33104281E-02	0.72655488E+03
42	34	0.30581676E-02	0.67119011E+03
42	35	0.27991597E-02	0.61434447E+03
42	36	0.25334692E-02	0.55603214E+03
42	37	0.22611635E-02	0.49626796E+03
42	38	0.19823136E-02	0.43506747E+03
42	39	0.16969934E-02	0.37244695E+03
42	40	0.14052808E-02	0.30842345E+03
42	41	0.11072572E-02	0.24301483E+03
42	42	0.80300803E-03	0.17623987E+03
42	43	0.49262309E-03	0.10811825E+03
42	44	0.17619678E-03	0.38670717E+02
43	0	0.50275294E-02	0.11034150E+04
43	1	0.50200942E-02	0.11017832E+04
43	2	0.50052255E-02	0.10985199E+04
43	3	0.49829266E-02	0.10936258E+04
43	4	0.49532028E-02	0.10871022E+04
43	5	0.49160609E-02	0.10789505E+04
43	6	0.48715094E-02	0.10691726E+04
43	7	0.48195586E-02	0.10577707E+04
43	8	0.47602205E-02	0.10447475E+04
43	9	0.46935089E-02	0.10301060E+04
43	10	0.46194394E-02	0.10138496E+04
43	11	0.45380294E-02	0.99598218E+03
43	12	0.44492979E-02	0.97650787E+03
43	13	0.43532659E-02	0.95543129E+03
43	14	0.42499563E-02	0.93275746E+03
43	15	0.41393938E-02	0.90849179E+03
43	16	0.40216050E-02	0.88264015E+03
43	17	0.38966185E-02	0.85520879E+03
43	18	0.37644649E-02	0.82620442E+03
43	19	0.36251768E-02	0.79563422E+03
43	20	0.34787888E-02	0.76350578E+03
43	21	0.33253379E-02	0.72982720E+03
43	22	0.31648630E-02	0.69460705E+03

```

43 23 0.29974056E-02 0.65785439E+03
43 24 0.28230091E-02 0.61957879E+03
43 25 0.26417198E-02 0.57979039E+03
43 26 0.24535862E-02 0.53849984E+03
43 27 0.22586595E-02 0.49571840E+03
43 28 0.20569939E-02 0.45145790E+03
43 29 0.18486460E-02 0.40573033E+03
43 30 0.16336757E-02 0.35855033E+03
43 31 0.14121462E-02 0.30993022E+03
43 32 0.11841237E-02 0.25988507E+03
43 33 0.94967812E-03 0.20843023E+03
43 34 0.70888319E-03 0.15558186E+03
43 35 0.46181656E-03 0.10135700E+03
43 36 0.20856015E-03 0.45773657E+02
44 0 0.26636658E-02 0.58460698E+03
44 1 0.26565648E-02 0.58304849E+03
44 2 0.26423648E-02 0.57993197E+03
44 3 0.26210700E-02 0.57525830E+03
44 4 0.25926865E-02 0.56902883E+03
44 5 0.25572224E-02 0.56124536E+03
44 6 0.25146880E-02 0.55191014E+03
44 7 0.24650956E-02 0.54102588E+03
44 8 0.24084598E-02 0.52859575E+03
44 9 0.23447971E-02 0.51462340E+03
44 10 0.22741262E-02 0.49911294E+03
44 11 0.21964681E-02 0.48206897E+03
44 12 0.21118461E-02 0.46349658E+03
44 13 0.20202855E-02 0.44340135E+03
44 14 0.19218142E-02 0.42178939E+03
44 15 0.18164623E-02 0.39866733E+03
44 16 0.17042624E-02 0.37404231E+03
44 17 0.15852498E-02 0.34792206E+03
44 18 0.14594620E-02 0.32031485E+03
44 19 0.13269396E-02 0.29122955E+03
44 20 0.11877258E-02 0.26067564E+03
44 21 0.10418665E-02 0.22866324E+03
44 22 0.88941099E-03 0.19520312E+03
44 23 0.73041139E-03 0.16030675E+03
44 24 0.56492328E-03 0.12398631E+03
44 25 0.39300569E-03 0.86254768E+02
44 26 0.21472134E-03 0.47125880E+02
44 27 0.30136817E-04 0.66142658E+01
45 0 0.50447754E-03 0.11072001E+03
45 1 0.49779211E-03 0.10925272E+03
45 2 0.48442388E-03 0.10631874E+03
45 3 0.46437814E-03 0.10191921E+03
45 4 0.43766285E-03 0.96055879E+02
45 5 0.40428864E-03 0.88731087E+02
45 6 0.36426885E-03 0.79947761E+02
45 7 0.31761961E-03 0.69709436E+02
45 8 0.26435979E-03 0.58020260E+02
45 9 0.20451118E-03 0.44885010E+02
45 10 0.13809846E-03 0.30309103E+02
45 11 0.65149303E-04 0.14298617E+02
45 27 0.30136817E-04 0.66142658E+01

```